10-UNDECENOIC ACID-BASED BIODEGRADABLE HYDROXY POLYESTERS: A PLATFORM FOR AMINOACID BIOCONJUGATES AND PEG-DERIVED AMPHIPHILIC COPOLYMERS

Carmen Valverde Sarmiento

UNIVERSITAT ROVIRA i VIRGILI

10-Undecenoic acid-based biodegradable hydroxy polyesters: a platform for amino acid bioconjugates and PEG-derived amphiphilic copolymers

CARMEN VALVERDE SARMIENTO

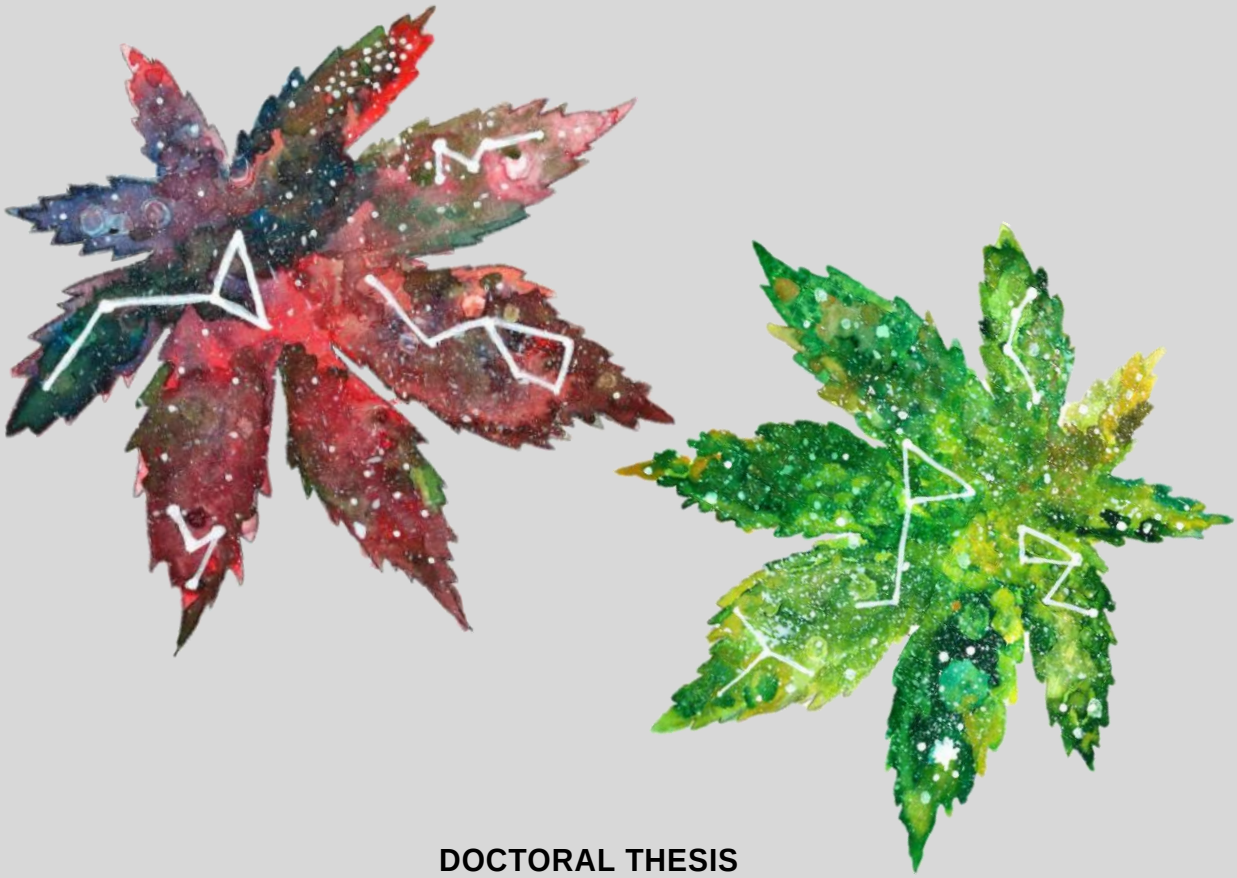

DOCTORAL THESIS
2018

UNIVERSITAT ROVIRA I VIRGILI
10-UNDECENOIC ACID-BASED BIODEGRADABLE HYDROXY POLYESTERS: A PLATFORM FOR AMINOACID BIOCONJUGATES AND PEG-DERIVED AMPHIPHILIC COPOLYMERS
Carmen Valverde Sarmiento

UNIVERSITAT ROVIRA I VIRGILI
10-UNDECENOIC ACID-BASED BIODEGRADABLE HYDROXY POLYESTERS: A PLATFORM FOR AMINOACID BIOCONJUGATES AND PEG-DERIVED AMPHIPHILIC COPOLYMERS
Carmen Valverde Sarmiento

Carmen Valverde Sarmiento

10-Undecenoic acid-based biodegradable hydroxy polyesters: a platform for amino acid bioconjugates and PEG-derived amphiphilic copolymers.

PhD Thesis

Supervised by Prof. Virginia Cádiz and

Prof. Juan Carlos Ronda

Department of Analytic Chemistry and Organic Chemistry

UNIVERSITAT
ROVIRA i VIRGILI

Tarragona

2018

UNIVERSITAT ROVIRA I VIRGILI
10-UNDECENOIC ACID-BASED BIODEGRADABLE HYDROXY POLYESTERS: A PLATFORM FOR AMINOACID BIOCONJUGATES AND PEG-DERIVED AMPHIPHILIC COPOLYMERS
Carmen Valverde Sarmiento

UNIVERSITAT ROVIRA i VIRGILI
Departament de Química Analítica i Química Orgànica
C/ Marcel·lí Domingo, 1
43007, Tarragona
Telf. 977 559 769
Fax. 977 558 446

Prof. Virginia Cádiz Deleito and Prof. Juan Carlos Ronda Bargalló from the Department of Analytical Chemistry and Organic Chemistry, University Rovira i Virgili,

We STATE that the present study, entitled:

"10-Undecenoic acid-based biodegradable hydroxy polyesters: a platform for amino acid bioconjugates and PEG-derived amphiphilic copolymers"

presented by Carmen Valverde Sarmiento for the award of the degree of Doctor, has been carried out under our supervision at the Department of Analytical Chemistry and Organic Chemistry of this University.

Tarragona, 03 September, 2018

Doctoral Thesis Supervisors

Prof. Virginia Cádiz Deleito

Prof. Juan Carlos Ronda Bargalló

UNIVERSITAT ROVIRA I VIRGILI
10-UNDECENOIC ACID-BASED BIODEGRADABLE HYDROXY POLYESTERS: A PLATFORM FOR AMINOACID BIOCONJUGATES AND PEG-DERIVED AMPHIPHILIC COPOLYMERS
Carmen Valverde Sarmiento

ABSTRACTS:

CATALÀ

El gran desenvolupament que actualment estan experimentant els biopolímers es deu fonamentalment als alts preus i a la disminució de les reserves de petroli, juntament amb la preocupació que existeix avui en dia en matèria de sostenibilitat ambiental. Entre els polímers d'origen renovable, els polièsters alifàtics són dels més estudiats ja que es consideren molt adequats per aplicacions com a biomaterials a causa de la seva biocompatibilitat i biodegradabilitat.

En aquesta tesi s'han preparat polièsters renovables mitjançant química sostenible i utilitzant derivats de l'oli de ricí, com a producte de partença. Concretament, s'han fet servir reaccions amb àcid 10-undecenoïc per obtenir els monòmers, que contenen grups funcionals àcid carboxílic i epòxid o alcohol. Tots dos tipus de monòmer són capaços d'experimentar polimerització, obtenint així polímers lineals i ramificats amb grups hidroxilo funcionalitzables. S'ha demostrat que aquests polímers són degradables enzimàtica i hidrolíticament. A més a més s'han modificat aquests polièsters amb diferents biomolècules com els aminoàcids.

Finalment, utilitzant enzims com a catalitzador s'han sintetitzat copoliésters de bloc i d'empelt a partir d'aquests monòmers o polièsters i derivats del polietilenglicol. Com a resultat s'han obtingut polímers amfifílics capaços de formar micel·les en les quals és possible encapsular drogues per ser alliberades de forma controlada.

CASTELLANO

El gran desarrollo que están experimentando actualmente los biopolímeros se debe fundamentalmente a los altos precios y disminución de las reservas de petróleo, junto con la preocupación que existe hoy en día en materia de sostenibilidad ambiental. Entre los polímeros de origen renovable los poliésteres alifáticos son los que se han estudiado en mayor profundidad por ser los más adecuados como biomateriales, debido a su biocompatibilidad y biodegradabilidad.

En esta tesis se han preparado poliésteres renovables mediante química sostenible y el uso de derivados de aceite de ricino como materia de partida. Concretamente, se han usado reacciones a partir del ácido 10-undecenoico para obtener monómeros que contienen grupos funcionales ácido carboxílico y epóxido o alcohol. Ambos monómeros son capaces de experimentar polimerización, obteniendo así polímeros lineales y ramificados con grupos hidroxilo funcionalizables. Se ha demostrado que estos polímeros son degradables enzimática e hidrolíticamente. Además, estos poliésteres se han modificado con diferentes biomoléculas como aminoácidos.

Finalmente, utilizando enzimas como catalizador se han sintetizado copoliésteres de bloque y de injerto a partir de estos monómeros o poliésteres y derivados del polientilenglicol. Como resultado, se han obtenido polímeros amfifílicos capaces de formar micelas, en las cuales es posible encapsular drogas para ser liberadas de forma controlada.

ENGLISH

Currently biopolymers experienced a great development due to the high prices and decrease of petroleum reserves along with the concern increasing in terms of environmental sustainability. Aliphatic polyesters are among the most studied polymers from renewable resources, because they are considered very suitable for applications as biomaterials due to their biocompatibility and biodegradability.

In this thesis, renewable polyesters have been prepared from derivatives of vegetable castor oil and using sustainable chemistry. Specifically, 10-undecenoic acid has been used to synthesize the monomers which contain carboxylic acid and epoxide or alcohol. These monomers by polymerization lead to linear or branched polymers with available reactive hydroxyl groups. It has been shown that these polymers are enzymatically and hydrolytically degradable. In addition, these polyesters have been modified with different biomolecules as amino acids.

Finally, using enzymes as catalyst have been synthesized block and grafted copolyesters from these monomers or polyesters and polyethylene glycol derivatives. As result, amphiphilic polymers capable of forming micelles have been synthesized, which can encapsulate drugs to be released.

UNIVERSITAT ROVIRA I VIRGILI
10-UNDECENOIC ACID-BASED BIODEGRADABLE HYDROXY POLYESTERS: A PLATFORM FOR AMINOACID BIOCONJUGATES AND PEG-DERIVED AMPHIPHILIC COPOLYMERS
Carmen Valverde Sarmiento

ACKNOWLEDGEMENTS

Esta Tesis ha sido posible gracias al soporte de todas las personas que han estado a mi lado y me han apoyado, por eso quiero dedicarles estas primeras páginas a ellos.

Quisiera agradecer a la Universitat Rovira i Virgili por haberme proporcionado la beca que me ha permitido realizar esta Tesis doctoral.

En primer lugar, me gustaría agradecer a mis directores Prof. Virginia Cádiz Deleito y Prof. Juan Carlos Ronda Bargalló por haberme dado la oportunidad de trabajar en el grupo de polímeros, Suspol. Gracias a ellos por su dedicación, orientación y apoyo durante estos cuatro años. Me han ayudado a llevar a cabo una investigación científica profesionalmente y además me han hecho crecer como persona. Por su espera y apoyo durante los duros meses de baja. También quisiera agradecer a la Prof. Marina Galià i Clua y al Dr. Gerard LLigadas Puig por su ayuda y colaboración en el trabajo de laboratorio y en sus comentarios constructivos durante estos años.

Así mismo quiero agradecer su interés y amabilidad a los profesores del Departamento: Prof. Àngels Serra, Prof. Sergio Castillón, Prof. Maribel Matheu, Dr. Toni Reina, Dra. Yolanda Díaz y Prof. Marisol Larrechi.

Me gustaría agradecer a los técnicos del Servei de Recursos Cientifics (SRCiT) por su inmensa colaboración: Irene Maijó, Francesc Gispert, Antonio de la Torre, Rita Marimon, Mercè Moncusí, Mariana Stefanova y en especial a Ramón Guerrero por su amabilidad y disponibilidad para ayudarme. También agradezco a las secretarias y técnicos del Departamento por su ayuda: Avelina, Dunia, Juan Luis y Tere.

Durante estos años han habido personas especiales, a las que ha sido un gran placer conocer. Entre estas personas están mis Suspoleros, los cuales no sólo han sido compañeros de trabajo, si no también han sido amigos. Mi hermana de Suspol Zeynep, mi querida amiga de locuras y canciones Alev, mi bebé melón Adri, el doctor y mánager Comí,

mi defensor Nabilsillo, mi compi de mesa el gatuno Pere, el noble chico de gustos refinados Aarón, la doctora Mariola, Lorena…. Y muchos más.

Agradecer su compañerismo a los chicos de sucres, que siempre estaban dispuestos a prestarme reactivos y ofrecerme pastas de cumpleaños.

A todos mis amigos y compañeros de polímeros gracias por vuestra compañía en estos años. Rubén, Xavi, los italianos, el descubrimiento de conocer más a Alberto y especialmente agradecer a Dailyn, no sólo su amistad, sino su cuidado y cariño hacia mí, porque ha sido como mi familia.

A los nuevos amigos, que estos años de Tesis me han permitido conocer, porqué gracias a ellos ha sido más llevadero este camino. Gracias a todos, entre los que están Marisa, Andreu, Bárbara, Vicky, Marsal, Lucía, los chicos del Cor Jove y a la familia Pokers, Emili y Jenny.

A mis amigos de toda la vida, los que son como mi familia, los que nunca fallan, a ellos les doy las gracias también porqué siempre me han apoyado y han estado a mi lado. Gracias por cómo sois y por lo que sois para mí, sin necesidad de escribirlo, cada uno de vosotros ya lo sabéis. A Juampe, Marta, Isa, Dani, Tillo, Lucía, Kiko, María, Andrea, Juli, Orta, Mercè, Alex, Mª del Mar, Lupe y Juanan.

Agradecer también a mi pareja Gerard por su apoyo y permanecer a mi lado en todo momento, también a su familia por darme su cariño y cuidado siempre, a l'avia por acogerme cuando estaba cojita.

Finalmente, agradecer a mi familia el hecho de haber podido realizar esta Tesis porqué sin ellos no sería posible haber llegado hasta aquí. Gracias por haberme dejado escoger mi camino, aconsejarme y apoyarme. En especial a mis padres Aurora y Nico, sin olvidarme de mis abuelas Carmen y Conchi. Gracias por su cuidado y dedicación durante mi convalecencia, sin ellos no estaría terminando esta Tesis, al menos de pie y andando.

UNIVERSITAT ROVIRA I VIRGILI
10-UNDECENOIC ACID-BASED BIODEGRADABLE HYDROXY POLYESTERS: A PLATFORM FOR AMINOACID BIOCONJUGATES AND PEG-DERIVED AMPHIPHILIC COPOLYMERS
Carmen Valverde Sarmiento

UNIVERSITAT ROVIRA I VIRGILI
10-UNDECENOIC ACID-BASED BIODEGRADABLE HYDROXY POLYESTERS: A PLATFORM FOR AMINOACID BIOCONJUGATES AND PEG-DERIVED AMPHIPHILIC COPOLYMERS
Carmen Valverde Sarmiento

GENERAL TABLE OF CONTENTS

General table of contents

UNIVERSITAT ROVIRA I VIRGILI
10-UNDECENOIC ACID-BASED BIODEGRADABLE HYDROXY POLYESTERS: A PLATFORM FOR AMINOACID BIOCONJUGATES AND PEG-DERIVED AMPHIPHILIC COPOLYMERS
Carmen Valverde Sarmiento

Chapter 1

Aim and outline

UNIVERSITAT ROVIRA I VIRGILI
10-UNDECENOIC ACID-BASED BIODEGRADABLE HYDROXY POLYESTERS: A PLATFORM FOR AMINOACID BIOCONJUGATES AND PEG-DERIVED AMPHIPHILIC COPOLYMERS
Carmen Valverde Sarmiento

1. AIM AND OUTLINE

Biopolymers are potential candidates for replacing fossil-derived polymers mainly due to their sustainability, biodegradability, and biocompability. Biobased polymers have had a significant increase of interest in the last years due to at least two important reasons. The first one is related to the availability of raw materials for the synthesis of polymers. Currently, the majority of polymers is produced from crude oil with the problems associated with the high prices and rapid fluctuations. The second reason of interest is related to waste management. Expected solution to this problem cannot rely on only one approach but rather on combination of a variety of them. Taking advantage of chemistry, the efficient transformation of renewable resources avoiding the use of fossil reserves that contributes negatively to the planet's energy problem, is a useful approach. Moreover, the synthesis of degradable polymers is also pursued, decreasing the negative environmental impact of huge amounts of plastic waste generation.

By selecting appropriate biomass feedstock and appropriate transformation processes, a wide range of molecules are accessible and these bioplatform molecules are a new challenge for chemistry. Then, the question is if we can build on these molecules as we have done over the last 70 years with the well stablished petroplatform molecules. A substantial grow in research activity on the conversion of these platform molecules to valuable and competitive products is needed.

The synthesis of polyesters and copolyesters made from monomers obtained by chemical modification of naturally-occurring compounds such as vegetable oils may lead to renewable polyesters with improved properties regarding to those displayed by the traditional ones.

Poly(lactic acid) or poly(lactide) (PLA) and poly(Ɛ-caprolactone) (PCL) are two of the leading and most mature biobased plastics among other aliphatic polyesters. However, the

versatility and successful use as commodity plastics are limited as is their exploitation in biomedical, electronic and optical sectors. The absence of reactive functionalities on the polymer backbone greatly limits their use. Thus, the introduction of functional groups can modulate their physical, chemical and biological properties.

General objective

The aim of this Thesis is preparing renewable functional polyesters from platform chemicals derived from vegetable oils, and developing environmentally friendly monomers and polymer synthesis strategies to keep moving toward more sustainable polymer chemistry. To achieve this goal special emphasis in no metallic and enzymatic catalysis has been done.

Specific objectives

The specific objectives are enumerated as follows:

- To prepare AB and AB_2 monomers using green methods exploiting the reactivity of 10-undecenoic acid, available from the pyrolysis of castor oil, as key substrate.
- To develop new linear and branched hydroxyl functionalized polyesters by chemical or enzymatic polymerizations.
- To study the enzymatic and hydrolytic degradation behaviour of these hydroxyl polyesters and to compare to that of poly(11-hydroxyundecanoate) and commercial poly(ε-caprolactone).
- To carry out the post-polymerization modification of free hydroxyl groups with N-Boc protected L-phenylalanine and L-serine, and a cysteine derivative as models for polymer bioconjugates.

- To develop hyperbranched amphiphilic copolyesters by copolymerization with methoxypolyethylenglycols or by grafting onto the polyesters using carboxyl functionalized di and triethyleneglycols.

- To study the ability of these amphiphilic copolyesters for self-assembling into micelles and to investigate their micellar behaviour.

Outline

The work presented in this Thesis is structured in seven chapters including aim and outline, general introduction, experimental part and general conclusions.

Chapter 1. The present chapter focuses on the objectives and the outline of the Thesis

Chapter 2. This chapter contains a general introduction and reviews the state-of-the-art of biobased polyesters from fatty acids, hydroxy functional polyesters and their postpolymerization modification and formation of micelles from amphiphilic copolyesters.

Chapter 3. Hydroxyl functionalized renewable polyesters derived from 10-undecenoic acid: polymer structure and postpolymerization modification.

Chapter 4. Hydrolytic and enzymatic degradation studies of aliphatic 10-undecenoic acid-based polyesters.

Chapter 5. PEG-modified poly(10,11-dihydroxyundecanoic acid) amphiphilic copolymers. Grafting *versus* macromonomer copolymerization approaches using CALB.

Chapter 6. This chapter deals with experimental part.

Chapter 7. General conclusions.

In the Annex part, the Supporting Information (SI) of Chapters 3, 4 and 5 is collected (Annexes A, B and C).

UNIVERSITAT ROVIRA I VIRGILI
10-UNDECENOIC ACID-BASED BIODEGRADABLE HYDROXY POLYESTERS: A PLATFORM FOR AMINOACID BIOCONJUGATES AND PEG-DERIVED AMPHIPHILIC COPOLYMERS
Carmen Valverde Sarmiento

Chapter 2

General introduction

UNIVERSITAT ROVIRA I VIRGILI
10-UNDECENOIC ACID-BASED BIODEGRADABLE HYDROXY POLYESTERS: A PLATFORM FOR AMINOACID BIOCONJUGATES AND PEG-DERIVED AMPHIPHILIC COPOLYMERS
Carmen Valverde Sarmiento

2.1 SUSTAINABILITY

Nowadays, plastics are the most important materials that we use in the modern life. However, this kind of materials is not new, early uses date back from 1600 B.C., when ancient Mesoamerican people harvested latex from *Castilla elastica* (Figure 2.1).[1]

Figure 2.1 Castilla elastica sheet.

In 1284 it was used horn and tortoiseshell as the predominant natural plastic.[2] In 1839 American Goodyear invented vulcanized rubber and a German apothecary Eduard Simon discovered polystyrene (PS).[3] He distilled an oily substance from storax, the resin of the Sweetgum tree, which he named "styrol". Several days later he found that the styrol had thickened, presumably due to polymerization, into a jelly which he named styrol oxide ("Styroloxyd"). However, the first synthetic polymer was Bakelite, that was developed by a Belgian chemist Leo Baekeland in 1907. Nevertheless, the great development of polymers was not until 20th century.

The plastics industry gives directly employment to over 1.5 million people in Europe currently. There are close to 60000 plastic companies, the European plastics industry ranks 7th in Europe in industrial value, at the same level as the pharmaceutical industry. The plastic world production is increasing and more than 300 Mt have been fabricated in 2016 (Figure 2.2). Its large annual production is due to plastic properties like: lightweight, resistance, versatility, economic, easy processing… becoming one of the

main materials we use daily in packaging, construction, medical industry, electronic devices, etc.[4]

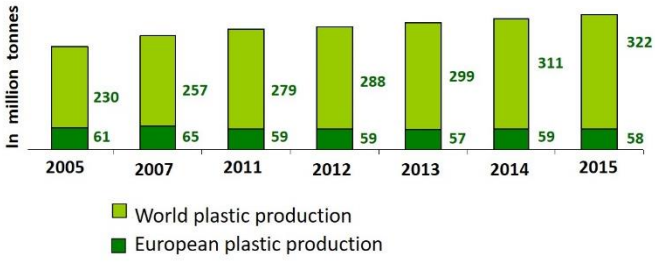

Figure 2.2 World and European production of plastic.

Within the last few decades plastics have revolutionized our daily lives. At the same time, the environmental consequences are being manifested so that the concern about the need to legislate its use is growing up. Owing to the wide usage of plastics and its additives, plastics can be a potential human health and environmental risks.[5] Figure 2.3 illustrates a historical summary in the development, production and use of plastics together with associated concerns and legislative measures.[6]

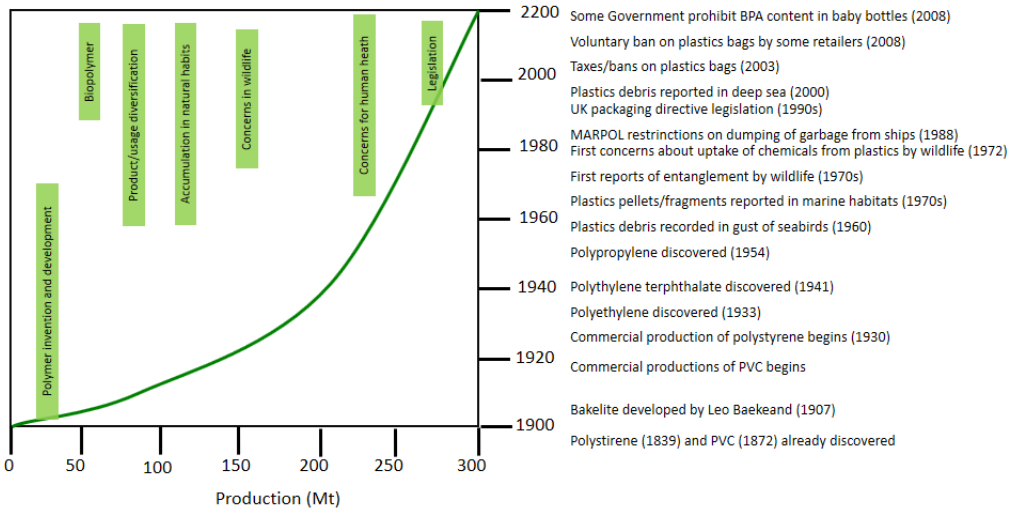

Figure 2.3 Historical overview summarizing the development and production of plastic, together with associated concerns, regulatory measures and some potential future trends.

Although there are regulatory measures in plastic materials, the growing up world global industrialization leads to the use of large quantities of fossil resources. More than 80 % of consumed energy is from fossil resources, and they have some inherent problems, they generate a lot of harmful emissions like as greenhouse gases (GHG), CO_2, methane and others pollutants, which are risks to the humankind and animal health. The different emissions are harmful for humankind, moreover they produce plastic wastes.

The polymer fossil-based industry is deeply rooted in European economy, with its well-known environmental and health consequences. With regard to this problem, the European Commission, in 2012, adopted strategies to change the European economy to bioeconomy. Bioeconomy is the sustainable exploitation of renewable biological resources from land and sea (such as crops, forests, fish, animals and microorganisms) to produce food, biomaterials and bioenergy.[7] So the plastic industry is inside of this new view of economy, and biopolymers are the most important alternative plastic materials to contribute with bioeconomy. Climate change and the associated need to reduce greenhouse gases mean it is time for a rethink.

The most the plastics come from crude oil, natural gas and coal. Some of the negative impacts could be reduced by bioplastics that are biodegradable o bio-based.[8] European bioplastics has done a forecast about bioplastics (Figure 2.4).[4] Bioplastics can be described by two different concepts:

• Biodegradable plastics: which are materials that are degraded by microorganisms into water, carbon dioxide (or methane) and biomass under specified conditions and can be made from organic and/or fossil resources.

• Bio-based plastics: which are materials made from biological and renewable resources such as grains, corn, potatoes, beet sugar, sugar cane or vegetable oils.

Introduction

Renewable resource can be described like: "any animal or vegetable specie which is exploited without endangering its survival and which is renewed by biological (short term) instead of geochemical (very long term) activities".[9]

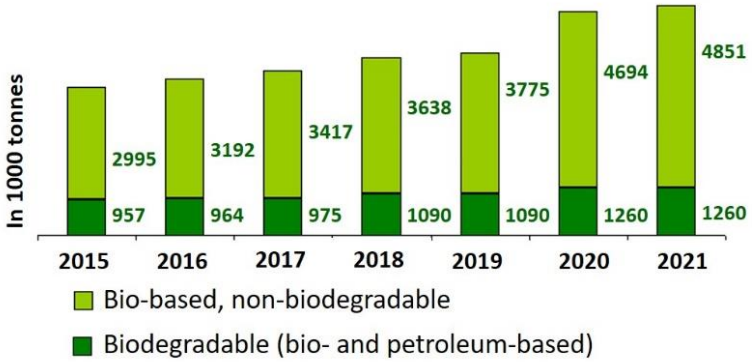

Figure 2.4 Forecast from European Bioplastics.

On the other hand, look for renewable resources in not new from 21st century, already in the 19th century renewable resources such as cellulose, vulcanised natural rubber and some vegetable oils were used. However, the interest in alternative sources fell in the 20th century due to the domination of the fossil sources. There is still one major problem usually associated with the biopolymers, it is their relatively high cost compared to their petrochemical homologues. Perhaps, the effective implementation of the biorefinery concept is the solution for the difference between prices and will make biopolymers available.[10]

Over the last decades, there is the trend in the development of polymer from renewable-based material.[9] Nowadays, there are a large quantity of materials derived from biological sources (cellulose, vegetable oils, sugars, proteins...) and other materials which microorganisms (bacterial or fungi) can convert into different monomers. Scheme 2.1 shows some examples of renewable monomers suitable for develop biopolymers.[11]

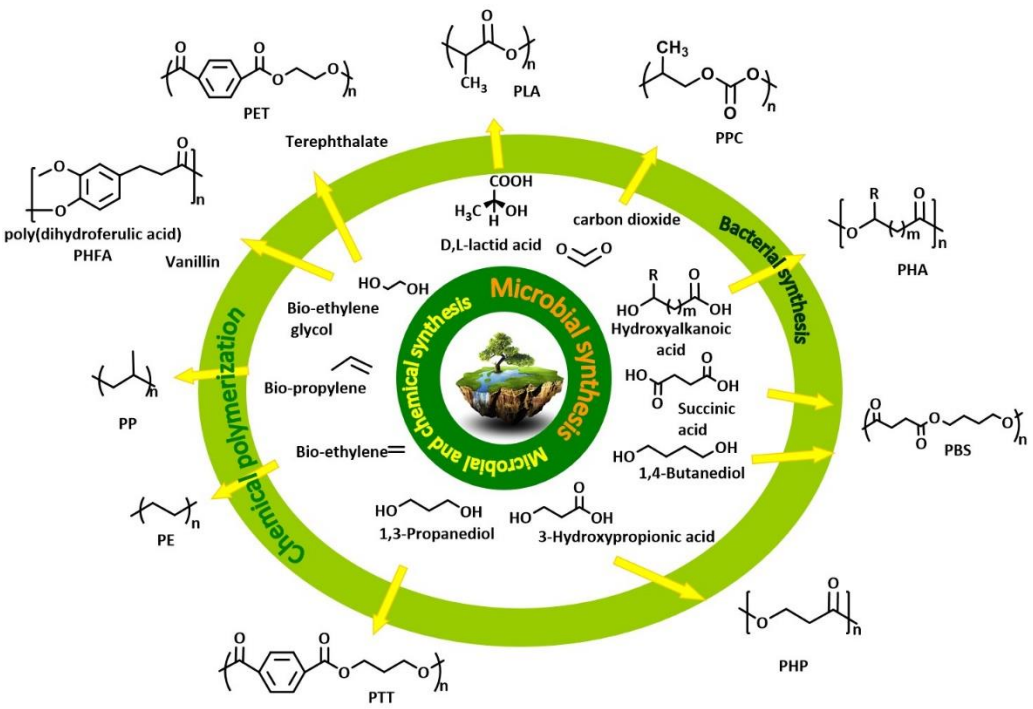

Scheme 2.1 Biomonomers and their biopolymers from renewable sources.

Development and production of polymers from renewable sources is currently a reality in some large companies. For example, The Coca-Cola Company launched its PlantBottle TM technology, they developed polyethylene terephthalate (PET) with 30 % plant-based material, in 2009. Afterwards, H. J. Heinz (ketchup producer) and Ford Motor Company used this material and Coca-Cola try to produce its PlantBottle using only renewable resources. LEGO, an important toy manufacturer, invested 135 € million in its own Sustainable Materials Centre, in 2015. Now, LEGO is using polymers from renewable resources in its building bricks. IKEA wants to manufacture all its plastic products from renewable and recycle materials (bags, toys, boxes…). Other example is Synvina, which is a joined venture company between BASF and Dutch Company Avantuim. Synvina produces the chemical building block furandicarboxylic acid (FDCA) from fructose. With FDCA it possible to develop polyethylenefuranoate (PEF) to

manufacture bottles and food packaging.[12] The mind of business is changing to have a sustainable world where we do not depend on fossil sources.

2.1.1 Vegetable oils as renewable feedstocks

Cellulose is the most abundant renewable polymer in nature because it is the main building component of our planet's vegetation, however one of the most widespread and used renewable source are vegetable oils (VOs).[13,14] VOs are considered to be one of the most important biological sources available which are alternative to fossil sources. [15,16] From 1950s decade vegetable oils are introduced into chemical industry because they are environmentally friendly, biodegradable, they have availability, low cost, high purity and low toxicity. Renewable feedstocks are replacing the use of fossil resources to make new polymers, as result of this, by green chemistry it is being developed a new polymer generation.[17,18] Vegetable oils meet with 7th point of 12 Principles of Green Chemistry which promote sustainability in chemistry.[18-20]

Vegetable oils are composed by mixtures of triglycerides. Triglycerides are three fatty acids linked to glycerol. By transesterification with monohydroxyalcohols they generate the corresponding esters and glycerol (Scheme 2.2).[17] Vegetable oils are liquids at room temperature and insoluble in water, about 95 % by weight are fatty acids.

Vegetable oils have some potential reactive sites which play an important role in its chemistry reactions and transformations. By esterification of a triglyceride, is obtained the corresponding esters and they can be reduced to alcohols. Scheme 2.2 shows esterification and reduction reactions and some examples of reactive groups, (1) reactions of the ester moiety, (2) reaction related to the methylene group directly attached to the carbonyl site of the ester moiety, (3) reaction involving the unsaturation and (4) reaction related to the allylic methylene.[21,22]

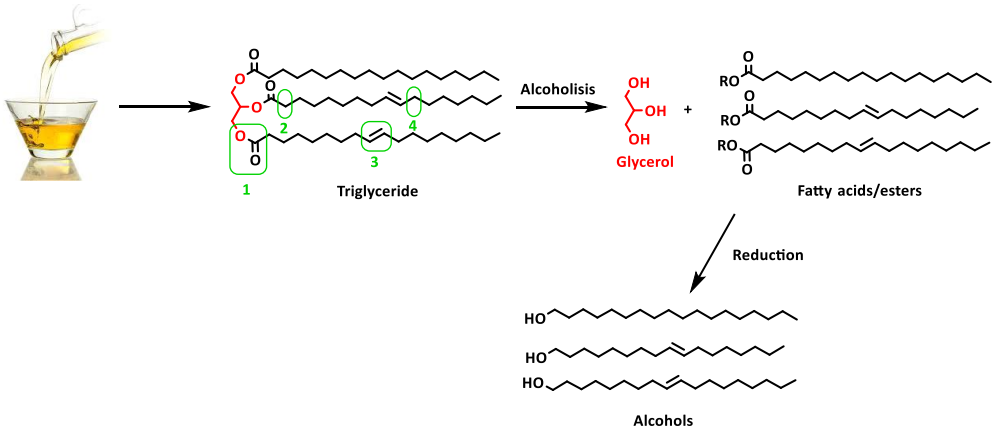

Scheme 2.2 Chemical conversion of a triglyceride from vegetable oil.

Vegetable oils have some potential reactive sites which play an important role in its chemistry reactions and transformations. By esterification of a triglyceride, are obtained the corresponding esters which can be reduced to alcohols. Scheme 2.2 shows esterification and reduction reactions and some examples of reactive groups, (1) reactions of the ester moiety, (2) reaction related to the methylene group directly attached to the carbonyl site of the ester moiety, (3) reaction involving the unsaturation and (4) reaction related to the allylic methylene.[23,24]

There are different vegetable oils naturally available and the composition of each vegetable oil is related to the natural species from where the oil is extracted. Glycerol and fatty acids are widely used in the industry. Glycerol is a versatile compound which can be converted in a wide range of products; it is very used in foods, pharmaceutical industry, cosmetics and biodiesel. [24,25]

Fatty acids can be used as starting materials to synthesize renewable oil-based monomers and polymers, with interesting hydrophobic and biodegradable properties.[26] They have a long aliphatic chain, saturated or unsaturated, with 0 to 3 double bounds per chain. Iodine value (IV) measures the average degree of unsaturations, that is the double bonds content in 100 g of oil. There are three groups of oils: drying (IV>130), semidrying (90<IV>130) or non-drying (90<IV). They have an

even number of carbon atoms, from 4 to 28 and the most common fatty acids have 14-22 number of carbon atoms.[27] Scheme 2.3 shows the most common fatty acids used as renewable feedstocks. The vegetable oils have different percentages of fatty acids according to their nature.

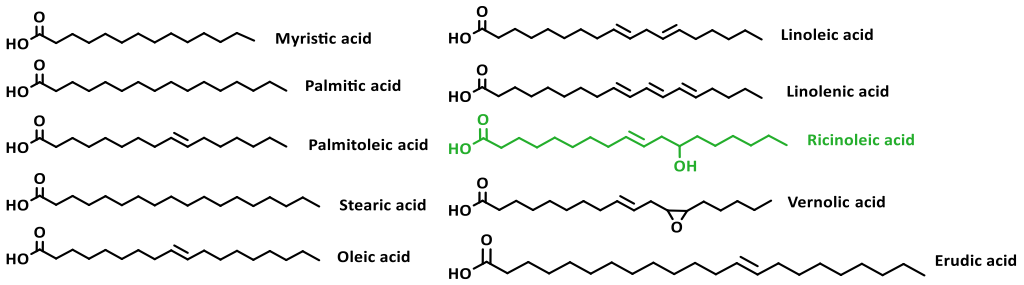

Scheme 2.3 Some fatty acids used as renewable feedstocks.

There is a large list of vegetable oils: canola, corn, linseed, olive, soybean, castor, palm, rapeseed, sunflower, however castor oil is one of the best renewable feedstocks alternative to fossil raw materials. [28,29] Castor oil is important due to biodegradability, not edible, low cost, environmentally friendly, easily extraction (50 % oil by weight), and renewability. Castor oil has carboxylic groups and unsaturations, both groups are highly reactive and modifiable, as well as the most of the fatty acids, and in addition it has a secondary hydroxyl group. Castor oil comes from castor plant and contains more than 90 % of ricinoleic acid (Table 2.1). Castor oil can be extracted from castor seeds by mechanical pressing, solvent extraction or both.

Table 2.1 Castor oil composition.

Fatty acid	Percentage (%)
Palmitic	0.8-1.1
Stearic	0.7-1.0
Oleic	2.2-3.3
Linoleic	4.1-4.7
Linolenic	0.5-0.7
Ricinoleic	>90

The castor plant (*Ricinus communis*) is from Euphorbiaceae family and it grows up in different climate (especially tropical climate). The plant is perennial, and usually is 10-12 m high. India is the largest producer (75 %), followed by China (12.5 %) and Brazil (5.5 %).[30] The production of castor plant is increasing 36 % in last decade because the chemical structure of the oil is very versatile in industry, thus decreasing its price in the market. Castor oil is non-edible because it has toxic compounds (ricine and ricinine), which are toxic proteins that inhibit some human and animal protein synthesis.

Castor oil hydrolysis easily produces ricinoleic acid which is a renewable raw material with a huge importance in chemical industry due to its three functional groups (Scheme 2.4). The polymerization of ricinoleic acid has been studied to obtain poly(ricinoleic acid) (PRA) by different polycondensation ways: acid catalysis or enzymatic catalysis. PRA has been exploited in different fields such as biomedicine and industrial preparation of polyesters, polyurethanes and polyamides.[31]

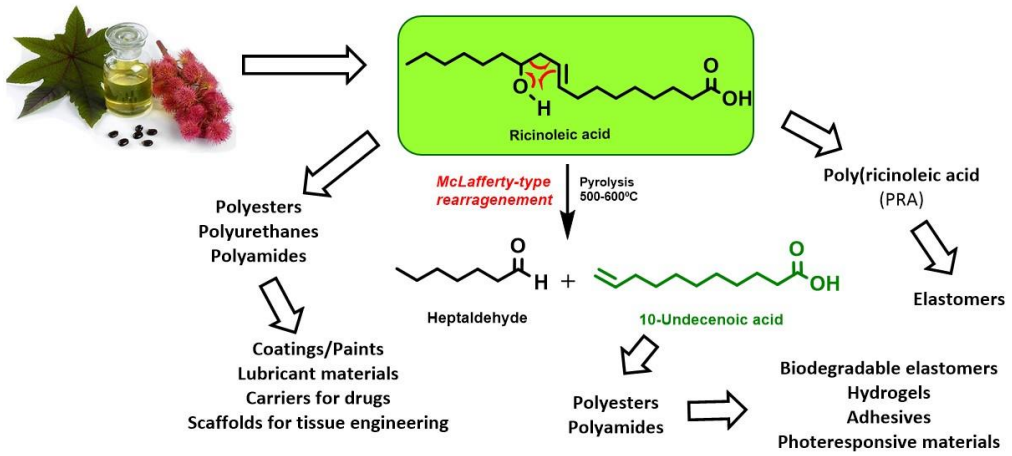

Scheme 2.4 Some potential applications from ricinoleic acid in the biopolymeric field.

Moreover, by pyrolysis under vacuum conditions, it can be obtained 10-undecenoic acid (UA) and heptaldehyde from crude castor oil or from ricinoleic acid (Scheme 2.4). Several mechanisms have been proposed to explain this pyrolysis: a McLafferty-like rearrangement in a concerted mechanism and free-radical mechanisms.[32,33] Nowadays,

Introduction

UA is a good antitumor and antibiotic precursor although the most important industry application is Nylon 11 synthesis. UA is also important in cosmetic, perfume, pharmaceutical and material applications.[34]

2.2 POLYESTERS

2.2.1 Historical overview

The polyesters are polymers which are synthesized by polycondensation process, by a wide range of reactions. The most common is the polyesterification between dihydroxyl compounds with diacids, or their derivatives by polycondensation reactions. The main chain in polyester is composed of aliphatic or aromatic moieties linked together by ester groups (R-COO-R'). Ester linkage can be easily cleaved by hydrolysis under alkaline, acid or enzymatic conditions, so that, polyesters can be biodegradable.

In the early nineteenth century General Electric Company developed resins from carboxylic polyacids and glycerol resulting in resinous compounds. This type of resins is still widely used for the production of coatings, varnishes and paints.

In 1930s Carothers synthesized for first time polyesters by the reaction between aliphatic diols and aliphatic diacids. He established the bases of step-growth polymerization through conversion, functionality and gel point studies.[35] At the begins these polyesters were not very promising because they had low melting points, they were sensitive to hydrolysis and no practical applications. These first polyesters could not compete with aliphatic polyamides or nylons, and the search for better polyesters continued, to get polyesters with higher melting points and better thermomechanical properties. In order to improve polyester properties, it was necessary to stiffen the polyester chain by using rigid aromatic monomers instead of flexible aliphatic.

In the early 1940s in United Kingdom, Calico Printers Association laboratories developed poly(ethylene terephthalate) (PET) synthesis.[36] Whinfield and Dickson, carried out the reaction between terephthalic acid and aliphatic diols, yielding high melting point fibre-forming polyesters. Nowadays, PET is one of the most produced polymers primarily for the textile and packaging applications. In Whinfield's patent is also described the synthesis of poly(butylene terephthalate) (PBT) and poly(trimethylene terephthalate) (PTT). PET, PBT and PTT (Scheme 2.5) are important in textile industry because aromatic polyesters have great mechanical properties and good heat resistance. Actually, aliphatic polyesters were the first fully characterized step-growth polymers, but they were not used in commercial applications until late 50s.

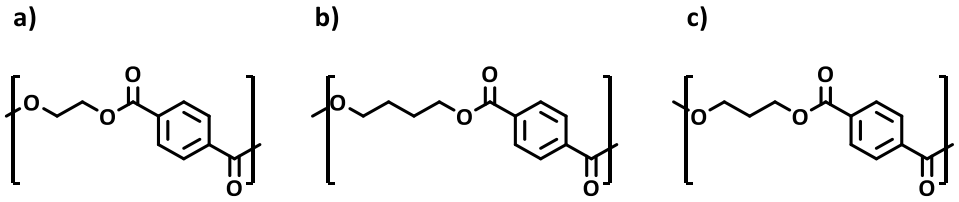

Scheme 2.5 Chemical structure of a) PET, b) PBT and c) PTT.

By the end of the 1930s, a new type of crosslinkable polyesters resins was discovered by Carothers and Flory. By the reacting mixtures of saturated and unsaturated diacids or anhydrides with aliphatic diols unsaturated polyesters were synthesized.[37]

The development of polyesters has continued until nowadays, so that polyesters become one of the most important polymers in wide variety of applications. Polyesters are present in fibres, engineering thermoplastics, resins, bottles, injection-moulding resins for UV-resistant, biomedical devices…[38]

In 1990s, environmental concerns began to be gaining ground so that, in the last decades development of polyesters focused on biodegradable and biobased polyesters. Due to the versatility of the ester linkage, able to undergo hydrolysis,

alcoholysis and acidolysis in some conditions, aliphatic polyesters are the polymers of choice to fulfil the increasing demand for recyclable and /or biodegradable polymers.[39]

Most polyesters are degraded after a few weeks or months in soils. Polyesters are hydro-biodegradables and they can be converted by microorganisms to carbon dioxide (or methane in anaerobic conditions), water and biomass. Currently there are many biodegradable polyesters type obtained from renewable resources, such as sugars, vegetable oils, organic acids, glycerol, suberin, cutin…

Biodegradable aliphatic polyesters can be used to implants for orthopaedic fixations or sutures, because polyesters are slowly degraded in the body so that a second surgical intervention is not required for implant removal after healing. Some examples of biobased aliphatic polyesters are poly(lactic acid) (PLA), poly(ε-caprolactone) (PCL), poly(trimethylene carbonate) (PTMC), poly(glycolic acid) (PGA) or their copolyesters which are used in food tray, cosmetic bottles, beverage bottles, shopping bags...[40]

Nowadays, poly (lactic acid) (PLA) is the most relevant industrial biobased aliphatic polyester. Polyesters from lactic acid have been used since 1960s in medical sutures because PLA is bioresorbable. It can be considered as a green polymer because it is biobased and degradable to CO_2 and H_2O through microorganisms forming a closed cycle (Scheme 2.6).[41]

Aromatic polyesters resist microbial attack and do not degrade under normal conditions, and they show great mechanical properties and good heat resistance. Several companies commercialize fully or partially biodegradable aromatic polyester: BASF developed Ecoflex® that is poly(butylene adipate-co-terephthalate) (PBAT) which is biodegradable by some plastic-degrading enzymes, DuPont™ developed Sorona® EP and Hytrel® RS, which are poly(trimethylene terephthalate) (PTT) and poly(tetramethylene glycol) (PBT-b-PTMG), respectively. They contain between 20 %

and 60 % renewable sourced polyether glycol derived from non-food biomass. Other example is PlantBottle™ from recyclable PET from The Coca-Cola Company.[10]

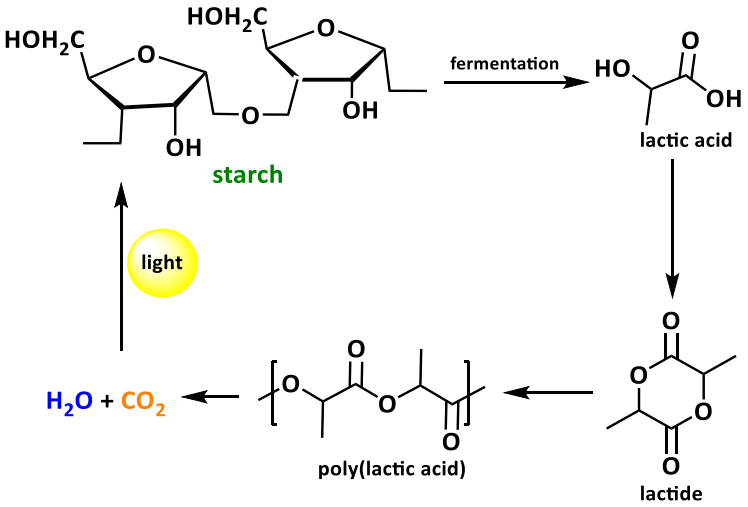

Scheme 2.6 PLA cycle.

2.2.2 Synthetic methods

Polyesters can be produced *via* several methods such as high-temperature bulk esterifications, low temperature enzyme-catalysed esterifications. Moreover, solid state is also used to restrain side reaction and thermal degradation of the products. Polycondensations can be carried out in solution, however, the use of solvents hinders applications at industrial scale.[42]

The synthesis of polyesters can be performed by polycondensation of hydroxyacids, diacids and diols or by ring opening polymerization of cyclic esters (Scheme 2.7).

These reactions are usually carried out in presence of catalyst. There are different kind of catalysts: metallics and organometallics, organics and enzymatics (lipases).

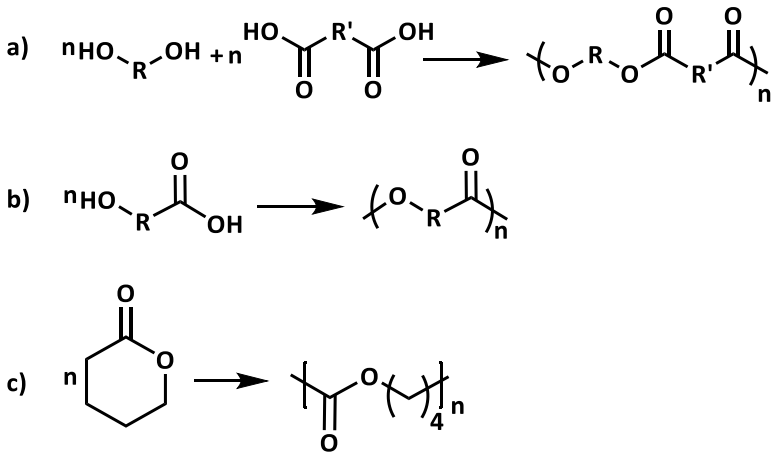

Scheme 2.7 Polyester synthesis from a) polycondensation of a diacid and a diol (AA + BB), b) polycondensation of a hydroxy acid (AB), and c) ring-opening polymerization of a lactone (ROP).

2.2.2.a Polycondensations

Polycondensation (Scheme 2.7, reaction a and b) is an equilibrium process. The synthesis of polyesters is carried out by a stoichiometric reaction between bifunctional reactants and are accompanied by the release of low molecular weight condensation products. To get high molecular weight polymers, vacuum is generally applied during last steps. So, it is possible to remove water and get conversions close to 100 %.[43]

Moreover, the synthesis of high molecular weight polyesters requires maintaining proper end-groups stoichiometry and the continuous removal of the condensate to prevent depolymerization. Side reactions may cause imbalance of reactive groups and limit the molar mass or may led to produce undesired polymer structures. Sometimes with high temperature (150-300 ºC) and bulk conditions these problems are minimized.

The synthesis of polyesters can be also carried out utilizing an AB monomer. An advantage of utilizing this AB monomer is the inherent balance of the two reactive groups in a single molecule as the absolute precision of the reactant's molar ratio is a necessary requirement to obtain polymers of sufficient molecular weight.[44]

The direct reaction between alcohol and carboxylic acid to get polyester is conducted under acid or basic catalysis conditions when the reaction is without activator, although catalyst-free conditions are more desirable. Esterification or transesterification polycondensation reactions from melt usually employ metal salts, metal oxides or metal alkoxides as catalysts, reaching high molar mass polyester, so that this kind of catalysts is widely used.[45]

When the substrates are acids-resistant, usually the reaction is carried out in presence of Brønsted acid (HCl, HBr, H_2SO_4, $NaHSO_4$, HSO_3Cl, NH_2SO_3, H_3PO_4, HBF_4, AcOH, camphorsulfonic acid…). If the acid is not high enough to trigger the reaction, an activator of acid can be added. Also, the use of Lewis acids, milder than Brønsted acids, are rapidly increasing. $BF_3{\cdot}OEt_2$, $FeCl_3$, $SnCl_2$, Sn $(Oct)_2$, $Sc(OTf)_3$, $HfCl_4{\cdot}2THF$ are some of the most important Lewis acids catalysts.

Other usual catalysts in polyesterification are organic catalysts, such as diclyclohexylcarbodiimide (DCC) or N-(3-dimethylamino-propyl)-N'-ethylcarbodiimide hydrochloride (DECH). The use of DCC as a promoter in polyesterifications, represents one of the most versatile polymerization and post-modification methods. The reactions usually proceed at room temperature and the reactions conditions are so mild that substrates with various functional groups can be employed. As such, a wide range of applications have been achieved in the fields of natural products, peptides, nucleotides, etc… The applications of the DCC methods in pure organic synthesis dates back to 1967.

In addition to the metallic and organic catalysts, enzymatic catalysts are frequently used in polyesterification. Enzymes are non-toxic, recyclable and eco-friendly biocatalysts… They can be easily removed from the reaction and play an important role in polyesterification technology.

Introduction

Hydrolase enzymes can performance polymerizations of various sugar and natural monomers *in vitro* with bond-formation to made polyesters (polysaccharides). So, enzymes catalyse the reaction in a reverse direction *in vitro* to *in vivo* (Figure 2.5).

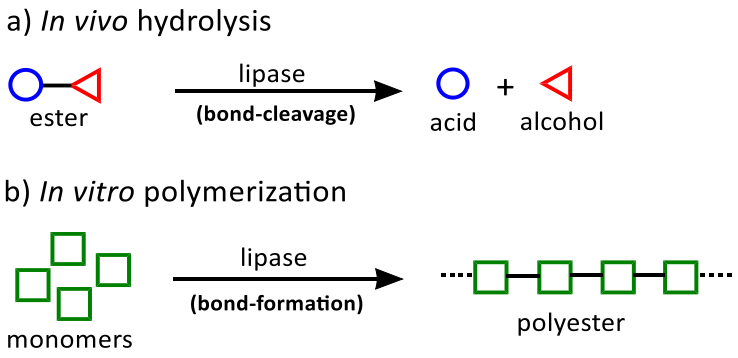

Figure 2.5. A model expression of lipase-catalysed reactions: a) in vivo hydrolysis and b) in vitro polymerization of monomers to procedure a polyester molecule.

In the three last decades, a lot of polyesters were synthesized by enzymes; the most used for *in vitro* polyesterifications are in the next table (Table 2.2).[46]

Table 2.2 Origen of enzymes used for in vitro polyesterification and their abbreviations.

Enzyme origin	abbreviation
Candida cylindracea	lipase CC
Pseudomonas fluorescens	lipase PF
porcine pancreas lipase	PPL
Aspergillus niger	lipase A
Candida rugosa	Lipase CR
Penicillium roqueforti	lipase PR
Pseudomonas cepacia	lipase PC
Rhizopus japonicus	lipase RJ
Rhizomucor meihei	lipase RM
Mucor meihei	lipase MM
Candida antarctica	lipase CA
Candida antarctica lipase B	CALB (Novozym 435)[a]
Yarrowia lipolytica	lipase YL

[a]CALB immobilized on an acrylic resin is commercially called as Novozym 435.

In order to improve its efficiency, enzymes are immobilized as cross-linked enzyme aggregates, call them CLEAs (cross-linked enzyme aggregates).[47] The CLEA technology is a simple and effective way of immobilizing enzymes that offer several advantages when compared to the corresponding free enzymes, such as increased thermal stability, facile recovery and reuse, and high productivities as compared to carrier-bound enzymes. Some of materials which are used to immobilized are celite or acrylic resin.[48]

Lipases are nature proteins so that polyesterifications are carried out in mild conditions, below 100 °C (20-90 °C) and low or not pressure. Solvent hydrophobicity plays an important role in enzymatic activity, particularly for lipases which normally act at oil-water interfaces in living cells. The best reactivity is found for hydrophobic solvents such as hexane, toluene, diisopropylether or diphenylether. Hydrophilic polar solvents such as DMSO or methanol lead to significant modifications in enzyme conformation and, therefore, to a dramatic decrease in catalytic activity. Water, supercritical carbon dioxide and ionic liquid are also used as solvents, although the use of water is more limited because of monomer and polymer solubility and the unfavourable equilibrium.[49]

Nowadays, *Candida antarctica* lipase B (CALB) is the most used lipase in organic synthesis. In 1994 Uppenberg research group described the amino acid and genic sequence of CALB which consists of 317 amino acid residues giving molar mass 33 $kg \cdot mol^{-1}$.[50] Its active site is composed of a nucleophilic serine residue activated by a hydrogen bond in relay with histidine and aspartate or glutamate, and the binding site is directly exposed to the solvent.[51,52] When the CALB is immobilized is more effective catalytically, it is possible to remove it from reaction mixture and reuse it even up to ten times. Furthermore, CALB immobilized in poly(methylmethacrylate) resin (PMMA, Lewatit VP OC 1600, Bayer), it knows as Novozym 435, is stable until 100 °C, and its optimal conditions are pH 5-9 and 90 °C.[53-56]

2.2.2.b Ring opening polymerization

Ring-opening polymerization (ROP) is used with a large number of cyclic monomers to prepare degradable aliphatic polyesters, using organometallic catalysts, enzyme catalysts (eROP) and organic catalyst (nucleophilic ROP and metal-free ionic ROP).[57] The most used cyclic monomers are cyclic esters such as lactones and lactides, although others cyclic monomers are also used (Scheme 2.8). Polycaprolactone (PCL), polylactic acid (PLA), poly(glycolic acid) (PGA) and their copolymers are usually synthesized by ROP, being PCL the most studied.[58]

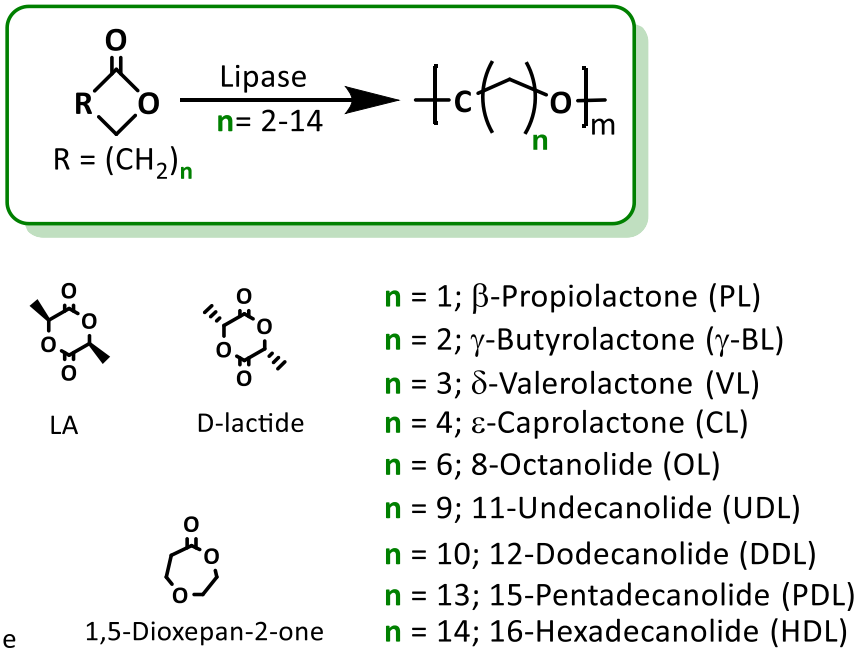

Scheme 2.8 eROP by lipase catalysts of lactones and lactides.

The thermodynamic polymerizability of lactones is strongly related to ring size, and some computational studies show that ring strain is highest for β-propiolactone (4-membered ring) and much lower for γ-butyrolactone (5-membered ring) and δ-valerolactone (6-membered ring).[59,60]

Some cyclic monomers were polymerized using metal salts, organometallic and organic catalysts such as zinc complexes, Tin (II) chloride, stannous octoate or 1,5,7-Triazabicyclo[4.4.0]dec-5-ene (TBD).[61-63] More recently, in order to decrease the toxicity to be used as biomaterials, a large number of cyclic monomers have been polymerized by enzyme catalysts and definitively, CALB is the most used enzyme in ROP.[64-70] In order to start the propagation of the polymer chain, an initiator such as water, aliphatic alcohol or primary amine, is added to CALB.

In vitro enzyme-catalysed ROP in non-aqueous medium has been also extensively studied.[67] Scheme 2.9 shows the mechanism of enzyme-catalysed ROP with CL as substrate. The active site of a lipase comprises a triad consisting of serine, histidine and aspartate. The ester moiety of CL undergoes a nucleophilic attack from the primary alcohol group of serine in the enzyme's active site. *Via* the enzyme intermediate species, the original alkoxy group is released, forming the so-called enzyme-activated monomer (EAM) species. Subsequently, a nucleophile R_1-OH can attack these EAM-species releasing the final product and thereby regenerating the enzyme. In the propagation step, the EAM is nucleophilically attacked by the terminal hydroxy group with a growing polymer moiety extending the polymer chain by one more monomer unit. Thus, the polymerization proceeds *via* an activated monomer mechanism, and the rate determining step of the overall polymerization is the formation of the EAM.[68]

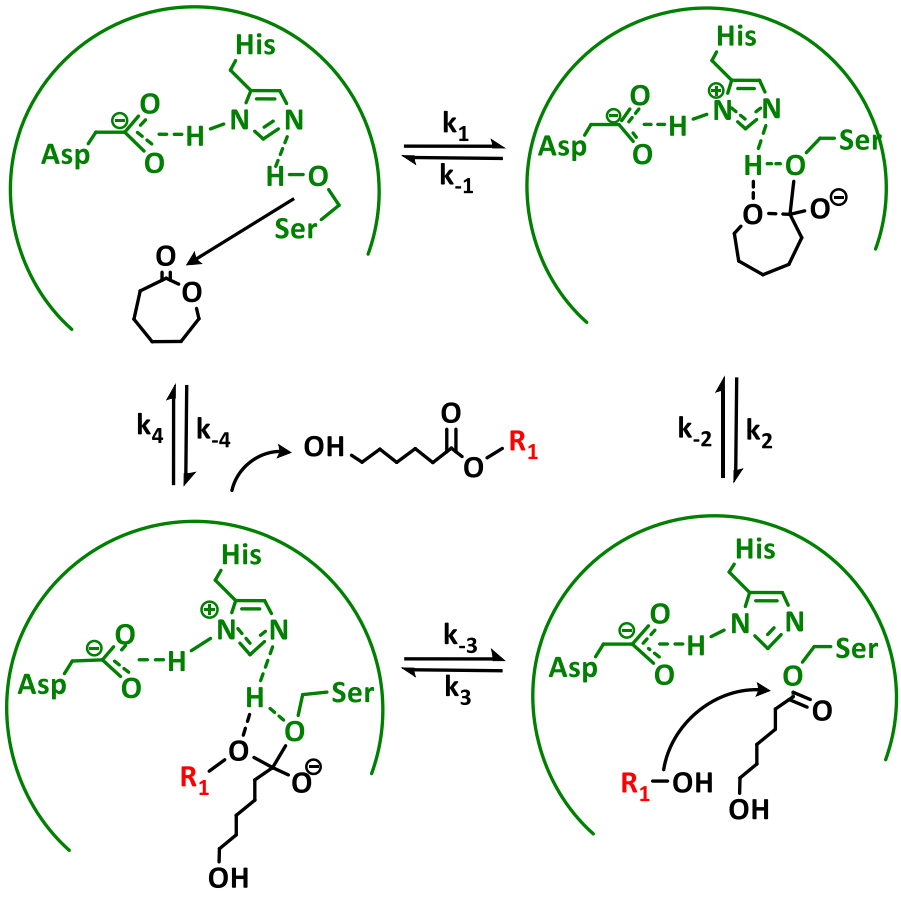

Scheme 2.9 Mechanism of enzyme-catalysed ring opening polymerization of ε-caprolactone.

2.2.3 Polyesters from vegetable oil-derivatives

Vegetable oils and their corresponding fatty acids are some of the most promising raw materials for polymeric synthesis and constitute an interesting source to obtain aliphatic polyesters.

Castor oil has attracted much attention to polyester synthesis because the 85-95 % of its composition is ricinoleic acid (RA) (12-hydroxy-cis-9-octadecenoic acid). RA has an

unsaturation in carbon 9 (fatty acid ω9), a secondary hydroxyl in carbon 12 and a carboxyl group. Moreover, it can be obtained in large quantities from agricultural crops and it is considered as not edible. RA is highly valued as raw material for polymer synthesis.[69-71]

In 1986, Matsumura et al. obtained polyricinolate (M_n 600-1307 g·mol^{-1}) by enzymatic dehydration-polycondensation using *Candida rugosa* lipase or *Chromobacterium viscosum* lipase of RA from castor oil under mild conditions (35 °C).

Moreover, copolymers from RA and other monomers have also been described, for example, Slivniak and Domb, in 2005, synthetized copolymers from RA and lactic acid (LA) by direct polycondensation and transesterification with different RA:LA ratios. The obtained polyesters by direct polycondensation had 2-8 kg·mol^{-1} whereas the polyesters obtained by transesterification reached 6-14 kg·mol^{-1}, both were liquid at room temperature and they found applications in the biomedical field (Scheme 2.10).[69]

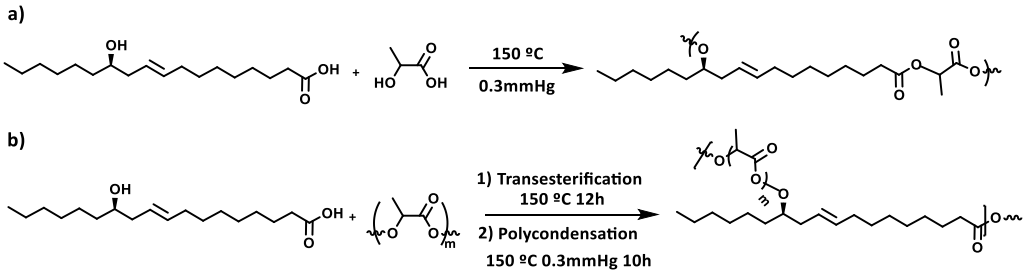

Scheme 2.10 Poly(RA-LA) synthesis by a) random condensation of LA and RA acids or b) transesterification with PLA and further RA polycondensation.

Afterwards, in 2007 Ebata et al. obtained also polyricinolate (PRA) (M_n 2.1-73.2 kg·mol^{-1}) from methyl ricinolate (MR) with *Pseudomonas cepacia* immobilized on ceramics (IM-PC) as catalyst which was further crosslinked to produce thermosetting elastomers. Furthermore, it has been also demonstrated that PRA can be easily recycled by enzymatic hydrolysis followed by repolymerization (Scheme 2.11). The result of this

study showed a notable catalyst activity for RA polymerization although lipases are known to have low reactivity for the esterification of secondary hydroxyl groups.[72,73]

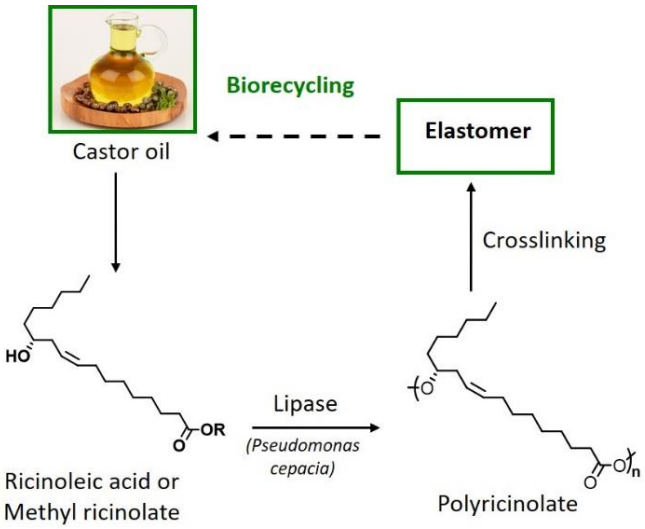

Scheme 2.11 Lipase-catalysed preparation and curing of polyricinolate.

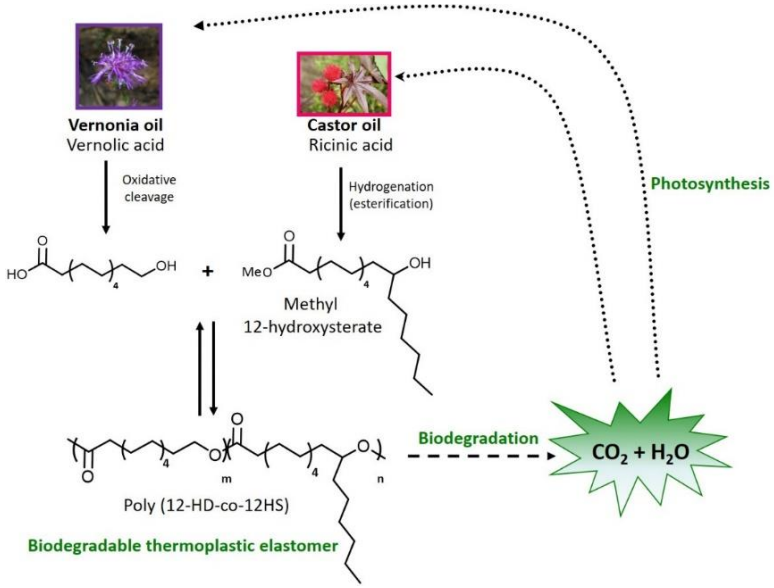

Scheme 2.12 Copolymerization of 12-hydroxydodecanoic acid and methyl 12-hydroxystearate by IM-CA and recyclability.

Polycondensation of hydroxyl groups in internal positions led to polyesters with alkyl dangling chains which serve as internal plasticizer. In this way, in 2008, Ebata et al. prepared thermoplastic polyesters by polycondensation of 12-hydroxydodecanoic acid and methyl 12-hydroxystearate using *Candida Antarctica* lipase. Both monomers were obtained from vernolic acid and hydrogenated methyl ricinoleate respectively (Scheme 2.12). These polymers are a novel green and sustainable elastomers having both good biodegradability and chemical recyclability properties.[74]

In 2010, Petrović et al. obtained a castor oil-derived linear polyester with high molecular weight (62 kg·mol^{-1}). Starting from castor oil, after ozonolysis followed by reduction and transesterification they obtained 9-hydroxynonanoic acid (Scheme 2.13). The polymer was synthesized in the presence of Ti(IV) isopropoxide by bulk esterification. This polyester is potentially biodegradable with interesting applications in industry as substitute for PCL, because it has higher melting point (70 °C) and glass transition temperature (-31 °C).[75]

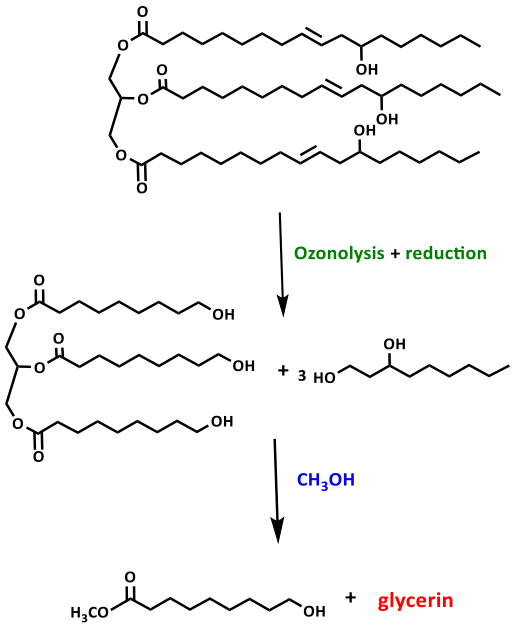

Scheme 2.13 Preparation of methyl 9-hydroxynonanoate from castor oil.

Also, in 2010 Quinzler et al. reported a semicrystalline polyester with long-chain hydrocarbon segments by combining oleic acid and erucic acids, which have C_{18} and C_{22} length. Oleic acid is the major fatty acid in plants such as sunflowers or olive trees and erucic acid is readily available from rape seed oil (Scheme 2.14).[76]

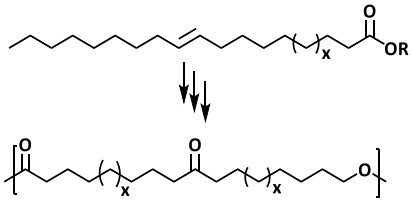

Scheme 2.14 Long-chain linear polyester synthesis (x=1: oleic acid or x=5: erucic acid).

In the same year, methyl 10-undecenoate was used to prepare α,ω-bifunctional fatty acids. Türünç et al. used thiol-ene additions to methyl 10-undecenoate to synthesize renewable monomers and polymers (Scheme 2.15).[77]

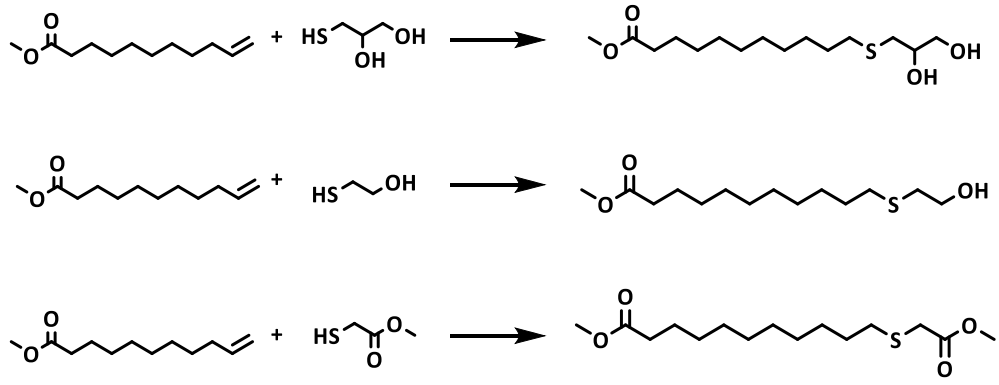

Scheme 2.15 Some renewable monomers from castor oil-derived methyl 10-undecenoate.

Polyesters from polyesterification of aliphatic α,ω-dicarboxylic acid (α,ω-diacids) with diols are widely used for engineered plastics, adhesives, lubricants… The majority of α,ω-dicarboxylic acid come from non-renewable petrochemical feedstocks. However, Gross et al. (2010) synthesized polyesters from diacids with diols from vegetable oils by microorganisms as catalysts (Scheme 2.16). It is well-known that many microorganisms such as *Candida tropicalis*, *Candida cloaca*, *Cryptococcus neoforman* and

Corynebacterium sp can convert n-alkanes and fatty acids to their corresponding α,ω-dicarboxylic acid. For example, *Candida tropicalis* (*C. tropicalis*) can hydroxylate the terminal methyl group by *cytochrome P450 monooxygenase* that is further transformed *via* the addition of *fatty alcohol oxygenase* and *aldehyde dehydrogenase* to form the corresponding diacids (Scheme 2.16 a). Moreover, CALB (*Candida antarctica* lipase B) can epoxidize double bounds to convert unsaturated dicarboxylic fatty acids to epoxidized monomers for preparing functional polyesters (Scheme 2.16 b). These linear and epoxidized polyesters have high molecular weight (25-57 kg·mol^{-1}) with low melting points (23-40 °C).[78]

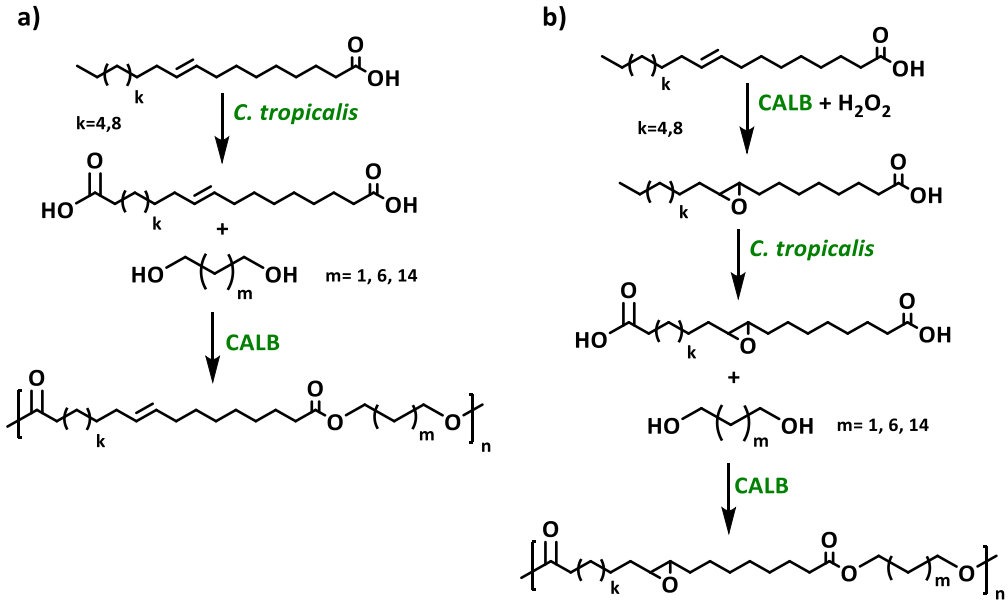

Scheme 2.16 Lipase-catalysed polycondensation of unsaturated a) dicarboxylic acids and diols and b) epoxidized dicarboxylic acid and diols.

In 2011, Matsumura focused on the preparation of biodegradable and biobased thermoplastic elastomers from macrolides (dodecanolide, pentadecanolide and hexadecanolide) as hard segment and methyl 12-hydroxystearate as soft segment, by lipase catalysed copolymerization.[79] Moreover, α,ω-hydroxy-terminated poly(ricinoleic

acid) was used as macroinitiator for the ring opening polymerization of LA.[80] A series of triblock copolymers with composition ranging from 35-83 % of PLA was prepared. The fatty acid-derived aliphatic polyesters are highly hydrophobic and have functional groups prone for further modification. Reactions to induce branching, grafting or crosslinking as well as functionalization with macromolecules are well known strategies for improving thermomechanical, chemical and biological properties.

Also, Vilela et al. prepared long-chain polyesters using erucic acid by self-metathesis to synthesize dicarboxylic monomers. This renewable aliphatic polyester was proposed for replacing PE or other polyolefins (Scheme 2.17).[81]

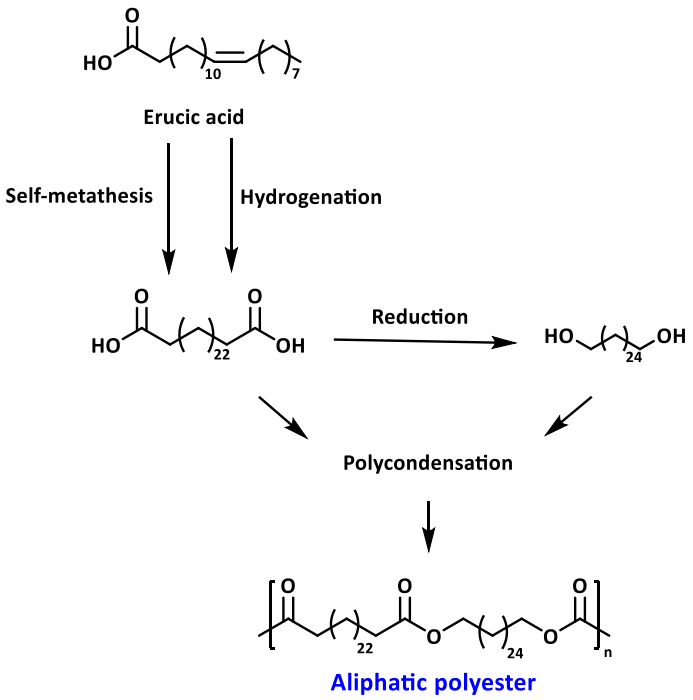

Scheme 2.17 Renewable aliphatic polyesters from erucic acid.

Aliphatic polyesters are one of materials that can potentially meet the varying requirements required for tissue scaffolds: synthesis simplicity, use of low cost and non-toxic monomers and ease control of the properties of the obtained materials.

2.3 FUNCTIONAL POLYESTERS: HYDROXYPOLYESTERS

Functional polyesters are biodegradable polymers with the ability to modulate their physico-chemical characteristics such as hydrophilicity and degradation rate through the introduction of additional functional groups, making thus suitable materials for many applications.[82] Among all biodegradable polymers, aliphatic polyesters are used in the medical field as bone screws, tissue engineering scaffolds, sutures and drug delivery systems. These aliphatic polyesters generally can be degraded by hydrolysis of main chain ester bonds and the time/rate of degradation depends on the polymer characteristics (hydrophobicity, crystallinity…) and the introduction of additional functional groups can improve their degradation behaviour. Biodegradable polyesters can be completely degraded in landfills, composters or sewage treatment plants by the action of naturally occurring microorganisms. Truly biodegradable plastics leave no toxic, visible or distinguishable residues following degradation. There are so many studies reported to improve the properties of aliphatic polyesters in order to gain sustainability.[83-85]

One of the different methods to synthesize functional polyesters is the post-polymerization functionalization. The main drawback of this method is the competence of side reactions so post-polymerization functionalization is not the preferred route of choice to obtain functional polyesters. Another way to synthesize functional polyesters is the homopolymerization of functional (protected) monomers or its copolymerization with commercially available non-functionalized monomers. As monomers have to be protected to allow polymerization and avoid side reactions an additional deprotection step is always mandatory.[86]

The ROP of lactones or different ring sizes, with or without protected functional groups constitutes another approach to functional polyesters and has extensively been

explored in the case of ε-CL derivatives.[87, 88] The enzymatic polymerization using lipases is very selective and thus protection/deprotection steps are not necessary.[89]

Recently, bio-based triblock copolyesters with free hydroxy groups were synthesized by Muñoz-Guerra et al. by ROP of L-lactide in solution using hydroxyl-ended polytartrate as di-functional macroinitiator.[90]

Industrially, the most common route to prepare polyesters is the step-growth polymerization of diacids or diesters with diols. This method is energy-intensive because it is necessary to remove small byproduct molecules such as water or alcohol and high temperatures are necessary to reach high molecular weights.

The polycondensation of hydroxyl-containing dicarboxylic acids under certain conditions allow preparing hydroxy functionalized polyesters. These aliphatic hydroxypolyesters easily degrade under physiologic conditions allowing to be used in medical devices. Moreover, the presence of *vic*-diols conferes antibacterial and antifungal properties as demonstrated in *in vitro* and clinical studies, in addition to enhanced biocompatibility.[91-94]

In 2005, poly(butylene tartrate) (PBT) was developed (Scheme 2.18). This biodegradable and biocompatible polyester has been studied as steroid-type anti-inflammatory drug carrier.

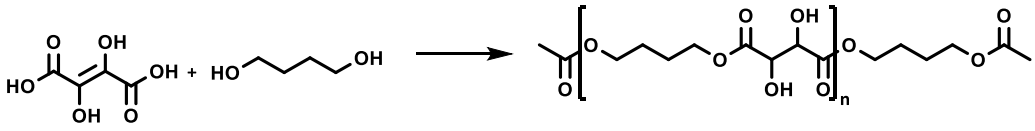

Scheme 2.18 Synthetic pathway for the preparation of PBT.

Poly(1,8-octanediol-co-citrate) (POC) has been reported in 2011. POC is biodegradable hydroxypolyester compatible with vascular cells, subcutaneous tissues and bone cells. Moreover, POC has antibacterial properties having important engineering and

biomedical applications (Scheme 2.19).[95,96] Actually, three-dimensional POC has been used as scaffold with different pore shapes and permeabilities on chondrogenesis using primary chondrocytes *in vivo*.[97]

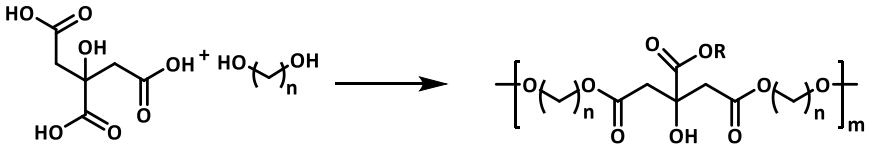

Scheme 2.19 Chemical reaction of POC synthesis.

Besides the examples commented before, the synthesis of linear polyesters having pendent hydroxyl groups is generally difficult requiring of multistep reactions including tedious protection and deprotection of the hydroxyl groups in the repeating units, which often engender degradation of the polymer backbone. The synthesis of poly(sebacoyl diglyceride) (PSeD) and poly(butylene succinate-co-butylene malate) have been reported through a simple protection and deprotection strategy, however sometimes, undesirable degradation and gelation occurred during deprotection step (Scheme 2.20 a). Using a similar protection-deprotection strategy hydroxypolyesters derived from malic and succinic acids have also been described and used for post-polymerization modification with biomolecules (Scheme 2.20 b).[98,99]

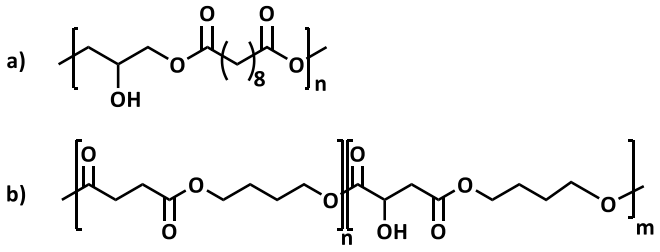

Scheme 2.20 Functionalizable hydroxypolyestres. a) poly(sebacoyl diglyceride) (PSeD). b) poly(butylene succinate-co-butylene malate).

Hydroxypolyesters can be also obtained by reaction of carboxylic acid with epoxide groups. This methodology has been extensively described for crosslinking oxirane

resins with dicarboxylic acids and/or dicarboxylic anhydrides. The reaction of epoxy groups with carboxylic and anhydride groups have a huge economic importance in the coating and polymer industry. However, these approaches can be used to produce linear hydroxypolyesters by reaction of epoxidized fatty acids.[100] Oxirane ring can be easily introduced in unsaturated fatty acids by selective oxidation of double bonds. Although a great number of epoxidation procedures have been described, most of them use metallic oxidizing reagents or catalysts. As green and environmentally friendly alternative, enzymatic methodologies through *in situ* formed peroxy acids using CALB and hydrogen peroxide have been extensively described (Scheme 2.21).[101-103]

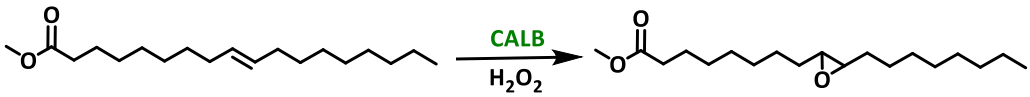

Scheme 2.21 Epoxidation of methyl oleate acid with CALB and hydrogen peroxide.

The reaction between carboxyl groups and oxirane rings and can be catalysed by a wide range of catalyst such as amines, ammonium and phosphonium salts, polyoxometalates, organic and phosphazene bases and enzymes. The reaction has also been described to proceed when acid halides instead of carboxylic acids are used.[104-107]

Rhodococcus sp. NCIMB 11216, *Candida rugose*, *porcine pancreatic* lipase, *Pseudomonas* sp, CALB and some others lipases have been described to polymerize oxirane rings with carboxylic derivatives (dicarboxylic anhydrides).[108] Moreover, some ionic liquids have been used as catalyst in the reaction of oxirane ring-opening with carboxylic acids ([bmim]Cl, [bmim]Br, [hmim]Br…), avoiding the use of toxic solvents and harsh conditions.[109]

Carboxylic acid oxirane ring opening reaction can be also catalysed with active hydrogen compounds such as phenols or acids. The carboxylic acid ring opening condensations have the additional advantage of not producing volatile by-products.

The reaction between epoxy and carboxyl groups (nucleophilic group) can proceed leading two different hydroxy esters, depending on the nucleophilic attack of the carboxylic acid occurs on the less substituted position of the oxirane ring, usually named normal ring opening, or in the more substituted position, usually named abnormal ring opening (Scheme 2.22 a).

As a consequence of the two reaction pathways, the resulting product from the normal ring opening is a primary ester with a secondary hydroxyl group and the resulting product from the abnormal ring opening is a secondary ester with a primary hydroxyl group (Scheme 2.22 a). However, the reaction does not necessary stop here, as the resulting hydroxyesters can be further esterified by the carboxylic acid to lead a diester and water as byproduct (Scheme 2.22 b). Water and the hydroxyl compounds mixture can also react with epoxy groups producing new hydroxylic compounds having ether linkages (Scheme 2.22 c).

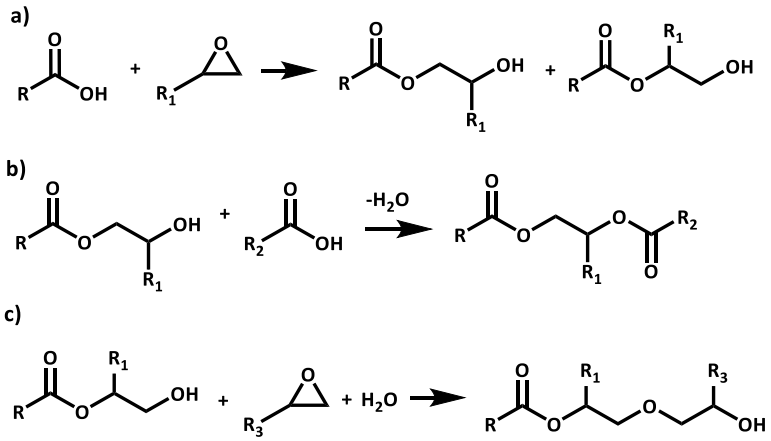

Scheme 2.22 Possible reaction products on the oxirane ring-opening by carboxylic acids.

Epoxide ring opening by carboxylic acids can be catalysed by cationic and anionic catalysts. Anionic catalysts, usually metallic or organic bases, act producing more nucleophilic carboxylate anions that attack preferentially on the less substituted carbon of the oxirane ring following a S_N2 mechanism (Scheme 2.23 a). The activity of different

bases was found to decrease in the following order: pyridine > isoquinoline > quinoline > N,N-dimethylcyclohexylamine > tributylamine > N-ethylmorpholine > dimethylamine > potassium hydroxide.[110]

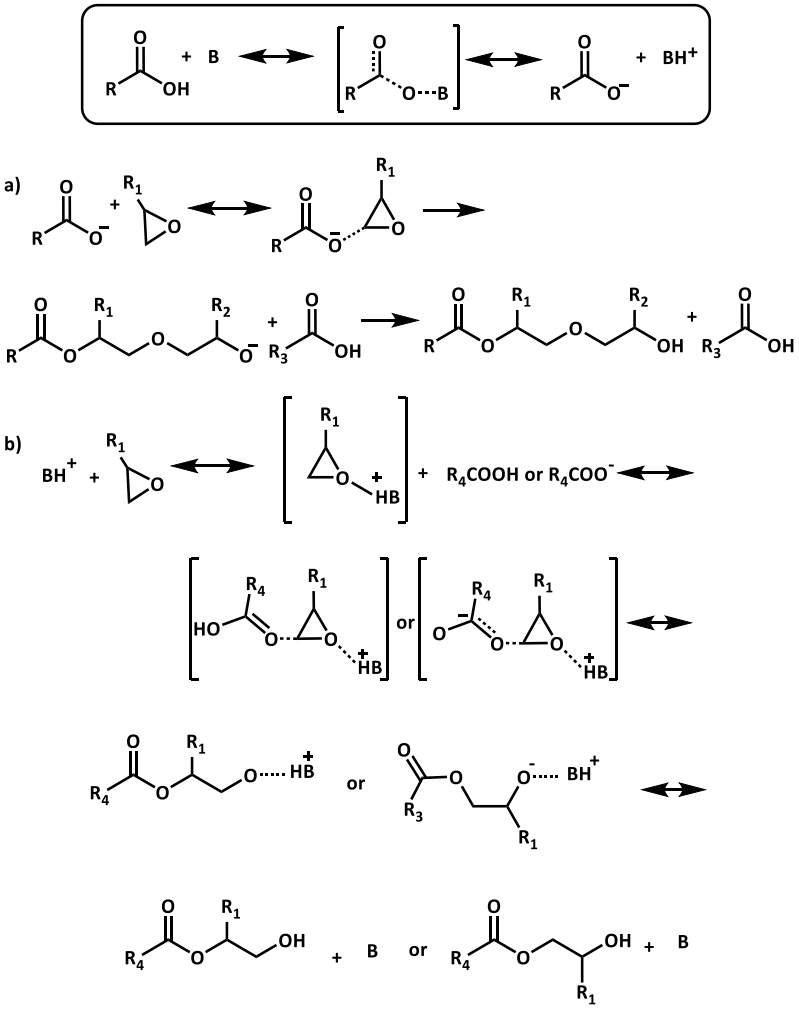

Scheme 2.23 Anionic and cationic catalysed oxirane ring-opening by carboxylic acids.

Cationic catalysts, usually protic or Lewis acid, activate oxirane ring opening by coordinating to the oxygen of the oxirane ring increasing the electrophilic character of the oxirane carbons (Scheme 2.23 b). Inorganic salts from Al, B, Be, Fe (III), Sn, Ti, Zr

and Zn halides are frequently used as active catalysts, being the boron trifluoride (BF_3) the most extensively used cationic catalyst (Scheme 2.24).

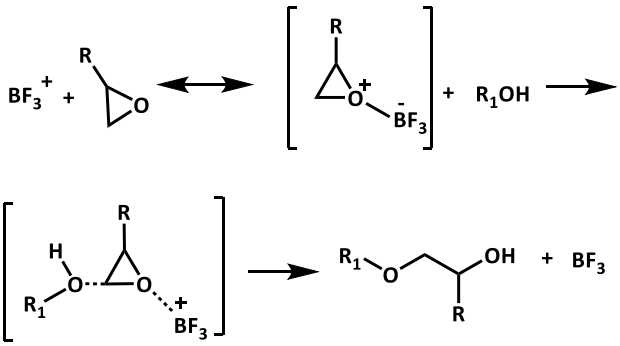

Scheme 2.24 Oxirane ring opening catalysed by boron trifluoride.

Metal alkoxides, metal chelates, dionate complexes, metal oxides and in general bidentate metallic compounds typically follow a more complex ring opening mechanism that combines both of the characteristics of the anionic and cationic ones. This named coordinative mechanism involves the coordination of the epoxy and carboxylic groups to two different metallic centres close to each other producing the activation of both the oxirane ring and the carboxylic nucleophile (Scheme 2.25).[111]

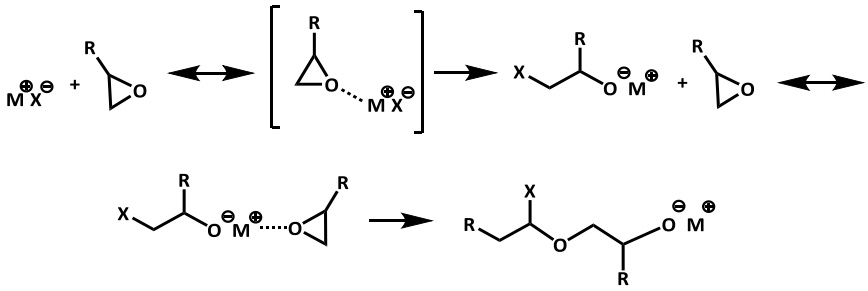

Scheme 2.25 Coordinative oxirane ring opening with metal oxides, alkoxides and derivatives.

The aliphatic hydroxypolyesters obtained by ROP with carboxylic acids or carboxylic acids derivatives have similar properties than the parent aliphatic polyesters described previously. These aliphatic hydroxypolyesters usually show enhanced biodegradability

which is mandatory in most biomedical engineering applications. So, many authors have described the synthesis of hydroxypolyesters by cationic ROP for uses in biomedical fields. Scheme 2.26 shows the preparation of hydroxypolyesters by reaction of sebacic acid with diglycidyl sebacate using bis(tetrabutylammonium) sebacate (TBAS) as catalyst.[112,113]

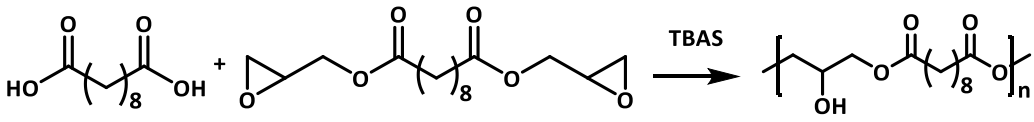

Scheme 2.26 ROP of diglycidyl sebacate with sebacic acid.

Oxirane-carboxylic acid ROP can also be carried out using AB monomers, for example White et al. synthetized a polyester from 10,11-epoxyundecanoic acid with phosphonium and ammonium salts (Scheme 2.27).[114] And some authors have described the use of the resulting hydroxypolyester as macroinitiator for RAFT polymerizations.[115]

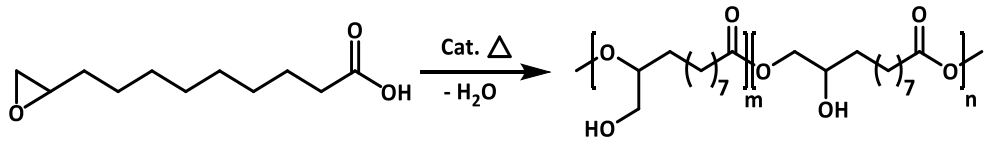

Scheme 2.27 Oxirane-carboxylic acid ROP using an AB monomer.

According these precedents, the reaction between oxirane and carboxyl groups constitute a straightforward way to produce polyesters with reactive pendant hydroxyl groups. The availability of new hydroxylated aliphatic polyesters can play an important role in biotechnological fields, such as release systems for pharmaceutical drugs and diagnostic systems.[116] Some biotechnology labile products (such as proteins, peptides, biomolecules…) are supported on polyesters for treatments of patients suffering from different chronic and life-threatening, because these scaffold polyesters are biodegradable, biocompatible and non-toxic. So that, functional biodegradable

polyesters with hydrophilic reactive pendant groups such as hydroxyl, carboxyl and amino have become attractive biomaterials because they have tuneable biodegradability and they can be applied in novel biotech fields (Figure 2.6).[117]

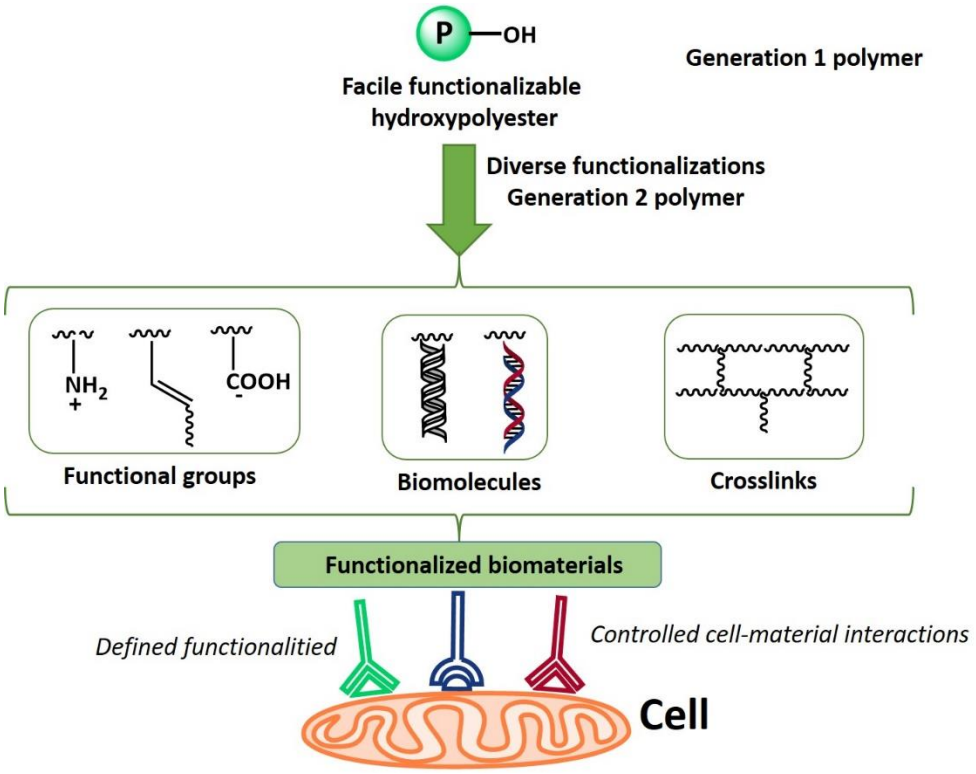

Figure 2.6 Schematic simple synthetic platform to novel biomaterials with a wide range of functionalities that can offer fine control of cell-material interactions.

Linear aliphatic polyester with lateral hydroxyl groups could offer additional benefits such as: tuning of the hydrophilic-hydrophobic imbalance resulting in a variety of self-assembled macromolecular structures like cylinder or core-shell shaped morphologies, also a further living/controlled ring opening polymerization of reactive cyclic monomers grafted onto the reactive hydroxyl sites to construct functional brush- or comb-like macromolecular architectures through controlling the graft density and length.[118]

Introduction

In the last decade several hydroxypolyester-based drug release systems have been developed to supplant the oral administration. Microspheres of functionalized hydoxypolyester are injected and the encapsulated drugs are released over a predetermined time. Some examples are poly(HMMG-L) and poly(HMG-CL) (Scheme 2.28).[119]

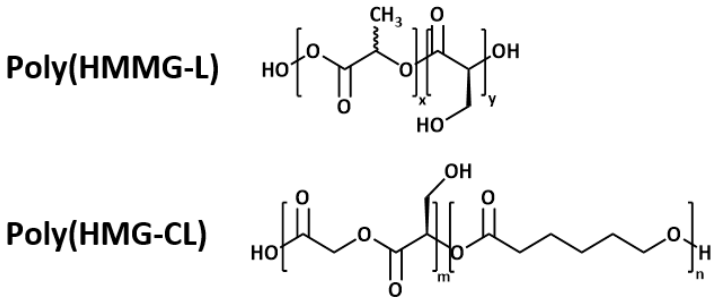

Scheme 2.28 Hydroxypolyesters used in microsphere encapsulation systems.

Some functional hydroxypolyesters have been used as bioadhesives or mucoadhesives. The concepts have been introduced into the pharmaceutical field from 1980s. These polymers are able to increase the epithelial permeability for many drugs by intensifying contact to the mucosa through the formation of covalent linkages (such as disulphide bonds) or weak interaction. Moreover, this kind of polymers allows the persistence of orally administered drugs by avoiding their enzymatic degradation.

Superior mucoadhesive polymers have been developed from natural and synthetic hydroxyl containing polymers, including hydroxypolyesters as a promising tool in therapy and drug delivery (Figure 2.7). Cysteine is usually linked covalently to the polymer giving the called thiolated polymers or thiomers that were first described by Andreas Bernkop-Schnürch et al in 1999.[120] It has been demonstrated that thiomers exhibit mucoadhesive properties, permeation enhancement, controlled release as well as enzyme and efflux pump inhibitory properties because of the formation of

disulphide bonds between thiol bearing side chains of the polymer and cysteine-rich subdomains of mucus glycoproteins (mucins).[121-126]

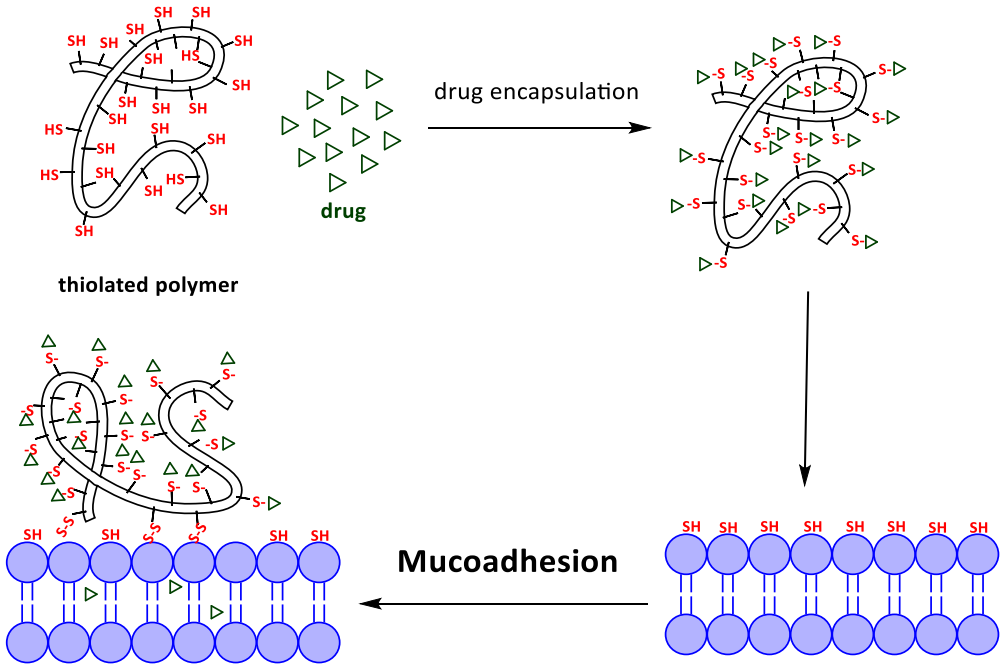

Figure 2.7 Mechanism of action of thiomers: drug encapsulation via disulphide formation and precise drug release with covalent binding between thiomer and mucin.

2.4 POLYMERIC MICELLES

Amphiphilic polymers are macromolecules which have a polar or hydrophilic moiety and a nonpolar or hydrophobic moiety in the same structure. One of the main properties of amphiphilic polymers is the formation of molecular nanostructures by auto self-assembly under the appropriate conditions (temperature, solvent, concentration, etc). When they are exposed to a solvent can develop different complex macromolecular structures such as monomolecular layers, vesicles and micelles. In a hydrophilic solvent, the polar chain orients itself towards the solvent, while the hydrophobic chain of the polymer orientates away from the solvent. So that,

amphiphilic polymers can form multimolecular micelles where the hydrophobic portions are clustered in a core, away from the solvent, and the hydrophilic portions are aligned forming a shell towards the solvent. When amphiphilic polymers form micelles in water (most usually) or polar solvents the aggregates are known as normal or regular micelles. When amphiphilic polymers are exposed to an hydrophobic solvent, they can form micelles with an opposite orientation, that is, with the hydrophobic chains on the shell and hydrophilic chains on the core. These micelles are known as reverse micelles (Figure 2.8).

Micelles based on amphiphilics polymers have a large number of potential applications as *stimuli* responsible and drug delivery systems being one of the most promising future improvements in therapy and drug administration.

Drugs generally have poor aqueous solubility and therefore they have low bioavailability after oral administration. On average, approximately 40 % of drugs available in the market and around 75 % of drugs currently in development stage are poorly soluble in water. Amphiphilic polymers have been extensively investigated for pharmaceutical applications when they form regular micelle aqueous media. Inside of the hydrophobic core, insoluble drugs can be loaded and transported in water media. These drugs can be delivered in a controlled way through external *stimuli*, for example light, pH, temperature or oxidant agents (Figure 2.8).[127-130]

Micelles are dispersed in aqueous media above their critical micelle concentration (CMC) and under the appropriate conditions drugs can be encapsulated in the core. The CMC is defined as the concentration of amphiphilic molecules above which micelles start to form.

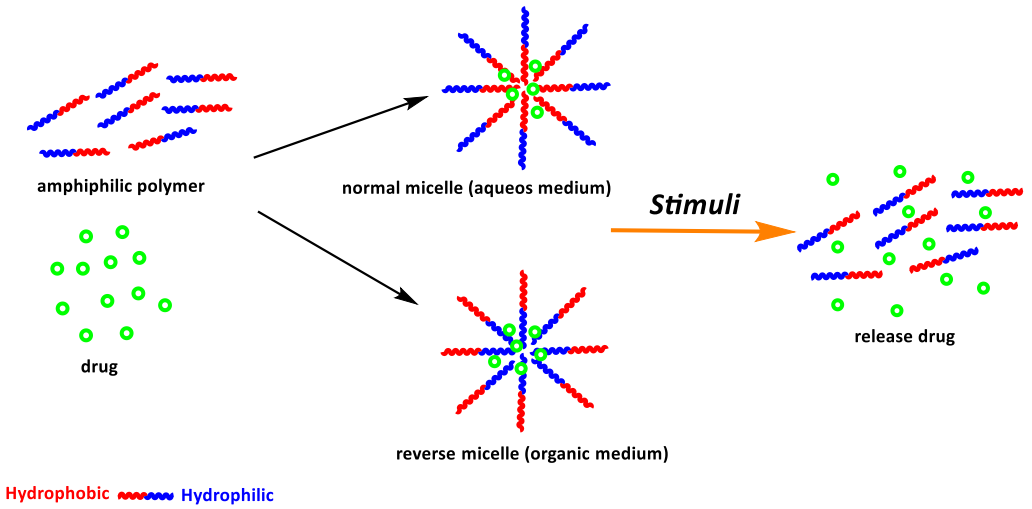

Figure 2.8 Normal and reverse micelle micelle formation and their use in drug delivery systems.

Different methods have been described to prepare micelles. The most frequent are: dialysis, oil/water emulsion, solvent evaporation (or film method), co-solvent evaporation and nanoprecipitation (Figure 2.9). In the dialysis method, the amphiphilic polymer is dissolved in a water miscible non-volatile organic solvent (such as DMF, DMSO…) followed by dialysis of the obtained solution against water. In the oil/water emulsion method the polymer is dissolved in a water immiscible volatile organic solvent (such as chloroform ethyl acetate or methylene chloride). This solution is slowly added to the aqueous phase under stirring to make an oil-in-water emulsion. In the solvent evaporation or film method, the amphiphilic polymer is dissolved in a volatile organic solvent and then the solvent is evaporated to make a thin polymer-drug film on a flask. The film is then reconstituted with the aid of aqueous solvent by vigorous shaking to produce polymeric micelles. Finally, in the co-solvent evaporation method the polymer is dissolved in a water miscible volatile organic solvent and then added drop wise to water under stirring, by the diffusion of solvent in water with simultaneous evaporation triggered the self-assembly of copolymer, yielding the polymeric micelles.[131-133]

Introduction

To prepare drug loaded polymeric micelles the same methodologies are used but starting from solutions of the amphiphilic polymer in which the targeted drug has been co-dissolved.

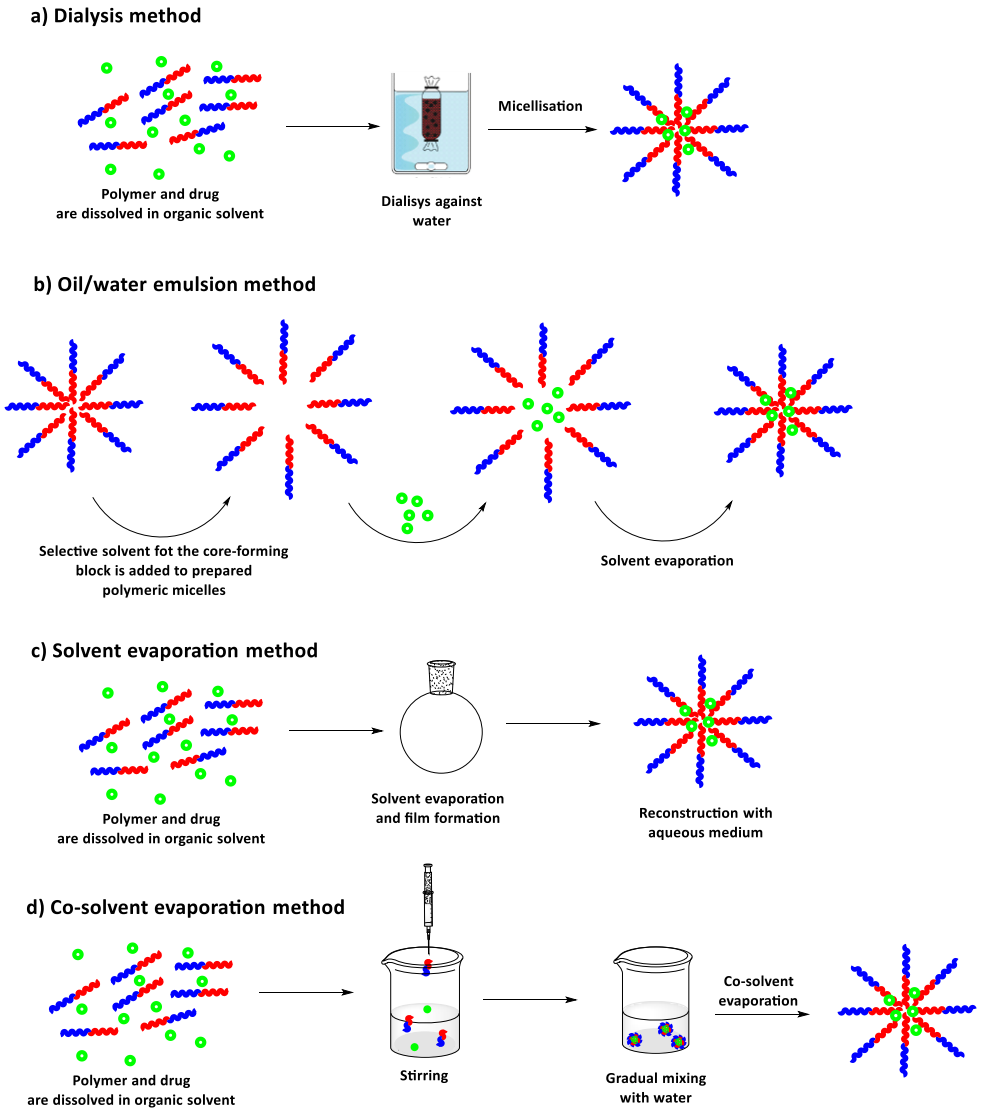

Figure 2.9 Different methods used for micelle preparation and drug encapsulation.

The hydrophobic core serves as a reservoir for drugs with low aqueous solubility with the hydrophilic shell preventing the adsorption of opsonins on the surface.

Polyethyleneglycol (PEG), is by far the polymer most used as hydrophilic block whereas the hydrophobic block can be chosen based on the required application.[134] PEG is an inexpensive, non-toxic and FDA (United States governmental agency for Food and Drug Administration) approved polymer for the use in drug products.[135] Moreover, the formed nanoscopic sized micelles (10-200 nm in diameter) are sufficiently large to avoid renal excretion (≥ 50 kg·mol^{-1}) as well as small enough to bypass the filtration of inter-endothelial cells in the spleen.

Amphiphiles can self-assemble into nano-sized micelles, also known as multimolecular micelles, of various morphologies in aqueous solution. However, conventional polymeric micelles represent thermodynamic aggregations of multiamphiphilic macromolecules above their critical micelle concentration (CMC). When these polymeric micelles are subjected to high dilution and alterations in other factors such as temperature, pH and ionic strength, they disassemble into free polymeric chains.[136]

To overcome the thermodynamic instability issue of polymeric micelles, core and/or shell cross-linking approaches have been proposed. Shell and/or core cross-linking endows polymeric micelles with excellent structural stability. However, their biodegradability or drug release profiles are compromised after cross-linking. From certain respects, the crosslinked core-shell particle can be also considered as single macromolecules.[137]

In addition to the cross-linking approach, design of unimolecular micelles provides an alternative strategy and opportunity to prepare stable polymeric micelle. Unimolecular micelles are defined as a class of single-molecule micelle with a distinct core and shell that are covalently bound together. Due to their unique architecture, unimolecular micelles show excellent stability regardless of the high dilution condition and other microenvironment changes, making them particularly attractive for the design of stable micelles for specific applications (Figure 2.10). Unimolecular micelles are covalently

bound molecular architecture than can be made from a variety of amphiphilic polymers, for example from amphiphilic dendrimers, amphiphilic hyperbranched polymers, amphiphilic dendrimers-like polymers, amphiphilic star polymers and other amphiphilic polymers.[138]

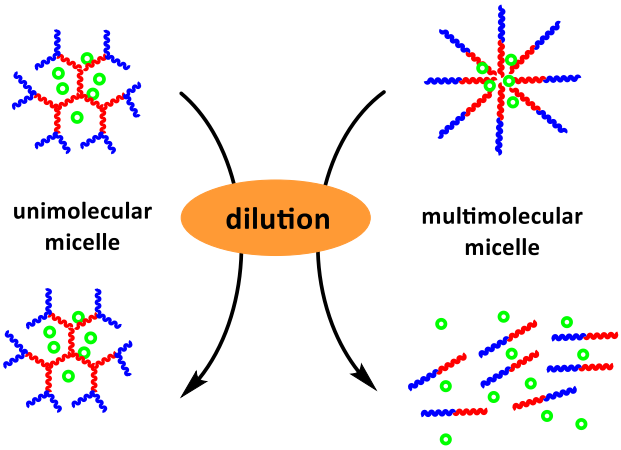

Figure 2.10 Different behaviours of unimolecular and multimolecular micelles under dilution. Unimolecular micelles are stable and multimolecular micelles can fall apart.

2.5 REFERENCES

[1] Hosler D.; Burkett S. L.; Tarkanian M. J.; Prehistoric polymers: Rubber processing in ancient Mesoamerica, **1999**, *Science,* 284, 1998-1991.

[2] British Plastic Federation http://www.bpf.co.uk/Plastipedia/Plastics_History/Default.aspx.

[3] Andray A. L.; Neal M. A.; Applications and societal benefits of plastics, **2009**, *Philos. Trans. R. Soc. Lond. B Biol. Sci.*, 364, 1977-1984.

[4] European bioplastics, Bioplastics facts and figures, *http://en.european-bioplastics.org/* accessed March, 2, **2017**.

[5] Halden R. U.; Plastics and Health Risk, **2010**, *Annu. Rev. Public Health*, 31, 179-194.

[6] Thompson R. C.; Swan S. H.; Moore C. J.; Vom Saal F. S.; Our plastic age, **2009**, *Philos. Trans. R. Soc. Lond. B Biol. Sci.*, 364, 1973-1976.

[7] Cristóbal J.; Matos C.T.; Aurambout J. P.; Manfredi S.; Kavalov B.; Enviromental sustainability assessment of bioeconomy value chains, **2016**, *Biomass and Bioenergy*, 89, 159-171.

[8] Nair L. S.; Laurencin C. T.; Biodegradable polymers as biomaterials, **2007**, *Prog. Polym. Sci.*, 32, 762-798.

[9] Belgacem M. N.; Gandini A.; Monomers, polymers and composites from renewable resources, **2008**, *Elsevier, Oxford 1st edn.*

[10] Vilela C.; Sousa A. F.; Fonseca A. C.; Serra A. C.; Coelho J.F.J.; Freire C.S.R.; Sylvester A.N.D.; The quest for sustainable polyesters –insights into the future, **2014**, *Polym. Chem.,* 5, 3119-3141.

[11] Chen G. Q.; Patel M. K.; Plastics derived from biological sources: Present and future: a technical and environmental review, **2012**, *Chem. Rev.*, 112, 2089-2099.

[12] BASF web, https://www.basf.com/en/we-create-chemistry/creating-chemistry-magazine/resources-environment-and-climate/naturally-good-searching-for-new-bio-based-raw-materials-for-industry.html accessed March, 3, **2017**.

[13] Metzger J. O.; Bornscheuer U.; Lipids as renewable resources: current state of Chemicals and biotechnological conversion and diversification, **2006**, *Appl. Microbiol. Biotechnol.*, 71:13-22.

[14] Bayer I. S.; Guzman-Puyol S.; Heredia-Guerrero J. A.; Ceseracciu L.; Pignatelli F.; Ruffilli R.; Cingolani R.; Athanassiou A.; Direct transformation of edible vegetable waste into bioplastics, **2014**, *Macromolecules*, 47, 5135-5143.

[15] Lligadas G.; Ronda J. C.; Galià M.; Cádiz V.; Renewable polymeric materials from vegetable oils: a perspective, **2013**, *Mater. Today*, 16, 9, 337-343.

[16] Xia Y.; Larock R. C.; Vegetable oil-based polymeric materials: synthesis, properties, and applications, **2010**, *Green Chem.,* 12,1893-1909.

[17] Gandini A.; Lacerda T. M.; Carvalho A. J. F.; Trovatti E.; Progress of Polymers from Renewable Resources: Furans, Vegetable Oils, and Polysaccharides, **2016,** *Chem. Rev.,* 116, 1637-1669.

[18] Lligadas G.; Ronda, J. C.; Galià M.; Cádiz V.; Oleic and Undecenoic Acids as Renewable Feedstocks in the Synthesis of Polyols and Polyurethanes, **2010**, *Polymers*, 2, 440-453.

[19] Anastas P.; Eghbali N.; Green Chemistry: Principles and Practice, **2009**, *Chem. Soc. Rev.*, 39, 301-312.

[20] Sheldon R. A.; Green and sustainable manufacture of Chemicals from biomass: state of the art, **2014**, *Green Chem.*, 16, 950-963.

[21] Galià M.; Espinosa L. M.; Ronda J. C.; Lligadas G.; Cádiz V.; Vegetable oil-based thermosetting polymers, **2010**, *Eur. J. Lipid Sci. Tecnhol.*, 112, 1, 87-96.

[22] Gandini A.; Lacerda T. M.; From monomers to polymers from renewable resources: Recent advances, **2016**, *Progress in Polymer Science,* 48, 1-39.

[23] Galià M.; Espinosa L. M.; Ronda J. C.; Lligadas G.; Cádiz V.; Vegetable oil-based thermosetting polymers, **2010**, *Eur. J. Lipid Sci. Tecnhol.*, 112, 1, 87-96.

[24] Gandini A.; Lacerda T. M.; From monomers to polymers from renewable resources: Recent advances, **2016**, *Progress in Polymer Science,* 48, 1-39.

[25] Gallezot P.; Direct routes from biomass to end-products, **2011**, *Catalysts Today,* 167, 31-36.

[26] Gandini A.; Polymers from Renewable Resources: A Challenge for the Future of Macromolecular Materials, **2008**, *Macromolecules,* Vol. 42, No. 24, 9491-9504.

[27] Khot S. N.; Lascala J. J.; Can E.; Morye S. S.; Williams G. I.; Palmese G. R.; Kusefoglu S. H.; Wool P. R.; Development and Application of Triglycerides-Based Polymers and Composites, **2001**, *J. Appl. Polym. Sci.*, Vol. 82, 703-723.

[28] Canakei M.; Sanli H.; Biodiesel production from various feedstocks and their effects on the fuel properties, **2008**, *J. Ind. Microbiol. Biotechnol.,* 35:431-441.

[29] Patel V. R.; Dumancas G. G.; Viswaneth L. C. K.; Maples R.; Subong B. J.; Castor oil: properties, uses, and optimization of processing parameters in commercial production, **2016**, *Lipid insights*, 9, 1-12.

[30] Mubofu E. B.; Castor oil as a potential renewable resource for the production of functional materials, **2016**, *Sustain. Chem. Process*, 4:11.

[31] Totaro G.; Cruciani L.; Vannini M.; Mazzola G.; Gioia D. D.; Celli A.; Sisti L.; Synthesis of castor oil-derived polyesters with antimicrobial activity, **2014**, *Eur. Polym. J.,* 56, 174-184.

[32] Van Steen M.; Stevens C. V.; Undecylenic Acid: A Valuable and Physiologically Active Renewable Building Block from Castor Oil, **2009**, *ChemSusChem*, 2, 692-713.

[33] Das G.; Trivedi R. K.; Vasishtha A. K.; Heptaldehyde and undecylenic acid from castor oil, **1989**, *J. Am. Oil Chem. Soc.,* Vol. 66, no. 7.

[34] Bigot S.; Daghrir M.; Mhanna A.; Boni G.; Pourchet S.; Lecamp L.; Plasseraud L.; Undecylenic acid: A tunable bio-based synthon for materials applications, **2016**, *Eur. Polym. J.*, 74, 26-37.

[35] a) Carothers W. H.; Polymerization, **1931**, *Chem. Rev.*, 8, 359-368. b) Carothers W. H., Hill J.W.; Studies of polymerization and ring formation. XI. The use of molecular evaporation as a means for propagation chemical reaction, **1932**, *J. Am. Chem. Soc.,* 54, 1577-1579. c) Carothers W. H.; Polymers and polyfunctionality, **1936**, *Trans. Faraday Soc.*, 32, 39-49.

[36] a) Whinfield, J. R., **1946**, *Nature* (London), 158, 930. b) Whinfield, J. R., Dickson J. T; British Patent, **1946**, 578, 079 (to ICI).

[37] Ellis C.; U.S. Patent, **1937**, 2,225, 313 (to Ellis-Foster Co).

[38] Ikada Y.; Tsuji H. Biodegradable polyesters for medical and ecological applications, **2000**, *Macromol. Rapid Commun.*, 21, 117-132.

[39] Kunduru K. R.; Basu A.; Zada M. H.; Domb A. J.; Castor oil-based biodegradable polyesters, **2015**, *Biomacromolecules*, 16 (9), 2572-2587.

[40] Middleton J. C.; Tipton A. J. Synthetic biodegradable polymers as orthopedic devices, **2000**, *Biomaterials*, 21, 2335-2346.

[41] Tokiwa T.; Jarerat A.; Biodegradation of poly(L-Lactide), **2004**, *Biotech. Lett.,*26, 771-777.

[42] Otera J.; Nishikido J.; Esterification, methods, reactions, and applications. 2nd Ed., **2010**, *WILEY-VCH Verlang GmbH & Co, KGaA*, Weinheim, 5-51.

[43] Rogers M. E.; Long T. E.; Turner S. R.; Synthetic methods in step-growth polymers, **2003**, *John Wiley & Sons Inc*.

[44] Binder S., Gadwal I., Bielman A., Khan A.; Thiol-epoxy polymerization via an AB monomer: Synthetic access to high molecular weight poly(β-hydroxythio-ether)s, **2014**, J. *Polym. Sci. Part A: Polym. Chem.*, 52, 2014-2046.

[45] Fradet A.; Marechal E.; Kinetics and mechanism of polyesterifications, 1982, *Adv. Polym. Sci.*, 43, 51-96.

[46] Kobayashi S.; Lipase-catalyzed polyesters synthesis- A green polymer chemistry, **2010**, *Proc. Jpn. Acad.* Ser. B 86, 338-365.

[47] Sheldon R. A.; Pelt S.; Kanbak-Aksu S.; Rasmussen J. A.; Janssen M. H. A.; Cross-linked enzyme aggregated (CLEAs) in organic synthesis, **2013**, *Aldrichimica acta*, vol. 46, no 3, 81-93.

[48] Mateo C.; J. M. Palomo, Lorente G. F.; Guisan J. M.; Lafuente R. F.; Improvement of enzyme activity, stability and selectivity via immobilization techniques, **2007**, *J. enzyme Microb. Tech.*, 40, 1451-1463.

[49] Matsumura S.; Enzymatic synthesis of polyesters via ring-opening polymerization, **2006**, *Adv. Polym. Sci*., 194, 95-132.

[50] Uppenberg J.; Patkar S.; Bergfors T.; Jones T. A.; Crystallization and preliminary X-ray studies o lipase B from *Candida antarctica*, **1994**, J. Mol. Biol. *235, 790-792*.

[51] Li C.; Tan T.; Zhang H.; Feng W.; Analysis of the conformational stability and activity of *Candida antarctica* lipase B in organic solvents, **2010**, *J. Biol. Chem*., 285, 28434-28441.

[52] Lund I. T.; Bockmann P. L.; Jacobsen E. E.; Highly enantioselective CALB-catalyzed kinetic resolution of building blocks for β-blocker atenolol, **2016**, *Tetrahedron*, 72, 7288-7292.

[53] Poojari Y.; Clarson S. J.; Thermal stability of *Candida antarctica* lipase B immobilized on macroporous acrylic resin particles in organic media, **2013**, *Biocatal. agric. biotech.,* 2, 7-11.

[54] Mahapatro A.; Kumar A.; Kalra B.; Gross R. A.; Solvent-free adipic acid/1,8-octanediol condensation polymerizations catalyzed by *Candida antarctica* lipase B, **2004**, *Macromolecules*, 37, 35-40.

[55] Mahapatro A.; Kumar A.; Gross R. A.; Mild, solvent-free ω-hydroxy acid polycondensations catalyzed by *Candida antarctica* Lipase B, **2004**, *Biomacromolecules*, 5, 62-68.

[56] Kumar A.; Gross R. A*.; Candida antarctica* Lipase B-catalyzed transesterification: new synthetic routes to copolyesters, **2000**, *J. Am. Chem. Soc.,* 122, 11767-11770.

[57] Shuai X.; Jedlinski Z.; Kowalczuk M.; Rydz J.; Tan H.; Enzymatic synthesis of polyesters from hydroxyl acids, **1999**, *Eur. Polym. Enzymatic J.*, 35, 721-725.

[58] Dechy-Cabaret O.; Martin-Vaca B.; Bourissou D.; Controlled ring-opening polymerization of lactide and glycolide, **2004**, *Chem. Rev.,* 104, 6147-6176.

[59] Duda A.; Kowalski A.; Libiszowski J.; Penczek S.; Thermodynamic and kinetic polymerizability of cyclic esters, **2005**, *Macromol. Symp.*, 224, 71-84.

[60] Hong M.; Chen E. Y. X.; Completely recyclable biopolymers with linear and cyclic topologies via ring-opening polymerization of γ-butyrolactone, **2015**, *Nat. Chem.,* 8, 42-49.

[61] a) Schwach G.; Coudane J.; Engel R.; Vert M.; Stannous octoate- versus zinc-initiated polymerization of racemic lactide, **1994**, *Polym. Bull.*, 32, 617-623. b) Schwach G.; Coudane J.; Engel R.; Vert M.; Ring opening polymerization of D, L-lactide in the presence of zinc metal and lactate, **1998**, *Polym. Int.*, 46, 177-182.

[62] Dove A. P.; Organic catalysis for ring-opening polymerization, **2012**, *Macro. Lett.,* 1, 1409-1412.

[63] Song F.; Wu L.; Synthesis of high molecular weight poly(L-lactic acid) via melt/solid polycondensation: intensification of dehydration and oligomerization during melt polycondensation, **2010**, *J. Appl. Polym. Sci.*, 120, 2780-2785.

[64] Polloni A. E.; Rebelatto E. A.; Veneral J. G.; Oliveira D.; Oliveira J. V.; Araújo P. H. H.; Sayer C.; Enzymatic ring-opening polymerization of ω-pentadecalactone in different solvents in a variable-volume view reactor, **2017**, *J. Polym. Sci. part A: Polym. Chem*., 55, 1219-1227.

[65] Kundys A.; Florjanczyk E. B.; Fabiszewska A.; Malajowiez J.; *Candida antarctica* lipase B as catalyst for cyclic esters synthesis, their polymerization and degradation of aliphatic polyesters, **2017***, J. Polym. Environ.*, DOI 10.1007/s10924-017-0945-1.

[66] Binns F.; Harffey P.; Roberts S. M.; Taylor A.; Studies leading to the large-scale synthesis of polyesters using enzymes, **1999**, *J. Chem. Soc., Perkin Trans.,* 1, 2671-2676.

[67] Xie W.; Li J.; Chen D.; Wang P. G.; Ring-opening polymerization of β-butyrolactone by thermophilic lipases, **1997**, *Macromol.*, 30, 6997-6998.

---

[68] Heise A.; Duxbury C. J.; Palmans R. A.; Enzyme-mediated ring-opening polymerization, **2009**, Handbook of Ring-Opening Polymerization, 379-399 (eds. Dubois P., Coulembier O., Marquez J. M.), *Wiley-VCH Verlag GmbH & Co. KgaA*, Weinheim.

[69] Slivnyak D. R.; Domb A. J.; Lactic acid and ricinoleic acid based polyesters, **2005**, *Macrom., 38,* 5545-5553.

[70] Maisonneuve L.; Chollet G.; Grau E.; Cramail H.; New perspective of european oleochemistry, 2016, OCL, 23 (5) D508.

[71] Zhu Y.; Romain C.; Williams C. K.; Sustainable polymers from renewable resources, **2016**, *Nature*, 540, 354-362.

[72] Kunduru K. R.; Basu A.; Zada M. H.; Domb A. J.; Castor Oil-Based Biodegradable Polyesters, **2015**, *Biomacromolecules*, 16, 2572-2587.

[73] Mutlu H.; Meier M. A. R.; Castor oil as a renewable resource for the Chemicals industry, **2010**, *Eur. J. Lipid Sci. Technol.*, 112, 10-30.

[74] Ebata H.; Toshima K.; Matsumura S.; Lipase-Catalyzed Synthesis and Properties of Poly[(12-hydroxydodecanoate)-co-(12-hydroxystearate)] Directed towards Novel Green and Sustainable Elastomers, **2008**, *Macromol. Biosci.*, 8, 38-45.

[75] Petrović Z. S.; Millić J.; Xu Y.; Cvtković I.; A chemical route to high molecular weight vegetable oil-based polyhydroxyalkanoate, **2010**, *Macromol.*, 43, 4120-4125.

[76] Quinzler D.; Mecking S.; Linear semicrystalline polyesters from fatty acids by complete feedstock molecule utilization, **2010**, *Angew. Chem. Int. Ed.*, 49, 4306-4308.

[77] Türünç O.; Meier M. A. R.; Fatty acid derived monomers and related polymers via thiol-ene (click) additions, **2010**, *Macromol. Rapid Comm.*, 31, 1822–1826.

[78] Yang Y.; Lu W.; Zhang X.; Xie W.; Cai M.; Gross R. A.; Two-step biocatalytic route to biobased functional polyesters from ω-carboxy fatty acids and diols, **2010**, *Biomacromolecules*, 11, 259–268.

[79] Kobayashi T.; Matsumura S.; Enzymatic synthesis and properties of novel biodegradable and biobased thermoplastic elastomers, **2011**, *Polym. Degrad. Stab.*, 96, 2071-2079.

[80] Lebarbe T; Ibarboure E.; Gadenne B.; Alfos C.; Cramail H.; Fully bio-based poly(L-lactide)-b-poly(ricinoleic acid)-b-(poly(L-lactide) triblock copolyesters: investigation of solid-state morphology and thermo-mechanical properties, **2013**, *Polym. Chem.,* 4, 3357-3369.

[81] Vilela C.; Silvestre A. J. D.; Meier M. A. R.; Plant oil-based long-chain C26 monomers and their polymers, **2012**, *Macromol. Chem. Phys.*, 213, 2220–2227.

[82] Tong R.; New chemistry in functional aliphatic polyesters, **2017**, *Ind. Eng. Chem. Res*., 56 (15), 4207−4219.

[83] Mooney B. P.; The second green revolution? Production of plant-based biodegradable plastics, **2009**, *Biochem. J.,* 418, 219-232.

[84] Vert M.; Aliphatic polyesters; great degradable polymers that cannot do everything**,** **2005**, *Biomacromolecules,* 6, 538-546.

[85] Guo B.; Peter M. A.; Synthetic biodegradable functional polymers for tissue engineering: a brief review, **2014**, *Chem. China Sci.*, 57, 4, 490-500.

[86] Seyednejad H.; Ghassemi A. H.; van Nostrum C. F.; Vermonden T.; Hennink V. E.; Functional aliphatic polyesters for biomedical and pharmaceutical applications, **2011**, *J. control. release*, 152, 168-176.

[87] Trollsås M.; Lee V. Y.; Mecerreyes D.; Löwenhielm P.; Möller M.; Miller R. D.; Hedrick J. L.; Hydrophilic Aliphatic Polyesters: Design, Synthesis, and Ring-Opening Polymerization of Functional Cyclic Esters, **2000**, *Macromol*ecules, 33, 4619-4627.

[88] Tong R.; New chemistry in functional aliphatic polyesters, **2017**, *Ind. Eng. Chem. Res.,* 4207−4219.

[89] Gross R. A.; Kumar A.; Kalra B.; Polymer Synthesis by In Vitro Enzyme Catalysis, **2001**, *Chem. Rev*., 101, 2097−2124.

[90] Zakharova E.; Martínez de Ilarduya A.; León S.; Muñoz-Guerra S.; Hydroxyl-functionalized amphiphilic triblock copolyesters made of tartaric and lactic acids: Synthesis and nanoparticle formation, **2018**, *React. Funct. Polym.,* 126, 52-62.

[91] Gershon H.; Shanks L.; Antifungal properties of *n*-alkanols, α,ω,n-alkanediols, and ω-chloro-α-alkanols, **1979**, *J. Pharm. Sci., Vol. 69, No. 4.*

[92] Takasu A.; Shibata Y.; Narukawa Y.; Hirabayashi T.; Chemoselective dehydration polycondensations of dicarboxylic acids and diols having pendant hydroxyl groups using the room temperature polycondensation technique, **2007**, *Macromolecules*, 40, 151-153.

[93] Karami N.; Alsterholm M.; Faergemann J.; In vitro activity of chlorhexidine and pentane-1,5-diol and their combination on *Candida albicans, Staphylococcus aureus* and *Propionibacterium acnes*, **2009**, *Acta Derm. Venereol.;* 89: 514–547.

[94] Slavko E.; Taylor M. S.; Catalyst-controlled polycondensation of glycerol with diacyl chlorides: linear polyesters from a trifunctional monomer, **2017**, *Chem. Sci.,* 8, 7106-7111.

[95] Yang J.; Webb A. R.; Pickerill S. J.; Hageman G.; Ameer G. A.; Synthesis and evaluation of Poly(diol citrate) biodegradable elastomers, **2005**, *Biomaterials*, 27: 1889-1898.

[96] Widiyanti P.; Sholikhah I.; Isfandiary A.; Hasbiyani N.; Lazuardi M. B.; Laksana R. D.; Poly (1,8-octanediol-co-citrate) hydroxyapatite composite as antibacterial biodegradable bone screw, **2017**, *IOP Conf. Ser.: Mater. Sci. Eng.,* 202: 012082.

[97] Jeong C. G.; Zhang H.; Hollister S. J.; Three-dimensional poly(1,8-octanediol–co-citrate) scaffold pore shape and permeability effects on sub-cutaneous in vivo chondrogenesis using primary chondrocytes, **2011**, *Acta Biomaterialia*, 7: 505–514.

[98] You Z.; Bi X.; Jeffries E. M.; Wang Y.; A biocompatible, metal-free catalyst and its application in microwaves-assisted synthesis of functional polyesters, 2012, Polym. Chem., 3, 384.

[99] You Z.; Cao H.; Gao J.; Shin P. H.; Day B. W.; Wang Y.; A functionalizable polyesters with free hydroxyl groups and tunable physicochemical and biological properties, **2010**, *Biomaterials*, 31, 3129-3138.

[100] Thibodeaux C. J.; Chang W. C.; Liu H. W.; The enzymatic chemistry of cyclopropane, epoxide, and aziridine biosynthesis, **2012**, *Chem. Rev.*, 112(3): 1681-1709.

[101] Miao S.; Zhang S.; Su Z.; Wang P.; Chemoenzymatic synthesis of oleic acid-based polyesters for use as highly stable biomaterials, **2008**, *J. Polym. Sci. Part A: Polym. Chem.,* 4243-4248.

[102] Warwel S.; Klass M. R.; Chemo enzymatic epoxidation of unsaturated carboxylic acids, **1995**, *J. Mol. Cat. B: enzymatic*, 1, 29-35.

[103] Wang X.; Tang Q.; Popowicz G.M.; Yang B.; Wang Y.; A mechanistic study into the epoxidation of carboxylic acid and alkene in a mono, di-acylglycerol lipase, **2015**, *Biochem. Biophys. Res. Commun.*, 460, 392-396.

[104] Nakano K.; Kodama S.; Permana Y.; Nozaki K.; Regioselective synthesis of halohydrin esters from epoxides: reaction with acyl halides and rhodium-catalyzed three-component coupling reaction with alkyl halides and carbon monoxide, **2009**, *Chem. Commun*., 6970-6972.

[105] Gros P.; Perchec P. L.; Senet J. P.; Reaction of epoxides with chlorocarboylated compounds catalyzed by hex alkyl guanidinium chloride, **1994**, *J. Org. Chem.,* 59, 4925-4930.

[106] Hu S.; Zhao J.; Zhang G.; Noncopolymerization approach to copolymers via concurrent transesterification and ring-opening reactions, **2016**, ACS Macro Lett., 5, 40−44.

[107] Zhao J.; Pahovinik D.; Gnanou Y.; Hadjichristidis N.; Phosphazene-promoted metal-free ring-opening polymerization of ethylene oxide initiated by carboxylic acid, **2014**, *Macromolecules*, 47, 1693-1698.

[108] Soeda Y.; Okamoto T.; Toshima K.; Matsumura S.; Enzymatic ring-opening polymerization of oxiranes and dicarboxylic anhydrides, **2002**, *Macromol. Biosci.*, 2, 429-436.

[109] Rad M. N. S.; Behrouz S.; The base-free chemoselective ring opening of epoxides with carboxylic acids using [bmim]Br: a rapid entry into 1,2-diol mono-esters synthesis, **2013**, *Mol. Divers.,* 17;9-18.

[110] Zhao Y.; Wang W.; Li J.; Wang F.; Zheng X.; Yun H.; Zhao W.; Dong X.; FeCl3/pyridine: dual-activation in opening of epoxide with carboxylic acid under solvent free condition, **2013**, *Tetrahedron letters*, 54, 5849-5852.

[111] Blank W. J.; He Z. A.; Picci M.; Catalysis of the epoxy-carboxyl reaction, **2001**, *International Waterborne, High-Solids and Powder Coatings Symposium*.

[112] You Z.; Wang Y.; A versatile synthetic platform for a wide range of functionalized biomaterials, **2012**, *Adv. Funct. Mater.,* 22, 2812-2820.

[113] You Z.; Cao H.; Gao J.; Shin P. H.; Day B. W.; Wang Y.; A functionalizable polyester with free hydroxyl groups and tunable physiochemical and biological properties, **2010**, *Biomaterials*, 31, 3129-3138.

[114] White J. E.; Earls J. D.; Sherman J. W.; López L. C.; Dettloff M. L.; Step-growth polymerization of 10,11-epoxy undecanoic acid. Synthesis and properties of a new hydroxyl-functionalized thermoplastic polyester, **2007**, *Polymer*, 48, 3990-3998.

[115] De Smet S.; Lingier S.; Du Prez F. E.; MacroRAFT agents from renewable resources and their use as polymeric scaffolds in a grafting from approach, **2014**, *Polym. Chem.,* 5, 3163- 3169.

[116] Sudesh K.; Abe H.; Doi Y. Synthesis, structure and properties of polyhydroxyalkanoates: biological polyesters, **2000**, *Prog. Polym. Sci.*, 25, 1503-1555.

[117] Hao Q.; Yang J.; Li Q.; Li Y.; Jia L.; Fang Q.; Cao A.; New facile approach to novel water-soluble aliphatic poly(butylene tartarate)s bearing reactive hydroxyl pendant groups, **2005**, *Biomacromol*., 6, 3474-3480.

[118] Zhang S.; Yang J.; Liu X.; Chang J.; Cao A.; Synthesis and characterization of poly(butylene succinate-co-butylene malate): a new biodegradable copolyester bearing hydroxyl pendant groups, **2003**, *Biomacrom.*, 4, 437-44.

---

[119] Ghassemi A. H.; van Steenbergen M. J.; Talsma H.; van Nostrum C. F.; Jiskoot W.; Crommelin D. J. A.; Hennink W. E.; Preparation and characterization of protein loaded microspheres based on a hydroxylated aliphatic polyester, poly(lactic-co-hydroxymethyl glycolic acid), **2009**, *J. Controlled Release*, 138, 57–63.

[120] Bernkop-Schnürch A.; Schwarz V.; Steininger S.; Polymers with thiol groups: a new generation of mucoadhesive polymers?, **1999**, *Pharmaceutical research*, vol 16, nº 6.

[121] Bhalekar M.; Sonawane S.; Shimpi S.; Synthesis and characterization of a cysteine xyloglucan conjugate as mucoadhesive polymer, **2013**, *Brazilian Journal of Pharmaceutical Sciences*, vol, 49, n. 2, 285-292.

[122] Madgulkar A. R.; Bhalekar M. R.; Asgaonkar K. D.; Dikpati A. A.; Synthesis and characterization of a novel mucoadhesive derivative of xyloglucan, **2016**, *Carbohydrate Polymers*, 135, 356–362.

[123] Lan H. T.; Leonaviciute G.O..; Zupančič O.; Bernkop-Schnürch A.; Thiomers: impact of in situ cross-linkers on mucoadhesive properties, 2017*, Eur. J. Pharm. Sci.*, 106, 41-48.

[124] Sosnik A.; Neves J.; Sarmento B.; Mucoadhesive polymers in the design of nano-drug delivery systems for administration by non-parenteral routes: a review, **2014**, *Prog. Polym. Sci.,* 39, 2030-2075.

[125] Fuoco T.; Finne-Wistrand A.; Pappalardo D.; A route to aliphatic poly(ester)s with thiol pendant groups: from monomer design to editable porous scaffolds, **2016**, *Biomacromolecules*, 17, 1383−1394.

[126] Neindre M.; Nicolaÿ R.; Polythiol copolymers with precise architectures: a platform for functional materials, **2014**, *Polym. Chem*., 5, 4601-4611.

[127] Bazban-Shotorbani S.; Hassani-Sadrabadi M. M., Karkhaneh A.; Serpooshan V.; Jacob K. I.; Moshaverinia A.; Mahmoudi M.; Revisiting structure-property relationship of pH-responsive polymers for drug delivery applications, **2017**, *J. Control. Realase*, 253, 46-63.

[128] Weber C.; Hoogenboom R.; Schubert U. S.; Temperature responsive bio-compatible polymers base on poly(ethylene oxide) and poly(2-oxazoline)s, **2012**, *Prog. Polym. Sci.*, 37, 686-714.

[129] Blasco E.; del Barrio J.; Sánchez-Somolinos C.M.; Piñol M.; Oriol L.; Light induced molecular reléase from vesicles base on amphiphilic linear-dendritic block copolymers, **2013**, *Polym. Chem.,* 4, 2246-2254.

[130] Zhang H.; Wang K.; Zhang P.; He W.; Song A.; Luan Y.; Redox-sensitive micelles assembled from amphiphilic mPEG-PLC-SS-DTX conjugates for the delivery of docetaxel, **2016**, *Colloids Surf. B*., 142, 89-97.

[131] Alibadi H. M.; Lavasanifar A.; Polymeric micelles for drug delivery, **2006**, *Expert Opin. Drug Deliv.,* 3(1), 139-162.

[132] Jee J. P.; McCoy A.; Mecozzi S.; Encapsulation and release of amphotericin B from an ABC triblock fluorous copolymer, **2012**, *Pharm. Res.*, 29 (1), 69-82.

[133] Gou M.; Men K.; Shi H.; Xiang M.; Zhang J.; Song J.; Long J.; Wan Y.; Luo F.; Zhao X.; Quian Z.; Curcumin-loaded biodegradable polymeric micelles for colon cancer therapy in vitro and in vivo, **2011**, *Nanoscale*, 3 (4), 1558-1567.

[134] Gaucher G.; Dufresne M. H.; Sant V. P.; Kang N.; Maysinger D.; Leroux J. C.; Block copolymer micelles: preparation, characterization and application in drug delivery, **2005**, *J. Control. Release*, 109 (3), 169-188.

[135] Torchilin V. P.; Micellar nanocarriers: pharmaceutical perspectives, **2007**, *Pharm. Res.*, 24 (1), 1-16.

[136] Fan X.; Li Z.; Loh X.J.; Recent development of unimolecular micelles as functional materials and applications, **2016**, *Polym. Chem.*, 7, 5898-5919.

[137] Hu X.; Liu Y.; Wang X.; Liu S.; Cell-Penetrating Hyperbranched Polyprodrug Amphiphiles for Synergistic Reductive Milieu-Triggered Drug Release and Enhanced Magnetic Resonance Signals, **2015**, *J. Am.Chem. Soc*., 137, 362-368.

[138] Lukowiak M. C.; Thota B. N. S.; Haag R.; Polymeric Soft Nanocarriers as Smart Drug Delivery Systems: State-of-the-Art and Future Perspectives, **2015**, *Biotechnol. Adv.*, 33, 1327-1341.

UNIVERSITAT ROVIRA I VIRGILI
10-UNDECENOIC ACID-BASED BIODEGRADABLE HYDROXY POLYESTERS: A PLATFORM FOR AMINOACID BIOCONJUGATES AND PEG-DERIVED AMPHIPHILIC COPOLYMERS
Carmen Valverde Sarmiento

Chapter 3

Hydroxyl functionalized renewable polyesters derived from 10-undecenoic acid: polymer structure and post-polymerization modification

Publication derived from this work: *European Polymer Journal*, 2018, 105, 68-78.

Supporting Information (SI) to this chapter in Annex A.

UNIVERSITAT ROVIRA I VIRGILI
10-UNDECENOIC ACID-BASED BIODEGRADABLE HYDROXY POLYESTERS: A PLATFORM FOR AMINOACID BIOCONJUGATES AND PEG-DERIVED AMPHIPHILIC COPOLYMERS
Carmen Valverde Sarmiento

3.1 INTRODUCTION

Nowadays, the interest in polymers from renewable resources has been witnessing an incessant growth in both academy and industry. The situation has advanced to such extreme that it does no longer need the arguments previously put forward to justify its relevance.[1,2] The proposed bio-based economy by the incorporation of renewable raw materials, in particular from the biomass, is found on the full utilisation of agricultural biomass for the production of fuels and chemicals by employing green and sustainable chemistry.[3,4] This is also true in the field of materials for which the development and study of new bio-based polymers is a growing worldwide interest.

Natural oils, such as vegetable oils provide interesting feedstock -triglyceride fatty acids- that beyond their use in food allow additional chemistry that yields opportunities for replacing petrochemicals. Fatty acids are among the most promising candidates for the preparation of polymers as they are easily accessible and present in quantity, but the rather low reactivity of their unsaturated aliphatic chains makes them ineffective monomers when used as such. However, this drawback can be overcome by functionalizing them with polymerizable moieties, for instance to introduce hydroxyl groups leading to polyols, which can be used for polyurethane synthesis.[5] Ricinoleic acid is the main fatty acid in castor oil (> 90 %) and its pyrolysis leads to 10-undecenoic acid, a key substrate in polymer chemistry for the synthesis of fully renewable Nylon-11 and other precursors for the preparation of sustainable polymers.[6,7]

Aliphatic polyesters are generally considered to be well-suited for applications as polymer-based biomaterials due to their demonstrated biocompatibility and biodegradability.[8-13] While polymeric materials based on ε-caprolactone, lactide and glycolide are currently used in numerous biomedical applications, such polyesters are limited in scope due to their hydrophobic and semicrystalline properties and the absence of functionality on the polymer backbone, which could otherwise be used for tailoring physical properties and

introducing bioactive moieties.[14] To widen the versatility of aliphatic polyesters, special efforts have been devoted to the functionalization of the polyester backbone.[15,16] Thus, different strategies *via* polymerization of functionalized monomers, post-polymerization modification or a combination of both, have been used.[17-27]

Our group is interested in extending the use of vegetable oils in the synthesis of functionalized polyesters and we recently described some works by design of specialty monomers.[28-31]

In this work, we describe an efficient synthesis of new functional biodegradable polyesters bearing hydrophilic reactive pendent groups according to the following criteria:

a) Functionality: we chose the versatile hydroxyl group as the pendent group, as it is one of the best understood organic functional groups, and many mild reactions are available for further modifications with biomolecules such as peptides.[32]

b) Easy preparations: polymerization *via* nucleophilic ring-opening of an epoxide group with carboxylic acid moiety forms the polyester backbone and the pendent hydroxyl groups in one step. An added advantage is that the reaction does not produce small molecule by-products.

c) Availabilities: the monomer precursor was prepared from bio-based low-cost reagents by a simple synthetic transformation in one step. Using renewable monomers with potential biocompatibility is not enough when sustainability is pursued and thus, their transformation in polymers must be done avoiding metallic and toxic catalyst and using benign solvents or no solvent whenever possible.

Using these criteria, the condensation of sebacic acid and their glycidyl derivatives to obtain polyesters with free hydroxyl groups has been described.[25] Moreover, approaches with AB monomers, containing both epoxy and carboxylic acid groups, using as synthetic strategy the oxirane ring opening polymerization, have also been reported.[33-35] An advantage of

utilizing an AB system for polymerization is the inherent balance of the two reactive groups in a single molecule which is desirable to minimize termination or other beside reactions.

In this contribution, we study the simple route to polyhydroxyester regarding the use of 10,11-epoxyundecanoic acid as an AB type monomer. Although, the synthesis of this polyhydroxyester has been previously reported by White et al. we believe this aliphatic polyester having secondary and primary hydroxyl functions on the backbone has a great potential as starting biobased polymer, thus, we have thought the convenience to study this polymerization in depth.[33] For this purpose, systematic variation in the reaction conditions of carboxyl-epoxy polyaddition was carried out. Insights into their fine structure of obtained polyesters are provided by ^{1}H, ^{13}C, and ^{19}F NMR spectroscopy. In addition, synthesized polyesters were characterized by means of size exclusion chromatography (SEC), FT-IR and thermal analysis.

To test the ability of these polyesters with free hydroxyl groups to prepare protein bioconjugates, three chemical modifications with N-Boc protected L-phenylalanine, L-serine and a cysteine derivative were essayed.

3.2 MONOMER SYNTHESIS

3.2.1 Synthesis of 10,11-Epoxyundecanoic acid

As introduced above, our goal is the synthesis of aliphatic polyesters based on 10-undecenoic acid by using an AB monomer capable to undergo self-polymerization. For this purpose 10,11-epoxyundecanoic acid (EUA) was synthesized from 10-undecenoic acid using H_2O_2 in presence of an enzymatic catalyst (Scheme 3.1). *Candida Antarctica* lipase B (CALB), has been demonstrated as very effective for catalysing the formation of peroxyacid which acts as reagent for double bond epoxidation.[36, 37]

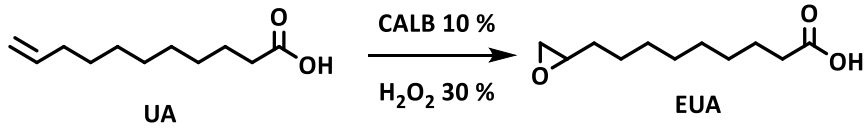

Scheme 3.1 Synthesis of 10,11-epoxyundecanoic acid (EUA).

Thus, using the procedure and work up described in the experimental part (Chapter 6.4.1), complete conversion of double bond was obtained. The resulting EUA monomer does not contain detectable amounts of hydroxyl or other impurities according to ^{1}H NMR spectroscopy (Figure 3.1 and Figure SI.1) and was used without any further purification. It must be pointed out the EUA (Figure 3.1), under dry and sealed conditions, remains stable at room temperature for more than one year.

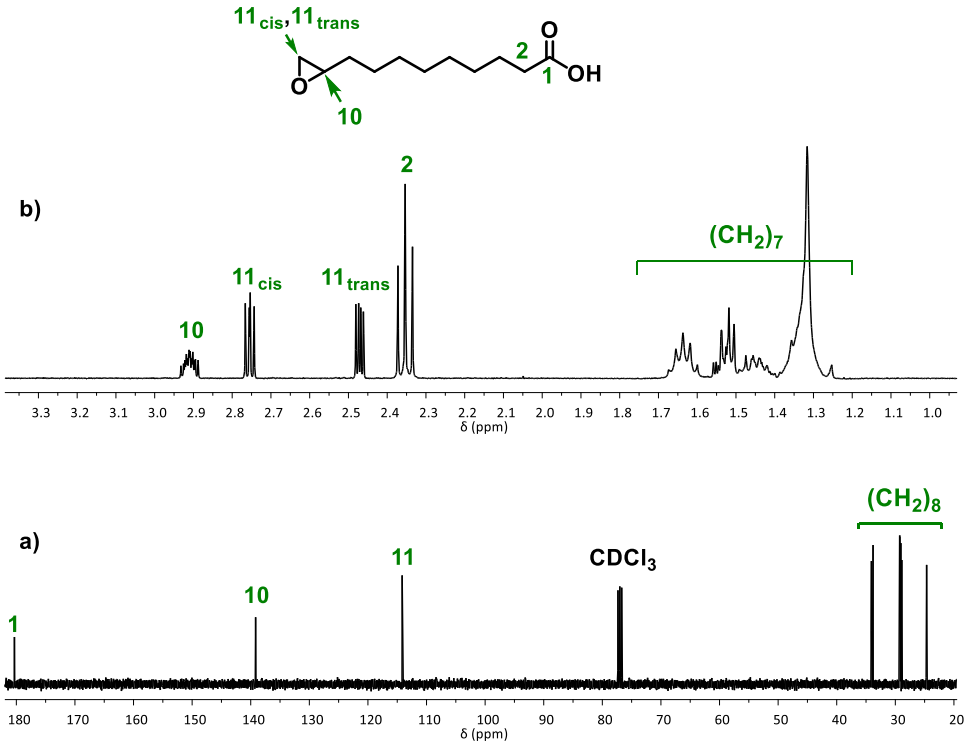

Figure 3.1 EUA monomer spectra of a) ^{13}C NMR and b) ^{1}H NMR.

3.3 MODEL REACTION

3.3.1 Reaction of 1,2-epoxyhexane and hexanoic acid

Prior to polyester preparation, the oxirane ring opening efficiency and selectivity of some catalysts were studied by reaction of 1,2-epoxyhexane (EH) and hexanoic acid (HA) in stoichiometric amounts as model reaction (Scheme 3.2).

The oxirane ring opening with carboxylic acids has been widely reported using several conventional acidic and basic catalysts.[38,39] Later, quaternary ammonium and phosphonium catalysts have been found as efficient catalyst under mild conditions.[40,41] In this reaction have been tested some of the next catalysts: $BF_3{\cdot}Et_2O$, tetrabutylphosphonium bromide (TBPB), tetraethylammonium bromide (TEAB) and 1,5,7-triazabicyclo[4.4.0]dec-5-ene (TBD).[42,43] Also, enzymatic catalysts have been extensively used in polyester synthesis.[44-46] However, although biocatalytic transformation of epoxides is well known, it has been scarcely applied to the synthesis of polyesters.[47,48] So, we also tested two enzymatic catalysts: *Candida Antarctica* immobilized on acrylic resin (5.000 U/g) (CALB) and *Candida Rugose* (CR) lipase immobilized on acrylic-epoxy resin (immobead 150) (100 U/g).

As a general trend, in a reaction of epoxy groups with carboxylic groups different consecutive reaction pathways should be expected (Scheme 3.2). The main is the direct nucleophilic attack of the carboxylic group on the oxirane ring. This reaction follows a typical S_N2 mechanism and consequently the nucleophilic attack proceeds preferentially at the less substituted carbon producing the named 'normal ring-opening' product (A).

Moreover, especially under neutral or acidic conditions, the nucleophilic attack on the more substituted carbon of the oxirane ring is also possible yielding the named "abnormal ring-opening" product (B).[39] The ratio between "normal" and "abnormal" oxirane ring opening depends on the reaction conditions, solvent polarity and more importantly on the nature of catalyst, thus, when protonic or Lewis acids are used as catalyst, the cationic

activation of the oxirane ring produces changes in selectivity increasing the attack on the more substituted carbon. These reactions do not necessarily stop here since the carboxylic acid can produce an esterification reaction with the hydroxylic group of the above ring opening products giving a diester (C) and water as products. Moreover, water can open the epoxide to give a diol (D_1). Finally, etherification reaction of all hydroxylic compounds in the media should be considered (D_2-D_5). In the last reaction stages, oxirane ring opening by water could also lead to ring opening polymerization. In this case, the signals of the resulting oligomeric polyethers should have a very close chemical shift in the ^{1}H NMR spectrum and they would be hardly to differentiate from D_2–D_5 compounds signals. All these by-side possible reactions indicate that selection of reaction conditions and catalyst is mandatory to obtain linear polyesters.

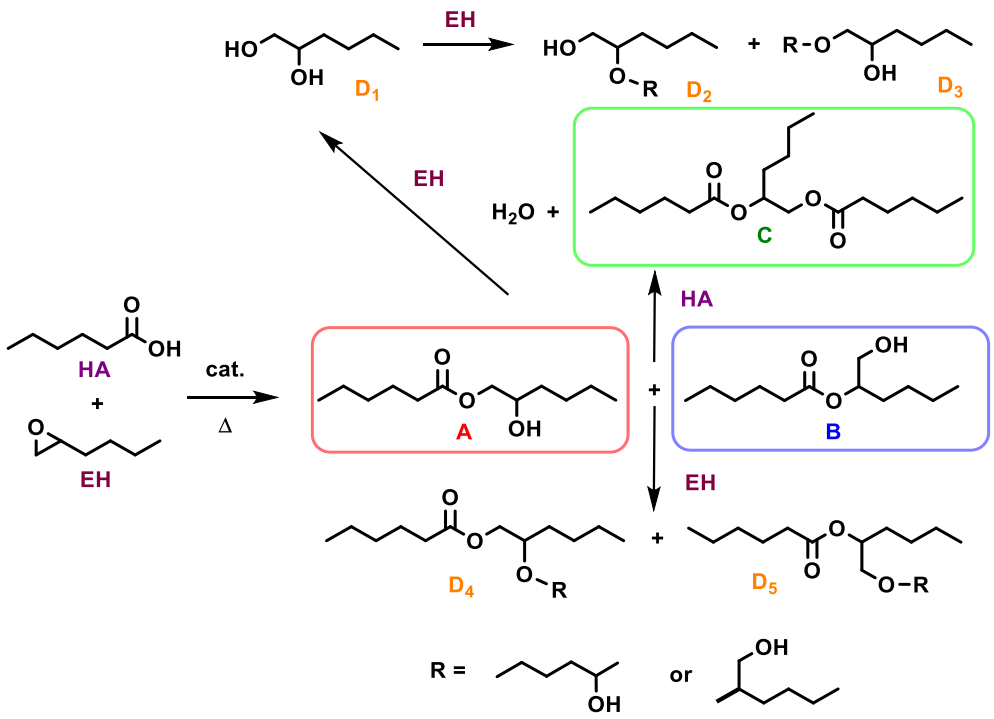

Scheme 3.2 Products in the catalysed ring opening of EH with HA in stoichiometric conditions.

The composition of the reaction mixture and the different conditions tested is collected in Table 3.1. The percentages of the different compounds were determined by ^{1}H NMR spectroscopy taking into account the assignments of the pure compounds A, B and C synthesized as model compounds (Figure 3.2 and Figure SI.2).

Derivatization with trichloroacetylisocyanate (TAI) and trifluoroacetic acid (TFAA) of A and B was carried out to determine the chemical shifts of methylene and methane signals arising from the hydroxyester moieties (Figure SI.3, Figure SI.4 and Table SI.1).[49-51]

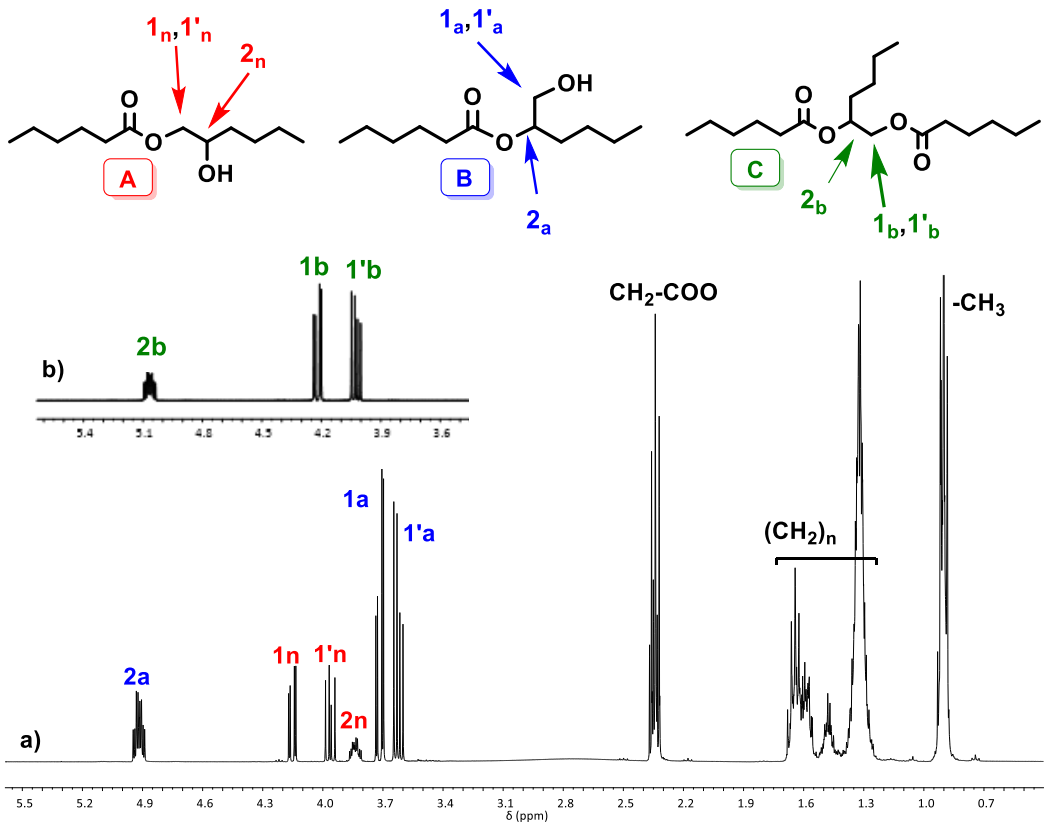

Figure 3.2 ^{1}H NMR spectra of a) A, B mixture and b) C.

Table 3.1 Composition of the crude reaction mixture in the ring opening of EH with HA.

Entry	Cat.	Solv.[a]	Conv. %[b]	A %[c]	B %[c]	C %[c]	D_2-D_5 %[d]
Conditions: 1 mol % catalyst, 100 ˚C, 24 h							
1	---	--	0	--	--	--	--
2	$BF_3.Et_2O$	--	~100	20.2	21.3	44.5	14.0
3	$BF_3.Et_2O$	Tol.	~100	13.1	15.9	25.5	45.4
4	TBD	--	93.3	40.9	27.2	11.7	20.1
5	TBD	Tol.	~100	58.2	32.3	2.8	6.7
6	TEAB	--	90.3	60.1	26.3	5.9	7.7
7	TEAB	Tol.	~100	64.3	29.3	1.1	5.3
8	TBPB	--	94.1	63.4	32.9	2.4	1.3
9	TBPB	Tol.	~100	63.4	31.8	1.2	1.0
Conditions: 10 % (w/w) enzyme, 90 ˚ C, 24 h							
10	CALB	--	~100	23.9	18.6	14.5	43.0
11	CALB	Tol.	91.7	17.5	15.8	20.7	45.9
12	CALB	DMF	96.4	60.1	29.4	3.0	7.5
13	CR	--	72.2	22.8	19.5	10.1	47.6
14	CR	Tol.	52.6	40.4	21.5	6.0	32.1
15	CR	DMF	~100	63.7	28.7	1.4	6.2

(a) Bulk or 2.5 M solution in toluene or DMF; (b) EH conversion determined by ^{1}H NMR from the signals at 2.92 and 2.76 ppm in the crude reaction mixture spectrum; (c) Percentage of A, B and C determined by ^{1}H NMR from the signals at 4.15 and 3.97 ppm (A), 3.70 and 3.65 ppm (B) and 4.20 ppm (C); (d) Percentage of ether compounds D_2 to D_5 determined by ^{1}H NMR from the signals between 3.40 and 3.20 ppm.

First, a control experiment without catalyst was carried out (entry 1). As expected no esterification occurs after 24 h at 100 °C. Next, the selected catalysts were used (1 % mol) at 100 °C for 24 h in bulk or in 2.5 M toluene solution. The classical Lewis acid $BF_3{\cdot}Et_2O$ was first tested (entries 2 and 3). As expected no regioselectivity in the ring-opening and predominance of secondary reactions were observed: esterification is favoured in bulk whereas etherification does in solution. When TBD as basic catalyst was tested (entries 4 and 5), selectivity toward normal opening increases but large amounts of diester and etherification products were observed. When ammonium (entries 6 and 7) and phosphonium salts (entries 8 and 9) were used, selectivity increases. In both cases results in toluene seem to be better reaching the lowest percentages of diester and etherification compounds. According to these results the 70:30 “normal opening/abnormal opening” ratio is the maximum selectivity reached. Moreover, ammonium salts (TBAB) seem to be less effective than phosphonium salts (TBPB) as lead to higher etherification extent. The

presence of about 30 % of units resulting from the attack of carboxylic acid on the more substituted carbon in the oxirane ring is consistent with the cationic-like activation by the onium salts.

Enzymatic catalysts CALB (entries 10–12) and CR (entries 13–15) were no selective neither in bulk nor in apolar solvent as toluene, rendering significant amounts of diester and specially etherification products. However, the polar DMF significantly improves selectivity and reduces esterification and etherification reactions although in lower extent than onium salts. It is worth to note that according to these results, these enzymatic catalysts are effective in the oxirane ring opening with carboxylic acids allowing a different approach, to prepare esters and polyesters.

3.4 POLYESTERS SYNTHESYS AND MICROSTRUCTURAL DETERMINATION

3.4.1 EUA polymerization with onium salts and CALB

In view of the above results (Table 3.1), the EUA polymerization (Scheme 3.3) have been tested using onium salts and CALB as catalysts. In Table 3.2 reaction conditions, crude composition and polyester characteristics are collected.

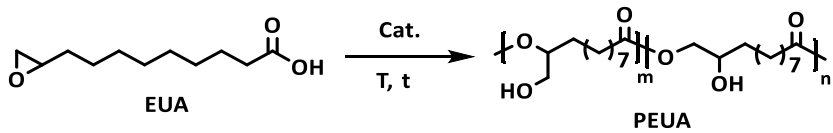

Scheme 3.3 Synthesis and polymerization of 10,11-epoxyundecanoic acid (PEUA).

In all cases, the crude polymerization mixture was analysed by ^{1}H NMR to determine the monomer conversion and next, polymers were isolated by precipitation to determine their molecular weight distribution and structural composition. The percentage of units arising from the attack to the less substituted oxirane carbon “normal ring-opening” (N_u), to the more substituted oxirane carbon “abnormal ring opening” (A_u) (not included in Table 3.2), branching by esterification (B_u) and etherification (E_u) was calculated by ^{1}H NMR

spectroscopy using the methylene and methine signals whose assignments will be commented in detail *vide infra*.

Table 3.2 Conversion, molecular weight and polyester composition obtained in the EUA polymerization.

Ent.	Cat.	Solv.	T(h)	Conv. %[a]	IF %[b]	SF %[c]	Mn[d]	Đ[d]	N_u %[e]	B_u %[e]	E_u %[e]
Conditions: 1 mol % catalyst, 100 ˚C (bulk or 2.5 M in toluene)											
1	--	--	8	70.0	--	[(f)]	--	--	--	--	--
2	TEAB	--	2	86.2	--	67.8	4110	2.9	60.9	3.2	4.9
3	TEAB	--	4	~100	--	92.2	4950	3.0	58.0	6.0	11.2
4	TBPB	--	2	91.9	--	87.7	4350	2.0	67.7	--	--
5	TBPB	--	4	~100	--	96.4	9050	3.0	68.7	--	--
6	TBPB	--	8	~100	30.2	67.2	14250	4.5	59.2	4.0	--
7	TBPB	Tol.	2	98.0	--	88.2	6030	2.3	69.8	--	--
8	TBPB	Tol.	4	~100	--	97.0	7560	3.3	68.6	--	--
9	TBPB	Tol.	8	~100	--	96.8	8570	3.5	70.3	--	--
10	TBPB	Dowanol	8	93.5	--	94.2	6360	2.6	78.6	0.4	--
Conditions: 10 % (w/w) catalyst, 90 ˚C (2.5 M in DMF)											
11	CALB	DMF	2	47.2	--	21.7	1000	1.5	36.9	26.2	13.7
12	CALB	DMF	4	53.9	--	26.9	1810	2.0	42.3	21.5	12.2
13	CALB	DMF	8	73.9	--	55.9	2300	1.9	41.8	16.5	13.8
14	CALB	DMF	12	84.3	--	63.5	2630	1.7	43.6	13.8	16.4
15	CALB	DMF	48	100	--	72.4	3480	1.8	51.7	--	17.1

(a) Conversion of EUA calculated by ^{1}H NMR from the crude mixture; (b) Insoluble fraction in THF; (c) Polymer isolated from the soluble THF fraction; (d) Determined by SEC (g·mol^{-1}); (e) Percentage of normal (N_u), branched (B_u) and ether (E_u) units determined by ^{1}H NMR from the signals at 4.15 and 3.97 ppm (A), 3.70 and 3.65 ppm (B), 5.1 and 4.20 ppm (C) and 3.40 to 3.20 ppm (E); (f) dimer and trimer species.

First, a blank experiment without catalyst was carried out (entry 1, Table 3.2). After 8 h, 70 % of EUA was consumed but no polymer could be isolated. The analysis of the crude showed mainly the formation of dimeric species. With TEAB in bulk (entries 2 and 3, Table 3.2), 4 h were necessary to achieve complete conversion. Oxirane ring opening occurs with good regioselectivity but percentages of B_u and E_u increase with time. However, when TBPB was used at the same reaction times (entries 4 and 5, Table 3.2), conversions were similar but molecular weight was higher at 4 h and no B_u or E_u were detected indicating a linear structure. Attempts to increase Mn, by polymerizing during 8 h (entry 6, Table 3.2) led to a significant insoluble fraction and the soluble fraction showed B_u or E_u, indicating post-polymerization reactions such as transesterification.

The same conditions with this catalyst in toluene solution (entries 7, 8 and 9, Table 3.2) showed a similar behaviour but in all cases, soluble polymer without branching or ether links was obtained. For all onium catalysts, molecular weights and polydispersity index increase with reaction time as consequence of internal transesterification reactions. Referring to percentage of normal opening, this remains practically constant (about 70 %) except when branching occurs due to further esterification. The polymerization of EUA with tetraphenylphosphonium bromide and tetrabutylammonium bromide has been reported at higher temperatures (140 °C) and using Dowanol PMA™ (propylene glycol monomethyl ether acetate) as solvent. Under these conditions, polyesters with Mn 13000-30000 $g \cdot mol^{-1}$ and polydispersity (Đ) 3.7-13 were obtained.[33] We tested this solvent with our polymerization conditions (entry 10, Table 3.2) and obtained polyesters with narrower distribution but lower molecular weights.

Enzyme catalysed polyesterifications can proceed either in bulk or in solution. Solvent hydrophobicity usually plays an important role in enzymatic activity as hydrophilic polar solvents such as DMF or dimethyl sulfoxide (DMSO) cause considerable modification in enzyme conformation decreasing catalytic activity of lipase.[52] In our case, as observed in the model study (Table 3.1), the formation of ester linkages in DMF is clearly favoured, but we have to point out that in this case ester formation arises from the nucleophilic attack

on the oxirane ring by the carboxylic acid group, which is favoured by polar aprotic solvents. It must be point out that a blank experiment in DMF without CALB at 90 °C showed scarce oligomerization after 24 h, indicating that CALB plays a determining role. This reaction has not been reported for CALB, but other enzymes such as halohydrin dehalogenases are effective in oxirane ring opening with other nucleophiles such as azide and cyanide anions.[53]

Working with CALB in bulk and in toluene confirmed the model reaction results giving poor monomer conversion. In DMF solution (entries 11-15, Table 3.2), polymerization proceeds slowly to give lower polymer yields and lower Mn when compared to TBPB. Long-time reaction (48 h) (entry 15, Table 3.2) was necessary to reach 100 % conversion. Remarkably, structure of all polyester contains both branched polyester and polyether linkages. Whereas low conversion gives branched polyesters, longer times and conversions produce extensive etherification. This probably is due to the fact, that ester linkages formed can undergo a reverse reaction, catalysed also by lipase, in a similar way than equilibrium condensation reactions.[46] Thus, the resulting free hydroxyl groups can react with the epoxy groups of the unreacted monomer yielding polyether linkages in an irreversible process (Scheme 3.4). These transesterification and etherification reactions lead to polymers with a significant lower molecular weight and polydispersity when compared to those obtained with onium salts. This fact is probably due to differences on fractionation during isolation processes.

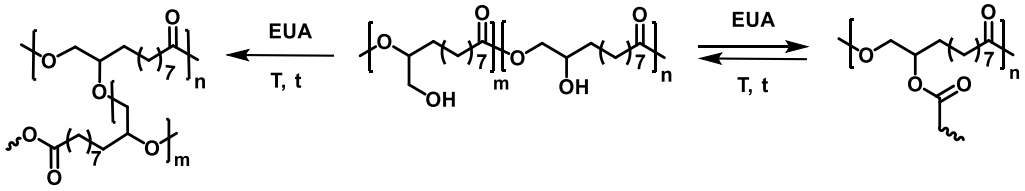

Scheme 3.4 Transesterification-etherification reactions in the polymerization of EUA with CALB in DMF.

According of these results, TBPB was considered the most suitable catalyst to obtain linear polyesters, and a kinetic study was carried out with different concentration of catalyst and

different temperatures in order to find out the better reaction conditions. Thus, the kinetic study was performed in toluene (100 °C), ethylbenzene (130 °C) and cumene (150 °C).

Figure 3.3 presents the evolution of monomer conversion and polymer molecular weight against time, calculated by ^{1}H NMR and SEC respectively. First, as expected, polymerization proceed much faster at 130 °C and 150 °C reaching complete conversion before 2 h. Thus, the effect of catalyst concentration was studied at 100 °C and a significant polymerization rate increase was observed when increasing TBPB from 0.5 % to 2 % (Figure 3.3 a).

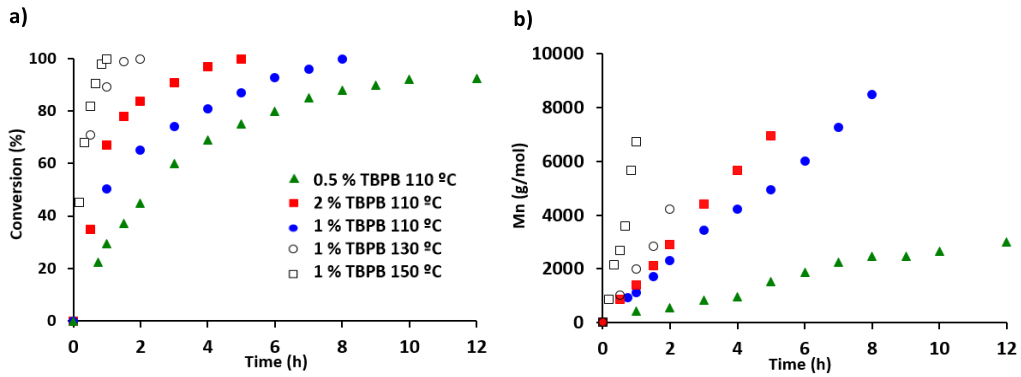

Figure 3.3 Polymerization of EUA with different TBPB concentrations and different temperatures: a) Conversion versus time, b) variation of M_n versus time.

The effect of temperature and catalyst concentration is also remarkable in molecular weights (Figure 3.3 b). As a general trend, either increasing catalyst concentration (0.5 to 2 %) or increasing temperature at (100 ˚C to 150 ˚C) produce a progressive and almost linear increase in Mn. Noteworthy, maximum molecular weights are reached using 1 % of catalyst at 100 °C. However, after the complete monomer conversion, longer polymerization times (not shown in Figure 3.3 b), seems to favour transesterification processes leading to branching, increasing molecular weight, and finally to the formation of increasing amounts of insoluble material. In polymerizations at 100 ˚C, this behaviour was significant after 12 h and 6 h when 1 % or 2 % of TBPB was used respectively. Higher temperatures (130 ˚C and 150 ˚C) accelerate even more these processes and significant amounts of insoluble crosslinked fraction were detected after only 6 h.

The progressive increase of the molecular weight can be followed by the evolution on the SEC traces versus conversion on the EUA polymerization with 1 % of TBPB at 100 °C (Figure 3.4). Molecular weights progressively increase up to Mn = 8600 g·mol^{-1} at 8 h when monomer is completely consumed. At 12 h, insoluble fraction was formed and the soluble fraction shows a higher Mn = 14500 g·mol^{-1}.

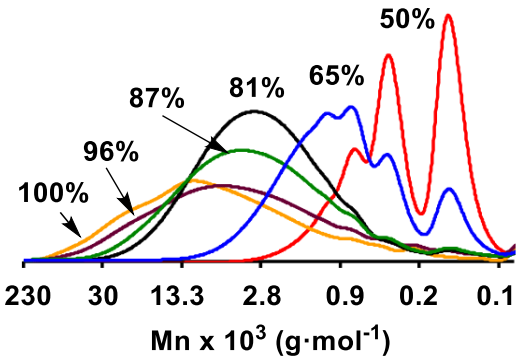

Figure 3.4 Molecular weights distributions according SEC traces for different monomer conversion on the EUA polymerization (1 % of TBPB in toluene at 100 °C).

With all this information in hand, the EUA scaled polymerization (10.0 g, 50.0 mmol) was carried out with 1 % of TBPB in a 2.5 M solution in toluene at 100 °C for 8 h (entry 9 in Table 3.2). In this way, a white polymer with a linear chain structure (PEUA-1) with Mn 9800 g·mol^{-1} and Đ 3.4 was obtained in 87 % yield. Moreover, for comparative purposes samples of partially branched (PEUA-2) and insoluble crosslinked polyester (PEUA-3) were prepared using 1 % of TBPB in bulk at 100 °C for 8 h (entry 6 in Table 3.2). Thus, starting from 2.0 g, 10.0 mmol of EUA, after fractionation in THF, a soluble polymer fraction with Mn 12400 g·mol^{-1} and Đ 4.1 (62 % yield) and an insoluble fraction (28 % yield) were obtained.

Molecular weights of all obtained linear and low branched hydroxypolyesters are in the range of 8.0–13.0 x 10^3 g · mol^{-1} which is quite low for most structural and engineering applications. However, a key issue for the potential applications of these hydroxypolyesters relies on the pendant hydroxyl free groups. The presence of these reactive groups together with low molecular weight of the linear or branched polyesters allows straight introduction

of diverse active biomolecules under mild conditions. Additionally, further modifications would allow molecular weight increasing obtaining reticulate materials with modulate final mechanical, thermal, chemical and biological properties. In fact, the beneficial effect of the hydroxyl pendant groups has been demonstrated improving polymer degradability in both hydrolytic and enzymatic media when compared with conventional polyesters such as poly(ε-caprolactone) and poly(11-hydroxyundecanoate) (see Chapter 4).

3.4.2 PEUAs microstructural characterization

In Figure 3.5, the region between 3.2 and 5.6 ppm of ^{1}H NMR spectra of linear PEUA-1 and partially branched PEUA-2 is shown. A representative general structure of these polyesters including the three possible different repetitive units arising from the attack to the less substituted oxirane carbon "normal ring-opening" (N_u), to the more substituted oxirane carbon "abnormal ring opening" (N_a), branching through transesterification, and the chain ends is also included. It must be pointed out that transesterification occurs either through primary or secondary alcohols giving non-distinguishable by NMR branching units.

The ^{1}H NMR spectra signals corresponding to the methine and methylene protons of the different units, named with the subscript n, a and b for "normal", "abnormal" or "branched" respectively, were unequivocally assigned by comparison with the methylene and methine signals of model compounds A, B and C (Figures 3.2 and Figure SI.2), and their corresponding trichloroacetylisocyanate (TAI) (Figure SI.3) and trifluoroacetic anhydride (TFAA) derivatives (Figure SI.4). Moreover, 10,11-dihydroxy-undecanoic acid was used as model for the polymer chain end groups (Figure 5.1 in Chapter 5).

The content of "normal", "abnormal" and "branched" units in PEUA-1 and PEUA-2 was determined by comparing the intensity of the integration of the corresponding ^{1}H and ^{19}F NMR signals of the pristine and their trifluoroacetylated derivatives (Table 3.3, Figure 3.6).

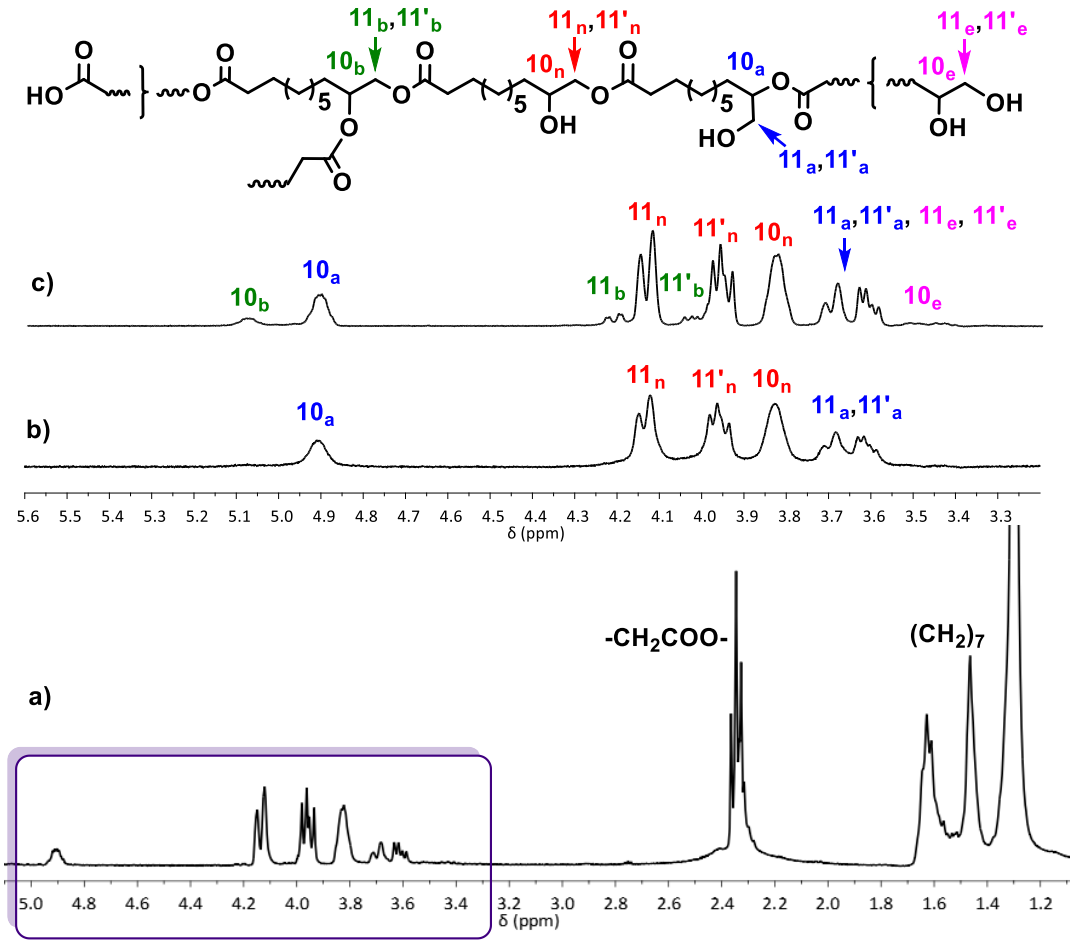

Figure 3.5 a) ^{1}H NMR PEUA; b) Region between 3.2 and 5.6 ppm of ^{1}H NMR spectra of PEUA-1; c) Region between 3.2 and 5.6 ppm of ^{1}H NMR spectra of PEUA-2 and the corresponding assignments in a representative structure.

Table 3.3 Quantifications of the different units (%) in PEUA-1 and PEUA-2 and their corresponding trifluoroacetates by ^{1}H NMR and ^{19}F NMR.

Polyester	^{1}H NMR				^{19}F NMR
	PEUA-1	PEUA-2	PEUA-1 TFA	PEUA-2 TFA	PEUA-1 TFA
n	71.1	63.9	66.7	61.7	66.5
a	28.6	28.4	33.2	30.8	33.5
b	< 0.5	7.6	< 0.5	7.5	--
e	--	1.6	--	--	--

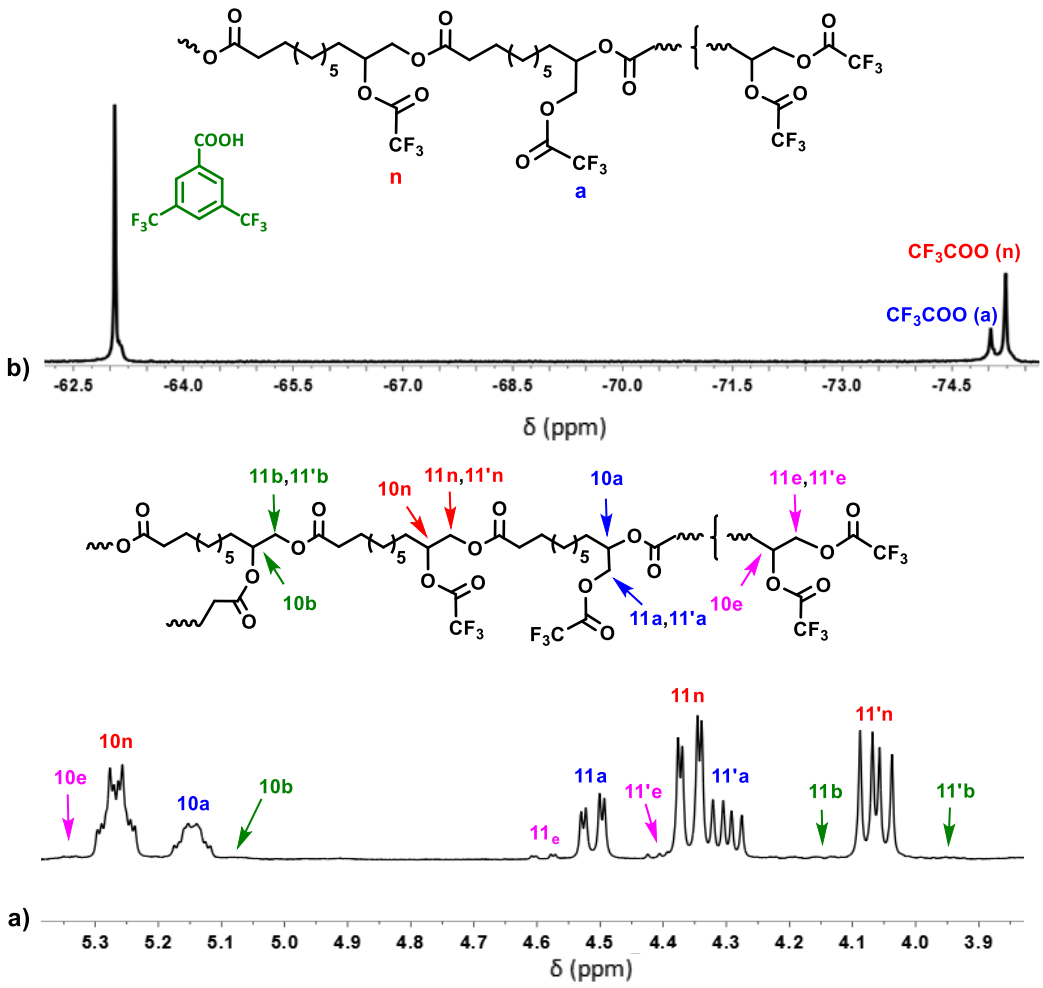

Figure 3.6 Spectra of a) ^{1}H NMR spectrum of PEUA-2 trifluoroacetate and b) ^{19}F NMR spectrum of the PEUA-1-trifluoroacetate and 3,5-bis(trifluoromethyl)benzoic acid mixture.

For linear PEUA-1, about 71 % of normal units were determined from the pristine polyester and a lower value (~67 %) from their TFA derivative, probably due to the signals of the TFA end groups are not included. In both cases, only a negligible number of branched units (less than 0.5 %) was detected. For PEUA-2, 62–64 % of "normal" units and 7.5 % of branched units were determined. These measurements confirm that, under the studied conditions and using onium salts as catalyst, the maximum selectivity toward the ring opening by attack to the less substituted oxirane carbon is about 70 %.

The absolute content of primary and secondary hydroxyl groups in PEUA-1 was determined by integration of the ^{19}F NMR signals using accurately weighted amounts of trifluoroacetylated PEUA-1 and bis (trifluoromethyl)benzoic acid as internal standard (Figure 3.6 b). In this way, 0.169 and 0.353 of primary and secondary hydroxyl equivalents per 100 g of polymer were determined (Figure 3.6 and equation 6.2 from Chapter 6). According to a linear structure and one hydroxyl group per repeating unit, it is possible to roughly estimate a Mn of 4000 $g \cdot mol^{-1}$ for this sample (equation 6.3 from Chapter 6), which is about one half of that determined by SEC (9800 $g \cdot mol^{-1}$).

Molecular weights determined by SEC are over or under estimated as consequence of differences in the hydrodynamic volume with the polystyrene standards used in the calibration. Thus, to validate the actual molecular weight, it was also calculated from the carboxylic end group by derivatization as methyl ester using trimethylsilyldiazomethane ($TMS\text{-}CHN_2$) (Figure 3.7 and equation 6.4 from Chapter 6). Thus, by comparing the ^{1}H NMR signal intensity of the methyl ester in the end group and the α-methylene in the repeating units, Mn of 4300 $g \cdot mol^{-1}$ was estimated which is in good agreement with the previous measurements and indicates that hydrodynamic volume of these polyesters in THF is greater than PS.

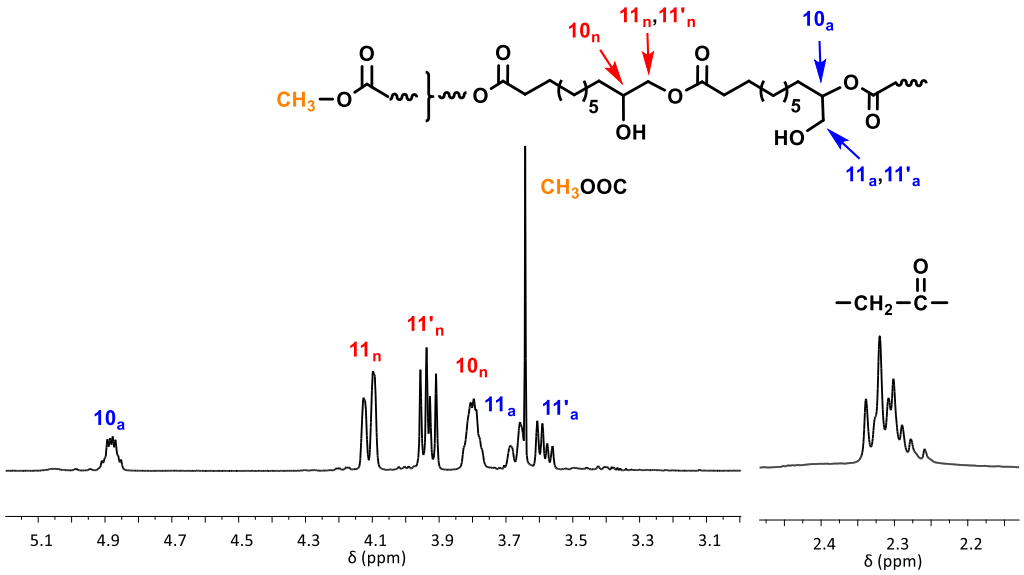

Figure 3.7 ^{1}H NMR of PEUA-TMS-CHN_2 derivative.

PEUAs ^{13}C NMR spectra assignments (Figure 3.8) were also undertaken by comparison with those of models A, B and C and ^{1}H–^{13}C heteronuclear bidimensional correlations (Figure SI.5). The methane and methylene carbons of the "normal" (70.1 and 68.7 ppm respectively) and "abnormal" (75.4 and 64.9 ppm respectively) units appear with different intensity sustaining the presence of about 70 % of normal units. Interestingly, ester groups in both units can be also differentiated by C=O signals at 174.5 ppm and 174.2 ppm, respectively. In the case of the spectrum of branched PEUA-2, four additional small signals appear: at 71.2 and 64.1 ppm assigned to the methine and methylene carbons of the branched units, and at 72.4 and 66.9 ppm assigned to the methine and methylene carbons of the diol end groups.

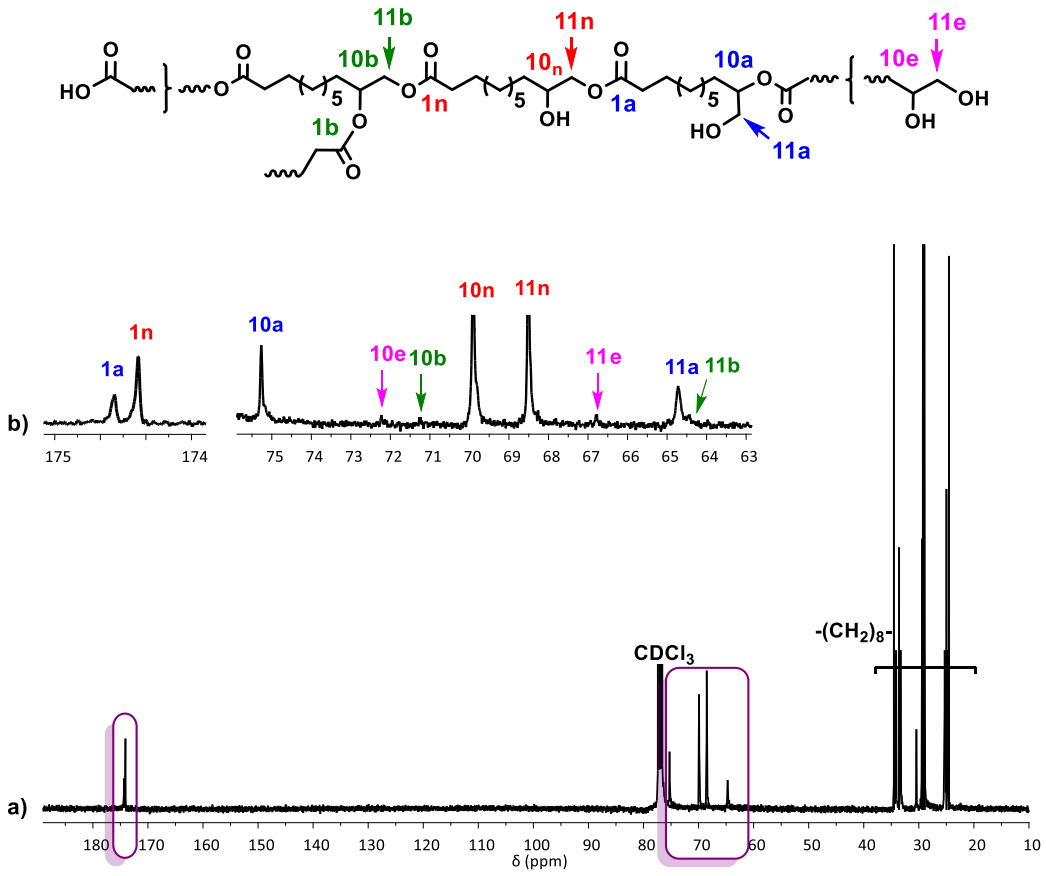

Figure 3.8 ^{13}C NMR spectra of a) PEUA-1, b) PEUA-2 (both recorded in $CDCl_3$).

As commented above EUA polymerization in bulk with TBPB at 8 h (entry 6 in Table 3.2) led also to the formation of some gel insoluble fraction (IF). Longer reaction times increase the content of this insoluble fraction up to 100 % at 4 days, presumably due to intramolecular transesterification reactions take place. So, to unravel the nature of the side cross-linking reactions ^{13}C NMR spectrum of the insoluble material was recorded as swollen gel in TCE-d_2 (Figure 3.9). The spectrum shows significant differences when compared to that of a linear PEUA-1 (Figure 3.8 a). In the carbonyl region, in addition to the signals at ca. 175.1 ppm and 165.6 ppm corresponding to “normal” and “abnormal” units, three additional signals are detected. A pair of signals having similar intensity, at 162.8 and 162.4 ppm

attributed to the branching units by comparison with the spectrum of a soluble branched PEUA sample, confirms the branching by transesterification. The third and more intense signal at 180.7 ppm can be attributed to free carboxylic group and could be related to etherification processes as signals at 78–82 ppm, characteristic of methine carbons in polyether chains, are also observed.[54]

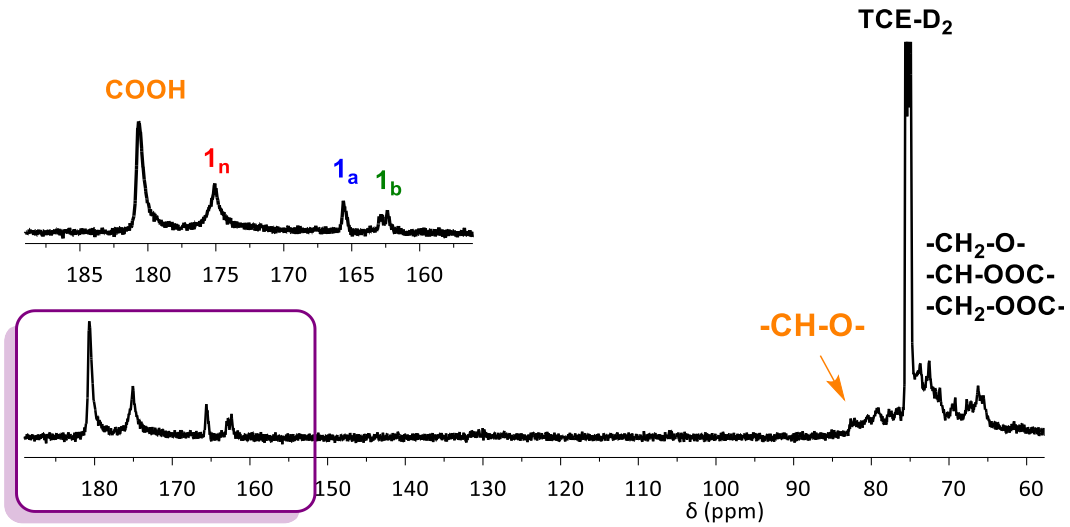

Figure 3.9 ^{13}C NMR spectra of PEUA-3 (recorded in TCE-D_2 as swollen gel).

These transesterification and etherification reactions were also confirmed by FTIR spectroscopy. In Figure 3.10, the spectrum of soluble PEUA-1 (top) shows the characteristic stretching vibration of hydroxyl groups at 3300 cm^{-1} and only a single carbonyl ester band at 1727 cm^{-1}. In the spectrum of insoluble PEUA-3 (bottom), the alcohol hydroxyl band disappears and a broad band at 3200–2500 cm^{-1}, characteristic of COOH, together with a new carbonyl band at 1707 cm^{-1} appear. Moreover, a new intense band at 1095 cm^{-1} indicates the presence of C-O-C ether linkages.

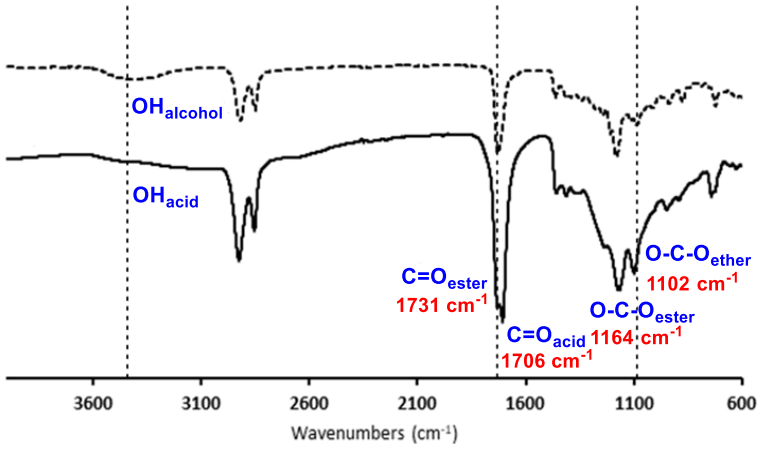

Figure 3.10 FT-IR spectra of PEUA-1 (top) and PEUA-3 (bottom).

According to these results, both transesterification and etherification reactions are responsible of the progressive cross-linking, when high temperatures or long polymerization times were used with TBPB, and indicate that an accurate control of polymerization conditions is mandatory to obtain linear polyesters. The first reaction (a in Scheme 3.5) involves the nucleophilic displacement of alkoxy groups giving new ester linkages leading to branching in a reversible way. The second one (b in Scheme 3.5) involves the nucleophilic displacement of alkoxycarbonyl leading to the formation of ether linkages and carboxylic acid moieties, in an irreversible way. These processes, including the direct etherification between two hydroxyl moieties, have been recently described for hyperbranched polyesters.[55]

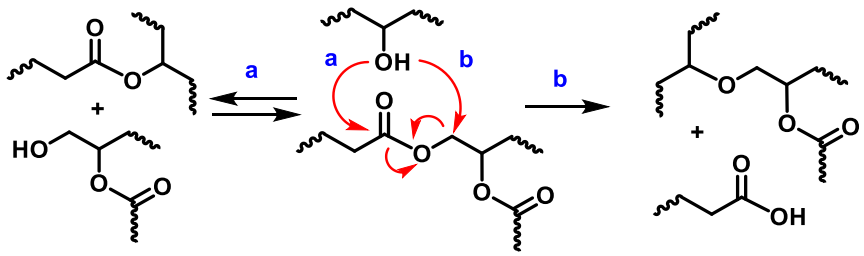

Scheme 3.5 Transesterification-etherification crosslinking reactions in the polymerization of EUA with TBPB.

It is worth to note that PEUA obtained with CALB in DMF also contained different percentages of etherification (determined by methane protons at 3.40–3.20 ppm in the ^{1}H NMR spectra).[56] However, in this case, ether formation most probably arises from oxirane ring opening as etherification is detected from the early stages of the polymerization when EUA is present.

The thermal behaviour of PEUAs has been examined by differential scanning calorimetry (DSC) and thermal gravimetric analysis (TGA) (Table 3.4). A DSC analysis was carried out in order to appraise the behaviour of the synthesized polyesters regarding reversible thermal transitions. Both PEUA-1 and PEUA-2 were found to be semicrystalline showing a double melting peak at ca. 85 and 99 °C in the first heating. However, the associated melting enthalpy is higher in PEUA-2 indicating a greater influence of sample molecular weight over its structure. In the second heating, melting temperatures and enthalpies decrease notably, but sample with higher molecular weight shows a higher crystallinity. The high melting point and crystallinity can be accounted by intermolecular interactions caused by the possible intermolecular hydroxyl bonds between two neighbouring hydroxyl and hydroxyl or carbonyl groups that can stabilize the aggregated solid crystalline structure. Tg values are the same in both polyesters (-16 °C) and fall into the range of polyhydroxyalkanoates.[57] Different behaviour is observed for PEUA-3, in which neither Tg or Tm is detected due to its cross-linked structure.

TGA traces PEAU-1 and PEUA-2 show that decomposition process happens in two main steps with maximum rates at temperatures of 385–390 °C and 462 °C, respectively. For PEUA-3, probably the ether linkages in its structure produce an increase in thermal stability, and maximum rates of both steps appear at higher temperatures. In all cases, the first peak contributing about 40 % weight loss corresponds to the decomposition of the ester bonds. The second peak could be related to the presence of hydroxyl groups leading to a progressive crosslinking on heating by dehydration/etherification reactions, as thermal degradation of aliphatic polyesters without reactive pendant groups, usually occurs in one main single step.[58]

Table 3.4 Thermal properties of PEUAs.

Sample	SEC[a]	DSC[b] 1st heating		DSC[b] 2nd heating			TGA[c]	
N_U/B_U %	Mn (Kg·mol^{-1})	Tm (°C)	ΔH (KJ·mol^{-1})	Tg (°C)	Tm (°C)	ΔH (KJ·mol^{-1})	$T_{5\%}$ (°C)	T_{max} (°C)
PEUA-1[d]	9.8	84/99	8.3	-16	35	5.6	341	386/462
PEUA-2[e]	12.4	86/98	16.6	-16	44	7.4	334	392/462
PEUA-3[f]	--	--	--	--	--	--	360	408/470

(a) Mn (Kg·mol^{-1}) determined by SEC. (b) DSC traces recorded under nitrogen atmosphere: Glass transition temperature (Tg) taken as the inflection point of the heating DSC traces recorded at 10 °C·min^{-1}.; melting temperature (Tm) and their enthalpy (ΔH) measured at heating rates of 10 °C·min^{-1}. (c) TGA traces recorded under nitrogen atmosphere at 10 °C·min^{-1}: ($T_{5\%}$) temperature of 5 % weight loss, (T_{max}) temperature of maximum degradation rate; (d) PEUA-1: 71 % N_U; (e) PEUA-2: 64 % N_U, 7.5 % B_U; (f) PEUA-3: insoluble crosslinked polyester.

3.5 POST-POLYMERIZATION MODIFICATION OF PEUA

The synthesized polyesters bearing reactive hydroxyl pendant groups are expected to be easily functionalized to ester function by reaction with acid or its derivatives. Alternatively, the hydroxyl groups can react with succinic anhydride to provide a polyester bearing active carboxylic groups thus investing the polymer reactivity. To demonstrate the potential ability to use these hydroxylic and carboxyl groups for biofunctionalization we investigated the coupling reaction between PEUA and PEUA-succinate respectively with three protected amino acids: phenylalanine, cysteine and serine derivatives as representatives for biomolecules (Scheme 3.6).[25]

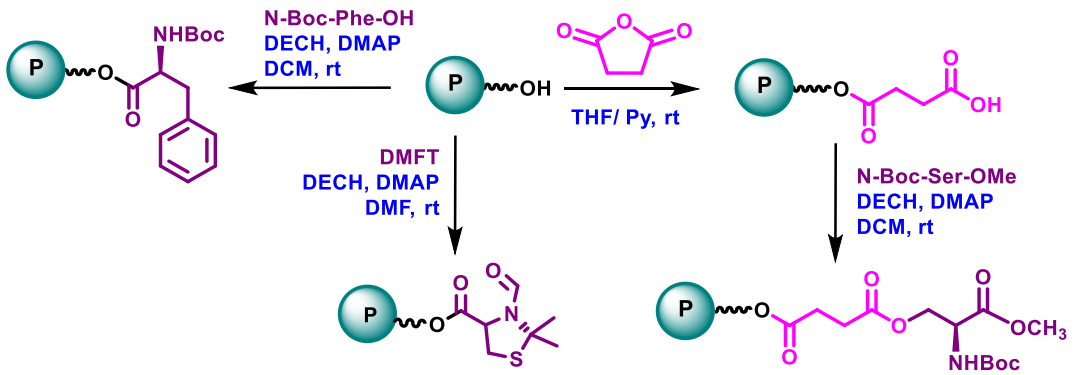

Scheme 3.6 Post-polymerization modification of PEUA-1.

PEUA-1 reacted with N-*tert*-butoxylcarbonyl (Boc)-protected phenylalanine in presence of excess of DECH and a catalytic amount of DMAP at room temperature to give PEUA-phenylalaninate (81 % yield). Its ^{1}H and ^{13}C NMR spectra and the corresponding peak assignments made on the basis of the starting reagents, are shown in Figure 3.11.[59] Polyester hydroxyl modification took place in a considerable extent (88-90 %) which was calculated by comparing the integration of the ^{1}H NMR signals of H_b and H_c,H'_c in the Boc-phenylalanine moiety, and those of α-methylene to carbonyl in polyester repeating units (signal noted 2 in Figure 3.11 a). It is worth to note, that protons H_b and H_c,H'_c appear as two different signals due to the presence of syn and anti rotamers (Figure 3.11 a).[60,61] From the relative intensity of these signals, $H_{b\ syn}$ (4.57 ppm), $H_{b\ anti}$ (4.40 ppm), H_c $H'_{c\ syn}$ (3.11-3.02 ppm) and H_c $H'_{c\ anti}$ (2.82 -2.76 ppm), about 84 % of "syn" configuration could be determined at the ^{1}H NMR recording conditions. ^{1}H NMR spectrum also shows small signals at 3.70-3.40 ppm attributable to unreacted polymer units (marked with an asterisk). ^{13}C NMR spectrum (Figure 3.11 b) shows differentiated signals for methines and methylenes of the normal and abnormal modified units (10_n, 11_n, 10_a and 11_a) but also signals of the remaining unmodified units (marked with an asterisk) can be observed. In this spectrum, only methine b appears unfolded due to the existence of syn-anti rotamers.

PEUA-1 reacted with 2,2-dimethylthiazolidin-3-(N-formyl)-4-carboxylic acid (DMFT) in presence of excess of DECH, DMAP and DMF as solvent, at room temperature to lead PEUA

modificated with protected L-cysteine (86 % yield). Its ^{1}H and ^{13}C NMR spectra and the corresponding peak assignments made on the synthetized starting reagent: 2,2-dimethylthiazolidin-3-(N-formyl)-4-carboxylic acid (Figure SI.6 and Figure SI.7) are shown in Figure 3.12.[62-64] Polyester hydroxyl modification was practically complete as observed by ^{1}H NMR and ^{13}C NMR spectra (signals noted in Figure 3.12). The methines and methylenes of the normal and abnormal units (10_n, 11_n, 10_a and 11_a) disappear signals (at 4.90 ppm and 4.2-3.35 ppm). In ^{13}C NMR appear duplicate signals due to the presence of syn and anti rotamers of protected L-cysteine (Figure 3.12 b). The anti rotamer is the most abundant, around 90 % of "anti" configuration as can be estimated from the relative intensities of the corresponding signals in the ^{13}C NMR spectrum.

PEUA-1 reacted with excess of succinic anhydride in a mixture of DCM and pyridine at room temperature to produce PEUA-succinic monoester in good yield. Their ^{1}H and ^{13}C NMR spectra (Figure 3.13) confirm the introduction of the succinate groups but some signals of remaining unreacted units were still detectable. From their relative intensity of this signals a modification degree of ca. 88 % was estimated.

This PEUA-succinic monoester reacted with N-*tert*-butoxylcarbonyl-protected serine methyl ester (N-Boc-SerOMe) in presence of excess of DECH and a catalytic amount of DMAP in similar conditions as employed for the phenylalanine derivative. The corresponding serine PEUA-succinate was isolated in 64 % yield. Its ^{1}H and ^{13}C NMR spectra and the corresponding peak assignments made on the basis of the starting reagents, are shown in Figure 3.14.

The spectra show the complete incorporation of the N-Boc-serine methyl ester to the succinic residues. No free carboxyl group were detected but the signals of original unmodified hydroxyl units can be observed (signals at 4.1 and 3.9 ppm in ^{1}H NMR and signals at ca. 69 and 67.5 ppm in ^{13}C NMR). Noteworthy, succinic groups seem to decouple the motions of the serine moieties from the polyester backbone thus resulting a simpler ^{1}H NMR spectrum with no evidence of rotamers.

Referring to the modified polyesters molecular weights in all cases were higher than the starting PEUA-1 (9800 g·mol^{-1}) and were in good agreement with the expected mass increase and the high modification degrees. All modified polymers showed narrower molecular weight distributions probably due to fractionation during the polymer isolation and purification.

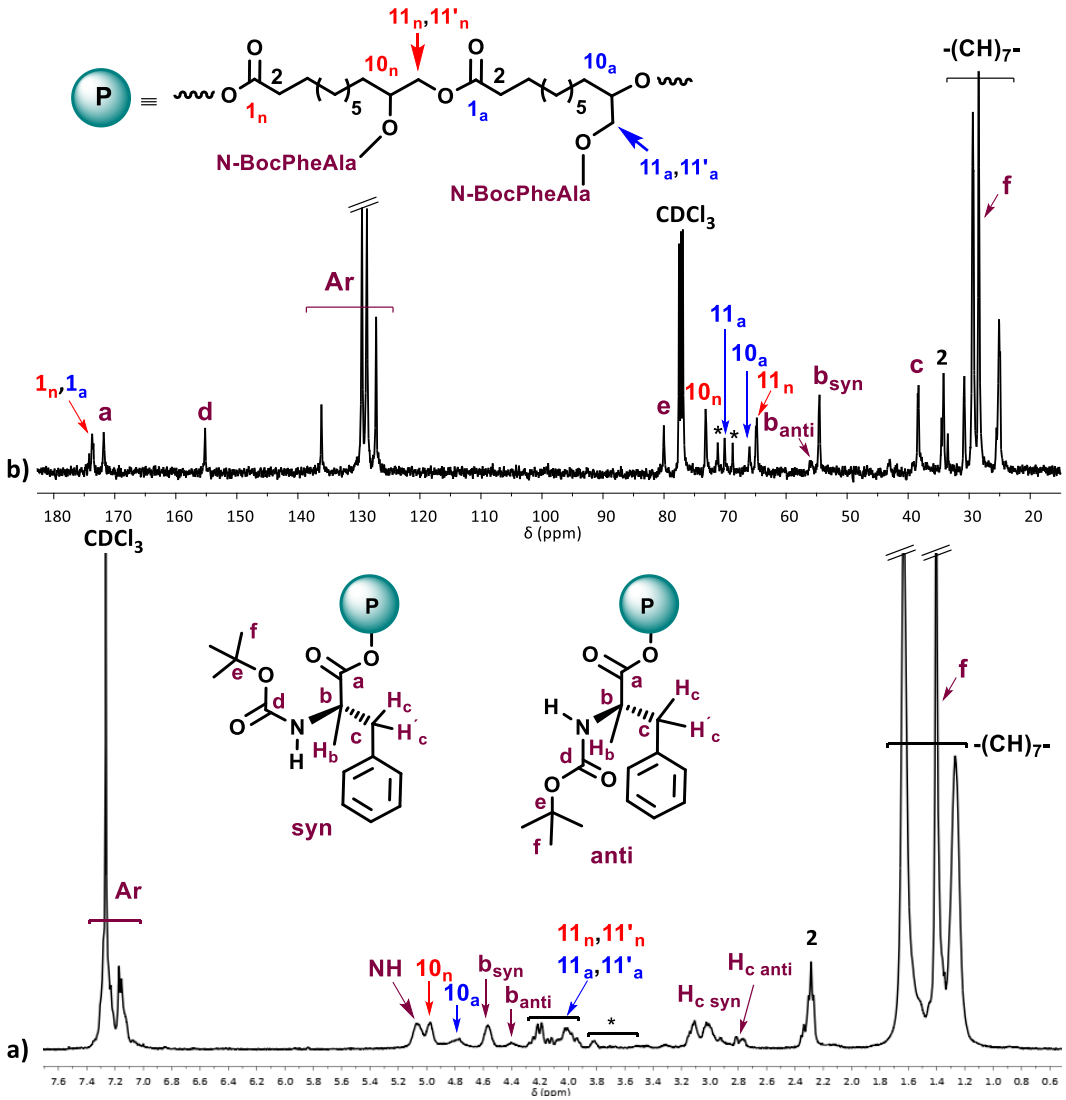

Figure 3.11 a) ^{1}H and b) ^{13}C NMR spectra of PEUA modified with N-Boc-Phe-OH. Signals of unmodified PEUA-1 are designed with one asterisk.

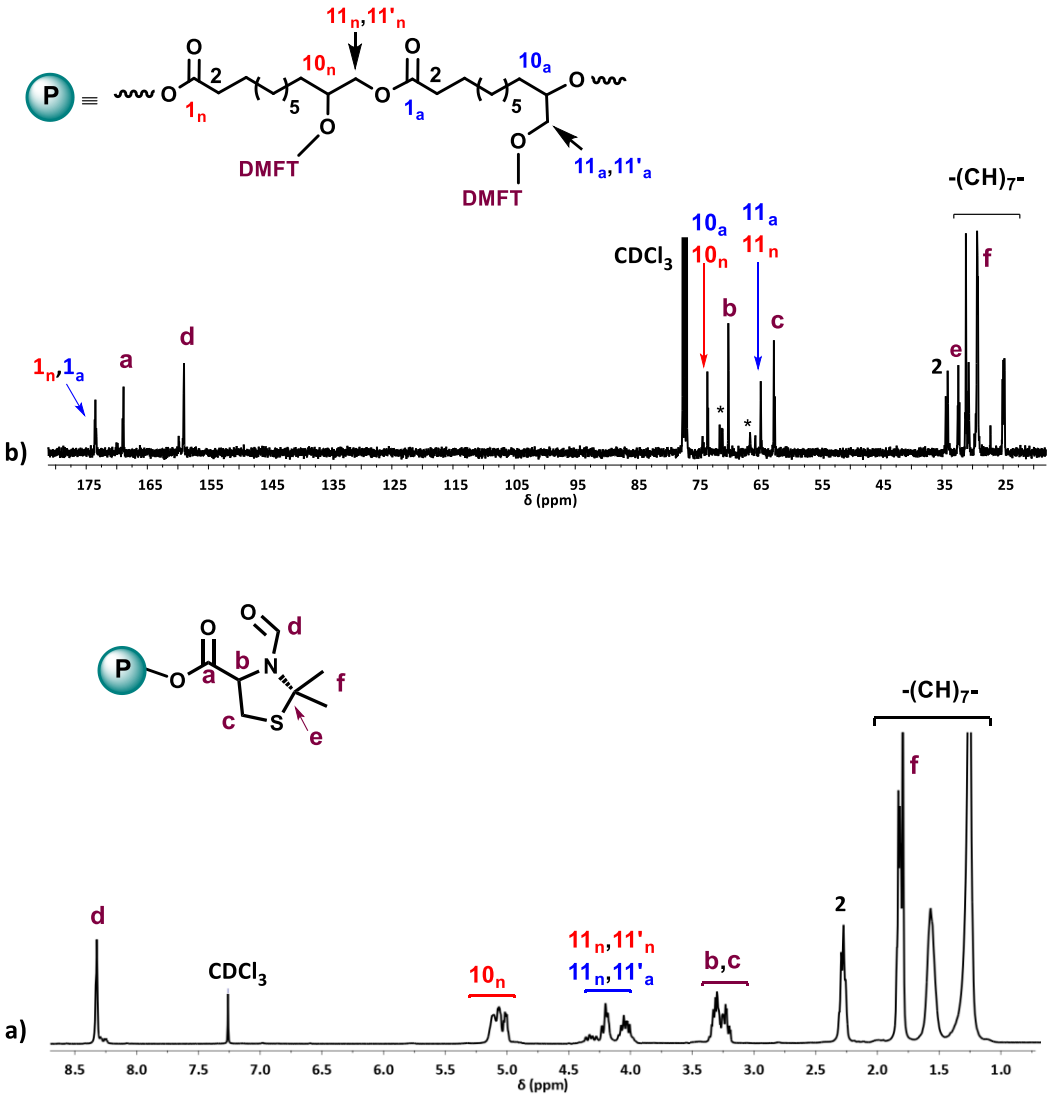

Figure 3.12 a) ^{1}H NMR of PEAU-1-DMFT and b) ^{13}C NMR spectra of PEUA-1- DMFT. Signals of syn rotamer are designed with one asterisk.

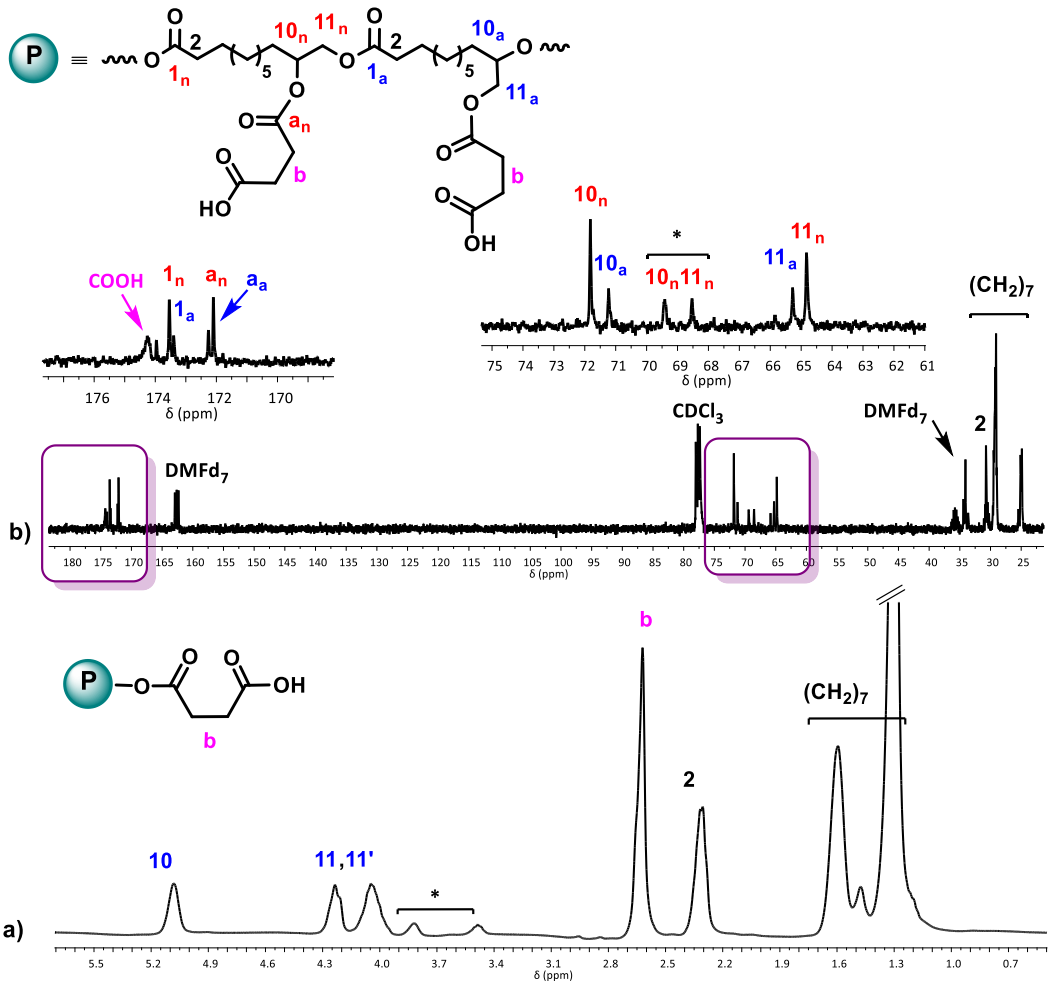

Figure 3.13 a) ^{1}H NMR of PEAU-1-succinate and b) ^{13}C NMR spectra of PEUA-1-succinate. Signals of unmodified PUEA-1 are designed with one asterisk.

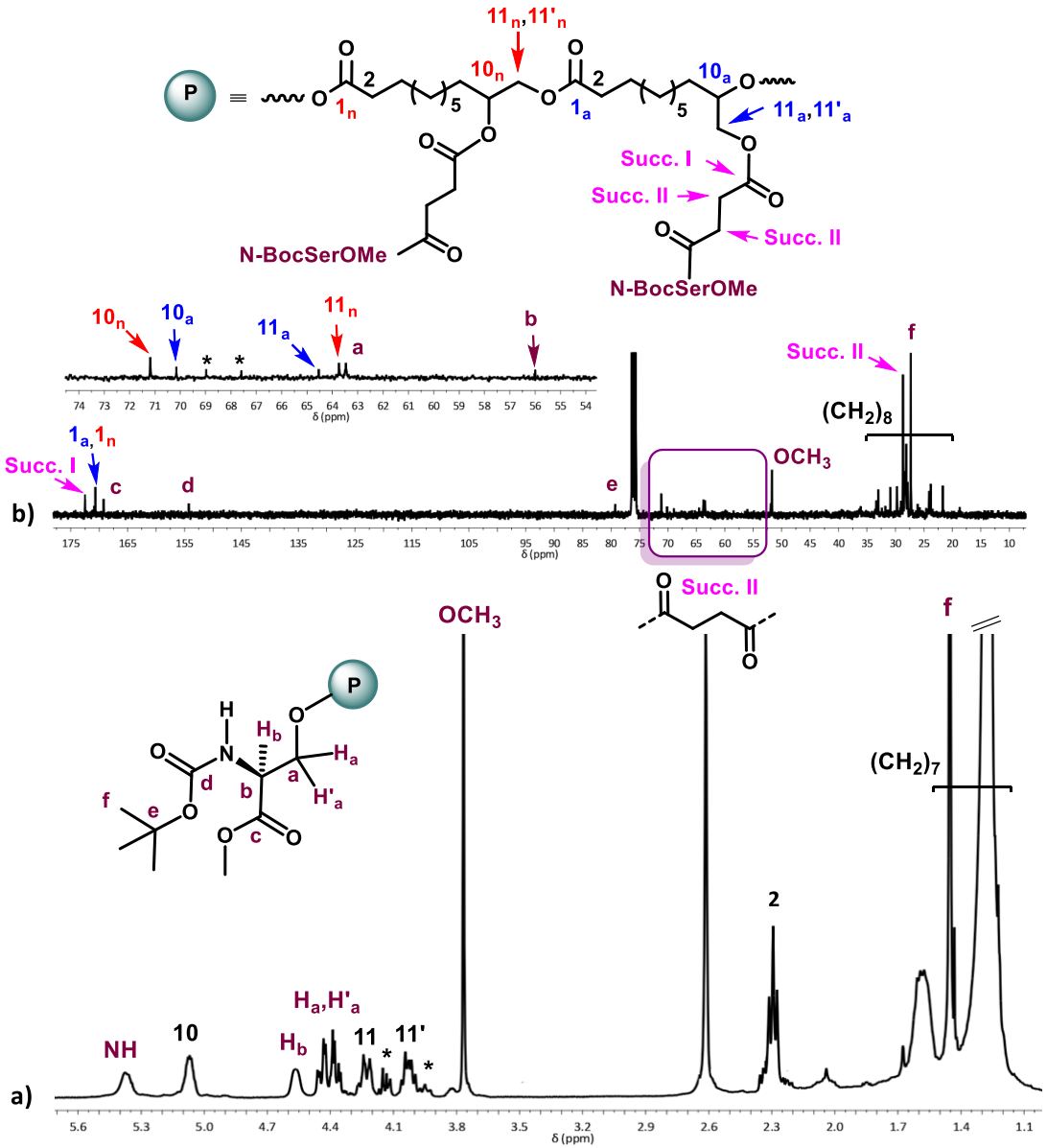

Figure 3.14 NMR spectra of PEUA-succinate modified with N-Boc-Ser-OMe, a) ^{1}H and b) ^{13}C NMR. Signals of unmodified PEUA are designed with one asterisk.

3.6 CONCLUSIONS

Biobased hydroxyl-functionalized aliphatic polyesters using 10,11-epoxyundecanoic acid as an AB type monomer were successfully synthesized *via* ROP with organic or enzymatic catalysts and thus avoiding metallic catalysts. Reaction with 1 % of tetrabutylphosphonium bromide in a 2.5 M solution in toluene at 100 °C for 8 h led to the highest conversion of linear polyesters with moderate molecular weights. Reaction in bulk, at higher temperatures or longer times gave branched polymers with increasing fractions of crosslinked polymers. In contrast, reaction with enzymatic catalyst (10 % CALB), in a 2.5 M solution in DMF at 90 °C for 48 h yielded branched polymers with polyether units. Under the appropriate conditions, both linear and branched polyesters could be prepared in multi-gram scale with complete monomer conversion either in bulk or in toluene solution.

The synthesis of model compounds and derivatization of polyesters allowed a detailed structural characterization of synthesized functionalized polyesters by ^{1}H, ^{13}C, and ^{19}F NMR. Likewise, the determination of normal/abnormal ratio (70/30), hydroxyl content (0.522 Eq OH/100 g polymer) and molecular weight (4000 g·mol^{-1}) for linear polyester was carried out.

Polyesters showed very good thermal stability and were found to be semicrystalline. The postpolymerization modification of the reactive hydroxyl sites present along the polymer backbone with N-Boc protected L-phenylalanine, protected L-cysteine and L-serine were successfully performed conferring them potential for the design of polymers with demand in biomedical applications. Moreover, thiolated polymers can be prepared from PEUA-DMFT.

3.7 REFERENCES

[1] Gandini A.; Lacerda T. M.; Carvalho A. J. F.; Trovatti T.; The progress of polymers from renewable resources: furans, vegetable oils and polysaccharides, **2016**, *Chem. Rev*., 116, 1637-1669.

[2] Gandini A.; Lacerda T. M.; From monomers to polymers from renewable resources: recent advances, **2015**, *Prog. Polym. Sci.,* 48, 1-39.

[3] Gallezot P.; Direct routes from biomass to end-products, **2011**, *Catal. Today*, 167, 31-36.

[4] Seldon R. A.; Green and sustainable manufacture of chemicals from biomass: state of the art, **2014**, *Gren Chem*., 16, 950-963.

[5] Lligadas G.; Ronda J. C.; Galià M.; Cádiz V.; Plant oil as platform chemicals for polyurethane synthesis: current state-of-the-art, **2010**, *Biomacromolecules*, 11, 2825-2835.

[6] Steen M. Van.; Stevens C. V.; Undecylenic acid: a valuable and physiologically active renewable building block from castor oil, **2009**, *ChemSusChem*, 2, 692-713.

[7] Bigot S.; Daghrir M.; Mhanna A.; Boni G.; Pourchet S.; Lecamp L.; Plasseraud L.; Undecylenic acid: a tuneable bio-based synthon for materials applications, **2016**, *Eur. Polym. J.*, 74, 26-37.

[8] Seyednejad H.; Ghassemi A. H.; van Nostrum C. F.; Vermonden T.; Hennink W. E.; Functional aliphatic polyesters for biomedical and pharmaceutical applications, **2011**, *J. Control. Rel.,* 152, 168-176.

[9] Oh J. K.; Polylactide (PLA)-based amphiphilic block copolymers: synthesis, self-assembly, and biomedical Applications, **2011**, *Soft Matter.*, 7, 5096-5108.

[10] Vilela C.; Sousa A. F.; Fonseca A. C.; Serra A. C.; Coelho J. F. J.; Freire C. S. R.; Silvestre A. J. D.; The quest for sustainable polyesters – insights into the future, **2011**, *Polym. Chem*., 5, 3119-3141.

[11] Kunduru K. R.; Basu A.; Zada M. H.; Domb A. J.; Castor oil based biodegradable polyesters, **2015**, *Biomacromolecules*, 16, 2572-2587.

[12] Hillmyer M. A.; Tolman W. B.; Aliphatic polyester block copolymers: synthesis, self-as-sembly, and biomedical applications, **2011**, *Soft Matter*., 5096-5108.

[13] Manavitehrani I.; Fathi A.; Badr H.; Daly S.; Shirazi N. A.; Dehghani F.; Biomedical applications of biodegradable polyesters, **2016**, *Polymers*, 8, 1-32.

[14] Vert M.; Aliphatic Polyesters: Great Degradable Polymers That Cannot Do Everything, **2005**, *Biomacromolecules*, 6, 538-546.

[15] Williams C. K.; Synthesis of functionalized biodegradable polyesters, **2007**, *Chem. Soc. Rev.*, 36, 1573-1580.

[16] Tong R.; New chemistry in functional aliphatic polyesters, **2017,** *Ind. Eng. Chem. Res.*, 56, 4207-4219.

[17] Gerhardt W. W.; Noga D. E.; Hardcastle K. I.; García A. J.; Collard D. M.; Weck M.; Functional lactide monomers: methodology and polymerization, **2006**, *Biomacromolecules*, 7, 1735-1742.

[18] Leemhuis M.; van Nostrum C.; Kruijtzer J. A. W.; Zhong Z. Y.; ten Breteler M. R.; Dijkstra P. J.; Feijen J.; Hennink W.E.; Functionalized Poly(α-hydroxy acid)s via ring-opening polymerization: Toward hydrophilic polyesters with pendant hydroxyl groups, **2006***, Macromolecules* , 39, 3500-3508.

[19] El Habnouni S.; Darcos V.; Coudane J.; Synthesis and ring opening polymerization of a new functional lactone, α-Iodo-Ɛ-caprolactone: a novel route to functionalized aliphatic polyesters, **2009**, *Macromol. Rapid. Commun.,* 30, 165-169.

[20] Hahn C.; Wesselbaum S.; Keul H.; Moller M.; OH-functional polyesters based on malic acid: influence of the OH-groups onto the thermal properties, **2013**, *E. Polym. J.*, 49, 217-227.

[21] Fuoco T.; Finne-Wistrand A.; Pappalardo D. A.; Route to aliphatic poly(ester)s with thiol pendant groups: From monomer design to editable porous scaffolds, **2016**, *Biomacromolecules*, 17, 1383-1394.

[22] Slavko T.; Taylor M. S.; Catalyst-controlled polycondensation of glicerol with diacyl chlorides: linear polyesters from a trifunctional monomer, **2017**, *Chem. Sci.,* 8, 7106-7111.

[23] Zhang S.; Yang J.; Liu X.; Chang J.; Cao A.; Synthesis and Characterization of Poly(butylene succinate-co-butylene malate): A New Biodegradable Copolyester Bearing Hydroxyl Pendant Groups, ***2003***, *Biomacromolecules*, 4, 437-445.

[24] Hao Q.; Yang J.; Li Q.; Li Y.; Fang Q.; Cao A.; New facile approach to novel water-soluble aliphatic poly(butylene tartarate)s bearing reactive hydroxyl pendant groups, **2005,** *Biomacromolecules*, 6, 3474-3480.

[25] You Z.; Cao H.; Gao J.; Shin P. H.; Day B. W.; Wang Y.; A functionable polyester with free hydroxyl groups and tunable physiochemical and biological properties, **2010**, *Biomaterials*, 31, 3129-3138.

[26] Y. Yan; Siegwart D.J.; Scalable synthesis and derivation of functional polyesters bearing ene and epoxide side chains, **2014**, *Polym. Chem*., 5, 1362-1371.

[27] Kalelkar P. P.; Alas G. R.; Collard D. M.; Synthesis of an alkene-containing copolylactide and its facile modification by the addition of thiols, **2016**, *Macromolecules*, 49, 2609-2617.

[28] Beyazkilic Z.; Lligadas G.; Ronda J. C.; Galià M.; Cádiz V.; Vinylsulfide-containing polyesters and copolyesters from fatty acids: Thiol-yne monomer synthesis and thiol-ene functionalization, **2014**, *Macromol. Chem. Phys.*, 215, 2248-2259.

[29] Moreno M.: Lligadas G.; Ronda J. C.; Galià M.; Cádiz V.; Polyketoesters from oleic acid. Synthesis and functionalization, **2014**, *Green. Chem.*, 4, 1847-1853.

[30] Beyazkilic Z.; Lligadas G.; Ronda J. C.; Galià M.; Cádiz V.; Synthesis and functionalization of vinylsulfide and ketone-containing aliphatic copolyesters from fatty acids, **2015**, *Polymer*, 79, 290-298.

[31] Lluch C.; Calle M.; Lligadas G.; Ronda J. C.; Galià M.; Cádiz V.; Versatile post-polymerization modifications of a functional polyester from castor oil, **2015**, *Eur. Polym. J*., 72, 64-71.

[32] Noga D. E.; Petrie T. A.; Kumar A.; Weck M.; García A. J.; Collard D. M.; Synthesis and modification of functional poly(lactide) copolymers: toward biofunctional materials, **2008**, *Biomacromolecules,* 9, 2056-2062.

[33] White J. E.; Earls J. D.; Sherman J. W.; López L. C.; Dettloff M. L.; Step-growth polymerization of 10,11-epoxyundecanoic acid. Synthesis and properties of a new hydroxy-functionalized thermoplastic polyester, **2007**, *Polymer*, 48, 3990-3998.

[34] Miao S.; Zhang S.; Su Z.; Wang P.; Chemoenzymatic synthesis of oleic acid-based polyesters for use as highly stable biomaterials, **2008**, *J. Polym. Sci. Part A: Polym. Chem.*, 46, 4243-4248.

[35] De Smet S.; Lingier S.; Du Prez F. E..; MacroRAFT agents from renewable resources and their use as polymeric scaffolds in a grafting from approach, **2014**, *Polym. Chem*, 5, 3163-3169.

[36] Warwel S.; gen Klaas M. R.; Chemo-enzymatic epoxidation of unsaturated carboxylic acid, **1995**, *J. Mol. Cat. B: Enzym.,* 1, 29-35.

[37] Aouf C.; Durand E.; Lecomte J.; Figueroa-Espinoza M. C.; Dubreucq E.; Fulcrand H.; Villeneuve P.; The use of lipases as biocatalysts for the epoxidation of fatty acids and phenolic compounds, **2014***, Green Chem.*, 16, 1740-1754.

[38] Alvey F. B.; Investigation of the epoxide-carboxylic acid reaction in model compound and polymerization reactions, **1969***, J. Polym. Sci. Part A: Polym. Chem*., 7, 2117-2124.

[39] Blank W. J.; He Z. A.; Picci M.; Catalysis of epoxy-carboxyl reaction, **2002**, *J. Coat. Technol*, 74, 33-41.

[40] You Z.; Wang Y.; A versatile synthetic platform for a wide range of functionalized biomaterials, **2012**, *Adv. Funct. Mater*., 22, 2812-2820.

[41] Kim J. W.; Cho D. W.; Park G.; Kim S. H.; Ra C. S.; Efficient ring opening reaction of epoxides with oxygen nucleophyles catalyzed by quaternary onium salt, **2013**, *Bull. Korean Chem. Soc*., 34, 2286-2290.

[42] Pratt R. C.; Lohmeijer B. G. G.; Long D. A.; Waymounth R. M.; Hedrick J. L.; Triazabicyclodecene: A simple bifunctional organocatalyst for acyl transfer and ring-opening polymerization of cyclic esters, **2006**, *J. Am. Chem. Soc.,* 128, 4556-4557.

[43] Tang D.; Noordover B. A. J.; Sablong R. J.; Koning C. E.; Metal-free synthesis of novel biobased dihydroxy-terminated aliphatic polyesters as building blocks for thermoplastic polyurethanes, **2011**, *J. Polym. Sci. Part A: Polym. Chem.*, 49, 2959-2968.

[44] Gross R. A.; Kumar A.; Kalra B.; Polymer synthesis by in vitro enzyme catalysis, **2001**, *Chem. Rev*., 101, 3793-3818.

[45] Matsumura S.; Enzymatic synthesis of polyesters via ring-opening polymerization, **2006**, *Adv. Polym. Sci.*, 194, 95-132.

[46] Kobayashi S.; Lipase-catalyzed polyester synthesis – A green polymer chemistry, **2010,** *Proc. Jpn. Acad. Ser.*, 86, 338-365.

[47] De Vries E. J.; Janssen D. B.; Biocatalytic conversion of epoxides, **2003**, *Curr. Opin. Biotechnol.,* 14, 414-420.

[48] Soeda Y.; Okamoto T.; Toshima K.; Matsumura S.; Enzymatic ring-opening polymerization of oxiranes and dicarboxylic anhydrides, **2002**, *Macromol. Biosci.,* 2, 429-436.

[49] Woodlett V. W.; Use on in situ reactions for characterization of alcohols and glycols by nuclear magnetic resonance, **1965**, *Anal. Chem*., 37, 431-431.

[50] Ranganathan M.; Balaram P.; Trifluoroacetic anhydride. A convenient NMR solvent for carbohydrates, 270 MHz ^{1}H NMR studies of 2-acetamido-2-deoxyhexoses, **1980**, *Org. Magn. Reson*., 13, 220-223.

[51] Rajan M.; Cotiuga I.; Ma Y.; Picchioni F.; Agarwal U. S.; Determination of acid and hydroxyl end-groups in end-functionalized polyestyrenes using ^{19}F NMR, **2003***, e-Polymers*,46, 1-7.

[52] Douka A.; Vouyiouka S.; Papaspyridi L-M.; Papaspyrides C. D.; A review of enzymatic polymerization to produce polycondensation polymers: the case of aliphatic polyesters, polyamides and polyesteramides. **2017***, Prog. Polym. Sci.,* https://doi.org/10.1016/ j.progpolymsci.2017.10.001.

[53] Elenkov M. M.; Hoeffken H. W.; Tang L.; Hauer B.; Janssen D. B.; Enzyme-catalyzed nucleophilic ring opening of epoxides for the preparation of enantiopure tertiary alcohols, **2007**, *Adv. Synth. Catal.,* 349, 2279-2285.

[54] Warwel S.; Wiege B.; Fehling E.; Kunz M.; Ring-opening of oleochemical epoxides catalyzed by aluminoxane/acetylacetone, **2000**, *Eur. Polym. J.,* 36, 2655-2663.

[55] Testud B.; Pintoni D.; Grau E.; Taton D.; Cramail H.; Hyperbranched polyesters by polycondensation of fatty acid-based ABn-type monomers, **2017,** *Green Chem.,* 19, 259-269.

[56] Lligadas G.; Ronda J. C.; Galià M.; Biermann U.; Metzger J. O.; **2006***, J. Polym. Sci. Part A: Polym. Chem*., 44, 634-645.

[57] Bengtsson S.; Pisco A. R.; Johansson P.; Lemos P. C.; M. Reis A. M.; Molecular weight and thermal properties of polyhydroxyalkanoates produced from fermented sugar molasses by open mixed cultures, **2010**, *J. Biotech.,* 147, 172-179.

[58] Brioude M. M.; Guimaräes D. H.; Fiúza R. P.; Prado L. A. S. A.; Boaventura J. S.; José N. M.; Synthesis and characterization of aliphatic polyesters from glycerol, by-products of biodiesel production, and adipic acid, **2007**, *Meter. Res*., 10, 335-339.

[59] Newmark R. A.; Miller M. A.; Nuclear magnetic resonance study of the conformations of valine and phenylalanine derivatives*,* **1971***, J. Phys. Chem.,* 75, 505-508.

[60] Marcovici-Mizrahi D.; Gottlieb H. E.; Marks V., Nudelman A.; On the stabilization of the syn-rotamer of amino acid carbamate derivatives by hydrogen bonding, **1996**, *J. Org. Chem*., 61, 8402-8406.

[61] Hu D. H.; Grice P.; Ley V.; Rotamers or diastereoisòmers? An overlooked NMR solution, **2012**, *J. Org. Chem.*, 77, 5198-5202.

[62] Howard-Lock H.E.; Lock C.J.L.; Martins M.L.; Smalley P.S.; Bell R.A.; Amino-acid zwitterion equilibria: vibrational and nuclear magnetic resonance studies of methyl-substituted thiazolidine-4-carboxylic acids, **1986**, *Can. J. Chem.*, 64, 1215-1219.

[63] Kuhlmann M.; Reimann O.; Hackenberger P.R.; Groll J.; Cysteine-Functional Polymers via Thiol-ene Conjugation, **2015,** *Macromol. Rapid. Commun.*, 36, 472-476.

[64] Sheehan J.C.; Yang D-D. H.; A new synthesis of cysteinyl peptides, **1957**, *J. Am. Chem. Soc*., 80, 1158-1164.

UNIVERSITAT ROVIRA I VIRGILI
10-UNDECENOIC ACID-BASED BIODEGRADABLE HYDROXY POLYESTERS: A PLATFORM FOR AMINOACID BIOCONJUGATES AND PEG-DERIVED AMPHIPHILIC COPOLYMERS
Carmen Valverde Sarmiento

Chapter 4

Hydrolytic and enzymatic degradation studies of aliphatic 10-undecenoic acid-based polyester

Publication derived from this work: *Polymer Degradation and Stability*, 2018, 155, 84-94.

Supporting Information (SI) to this chapter in Annex B.

UNIVERSITAT ROVIRA I VIRGILI
10-UNDECENOIC ACID-BASED BIODEGRADABLE HYDROXY POLYESTERS: A PLATFORM FOR AMINOACID BIOCONJUGATES AND PEG-DERIVED AMPHIPHILIC COPOLYMERS
Carmen Valverde Sarmiento

4.1 INTRODUCTION

For the last 60 years, synthetic polymeric materials have grown progressively basically due to their low cost, their reproducibility, and their resistance to physical aging and biological attacks. However, the resistance of synthetic polymers to the degrading action of living systems is becoming increasingly problematic in several domains where they are used for a limited period of time before becoming wastes. This is the case in surgery, in pharmacology, in agriculture, and in the environment as well.

Nowadays the open and the patent literature propose a large number of polymers whose main chains can be degraded usefully. Among these degradable polymers, aliphatic polyesters are receiving special attention because they are all more or less sensitive to hydrolytic and enzymatic degradation.[1-3] Aliphatic polyesters containing flexible ester bonds appear to be the most promising because of their excellent biocompatibility and variable degradability and are the most representative examples of environmentally relevant polymeric materials.[4-7]

Many aliphatic polyesters biodegrade *via* a two-step process. First, polymer backbone bonds must be enzymatically or otherwise hydrolysed to produce oligomers, which are subsequently broken down and further, in soil return water, carbon dioxide, and hummus.[8] Generally, polyester degradation rate is impacted by the structure of the polymer backbone, including the electrophilicity of the carbonyl atoms and the presence or absence of bulky substituents. Among the critical factors that affect the degradation rate of polyesters, one is the distance between ester groups in the polymer which determine the polymer character, e.g. hydrophobicity and crystallinity. Molecular weight and crystallinity have been shown to have the largest impact in polyester degradation due to a hindrance in water being able to diffuse into the matrix.

Moreover, the presence of hydrophilic (hydroxyl and carboxyl) end groups also promotes the polyester degradation. It is well known the effect of autocatalysis by the acid ended

chain fragments, which leads to a dramatic increase of the rate of degradation as degradation advances.[9] It is established that carboxyl end groups formed by chain cleavage catalyse degradation and that amorphous regions are preferably degraded.[5,10,11]

The introduction of functional groups into commonly used polyesters such as PLA and PCL provides polymers with tuneable degradation behaviour by suppression of crystallinity and enhanced hydrophilicity that also favours cell adhesion to the surfaces important for tissue engineering purposes.[12] Further, increased hydrophilicity results in a greater water absorbing capacity of the polymers, thereby increasing the degradation rate and probably preventing a pH drop inside the degrading matrices and hence preventing incomplete release of degraded fragment or encapsulated compounds.[13]

Aliphatic polyesters degrade either by bulk erosion or surface erosion.[14-16] Polymer hydrolytic degradation is produced by scission of chemical bonds in the polymer backbone, by water uptake, to form oligomers and finally monomers. In the first step, water molecules attack the water-labile bonds by either direct access to the polymer surface or by imbibition into the polymer matrix followed by bond hydrolysis. This nucleophilic attack by water can be catalysed by acids, bases or enzymes.[17]

In this work it studied the hydrolytic and enzymatic degradation of two aliphatic polyesters synthesized from castor oil-derived 10-undecenoic acid: poly(10,11-epoxyundecanoic acid) (PEUA from Chapter 3) which contains primary and secondary hydroxyl pendant functions along the main chain and poly(11-hydroxyundecanoate)diol, and compared with commercial poly(ε-caprolactonediol). Changes taking place in sample weight, molecular weight, chemical constitution, thermal properties, crystallinity and surface morphology of the polyesters were evaluated and related to the polymer structure and degradation conditions.

4.2 POLYESTER SYNTHESIS AND CHARACTERIZATION

Linear poly(10,11-epoxyundecanoic acid) (PEUA) was synthesized through carboxylic ring opening polymerization of 10,11-epoxyundecanoic acid catalysed by TBPB with high yields (87 %), described in Chapter 3.[18] Poly(11-hydroxyundecanoate)diol (PHU) was synthesized by transesterification reaction initiated by 1,6-hexanediol and catalysed by titanium tetraisopropoxide, with high yield (92 %). These two polymers are obtained from 10-undecenoic acid-derived monomers. The first contains primary and secondary hydroxyl pendant groups along the main chain in about 30:70 ratio, arising from normal and abnormal oxirane ring opening.[18] Poly(ε-caprolactone)diol (PCL) diethylenglycol initiated was purchased and used to compare the degradation behaviour of our 10-undecenoic acid-derived renewable polyesters with a commercial versatile and widely used polymer with similar structure.

Structure of the three polymers is represented in Scheme 4.1 and the main features in connection with the degradation study carried out in this work are listed in Table 4.1, Table 4.2 and Table 4.3.

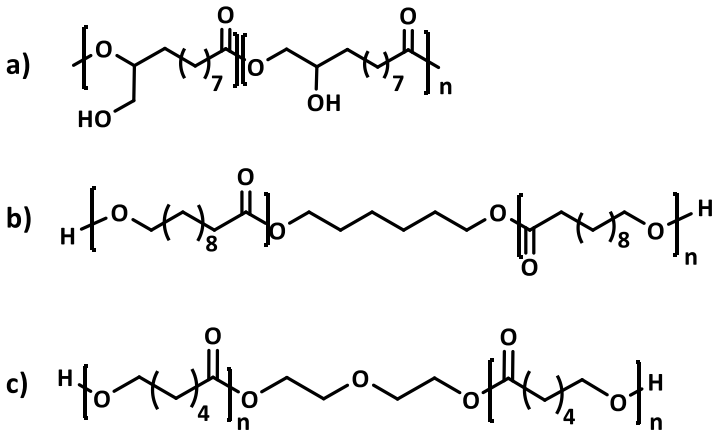

Scheme 4.1 Structure of polymers a) PEUA, b) PHU and c) PCL.

Table 4.1 Molecular weight of initial polymers.

	Molecular weight		
Polymer	**RMN**	**SEC**	
	Mn (kg·mol^{-1})^a	**Mn (kg·mol^{-1})^b**	**Đ^b**
PEUA	3.65	8.40	3.4
PHU	3.52	3.90	2.0
PCL	2.58	3.60	1.9

(a) Number average molecular weight determined by NMR; (b) Number average molecular weight and polydispersity index determined by SEC in THF relative to PS standards.

Table 4.2 Thermal properties and XRD of initial polymers.

		DSC 1st heating		DSC 2nd heating			TGA		XRD
Pol.	**Tg (°C)^a**	**T_m (°C)^b**	**ΔH_m (KJ·mol^{-1})^b**	**T_m (°C)^c**	**ΔH_m (KJ·mol^{-1})^c**	**χ_c %^{d}**	**$T_{5\%}$ (°C)^e**	**T_{max} (°C)^f**	**χ_c %^{g}**
PEUA	-12	92.1±0.6 100.1±0.5	17.5±0.6	43.2±0.2	7.1±0.3	--	342	386 432	54.2
PHU	--	73.8±0.3	27.7±0.4	72.9±0.3	22.4±0.4	56.7	327	425	66.3
PCL	--	58.0±0.6	11.7±0.3	52.0±0.4	9.8±0.2	54.7	217	413	62.0

(a) Glass-transition temperature (Tg) taken as the inflection point of the first heating DSC curves recorded at 10 °C·min^{-1}; (b) Melting temperatures (T_m) and enthalpies (ΔH_m) determined by DSC on the first heating scan at heating rates of 10 °C·min^{-1}; (c) Melting temperatures (T_m) and enthalpies (ΔH_m) determined by DSC on the second heating scan at heating rates of 10 °C·min^{-1}; (d) Fractional crystallinity estimated by DSC using ΔH^0_m described in literature; (e) Temperature at which 5 % weight loss was observed by TGA; (f) Temperature for maximum degradation rate from TGA; (g) Fractional crystallinity estimated by XRD from the amorphous and crystalline pattern areas.

The absolute molecular weights were determined by NMR measurements. Mn of PEUA was calculated by ^{19}F NMR of the corresponding trifluoroacetyl derivative as previously reported.[18] In the case of PHU and PCL, Mn was calculated by ^{1}H NMR spectroscopy by comparison of the intensities of signals corresponding to the α-methylene to ester group in the main chain at 2.3 ppm, and CH_2OH end groups at ca. 3.6 ppm in both cases (Figure 4.8 a and Figure 4.9 a). As can be seen, PEUA and PHU have similar Mn whereas Mn of commercial PCL is something lower. Mn of the three polyesters was also determined by

SEC which was the technique used to follow the hydrolytic and enzymatic degradation. The resulting values are higher, especially in the case of PEUA. This can be attributed to differences in the hydrodynamic volume with the PS standards. Moreover, as PEUA contains hydroxyl pendant groups it should be expected to have a more expanded coil in good solvents such as THF.

According to DSC scans, all polyesters PEUA, PHU and PCL are semicrystalline. Relatively small decreases in melting temperature and melting enthalpy between the first and second scan are observed for PHU and PCL indicating a strong tendency of the chains to reorganize and crystallize. Moreover, melting temperatures of PHU and PCL are lower than those reported for the pure crystalline samples, which confirms its semicrystalline character. [19] In regard to commercial PCL, it is reported that melting temperature occurs in the range of 59-64 °C depending upon the crystallite size.[20] PEUA shows a different behaviour having much higher melting temperature and melting enthalpy in the first scan, which is consistent with literature.[21] From the observed melting temperatures of pristine polyesters, it was established that 45 °C had to be the maximum incubation temperature to maintain the shape and integrity of all samples.

After erasing the thermal history, the fractional crystallinity (χ_c) of PHU and PCL based on their enthalpy of fusion in the second heating scan could be estimated, as the heat of fusion for the 100 % crystalline samples is reported (PHU 39.5 KJ·mol^{-1} and PCL 17.9 KJ·mol^{-1}).[22,19] According this estimation, PHU has slightly higher crystallinity degree than PCL and XRD measurements confirms the same result. The complete linear structure of both polymers favours aliphatic chain packing and fast reorganization. In the case of PEUA there is no reference for the pure crystalline sample. However, according to XRD data it seems to be less crystalline than PHU and PCL, which is concordant to its random copolymer structure and the presence of hydroxyl pendant groups**.**

TGA curves for the three polyesters have approximately the same shape with the only difference that the hydroxypolyester, PEUA, shows and additional decomposition process

and a slight lower thermal stability.[18] Aliphatic polyesters without reactive pendant groups usually have a single step degradation. Under the given experimental conditions, no measurable number of volatile compounds (moisture, unreacted monomers, and small molar mass product of reaction) is detected below 270 °C. From the measured TGA curves of three polyester samples, temperatures obtained for mass losses of 5 % and maximum rate temperatures for main decomposition processes were calculated and collected in Table 4.2.

Hydrophilic/hydrophobic behaviour of these polyesters (Table 4.3) was determined measuring their solubility, water uptake and contact angle.

Table 4.3 Solubility, water uptake and contact angle of PEUA, PHU and PCL.

	Solubility[a]						Water uptake[b]		Contact angle
Polymer	**H_2O**	**EtOH**	**DMSO**	**DMF**	**THF**	**$CHCl_3$**	**37 °C**	**45 °C**	**Θ_{water} (°)**
PEUA	-	-	+	+	+	+	1.5±0.1	1.86±0.0	79.1±1.4
PHU	-	-	-	+	+	+	0±0.0	0.23±0.0	83.4±1.3
PCL	-	-	-	+	+	+	2.2±0.2	5.25±0.2	66.2±2.6

(a) (-) insoluble, (+) soluble. (b) expressed as weight increase percentage.

Solubility properties were assessed in an assortment of representative polar, protic and aprotic solvents. As expected by their predominant polymethylene moieties, all polyesters were insoluble in water and ethanol but soluble in medium to high polarity aprotic solvents. The hydrogen bonding interactions between hydroxyl groups in PEUA and the highly polarized S=O groups could explain its different solubility in DMSO.

Polymer water uptake was measured at 37 °C and 45 °C, temperatures at which hydrolytic and enzymatic degradation were performed. It can be observed increasing values according to their expected hydrophilic character, PCL > PEUA > PHU taking into account their relative ester density and the presence of additional hydroxyl groups in PEUA. The

same behaviour was observed through water contact angle measurements (Figure 4.1) confirming the hydrophilicity order.

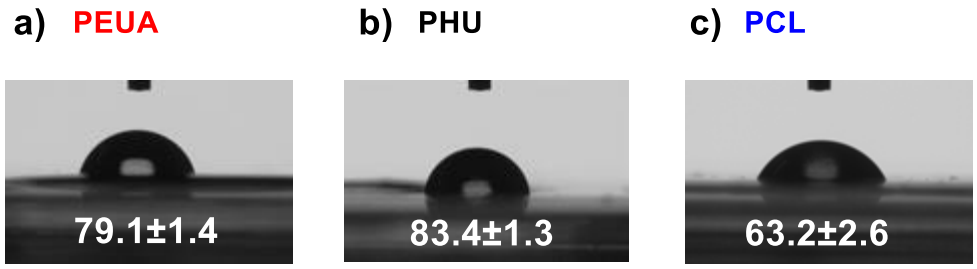

Figure 4.1 Water contact angle images of starting polymers a) PEUA, b) PHU and c) PCL.

4.3 HYDROLYTIC AND ENZYMATIC DEGRADATIONS

The study is focused on two main elements: composition of the polymer matrix during the hydrolysis (weight loss and molecular weight decrease) and composition of the degradation products.

The variation in sample weight and Mn for PEUA, PHU and PCL upon incubation in aqueous buffers at pH 2.0 and 45 ºC and at pH 7.4 with porcine pancreas lipase and 37 ºC, respectively, is depicted in Figure 4.2 and Figure 4.3.

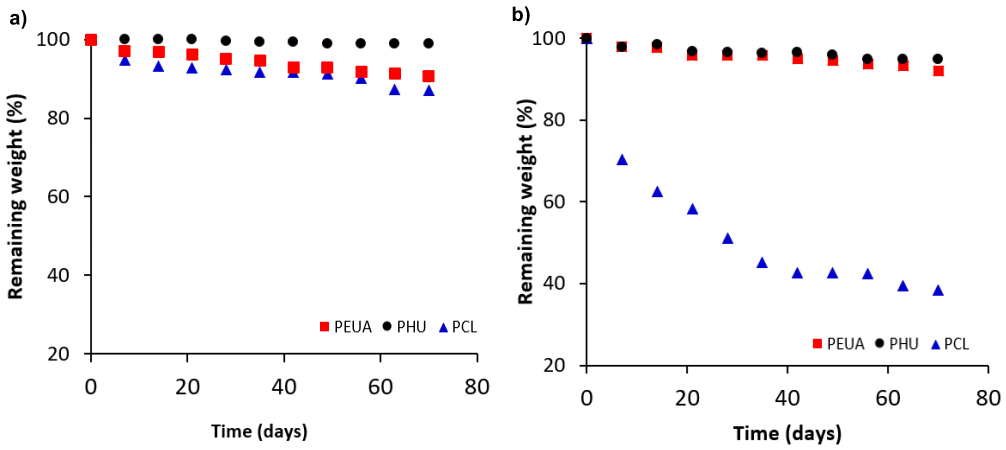

Figure 4.2 Remaining weight of polymers by measure of weight loss versus time: a) at pH 2.0 at 45 ºC; b) at pH 7.4 at 37 ºC with porcine pancreas lipase.

The weight losses undergone by PCL and PEUA were about 7 % and 5 %, respectively, after 10 weeks of incubation at pH 2.0 at 45 °C, thus showing the release of soluble oligomers produced by degradation. By contrast, the invariance observed for PHU in both weight loss and Mn is indicative of none degradation. When incubated under enzymatic conditions, after 10 weeks, scarce variance was observed in remaining weights in PEUA and PHU, therefore none of them underwent significant degradation. However, the weight loss for PCL was about 60 % but the fact that there was no significant change in molecular weight (Figure 4.3 b), indicates clearly a surface erosion mechanism for polymer degradation as confirmed by the observed sample size reduction.[14,23]

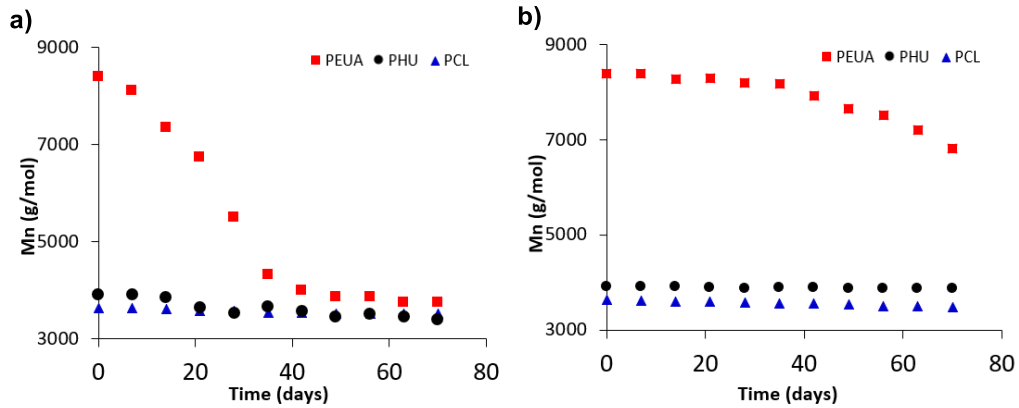

Figure 4.3 Degradation of polymers by SEC determination; a) Molecular weight at pH 2.0 at 45 °C; b) Molecular weight at pH 7.4 at 37 °C with porcine pancreas lipase.

In the case of PEUA, a significant decrease of Mn was observed for at pH 2.0 at 45 °C. The initial Mn was 8400 g·mol^{-1} with Đ 3.4 and the final Mn 3700 g·mol^{-1} with Đ 2.6, however, weight loss is very low (up to 5 %). This seems to indicate that, even in small extent, hydrolytic degradation proceeds through a bulk erosion mechanism. In enzymatic degradation, Mn also decrease but in a minor extension and without significant changes in Đ. This is consistent with the difficulty of enzymes to penetrate polymer systems and only to diffuse into poorly ordered amorphous regions.[24,25]

By comparison to PHU behaviour in both hydrolytic and enzymatic media it can be inferred that the pendant hydroxyl group and the superior amorphous character in PEUA play a

significant role in the degradation mechanism by increasing hydrophilicity, water uptake and swelling of the amorphous domains, facilitating the ester cleavage and the decrease of molecular weight. This behaviour is especially remarkable in acidic medium where the formation of shorter chains modify crystallinity (*vide infra).*

4.4 THERMAL ANALYSIS

To evaluate thermal changes during hydrolytic and enzymatic degradation, second heating DSC traces of the three polyesters after 10 weeks of incubation at pH 2.0 at 45 °C and at pH 7.4 at 37 °C with porcine pancreas lipase were carried out, and compared with those of the pristine polymers (in Table 4.3). DSC scans are shown in Figure 4.4 a and measured melting temperatures, melting enthalpies and estimated fractional crystallinities (χ_c) are collected in Table 4.4.

Table 4.4 Melting temperatures, melting enthalpies and crystallinity degrees estimated by DSC and XRD of polyesters after 10 weeks of incubation at pH 2.0 at 45 °C and at pH 7.4 at 37 °C with porcine pancreas lipase.

	pH 2.0 (45 °C)				pH 7.4 (37 °C) lipase			
Polymer	**T_m (°C)[a]**	**ΔH_m (KJ·mol^{-1})[a]**	**χ_c %[b]**	**χ_c %[c]**	**T_m (°C)[a]**	**ΔH_m (KJ·mol^{-1})[a]**	**χ_c %[b]**	**χ_c %[c]**
PEUA	29.2±0.2	6.2±0.3	--	54.4	52.5±0.2	7.7±0.3	--	57.9
PHU	72.9±0.2	21.7±0.2	54.9	65.1	73.2±0.2	21.4±0.3	54.2	67.0
PCL	49.3±0.4	9.5±0.2	53.0	66.6	50.9±0.2	9.8±0.2	54.7	66.4

(a) Melting temperatures and melting enthalpies measured by DSC at heating/cooling rates of 10 °C·min^{-1}; (e) Fractional crystallinity estimated by DSC using ΔH^0_m described in literature; (c) Fractional crystallinity estimated by XRD from the amorphous and crystalline pattern areas.

Several factors can provoke crystallinity changes during polymer degradation.[14] One is the generation of crystallizable oligomers and monomers. The other stems from the behaviour of semicrystalline polymers during erosion. It was well recognized that degradation is much faster in amorphous domains that in crystalline ones, mostly because water penetration is easier within a disordered network of polymer chains.[5,26,27.] Moreover, when introducing the samples in the incubation media, water uptake lowered the glass transition

temperature, increasing mobility of the chains making it possible for them to reorganize and crystallize.[23] In our case, from DSC traces different behaviour for the three polyesters is observed. For PCL, both melting enthalpy and melting temperature remain almost unaffected after incubation in both hydrolytic and enzymatic media. This confirms that surface erosion is the predominant degradation mechanism producing a layer-by-layer ester cleavage and solubilisation. This mechanism is especially remarkable under enzymatic conditions where about 60 % of the initial weigh is lost after 10 weeks. For PHU, also no significant changes in melting enthalpy and melting temperature are observed what is consistent with a scarce degradation observed. It must be pointed out that PHU, due to the linear aliphatic chain structure, possess the highest crystalline and hydrophobic character of the three samples studied, and shortage of amorphous domains to promote a fast degradation mechanism.

PEUA due to the presence of hydroxyl groups and the two different sequence monomeric units possess a lower ability to crystallize as it is shown by their relative lower melting enthalpy values (Tables 4.2 and 4.4). On incubation after 10 weeks at pH 2.0, a decrease in both melting temperature and melting enthalpy is observed as result of the formation of smaller crystals from shorter chains resulting after the bulky degradation process.[28] This behaviour is consistent with the significant molecular weight decrease produced in the degradation in this medium (Figure 4.3 a). On the contrary, on incubation after 10 weeks at pH 7.4 in enzymatic media, a moderate increase in both melting temperature and melting enthalpy is observed, suggesting a crystallinity increase. In this case, the observed decrease of molecular weight is much lower (Figure 4.3 b) and the increase of crystallinity could be related to the increased mobility and rearrangement of polymer chains promoted by water swelling during incubation.

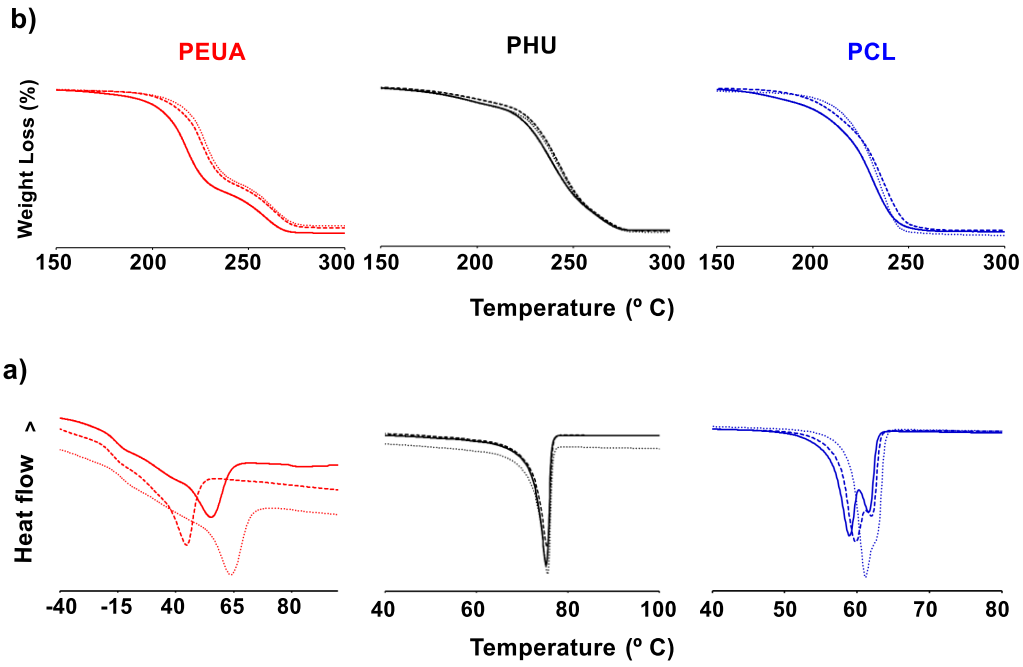

Figure 4.4 Second heating DSC (a) and TGA plots (b) of initial polyesters (——), polyesters after 10 weeks incubation at pH 2.0 at 45 ºC (----) and polyester after 10 weeks incubation at pH 7.4 at 37 ºC with porcine pancreas lipase (·····).

Thermal stability changes were studied by TGA (Figure 4.4 b). Curves of initial and incubated samples for each polymer, show the same degradation profile. For PHU no significant changes are observed according to the negligible degradation and no variation in the crystallinity degree. For PCL and PEUA a slight increase in thermal stability is observed, which can be related with the reduction of the low molecular weight fractions by degradation/solubilization after incubation.

4.5 XRD ANALYSIS

Although crystallinity can be roughly estimated by DSC, X ray measurements afford a more accurate crystallinity measurement and crystalline arrangement determination. XRD patterns of pristine and incubated samples of PEUA, PHU and PCL are shown in Figure 4.5. Moreover, fractional crystallinity (χ_c) determined from the amorphous and crystalline pattern areas are collected in Tables 4.2 and 4.4.

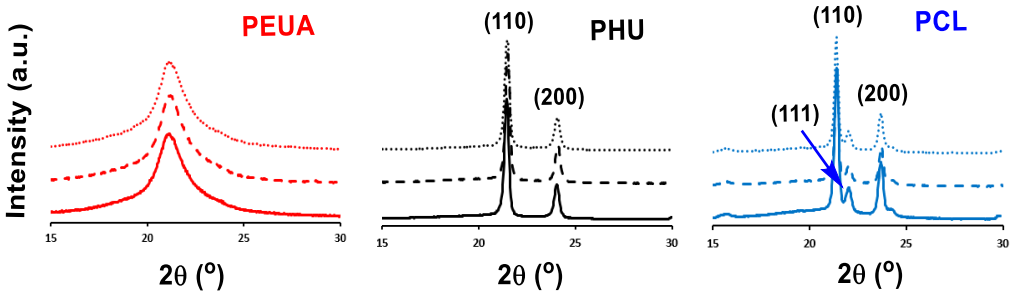

Figure 4.5 XRD patterns of initial polyesters (—), polyesters after 10 weeks incubation at pH 2.0 at 45 °C (- - -) and polyester after 10 weeks incubation at pH 7.4 at 37 °C with porcine pancreas lipase (·····).

XRD patterns for PHU and PCL coincide with the previously described in literature and confirm the high crystalline character of both polymers.[29,30] Calculated fractional crystallinities are systematically higher (χ_c = 62-67 %) than those estimated by DSC (χ_c = 54-57 %) and confirm the lower crystallinity of PEUA, also indicated by the significant broad dispersion pattern shown in Figure 4.5. In the case of PEUA, χ_c values before and after incubation at pH 2.0 at 45 °C are similar, although by DSC lower melting enthalpy and melting temperature are observed. Under incubation at pH 7.4 at 37 °C and lipase, a slight increase in crystallinity is observed which is in agreement with DSC results. In the case of PCL, despite the fact that by DSC no increase in melting enthalpy was observed, XRD pattern suggest a slight enrichment in crystallinity that could be related with the preferential degradation of the amorphous domains in the surface erosion.

4.6 MORPHOLOGICAL OBSERVATIONS

Surface morphology changes of PEU, PHU and PCL after hydrolytic and enzymatic degradation were observed by ESEM. PHU and PCL micrographs are shown in Figures 4.5. PHU ESEM micrographs (Figure 4.6 a, b and c) revealed that no changes in morphology had taken place upon incubation. For PCL (Figure 4.6 d, e and f) images are consistent with a degradation mechanism by erosion. Initially, the surface appears fairly flat, and surface morphology is induced by the mould used for compression moulding. After incubation 10

weeks, a homogeneous and porous structure indicating hydrolytic attack at the amorphous phase at the surface is observed. This erosion seems to be more prominent under enzymatic degradation conditions. This result is in agreement with the superior weight loss observed in Figure 4.2 b.

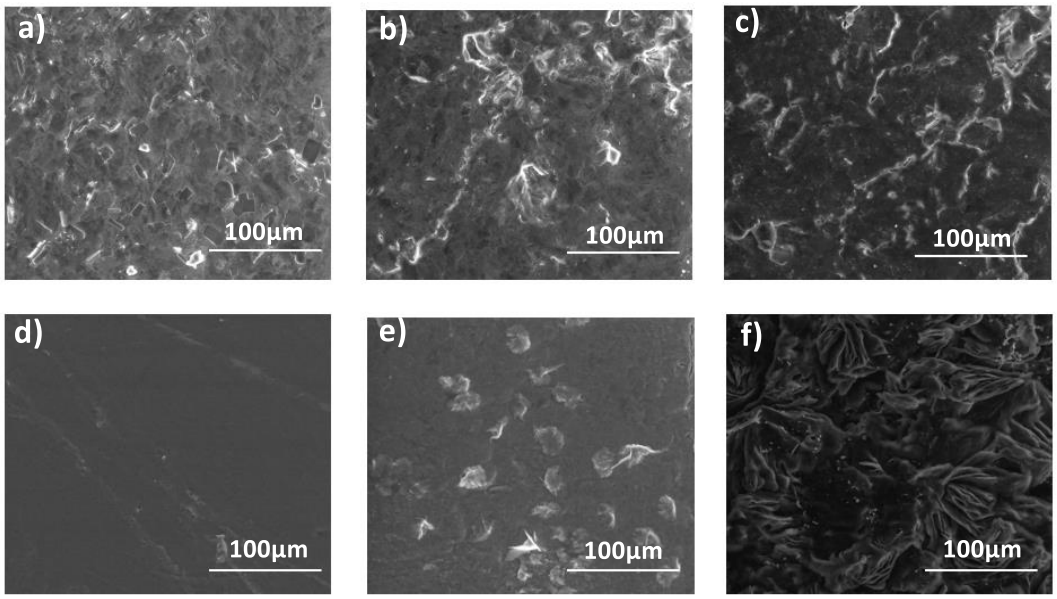

Figure 4.6 ESEM micrographs of a) initial PHU; b) PHU after incubation at pH 2.0 at 45 °C; c) PHU after incubation at pH 7.4 at 37 °C, d) initial PCL; e) PCL after incubation at pH 2.0 at 45 °C and f) PCL after incubation at pH 7.4 at 37 °C with porcine pancreas lipase.

ESEM micrographs of PEU are shown in Figure 4.7.

For PEUA surface, ESEM micrographs show that the initial flat surface is transformed in a porous structure indicating hydrolytic attack at the amorphous domains occurs both in acid and enzymatic media. This erosion mechanism can be visualized more clearly in the cut vertical edge (Figure 4.7 d and e) of samples degraded in acid media. The stretch marks induced by the cutting blade become deeper and in addition, some eroding regions can be observed in the surface.

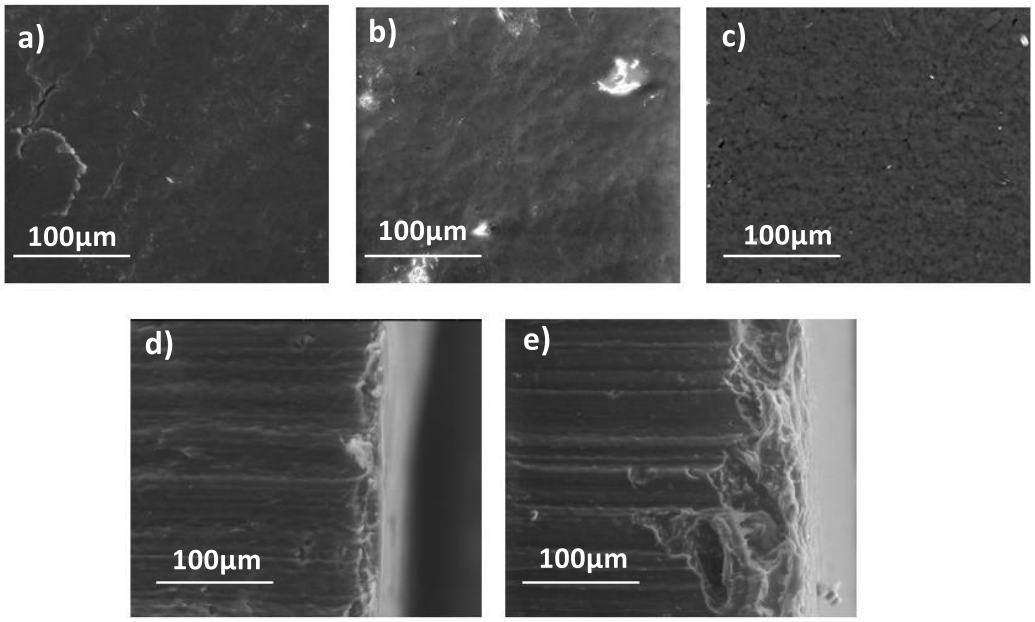

Figure 4.7 ESEM micrographs of a) initial PEUA, b) PEUA after incubation at pH 2.0 at 45 °C, c) PEUA after incubation at pH 7.4 at 37 °C, d) vertical initial PEUA and e) vertical APEUA after incubation at pH 2.0 at 45 °C.

To provide a better understanding of microstructural changes in PEUA morphology after incubation at pH 2.0 and 45 °C, we use atomic force microscopy (AFM) that provide high-resolution, three-dimensional imaging of material surface.[31] The three-dimensional topographic images and the corresponding two-dimensional images of initial PEUA and after incubation of 10 weeks are displayed in Figure 4.8. As can be seen after incubation in these conditions a significant surface erosion with deep valleys and pores is observed.

The processes involved in the erosion of a degradable polyester are complex. Water enters the polymer bulk, which might be accompanied by swelling. The intrusion of water triggers the chemical polymer degradation, leading to the creation of oligomers and monomers. Progressive degradation changes the microstructure of the bulk through the formation of pores.[14]

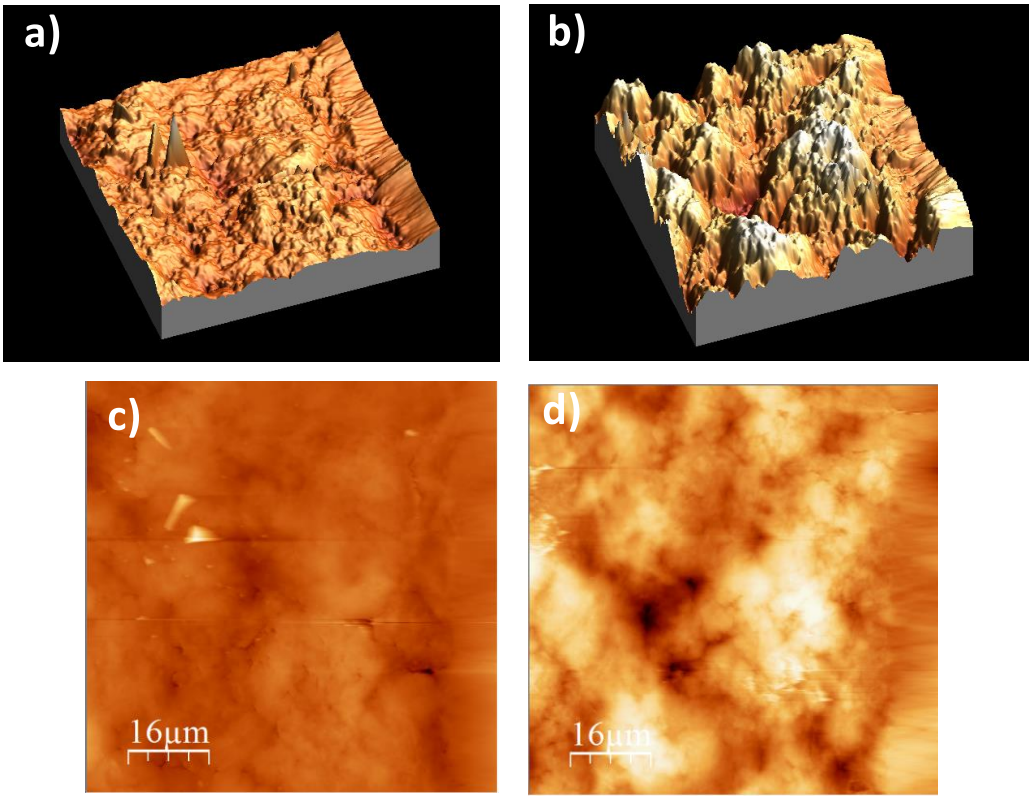

Figure 4.8 AFM images three-dimensional representation (top): a) initial PEUA; b) PEUA after incubation at pH 2.0 at 45 ºC and two-dimensional representation (bottom): c) initial PEUA; d) PEUA after incubation at pH 2.0 at 45 ºC.

4.7 DEGRADATION STUDY BY ^{1}H NMR

In order to deep insight the degradation of polyester chain at the molecular level a NMR study was carried out. ^{1}H NMR spectra of the residual material resulting after 10 weeks of incubation at pH 2.0 at 45 ºC, and at pH 7.4 at 37 ºC have been recorded. Residual material of PHU and PCL spectra showed only negligible differences with their initial spectra (Figures 4.9 b and c and 4.10 b and c respectively), confirming no significant variations in the chemical constitution. By contrast, some structural changes in residual material are observed after both hydrolytic and enzymatic degradation of PEUA (Figure 4.11 b and c), due to the progressive chain cleavage. These changes agree to the decrease of Mn observed by SEC (Figure 4.3).

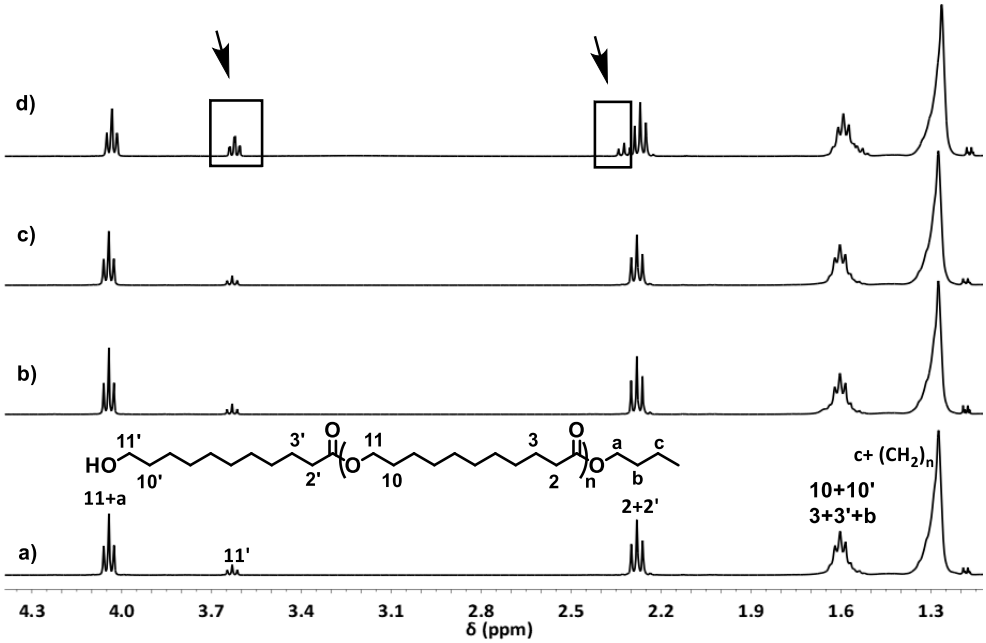

Figure 4.9 ^{1}H NMR spectra of PHU a) initial sample; b) after incubation at pH 2.0 at 45 °C; after incubation at pH 7.4 at 37 °C; d) after accelerated hydrolytic degradation at 100 °C.

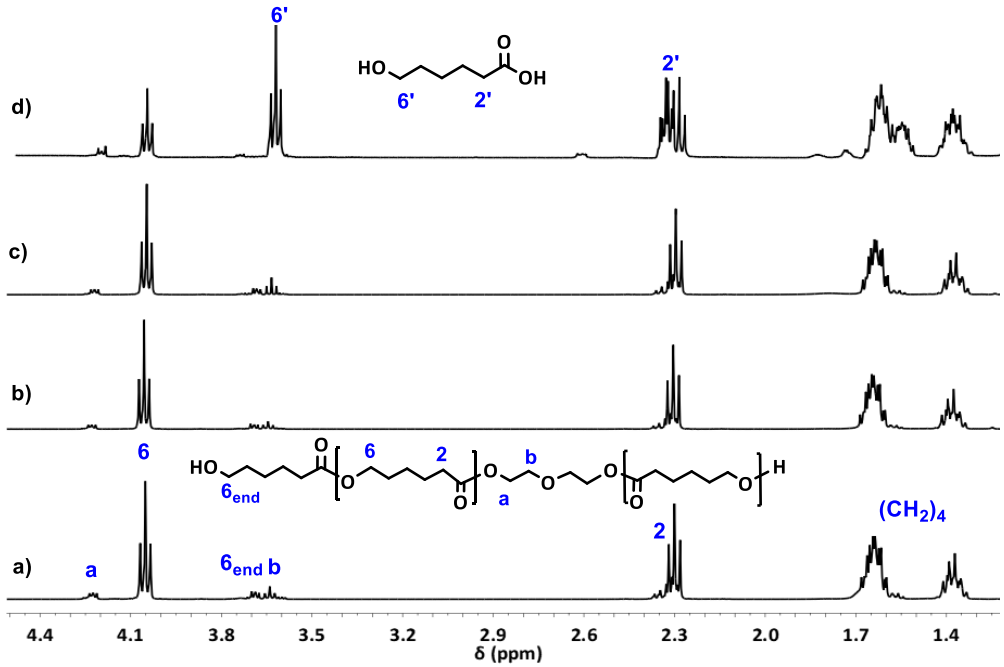

Figure 4.10 ^{1}H NMR spectra of PCL a) initial sample; b) after incubation at pH 2.0 at 45 °C; after incubation at pH 7.4 at 37 °C; d) after accelerated hydrolytic degradation after 100 °C.

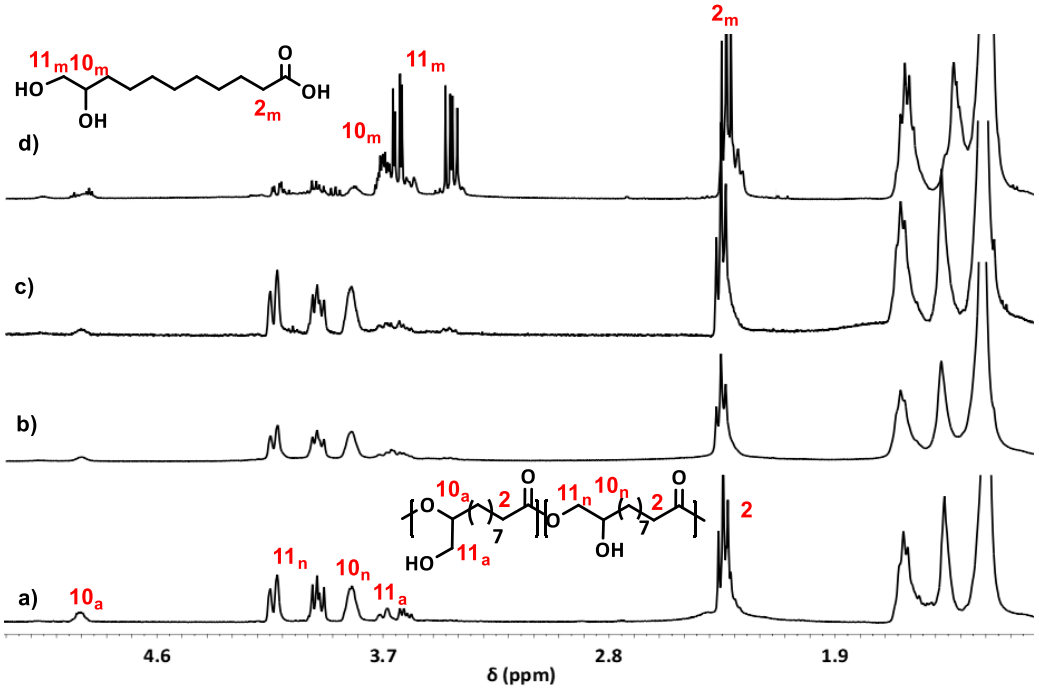

Figure 4.11 ^{1}H NMR spectra of PEUA: a) initial sample; b) after incubation at pH 2.0 at 45 °C; after incubation at pH 7.4 at 37 °C; d) after accelerated hydrolytic degradation at 100 °C.

4.8 ACCELERATED HYDROLYTIC DEGRADATION

To study in detail all residual material of three polyesters, accelerated degradation tests with methanesulfonic acid 1 M for 1 day at 100 °C were performed. Accelerated degradation methods allow obtaining degradation results in a shorter period of time.[32,33]

^{1}H NMR spectrum of residual material after accelerated degradation of PEUA (Figure 4.11 d) shows a great extent of polymer degradation giving mostly 10,11-dihydroxy undecanoic acid (DHU) and oligomers as bear out by SEC curves (Figure 4.12 a).

^{1}H NMR spectrum of residual material after accelerated degradation of PHU (Figure 4.9 d) shows an increase of hydroxyl end group signals (at 3.64 ppm) and the appearance of a new signal (at 2.35 ppm) corresponding to the carboxyl end group signals, confirming the partial cleavage of ester groups, leading to a polymer with lower molecular weight (Figure 4.12 b).

^{1}H NMR spectrum of residual material after accelerated degradation of PCL (Figure 4.10 d) reveals a great extent of polymer degradation giving mainly 6-hydroxy-hexanoic acid, confirming the almost complete degradation of PCL. (Figure 4.12 c).

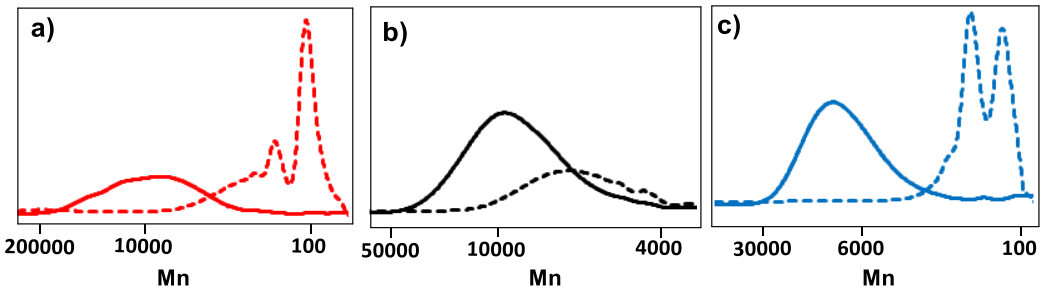

Figure 4.12 SEC traces for hydrolytic accelerated degradation with methanesulfonic acid at 100 ºC. a) PEUA; b) PHU; c) PCL. Initial sample (continue line) and after degradation (dashed line).

To study in detail the structural changes undertaken by PEUA during accelerated hydrolytic degradation a kinetic study was carried out by ^{1}H NMR spectroscopy (Figures 4.13 and 4.14). In Figure 4.13 a is shown the weight percentage decrease of PEUA and the increase of DHU *versus* time. As can be seen, although degradation occurs through intermediate oligomeric species, there is a complementary relationship between PEUA degradation and DHU formation (Figure 4.14, 5 h).

As commented above, on the structure of PEUA there are two kinds of repetitive units with pendant secondary or primary alcohols arising from the attack of the carboxylic acid either to the less (leading to a normal unit) or the more substituted carbon (leading to an abnormal unit) of oxirane ring on the starting 10,11-epoxyundecanoic acid. According to ^{1}H NMR microstructural determination these normal/abnormal units are present in a 72:28 molar ratio in the starting polymer (Figure 4.13 b and 14, 0 h). During degradation studies we observed a change in the comonomer composition due to the different hydrolysis rates of primary and secondary esters (Figure 4.13 b). Thus, as observed in the first degradation stages, selective primary ester (normal unit) degradation is predominant and consequently its relative content in the copolymer decreases. Moreover, a significant percentage of

branched units was detected from 1 h (Figure 4.13 b and 14, 2 h and 3 h). The characteristic NMR signals of these branched units in PEUA have been previously assigned and reported.[19] The formation of these units is related with transesterification reactions throughout process. These transesterification reactions have been previously reported for PEUA and similar polyesters.[19] Thus, progressive degradation of PEUA lead not only to a decrease in molecular weight but also to a change in its microstructure that goes from linear to branched oligomers.

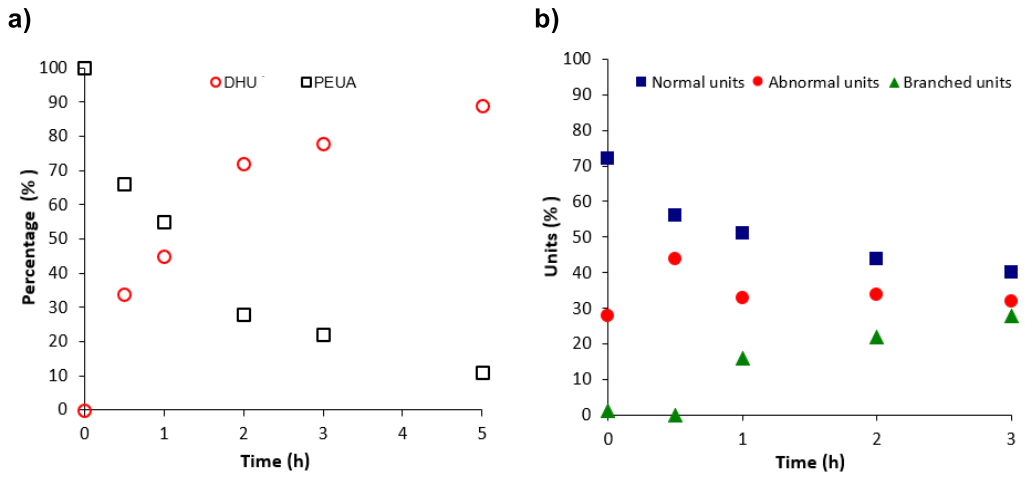

Figure 4.13 Accelerated hydrolytic degradation kinetic of PEUA with 0.5 M of methanesulfonic acid at 100 °C. a) Weight percentage of PEUA and PHU determined by ^{1}H NMR spectroscopy; b) Percentage of normal, abnormal and branched units in PEUA determined by ^{1}H NMR spectroscopy.

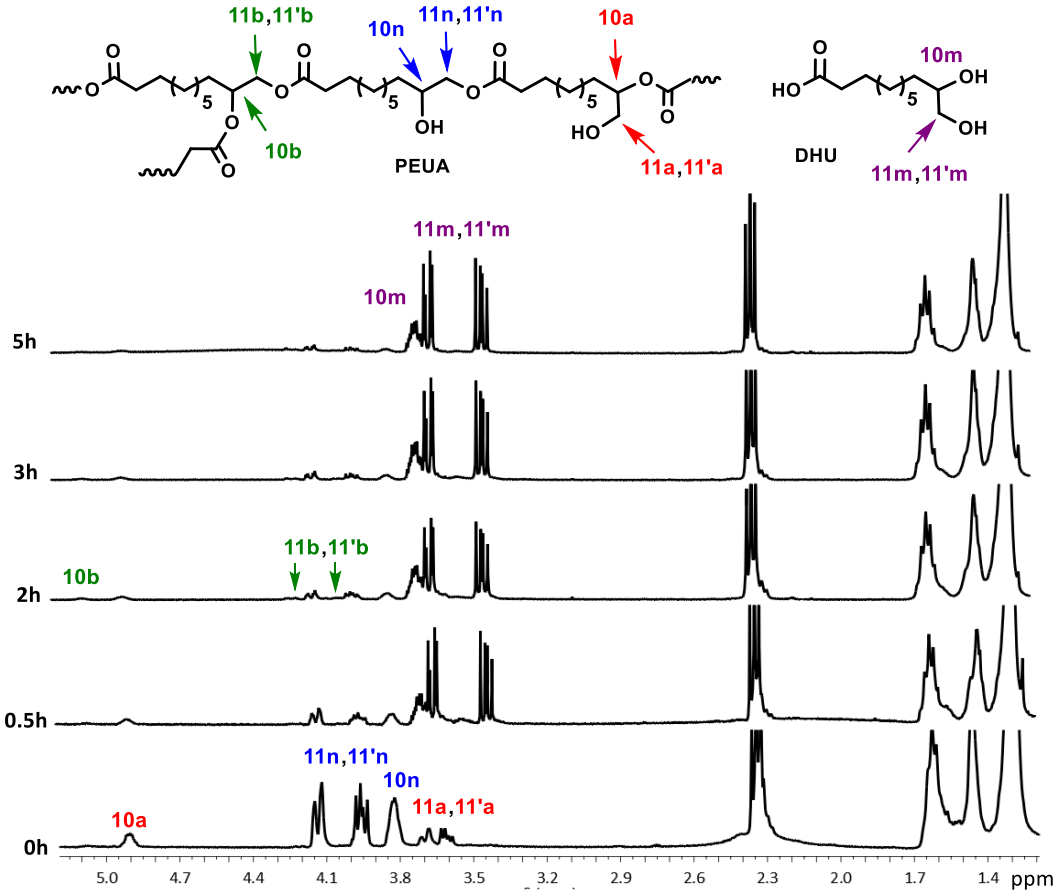

Figure 4.14 ^{1}H NMR spectra of PEUA accelerated hydrolytic degradation with 0.5 M of methanesulfonic acid at 100 ^{o}C versus time. Assigned signals correspond to normal (10n, 11,11'n), abnormal (10a, 11,11'a), branched (10b, 11,11'b) units and DHU monomer (10m, 11,11'm).

4.9 CONCLUSIONS

PEUA with hydroxy pendant groups and PHU, both derived from 10-undecenoic acid were synthesized with high yield. The hydrolytic and enzymatic degradations of PEUA and PHU were studied and compared with that of the commercial PCL. PEUA, PHU and PCL were characterized by ^{1}H RMN, SEC, DSC, TGA, XRD and hydrophilic/hydrophobic character. PHU showed the highest hydrophobicity and crystallinity, so that scarce hydrolytic degradation was detected. In contrast, in PEUA a Mn decrease by both hydrolytic and enzymatic

degradations was observed demonstrating that in this polyester the presence of hydrophilic pending group together with the superior amorphous character are determinant when comparing degradation of polyesters with the same chain length (C_{11}) and similar Mn. Significant weight loss (60 %) was only observed for PCL under enzymatic conditions. This different behaviour seems to indicate that PCL degrades through a surface erosion mechanism while PEUA do it through bulk erosion mechanism. Even after accelerated degradation in stronger conditions, PHU undergoes slight degradation whereas that PEUA and PCL suffer a significant degradation to produce low molecular weight products.

4.10 REFERENCES

[1] Vert M.; Aliphatic Polyesters: Great degradable polymers that cannot do everything, **2005**, *Biomacromolecules*, 6, 538-546.

[2] Bai Z.; Liu Y.; Su T.; Wang Z.; Effect of hydroxyl monomers on the enzymatic degradation of poly(ethylene succinate), poly(butylene succinate) and poly(hexylene succinate), **2018**, Polymers, 90, doi: 10.3390/polym10010090.

[3] Rowe M. D.; Eyiler E.; Walters K. B.; Hydrolytic degradation of bio-based polyesters: Effects of pH and time, **2016**, *Polym. Test.*, 52, 192-199.

[4] Holland S. J.; Tighe B. J.; Gould P. L.; Polymers for biodegradable medical devices. 1. The potential of polyesters as controlled macromolecular release systems, **1986**, *J. Control. Rel.,* 4, 155-180.

[5] Li S.; Vert M.; Biodegradation of aliphatic polyesters. In: Scott, G.; Gilead, D. Editors. Degradable polymers: principles and applications, **1995**, *London Chapman & Hall*, p. 43-87.

[6] Rydz J.; Zawidlak-Wegrzynnska B.; Christova D.; Degradable polymers. In Encyclopedia of Biomedical Polymers and Polymeric Biomaterials; **2015**, *M. K. Mishra, Ed.*, CRC Press: Boca Ratón, FL, USA.

[7] Rydz J.; Sikorska W.; Kyulavska M.; Christova D.; Polyester-Based (Bio)degradable Polymers as Environmentally Friendly Materials for Sustainable Development, **2015**, *Int. J. Mol. Sci.*,16, 564-596.

[8] ASTM Standard D6400, Standard specification for labelling of plastics designed to be aerobically compostable in municipal or industrial facilities; **2012** ASTM Annual Book of Standards; ASTM International: West Conshohocken, PA, 2012 (DOI 10.1520/D6400-12).

[9] Pitt C. G.; Gratzel M. M.; Kimmel G. L.; Surles J.; Schindler A.; Aliphatic polyesters II. The degradation of poly (DL-lactide), poly (ε-caprolactone), and their copolymers *in vivo,* **1981***, Biomaterials*, 2, 215-220.

[10] Lyu S.; Schley J.; Loy B.; Lind D.; Hobot C.; Sparer R.; Untereker D.; Kinetics and time–temperature equivalence of polymer degradation, **2007**, *Biomacromolecules*, 8, 2301-10.

[11] Gleadall A.; Pan J.; Kruft M-A.; Kellomäki M.; Degradation mechanisms of bioresorbable polyesters. Part 1. Effects of random scission, end scission and autocatalysis, **2014**, *Acta Biomater.*, 10, 2223-2232.

[12] Ken W.; Vladimir H.; Patrick A. T.; Relative importance of surface wettability and charged functional groups on NIH 3T3 fibroblast attachment, spreading, and cytoskeletal organization, **1998***, J. Biomed. Mater. Res.,* 41, 422-430.

[13] Ghassemi A. H.; van Steenbergen M. J.; Talsma H.; van Nostrum C. F.; Jiskoot W.; Crommelin D. J. A.; Hennink W. E.; Preparation and characterization of protein loaded microspheres based on a hydroxylated aliphatic polyester, poly(lactic-co-hydroxymethyl glycolic acid), **2009**, *J. Control. Release*, 138, 57-63.

[14] Göpferich A.; Mechanisms of polymer degradation and erosion, **1996**, *Biomaterials*, 17, 103-114.

[15] Albertsson A. C.; Varma I.; Aliphatic polyesters: synthesis, properties and applications, **2002**, *Adv. Polym. Sci*., 157, 1-40.

[16] Kasperczyk J.; Li S.; Jaworska J.; Dobrzynski P.; Vert M.; Degradation of copolymers obtained by ring-opening polymerization of glycolide and ε-caprolactone: a high resolution NMR and ESI-MS study, **2008**, *Polym. Degrad. Stab.,* 93, 990-999.

[17] Azevedo H. S.; Reis R. L.; Understanding the enzymatic degradation of biodegradable polymers and strategies to control their degradation rate, **2004**, *In Biodegradable Systems in Tissue Engineering and Regenerative Medicine; R. L. Reis, J. S. Roman, Eds., CRC Press: Boca Ratón*, FL. USA, pp 177-201.

[18] Valverde C.; Lligadas G.; Ronda J. C.; Galià M.; Cádiz V.; Hydroxyl functionalized renewable polyesters derived from 10-undecenoic acid: polymer structure and postpolymerization modification, **2018,** *Eur. Poly. J*., 105, 68-78.

[19] Wunderlich B.; Appendix 1: Table of thermal properties of linear macromolecules and related small molecules-The ATHAS data bank from Thermal Analysis of Polymeric Materials. Springer-Verlag Berlin Heidelberg, **2005,** p.777-800.

[20] Pitt C. G.; Poly (ε-caprolactone) and its copolymers. M. Chasin, **1990**, *R. Langer Eds. Marcel Dekker*, New York, NY, p. 81.

[21] White J. E.; Earls J. D.; Sherman J. W.; López L. C.; Dettloff M. L.; Step-growth polymerization of 10,11-epoxyundecanoic acid. Synthesis and properties of a new hydroxy-functionalized thermoplastic polyester, **2007**, *Polymer*, 48, 3990-3998.

[22] Kong Y.; Hay J. N.; The enthalpy of fusion and degree of crystallinity of polymers as measured by DSC, **2003**, *Eur. Polym. J.*, 39, 1721-1727.

[23] Castilla-Cortázar I.; Más-Estelles J.; Meseguer-Dueñas J. M.; Escobar J. L.; Martí B.; Vidaurre A.; Hydrolytic and enzymatic degradation of a poly(ε-caprolactone) network, **2012**, *Polym. Degrad. Stab.*, 971241-1248.

[24] Mochizuki M.; Hirami M.; Structural effects on the biodegradation of aliphatic polyesters, **1996**, *Polym. Adv. Tech*., 8, 203-209.

[25] Marten E.; Müller R-J.; Deckwer W-D.; Studies on the enzymatic hydrolysis of polyesters I. Low molecular mass model esters and aliphatic polyesters, **2003**, *Polym. Degrad. Stab*., 80, 485-501.

[26] Fisher E. W.; Sterzel H. J.; Wegner G.; Investigation of the structure of solution grown crystals of lactide copolymers by means of chemical reactions, **1973**, *Kolloid-Z.u.Z. Polymere*, 251, 980-990.

[27] Fernández J.; Larrañaga A.; Etxebarría A.; Sarasua J. R.; Effects of chain microstructures and derived crystallization capability on hydrolytic degradation of poly(L-lactide/ε-caprolactone) copolymers, **2013**, *Polym. Degrad. Stab*., 98, 481-489.

[28] Malberg S.; Höglund A.; Albertsson A. C.; Macromolecular design of aliphatic polyesters with maintained mechanical properties and a rapid, customized degradation profile, **2011**, *Biomacromolecules*, 12, 2382-2388.

[29] Kim E.; Uyama H.; Doi Y.; Ha C-S.; Iwata I.; Crystal structure and morphology of poly(11-undecalactone) solution-grown single crystals, **2004**, *Macromolecules*, 37, 7258-7264.

[30] Hu H.; Dorset D.L.; Crystal structure of poly(Ɛ-caprolactone), **1990**, *Macromolecules*, 23, 4604-4607.

[30] Gu X.; Raghavan D.; Nguyen T.; VanLandingham M. R.; Yebassa D.; Characterization of polyester degradation using tapping mode atomic force microscopy: exposure to alkaline solution at room temperature, **2001**, *Polym. Degrad. Stab.*, 74, 139-149.

[32] Ghaffar A.; Verschuren P. G.; Geenevasen J. A. J.; Handels T.; Berard J.; Plum B.; Dias A. A.; Schoenmakers P. J.; Van der Wal Sj.; Fast *in vitro* hydrolytic degradation of polyester urethane acrylate biomaterials: Structure elucidation, separation and quantification of degradation products, **2011**, *J. Chromatogr*. A, 1218, 449-458.

[33] Orozco-Castellanos L. M.; Marcos-Fernández A.; Martinez-Richa A.; Hydrolytic degradation of poly(ε-caprolactone-co-γ-butyrolactone: characterization and kinetics of hydrocortisone delivery, **2011**, Polym. Adv. Technol., 22, 430-436.

UNIVERSITAT ROVIRA I VIRGILI
10-UNDECENOIC ACID-BASED BIODEGRADABLE HYDROXY POLYESTERS: A PLATFORM FOR AMINOACID BIOCONJUGATES AND PEG-DERIVED AMPHIPHILIC COPOLYMERS
Carmen Valverde Sarmiento

Chapter 5

PEG-modified poly(10,11-dihydroxyundecanoic acid) amphiphilic copolymers. Grafting *versus* macromonomer copolymerization approaches using CALB

Publication derived from this work in *European Polymer Journal, 2018*. DOI: 10.1016/j.eurpolymj.2018.09.032

Supporting Information (SI) to this chapter in Annex C.

UNIVERSITAT ROVIRA I VIRGILI
10-UNDECENOIC ACID-BASED BIODEGRADABLE HYDROXY POLYESTERS: A PLATFORM FOR AMINOACID BIOCONJUGATES AND PEG-DERIVED AMPHIPHILIC COPOLYMERS
Carmen Valverde Sarmiento

5.1 INTRODUCTION

The development of polymers that are sustainable by combination of environmental, societal, human health and economic perspectives is a major challenge in polymer science. The key to shifting to sustainable alternatives will be to obtain both existing and new low-cost polymers with competitive performance properties from renewable resources.[1] Nowadays, the interest in polymers from renewable resources has been witnessing an incessant growth in both academic and industrial communities.[2,3] The situation has advanced to such extreme that it does no longer need the arguments previously put forward to justify its relevance. Among available renewable resources, vegetable oils and derived fatty acids represent a promising feedstock for the polymer industry, owing to their abundant availability, relative low cost and inherent degradability. Castor oil is one of the most valuable choices. Their high versatility and exclusion of alimentary sector convert this material in a good candidate to explore new routes to obtain biopolymers. 10-Undecenoic acid is available from the pyrolysis of castor oil, and it is a key substrate in polymer chemistry for the synthesis of precursors for the preparation of sustainable materials.[4]

The synthesis of vegetable oil-based linear polyesters has been extensively studied in the last years, including our group that has extended the use of 10-undecenoic acid to the synthesis of functionalized polyesters from specialty monomers.[5-14]

However, only limited attention has been dedicated to hyperbranched polyesters derived from plant oils. Related examples have involved the polycondensation of AB_n type precursors.[15-17] Oil-based polyesters bearing hydroxyl reactive pendent groups have also been reported.[14-21]

Interestingly, a linear hydroxyl functionalized hydrophobic polyester chain was modified to obtain a macro-chain transfer agent on which grafting from with bio-based acrylates was performed to prepare amphiphilic grafted copolymers.[21]

For many years, postpolymerization modification has been perceived as unavoidable, when one is unable to synthesize a polymer by direct polymerization. However, as it has become

apparent nowadays, the reasonable combination of efficient chemical transformations with macromolecular structures can provide a profusion of materials with irresistible properties, myriad functionalities, and elaborated architectures.[22]

By self-assembly or co-assembly of amphiphilic block copolymers have been prepared nanosized micelles with a core-shell architecture in a selective solvent and have attracted increasing attention for drug delivery.[23-26] The hydrophobic core serves as a natural carrier environment for hydrophobic drugs, and the hydrophilic shell stabilizes the particles in aqueous solution.[27] Micelles can be classified as simple and complex according to their structure and size. Primary micelles are generally smaller than 50 nm whereas complex micelles, larger in size (higher than 100 nm) are usually formed by secondary aggregation of primary micelles.[28]

Simple multimolecular micelles are generally formed by primary aggregation of block copolymers due to the microphase separation in selective solvents. The resulting self-assembled materials usually lack of the necessary thermodynamic stability when changes in concentration or other parameters as temperature or ionic strength occur, producing disassemble and the formation of free polymeric chains. These drawbacks can be overcome by core or shell crosslinking approaches endowing micelles with excellent structural stability although crosslinking generally compromises the final biodegradability. Alternatively, design of amphiphilic polymers with certain architectures such as dendritic, hyperbranched, star or heterografted brush-shaped molecules, provides an alternative strategy to prepare stable polymeric micelles. Due to their unique architecture can form unimolecular micelles with excellent stability regardless of the high dilution condition and other microenvironment changes.[29]

Amphiphilic hyperbranched polymers is one type of materials that have been widely used for unimolecular micelle preparation.[30] On contrary to other architectures such as dendritic polymers, these hyperbranched polymers can be synthesized following convenient one-step synthesis on a large scale and good yields, by simply polycondensation of ABx

monomers or ring opening polymerization of latent ABx monomers.[31] Strategies for preparing amphiphilic hyperbranched polymers include incorporation of hydrophobic components into a preformed hydrophilic polymeric chain, which essentially renders a block copolymer, or the modification of the hydrophobic hyperbranched core by the incorporation of multiple hydrophilic arms rendering graft polymers.[29,32] In this sense, PEGylation has for a long time been known as a simple and effective approach to provide the amphiphilic structures, enhanced water compatibility and self-aggregation properties.[33,34]

Both, amphiphilic PEG-derived block copolymers and grafted polymers can associate in the appropriate solvent to produce micellar architectures. Intramolecular assembly will lead to unimolecular micelles while intermolecular assembly will induce to multimolecular micelles. Moreover, in contrast to linear block copolymers, block hyperbranched and grafted polymers enable to tune the different associate structures by controlling branching degree or grafting density. Some examples of PEG-derived hyperbranched amphiphilic polyesters have been reported in the last decade including one that uses the environmentally friendly CALB as catalyst.[35-38]

In this report, we describe the synthesis and characterization of a renewable hydroxyl hyperbranched polyester: poly(10,11-dihydroxyundecanoic acid) (PDHU), by polycondensation using CALB as catalyst. Moreover, different approaches were used for the synthesis of partially renewable amphiphilic copolymers by incorporation of methoxypolyetileneglycol moieties ($mPEG_n$). First, copolymerization of $mPEG_n$-OH of different lengths and 10,11-dihydroxyundecanoic was used to produce block hyperbranched copolymers. Moreover, mPEG containing carboxylic acid groups ($mPEG_2OCH_2COOH$ and $mPEG_3OOC(CH_2)_2COOH$) was attached to hydroxyl groups of linear and hyperbranched PDHU to render different grafted polymers. The self-assembly and micellar behaviour of these amphiphilic structures was investigated.

5.2 MONOMER SYNTHESIS

5.2.1 Synthesis of 10,11-epoxyundecanoic acid (EUA)

Following a general procedure, 10,11-epoxyundecanoic acid (EUA) was synthesized from 10-undecenoic acid using 30 % H_2O_2 and CALB as catalyst as previously described (Chapter 3). This monomer was used to prepare linear PEUA for mPEG grafting (Chapter 5.5).[39,14]

5.2.2 Synthesis of 10,11-dihydoxyundecanoic acid (DHU)

Microbial fatty acid-hydroxylation enzymes, including P450, lipoxygenases, hydratases, 12-hydrolases and diol synthases allow regio-specific synthesis of a variety of hydroxyl fatty acids.[40] Dihydroxy fatty acids are also accessible using bacterial or fungal synthases, but generally mixtures of unsaturated diol compounds are obtained which are not easily scalable because imply biotechnological methodologies or the use of non-commercial enzymatic catalysts. Thus, transformation of fatty acid double bonds into *vic* diols *via* chemical transformation seems much more feasible. Several efficient methods for direct dihydroxylation have been described but rely on the use of metallic catalysts (Ag, Mn, Ru, Os, Rh) which, due to their toxicity, must be avoided specially in biomedical applications. In this sense, the ring opening of epoxy fatty acids is a more convenient way as can be easily carried out *via* simple acid or basic hydrolysis. Epoxides are readily accessible by conventional epoxidation with peracids without the aid of metallic catalysts. Moreover, epoxidation with hydrogen peroxide catalysed by lipases, is a more convenient route from the sustainability point of view.[41] Both transformations, epoxidation and oxirane ring opening, can be carried out under mild conditions and are easily scalable. Moreover, they have the additional advantage that can be performed in one pot reaction, by the consecutive double bond epoxidation with “in situ” generated performic acid, epoxide ring opening by formic acid and hydrolysis of the resulting mixture of *vic*-hydroxy formiates (Scheme 5.1).[42,43]

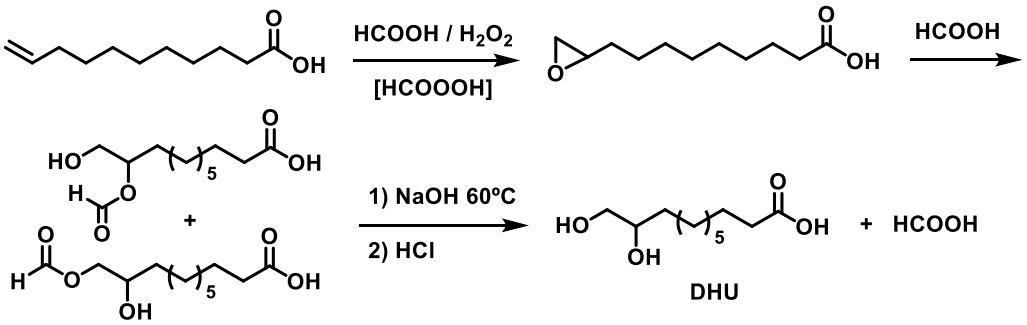

Scheme 5.1 One pot-three steps synthesis of 10,11-dihydroxyundecanoic acid.

This ancient procedure is nowadays envisaged as a green and useful synthetic tool because it uses water as solvent and hydrogen peroxide and formic acid as reagents. Formic acid is the major byproduct from lignocellulosic biomass processing and thus, constitutes a versatile new green reagent.[44,45] Using this procedure, 10,11-dihydroxyundecanoic acid (DHU) was synthetized in multigram scale with almost quantitative yield and high purity (Figure 5.1).

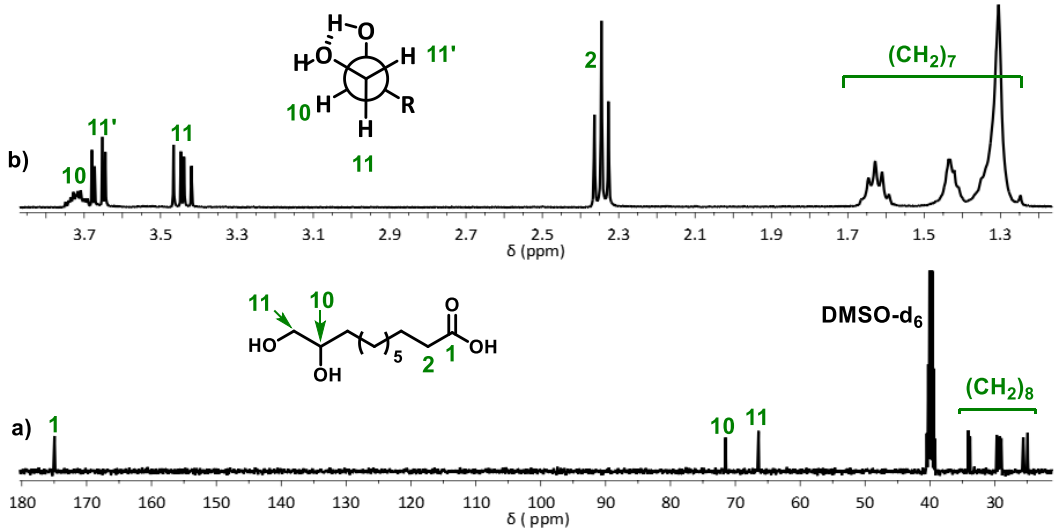

Figure 5.1 DHU monomer spectra of a) ^{13}C NMR recorded in DMSO-d_6 and b) ^{1}H NMR recorded in $CDCl_3$.

5.3 HOMOPOLYMER SYNTHESIS AND STRUCTURAL DETERMINATION

In a previous work our group reported the ring opening polymerization of 10,11-epoxyundecanoic acid catalysed by tetrabutylphosphonium bromide (TBPB to prepare linear hydroxypolyesters (PEUA) as precursors for amino acid decorated bio-polymers (Chapter 3.4).[14] This study demonstrated that, under certain conditions, (ie. T > 100 °C or long polymerization times) different percentages of branched structures were also obtained. However, attempts to extend this polymerization methodology to the preparation of hyperbranched polyesters led to the formation of important percentages of insoluble crosslinked materials. Thus, the polycondensation of dihydroxy fatty acid derivatives was considered as a more straightforward way to prepare these bio-based hyperbranched hydrophobic structures.

5.3.1 EUA polymerization

EUA homopolymerization was carried out with 1 % of TBPB in a 2.5 M solution in toluene at 100°C for 8 h following a described procedure.[14] Thus, a linear hydroxyl polyester (PEUA) with Mn 9800 g·mol^{-1} and Đ 3.4 was obtained. Its structure contained 71 % of normal ring-opening units (secondary hydroxyl groups) and 29 % of abnormal ring-opening groups (primary hydroxyl groups) (see Figure 3.5 and Figure 3.8 in Chapter 3).

5.3.2 DHU polymerization

5.3.2.a Synthesis of poly(10,11-dihydroxyundecanoic acid) (PDHU)

First, DHU homolymerization with different catalysts was considered to study the monomer polycondensation behaviour (Scheme 5.2).

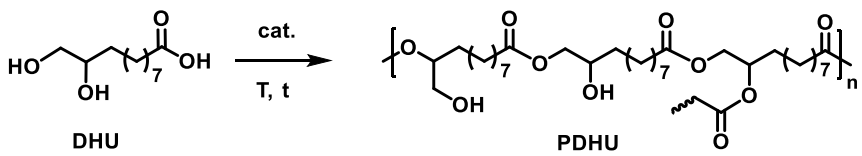

Scheme 5.2 Representative structure of PDHU indicating the three possible structural units *via* homopolymerization of DHU.

First metallic Lewis acid catalysts were considered. Metal salts, oxides or alkoxides have been described as effective condensation catalyst but usually require too high temperatures (160-250 °C) that, in the case of DHU, would lead to crosslinked materials. So only relatively low temperatures were tested with Ti(*t*-BuO)$_4$ and Sn(Oct)$_2$ as catalysts. At 120 °C either in bulk or in toluene solution (2.5 M) complete conversion was achieved after 24 h. Moreover, the obtained polyesters contained important fractions of crosslinked material. Working at 110 °C with Sn(Oct)$_2$, soluble polyesters could be obtained (Table 5.1, entries 1 and 2). After 6 h of reaction, monomer conversion was not complete and the resulting polymer had a predominant linear structure. Increasing polymerization time lead to almost complete conversion of branched polyester with moderate molecular weight was obtained. Lanthanide triflates have been described as effective catalysts under mild conditions allowing the condensation of dihydroxydicarboxylic acids with diols with good conversion and moderate molecular weight.[46] We tested the polymerization with Sc(OTf)$_3$ and Sm(OTf)$_3$ at 80 °C in solution of DPE (2.5 M) (Table 5.1, entries 3 and 4). After 24 h, in both cases, poor conversions of medium molecular weight polyesters with a branched structure were achieved. This behaviour is not in accordance with the described selectivity of these catalysts towards esterification of primary alcohols and evidences poor chemo-selectivity when both alcohol types are in vicinal positions.[47] Enzymatic catalysts, especially lipases, have been reported as a green alternative in the effective ring opening and polycondensation polymerization to produce polyesters under mild conditions.[48,49] *Candida antarctica* lipase B (CALB) is by far the most studied as it is available as an heterogeneous bio-catalyst consisting of CALB physically immobilized within a macroporous resin of poly(methylmethacrylate). This catalyst form, commercialized as

Novozym 435, offers additional advantages as easy manipulation, easy removal from the polymerization mixture and robust nature that, under certain conditions, allows recycling. The polycondensation of monomers containing both hydroxyl and carboxyl groups in the same structure have also been described with CALB.[50,51] The efficiency of enzymatic catalysts can be affected by process parameters such as polymerization temperature, polymerization technique (solution or solvent-free) as well as water removal methods (e.g. application of vacuum, water absorption in molecular sieves, azeotropic distillation).[49] Thus DHU polymerization was tested at 80 and 90 °C in bulk and in DPE solution (2 M) with continuous application of vacuum (200 mmHg) and in toluene solution (2 M) in presence and absence of 4 Å molecular sieves (MS) (Table 5.1).

CALB polymerization test in bulk and in DPE solution at 90 °C led to formation of extensive crosslinked insoluble fractions, but in toluene and in presence of MS (Table 5.1 entry 5) high conversion of soluble almost linear polyester was obtained after 24 h. Extending the polymerization time to 48 h (Table 5.1 entry 6) lead to complete conversion of branched polyester with increase of both molecular weight and polydispersity due to that transesterification reactions probably takes place. Working at 80 °C for 24 h in bulk (Table 5.1 entry 7) lead to good conversions of soluble branched polyester with lower molecular weight than those obtained in toluene at 90 °C. In DPE solution (Table 5.1 entry 8) noticeably better results were obtained with a complete conversion and the formation of a medium molecular weight polyester with considerable branching degree (~22 % of branched units) was observed.

Assays in toluene solution with and without the 4Å MS as water scavenger (Table 5.1 entries 9-10) gave much better results. Complete conversion of relatively high molecular weight branched polyester was obtained after 24 h indicating that under the studied conditions enzyme has higher activity when working at 80 °C in toluene (compare with Table 5.1 entry 8).

Table 5.1 Conversion, molecular weight and microstructure composition of PDHU obtained with various catalysts and conditions.

Ent.	Cat.	Solv.[a]	Temp (°C)	T (h)	Conv. %[b]	Mn (g·mol^{-1})[c]	Đ[c]	N_u %[d]	A_u %[d]	B_u %[d]
Conditions: 0.5 mol % metallic catalysts										
1	$Sn(oct)_2$	---	110	6	27.0	1450	1.30	80.0	18.0	2.0
2	$Sn(oct)_2$	---	110	24	95.5	3900	4.53	47.5	28.3	24.2
3	$Sc(OTf)_3$	DPE	80	48	52.2	2440	1.67	56.8	24.4	18.8
4	$Sm(OTf)_3$	DPE	80	48	48.2	1860	1.61	44.8	32.7	22.5
Ent.	**Water removal**	**Solv.[a]**	**Temp (°C)**	**T (h)**	**Conv. %[b]**	**Mn (g·mol^{-1})[c]**	**Đ[c]**	**N_u %[d]**	**A_u %[d]**	**B_u %[d]**
Conditons: 10 % (w/w) enzymatic catalyst [CALB]										
5	4Å MS	Tol.	90	24	92.3	11840	2.0	64.8	34.8	0.4
6	4Å MS	Tol.	90	48	~ 100	16080	3.2	58.3	18.7	23.0
7	vacuum	--	80	24	88.0	8500	2.1	64.2	20.9	14.9
8	vacuum	DPE	80	24	~ 100	14870	2.2	56.2	22.0	21.8
9	4Å MS	Tol.	80	24	~ 100	19700	2.3	50.0	23.4	26.6
10	4Å MS	Tol.	80	48	~ 100	25860	2.0	47.8	18.0	34.2
11	---	Tol.	80	24	~ 100	28470	1.6	49.0	18.3	32.7
12	---	Tol.	80	48	~ 100	39460	1.6	45.8	14.1	40.1

a) 2M solution; b) DHU conversion calculated by ^{1}H NMR from the crude mixture; c) Determined by SEC; d) Percentage of normal (N_u), abnormal (A_u) and branched units determined by ^{1}H NMR from the signals at 4.15 and 3.97 ppm (N_u), at 4.90 and 3.69 ppm (A_u) and 5.12 and 4.20 ppm (B_u).

Extending the polymerization time (48 h) translates into an increase in molecular weight and branching degree but a decrease in the polydispersity. This indicates that in these conditions, the post condensation transesterification processes recombine chains of different length furnishes a more uniform hyperbranched structure. Polymerizations in absence of water scavenger agent (Table 5.1 entries 11-12) led to similar good conversions

but, unexpectedly, narrower polyesters with significantly higher molecular weight were obtained. This behaviour is against the generally observed for esterification and transesterification polycondensations with CALB and could be related with the number of molecular sieves used in the polymerization tests. Excessive dehydrating conditions could remove part of tightly bound water from the enzyme domains which is essential for enzyme catalytic activity.[52,53] In any case, under these simple conditions, polyesters with the highest molecular weight (~39500 g·mol^{-1}) and branching degree (~40 % of branched units) were obtained.

At this point, it must be noted that according to the results, although it is described that esterification occurs selectively at primary hydroxyl groups during the initial polycondensation step (percentage of N_u is always greater than A_u), branching and post condensation transesterification processes seem to proceed indistinctly from both types of hydroxyl groups. (Increase in branching decreases N_u and A_u in a similar percentage).[54] CALB catalysts are described to be more active in transesterification of both primary and secondary alcohols than in their direct polycondensation. This fact could explain the minor selectivity observed in the final polyesters.[48,49]

To prepare a PDHU sample of intermediate molecular weight, polymerization of DHU using conditions in entry 6 table 5.1 was scaled to 3.0 g (15.0 mmol) to obtain a polyester sample with 15800 g·mol^{-1} and Đ 2.7, with 22.1 % of branching units, 57.5 % of secondary hydroxyl units and 20.3 % of primary hydroxyl units, which was used as substrate for the post-polymerization modification with mPEG carboxylic derivatives *vide infra*. In Figure 5.2 a the ^{1}H NMR spectrum of PHDU with the corresponding assignments in a representative structure is shown.

5.3.2.b Structural characterization of PDHU

In Figure 5.2 a is shown the ^{1}H NMR spectrum of PDHU. A representative general structure of polyester including the three possible different repetitive units arising from normal ring-opening, abnormal ring-opening and branching through transesterification, and the chain

ends is also included. It must be pointed out that transesterification occurs either through primary or secondary alcohols giving non distinguishable signals by NMR branching units.

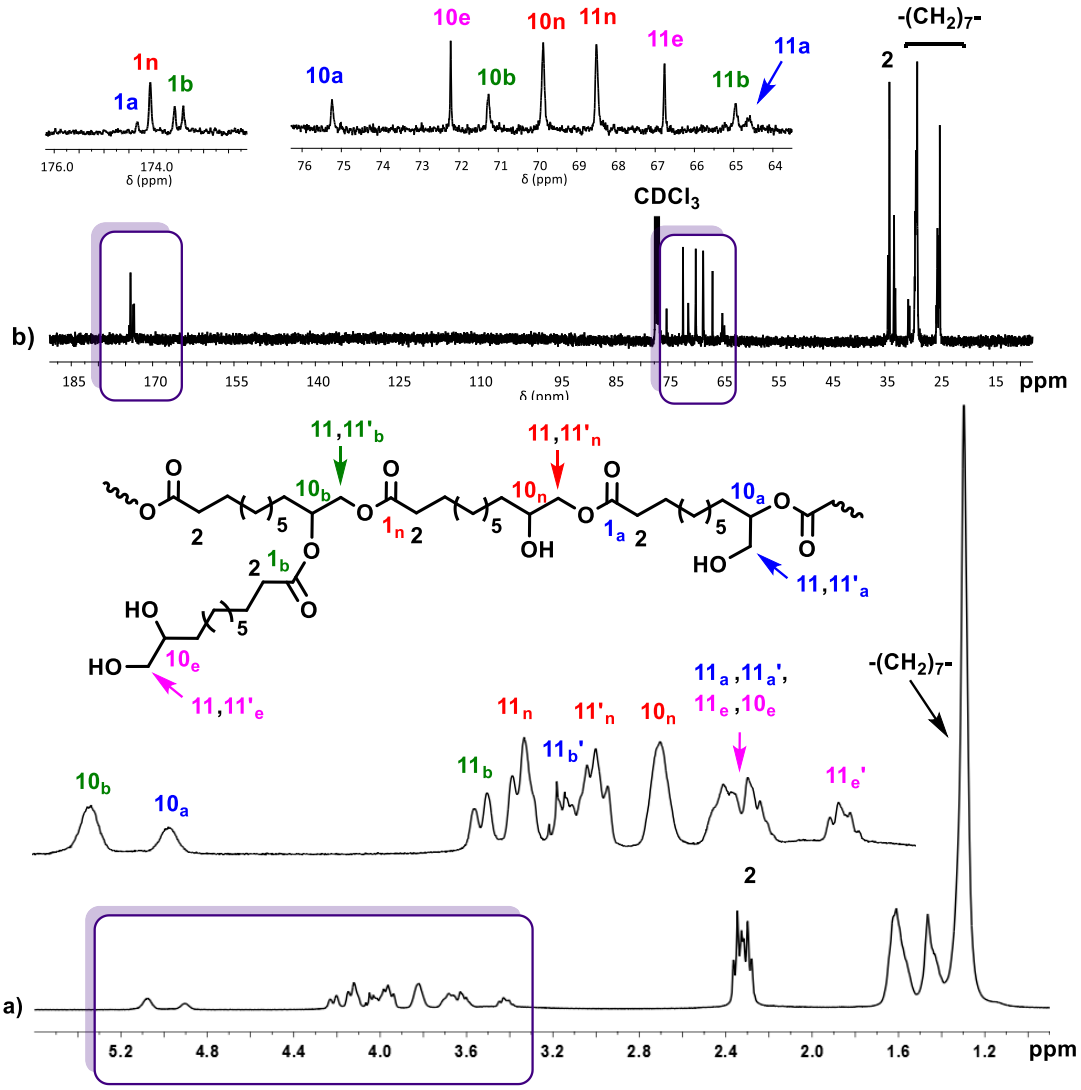

Figure 5.2 a) ^{1}H and b) ^{13}C NMR spectra of PDHU recorded in $CDCl_3$ with the corresponding assignments.

The ^{1}H NMR spectra signals corresponding to the methine and methylene protons of the different units, named with the subscript **n**, **a** and **b** for "normal", "abnormal" or "branched" respectively, were unequivocally assigned by comparison with the methylene and methine signals of model compounds (Figure SI.1), and their corresponding trifluoroacetate derivatives (Figure SI.2 and SI.3). Moreover, 10,11-dihydroxyundecanoic acid was used as model for the polymer chain end groups (Figure 5.1).

The content of normal, abnormal and branched units was determined by comparing the integration of the corresponding ^{1}H (Figure 5.2 a) and ^{19}F NMR (Figure 5.3) signals of the pristine and their trifluoroacetylated derivatives (see SI.4). The percentage of normal, abnormal, branched and diol end groups could be estimated from integration of the corresponding signals in the ^{1}H NMR spectrum of pristine polyester and ^{1}H and ^{19}F NMR spectra of the corresponding trifluoroacetylated derivative (PDHU-TFA) are collected in Table 5.2. As can be seen, all quantifications show acceptable concordance with the proposed unit distribution, with about 56-57 % of normal units and 21-23 % of branched units. It must be noted that percentage of diol end groups is slight lower than the expected according to the percentage of branched units what could be related to the different relaxation times in NMR of the corresponding protons.

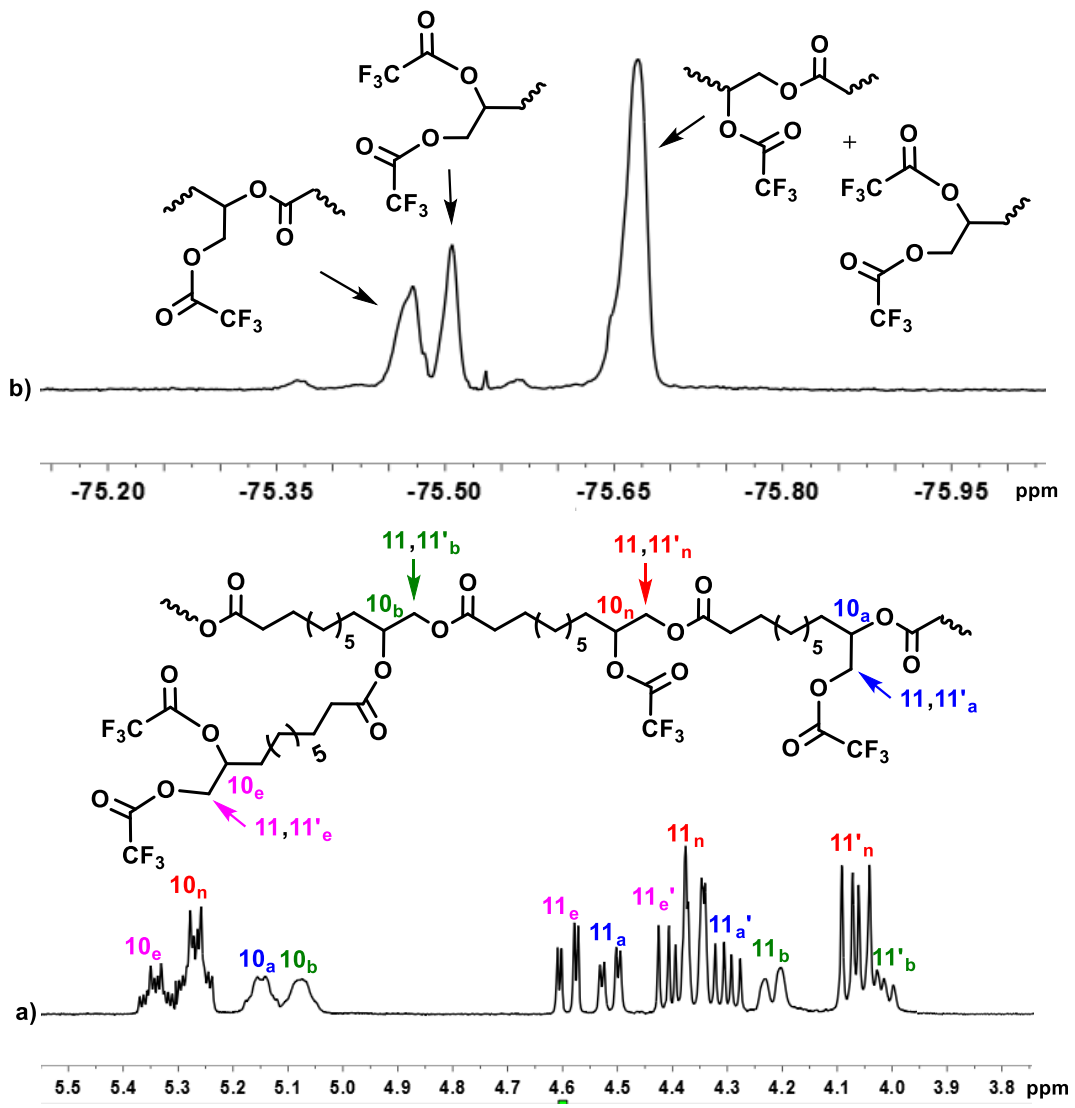

Figure 5.3 a) ^{1}H NMR and b) ^{19}F NMR spectra of PDHU-TFA with the corresponding assignments.

Table 5.2 Quantifications of the different units in PDHU and PDHU-TFA by ^{1}H NMR and ^{19}F NMR.

	PDHU		PDHU-TFA			
	^{1}H NMR		^{1}H NMR		^{19}F NMR	
Unit	δ ppm	%	δ ppm	%	δ ppm	%
n	3.83	57.5	5.27	56.5	-75.68	55.9
a	4.91	20.3	5.15	21.9	-75.47	23.5
b	5.08	22.1	5.08	23.0	-75.52/-75.68	20.6
e	3.62	19.5	5.34	20.9	--	---

PDHU ^{13}C NMR spectrum assignments (Figure 5.2 b) were also undertaken by comparison with those of models (compounds **A**, **B** and **C**) and ^{1}H-^{13}C heteronuclear bidimensional correlations (Figure SI.4). The methine and methylene carbons of the normal (70.0 and 68.7 ppm), abnormal (75.4 and 64.9 ppm), branched (71.4 and 65.1 ppm) units, and diol end groups (72.4 and 66.9 ppm) appear with different intensity sustaining the presence of about 56-57 % of normal units and 22-23 % of branched units. Ester groups in abnormal and normal units can be differentiated by C=O signals at 174.5 ppm and 174.2 ppm respectively. Moreover, branched units, that could not be differentiated by ^{1}H NMR, can be distinguished by C=O signals that appear at 173.9 and 173.7 ppm.

5.4 DHU COPOLYMERIZATION WITH mPEG-OH

The good results obtained in the homopolymerization of DHU led us to consider CALB in toluene at 80 °C as the catalyst and polymerization conditions of choice for the copolymerization of DHU using mPEG-OH as comonomer (Scheme 5.3). In the literature, amphiphilic copolymers were mostly prepared by CALB catalysed chemical modification of the corresponding methyl or vinyl esters through a transesterification reaction, but some few examples using free carboxylic acids also do exist.[55,56]

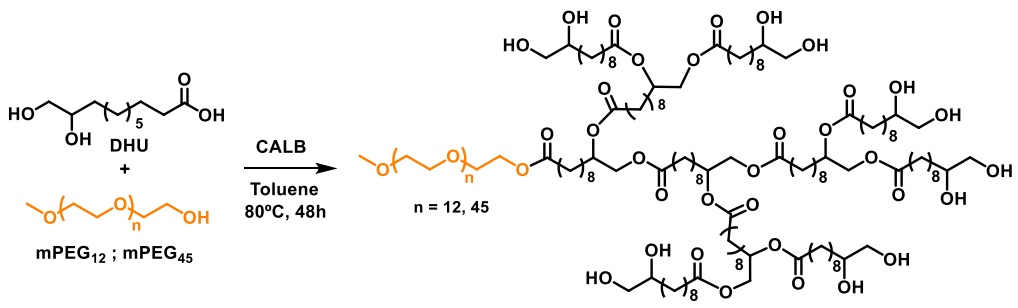

Scheme 5.3 Synthesis of amphiphilic polymers by copolymerization of DHU in presence of mPEG-OH, showing a representative mPEG-*b*-PDHU structure.

Two commercial monomethylated mPEGs of 550 and 2000 g·mol^{-1} were selected as hydrophilic macromonomers. Their formula weight corresponds to 12 and 45 ethylenoxy repeating units, and were named as mPEG$_{12}$OH and mPEG$_{45}$OH. The polymerizations were carried out in the same conditions as in Table 5.1, entry 12 (2 M toluene solution, 10 % (w/w) of CALB at 80 °C for 48 h). For each mPEG two different mPEG:DHU molar ratios in the feed were tested, 1:10 and 1:20. Using these conditions, according to the ^{1}H and ^{13}C NMR spectra of the crude reaction mixture, complete DHU conversion was achieved but incorporation of mPEG$_n$-OH was lower than those in the feed was. Even that, degrees of modification are considerable high (see SI.5) and repeated warm water washings could remove remaining unreacted mPEG-OH (confirmed by ^{13}C NMR spectroscopy).

Once purified, the copolymer compositions were determined by ^{1}H NMR (Figure SI.6 and SI.8) taking into account the relative intensities of the signals at ca. 2.35 ppm of the α-methylene to ester group (CH$_2$-COO), and at 3.38 ppm of methyl of mPEG$_n$. Thus, when working with 1:10 molar ratio, mPEG$_n$ incorporation was about 90 % of the feed which correspond to copolymers with molar composition mPEG$_{12}$-PDHU$_9$ and mPEG$_{45}$-PDHU$_9$. In the case of 1:20 molar ratio, incorporation decreases to 75 % which correspond to copolymers with molar composition mPEG$_{12}$-*b*-PDHU$_{15}$ and mPEG$_{45}$-*b*-PDHU$_{15}$ (Table 5.3). In Figure 5.4 b the ^{1}H NMR spectrum of mPEG$_{12}$-*b*-PHDU$_9$ with the corresponding assignments in a representative structure is shown.

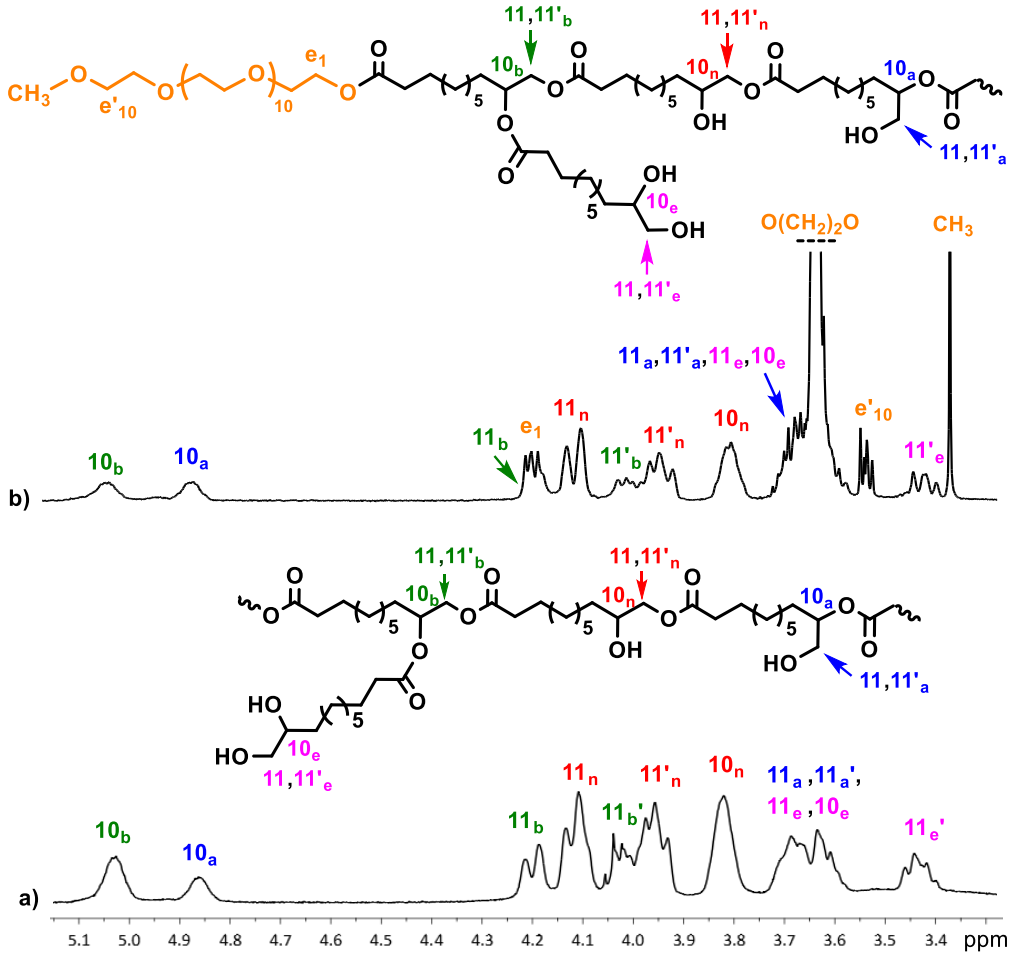

Figure 5.4 Region between 5.2 and 3.2 ppm ^{1}H NMR spectrum of a) PDHU and b) mPEG$_{12}$-*b*-PHDU$_{9}$ with the corresponding assignments in a representative structure.

Moreover, the microstructure of the PDHU block was determined by comparing the ^{1}H NMR intensity of the signals at ca. 5.07 ppm, 4.87 ppm and 3.83 ppm corresponding respectively to methines attached to an ester (in a branched unit), to a primary hydroxyl (in an abnormal unit) and to a secondary hydroxyl (in a normal unit) respectively. The results are collected in Table 5.3.

Table 5.3 Composition, molecular weight and microstructure of copolymers mPEG$_m$-*b*-PDHU$_n$ obtained after 48 h with CALB in toluene at 80 °C.

	mPEG:DHU molar ratio		Molecular weight			Structure	
Copolymer name	**feed**	**^{1}H NMR[a]**	**Mn (g·mol^{-1})[a]**	**Mn (g·mol^{-1}) [b]**	**Đ[b]**	**N_u %[c]**	**B_u %[c]**
mPEG$_{12}$-*b*-PDHU$_9$	1:10	1:09	2300	4100	2.5	54	23
mPEG$_{12}$-*b*-PDHU$_{15}$	1:20	1:15	3530	5300	2.1	53	27
mPEG$_{45}$-*b*-PDHU$_9$	1:10	1:09	3800	5500	2.1	52	29
mPEG$_{45}$-*b*-PDHU$_{15}$	1:20	1:15	5030	9100	2.3	48	32

a) Determined by ^{1}H NMR from signals at 3.38 and 2.35 ppm; b) Determined by SEC in THF; c) Percentage of normal (N_u) and branched units (B_u) determined by ^{1}H NMR from the signals at 3.83 ppm (N_u) and 5.07 ppm (B_u).

Polymerizations initiated by mPEG$_{12}$OH and mPEG$_{45}$OH with increasing amounts of DHU lead to copolymers with increasing molecular weight that according to their ^{1}H NMR spectra suppose the introduction of about 9 (mPEG$_n$-*b*-PDHU$_9$) and 15 (mPEG$_n$-*b*-PDHU$_{15}$) DHU units in an hyperbranched arrangement. Molecular weights determined by SEC are 60-80 % higher than those estimated by ^{1}H NMR spectroscopy. These differences are attributed to the different hydrodynamic volume when compared with polystyrene standards. This behaviour has been previously described for PEUA and it is also observed in PDHU homopolymers.[14] Referring to polydispersity indexes (Đ), they are in rang 2.1-2.5 and close to PDHU homopolymers. The microstructure of the PDHU block can be inferred from the relative percentage of normal, abnormal and branched units. In general, all copolymers show branching degree (23-32 %) and percentage of normal units (48-54 %) but branching seems to increase as DHU content does, as mPEG$_n$-*b*-PDHU$_9$ have lower branching degrees than mPEG$_n$-*b*-DHU$_{15}$. This behaviour, seems to indicate that the presence of mPEG-OH in the polymerization medium does not affect CALB activity in a measurable way.

5.5 PDHU AND PEUA GRAFTING WITH $mPEG_2OCH_2COOH$ AND $mPEG_3OOC(CH_2)_2COOH$

CALB has also been reported as efficient catalyst in the chemical functionalization of many different polymers and has specifically been used for preparing amphiphilic polymers by esterification-modification of polyglycerol with mPEG carboxylic derivatives.[57,24] According to that, polyester hydroxyl group modifications were carried out using CALB in toluene working at 80 °C during 48 h in order to achieve maximum modification degrees.

To study the possible effect of the starting polymer structure, two different hydroxypolyesters were tested: a hyperbranched PDHU of 15800 $g \cdot mol^{-1}$ and Đ 2.7 with 22.1 % of branched units and a linear PEUA of 9800 $g \cdot mol^{-1}$ and Đ 3.4. Also, two different carboxy-functionalized mPEG derivatives with different PEG length were used: 2-(2-(2-methoxyethoxy)ethoxy)acetic acid ($mPEG_2OCH_2COOH$) and 2-(2-(2-methoxyethoxy)ethoxy)ethyl monosuccinate ($mPEG_3OOC(CH_2)_2COOH$). The reaction is represented in Scheme 5.4.

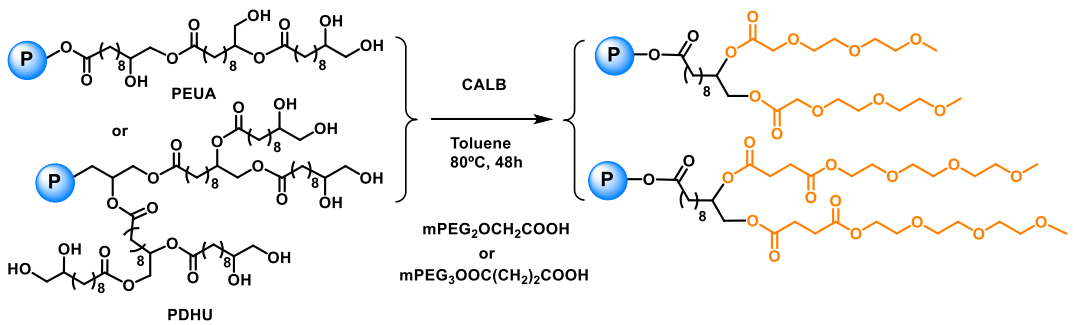

Scheme 5.4 Schematic representation of the CALB modification of PEUA and PDHU with $mPEG_2OCH_2COOH$ and $mPEG_3OOC(CH_2)_2COOH$ (in the grafted polyesters, only the modification of one *vic*-diol end group is represented).

In all cases, two equivalents of grafting acids per hydroxyl group were used. After 48 h, the partial grafting onto both polymers could be detected by ^1H and ^{13}C NMR spectroscopy (42-56 %, see SI.6) and quantified using the ^1H NMR signals at 3.38 and 2.35 ppm for $mPEG_2OCH_2COO$-*g*- (Figure SI.10 b and Figure SI.12 b) and at 3.35, 2.66 and 2.33 ppm for

$mPEG_3OOC(CH_2)_2COO$-*g*- (Figure SI.10 c and Figure SI.12 c) (Table 5.4). Moreover, ^{13}C NMR allowed confirming the complete elimination of unreacted acids after work-up. Percentages of grafting achieved with $mPEG_2OCH_2COOH$ are higher than those with $mPEG_3OOC(CH_2)_2COOH$, probably due to major reactivity of α-alkoxy carboxylic acid.

Microestructure of the remaining non grafted units was determined (see SI.6) by comparing the ^1H NMR intensity of the signals at ca. 5.06 ppm, 4.87 ppm and 3.82 ppm corresponding respectively to methines attached to an ester (B_u), to a primary hydroxyl (A_u) and to a secondary hydroxyl (N_u) respectively (Table 5.4). In Figure 5.5 the ^1H NMR spectrum of $mPEG_2OCH_2COO$-*g*-PEUA and $mPEG_3OOC(CH_2)_2COO$-*g*-PEUA with the corresponding assignments in a representative structure are shown.

As can be seen, grafting onto PDHU takes place without significant changes in the branching structure which remains about 20 %. On the contrary, grafting onto linear PEUA lead to a branched structure (16-17 %) which indicates that during grafting process CALB also catalyses transesterifications altering the linear structure. Mn determined by SEC, are significantly lower than those of starting PEUA and PDHU, which could be related to the drastic variation on the hydrodynamic volume when introducing hydrophilic side chains. Moreover, some CALB promoted ester cleavage and transesterification with the excess of grafting reagent should not be discarded. ^1H NMR spectroscopy does not allow confirming this ester cleavage since the expected resulting *vic*-diol moieties are also esterified by the carboxylic PEG derivatives. In any case, PDHU derivatives show higher Mn and Đ than PEUA derivatives.

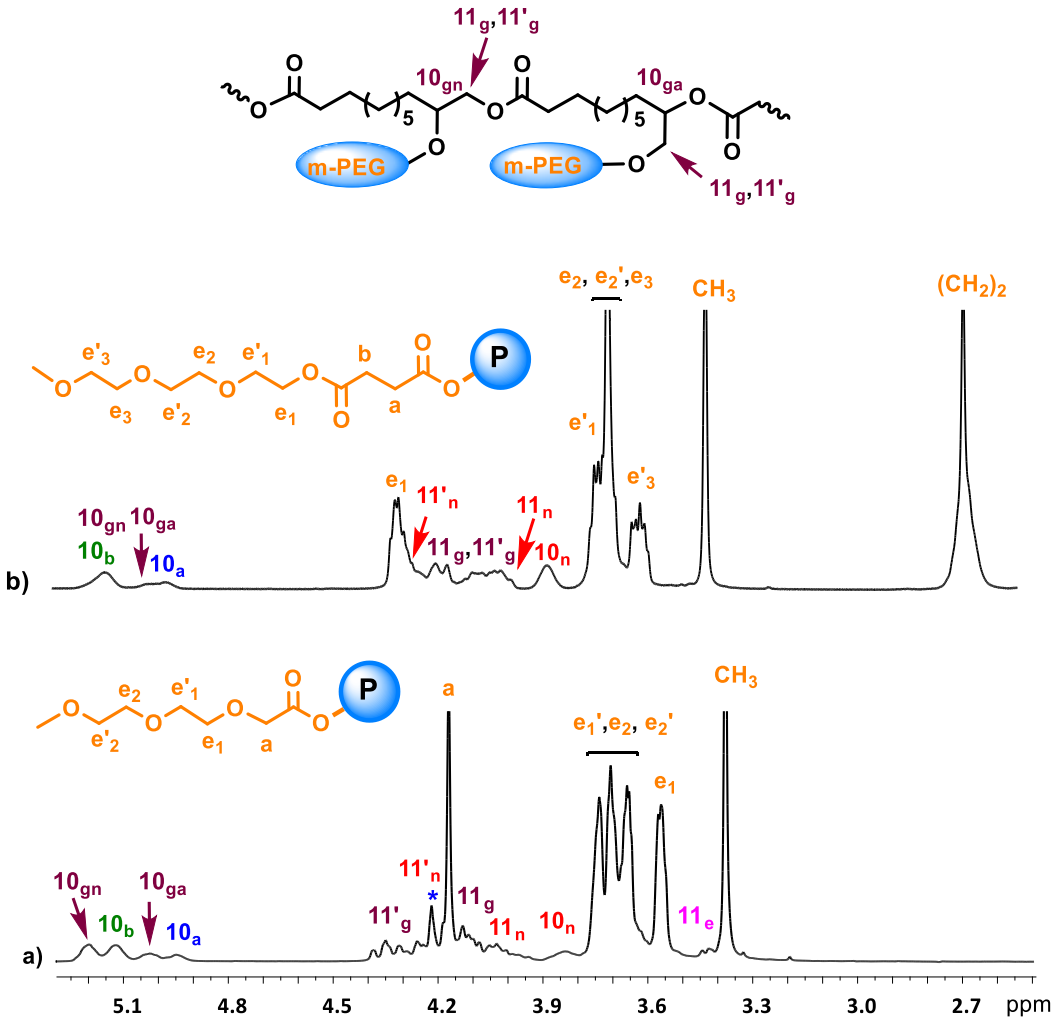

Figure 5.5 Region between 5.3 and 2.6 ppm of the ^{1}H NMR spectrum of a) mPEG$_2$OCH$_2$COO-*g*-PEUA and b) mPEG$_3$OOC(CH$_2$)$_2$COO-*g*-PEUA with the corresponding assignments in a representative structure. Assignments of the un-grafted starting units are indicated in Figure 5.4 a).

Table 5.4 Composition, molecular weight and microstructure of PEUA and PDHU grafted with $mPEG_2OCH_2COOH$ and $mPEG_3OOC(CH_2)_2COOH$ using CALB in toluene at 80 °C.

Polymer name	Grafting %[a]	Mn ($g \cdot mol^{-1}$)[b]	Đ[b]	N_u %[c]	B_u %[c]
$mPEG_2OCH_2COO$-*g*-PEUA	56	1600	2.0	20	16
$mPEG_3OOC(CH_2)_2COO$-*g*-PEUA	42	1700	2.2	33	17
$mPEG_2OCH_2COO$-*g*-PDHU	54	4500	3.0	19	20
$mPEG_3OOC(CH_2)_2COO$-*g*-PDHU	46	6700	3.6	28	20

a) Percentage of grafting determined by ^{1}H NMR from signals at 3.38 and 2.35 ppm for $mPEG_2OCH_2COO$-*g*-PEUE/PDHU and at 3.35, 2.66 and 2.33 ppm for $mPEG_3OOC(CH_2)_2COO$-g-PEUA/PDHU; b) Determined by SEC in THF; c) Percentage of normal (N_u) and branched units (B_u) determined by ^{1}H NMR from the signals at 3.82 ppm (N_u) and 5.07 ppm (B_u).

5.6 THERMAL CHARACTERIZATION OF mPEG BLOCK AND GRAFTED POLYMERS

The thermal characteristics of homopolymers, block copolymers and grafted polymers were determined by DSC and TGA and are collected in Table 5.5. PDHU is semicrystalline and shows a Tm of 39 °C which is lower than that of PEUA (43° C) according to its branched structure. Block copolymers also show semicrystalline character with Tm between 44 °C and 56 °C and superior melting enthalpies for those with longer mPEG.[14] Unlike PDHU, block copolymers do not show detectable Tgs. Concerning grafted polymers, they are amorphous with low Tgs indicating that grafting mPEG groups prevent crystallization of aliphatic polymer chains.

Thermal stability evaluated by TGA shows scarce differences between the homopolymer and its corresponding block copolymers. Different behaviour was observed for grafted polymers with a significant decrease in temperature at which 5 % weight loss takes place although temperature for maximum degradation rates are similar. This could be related to the higher percentage of labile ester groups and their lower molecular weight.

Table 5.5 Thermal properties of PDHU and their block and grafted polymers.

Polymer name	DSC analysis			TGA analysis	
	Tm (°C)[a]	ΔH (KJ·mol^{-1})[a]	Tg (°C)[b]	$T_{5\%}$ (°C)[c]	T_{max} (°C)[d]
PDHU	39.0	5.7	- 13	360	408/469
mPEG$_{12}$-*b*-PDHU$_9$	43.8	2.6	-	354	407/461
mPEG$_{12}$-*b*-PDHU$_{15}$	55.7	3.7	-	360	403/465
mPEG$_{45}$-*b*-PDHU$_9$	46.7	27.3	-	372	412/472
mPEG$_{45}$-*b*-PDHU$_{15}$	47.3	20.0	-	370	409/465
mPEG$_2$OCH$_2$COO-*g*-PEUA	-	-	- 64	200	401/455
mPEG$_2$OCH$_2$COO-*g*-PDHU	-	-	- 46	205	394/458
mPEG$_3$OOC(CH$_2$)$_2$COO-*g*-PEUA	-	-	- 58	204	399/448
mPEG$_3$OOC(CH$_2$)$_2$COO-*g*-PDHU	-	-	- 52	204	387/462

a) Melting temperatures (T_m) and enthalpies (ΔH_m) determined by DSC on the second heating scan at heating rates of 10 °C·min^{-1}; (b) Glass-transition temperature (T_g) taken as the inflection point of the second heating DSC curves recorded at 10 °C·min^{-1}; (c) Temperature at which 5 % weight loss was observed by TGA; (d) Temperature for maximum degradation rate from TGA.

5.7 SELF-ASSEMBLY BEHAVIOUR OF mPEG BLOCK COPOLYMERS AND GRAFTED POLYMERS

All DHU-based mPEG block copolymers and grafted polymers showed a great ability to self-assemble to form different unimolecular and mainly multimolecular round shaped micelles. The high hydrophobicity of the PDHU hyperbranched block allows forming a dense core arranging the mPEG hydrophilic block in the shell, thus leading to stable supramolecular micelles. The micellar characteristics of the different copolymers are collected in Table 5.6 and DLS plots measured at 0.5 mg·ml^{-1} solution in water are collected in Figure SI.18.

Table 5.6 Micellar characteristics of the block copolymers and grafted polymers obtained after 48 h with CALB in toluene at 80 °C.

		Micellar characteristics		
Polymer name	**CMC (mg L^{-1})[a]**	**Size (d/nm)[b]**	**PdI[b]**	**$Z_{average}$ (d/nm)[b]**
mPEG$_{12}$-PDHU$_9$	0.02	242±3	0.178±0.01	239±4
mPEG$_{12}$-PDHU$_{15}$	0.01	290±6	0.123±0.01	299±1
mPEG$_{45}$-PDHU$_9$	0.10	155±4 (78 %) 39±7 (22 %)	0.356±0.00	100±1
mPEG$_{45}$-PDHU$_{15}$	0.03	167±4	0.273±0.01	140±1
mPEG$_2$OCH$_2$OO-g-PEUA	nd	287±3 (92 %) 75±2 (8 %)	0.342±0.04	253±9
mPEG$_2$OCH$_2$COO-g-PHDU	0.20	284±1 (93 %) 68±7 (7 %)	0.188±0.01	239±4
mPEG$_3$OOC(CH$_2$)$_2$COO-g-PEUA	nd	328±3 (67 %) 106±3 (33 %)	0.325±0.11	270±4
mPEG$_3$OOC(CH$_2$)$_2$COO-g-PDHU	3.24	294±3 (89 %) 94±9 (11 %)	0.217±0.00	241±1

a) Determined using pyrene as fluorescence probe; b) Size, PdI (size polydispersity index) of micelles (0.5 mg mL^{-1}) and Z-average determined by DLS.

In all cases, unimolecular micelles were not detected by DLS at 0.5 mg·ml^{-1} concentration. Measurements at lower concentrations (0.01 and 0.05 mg·ml^{-1}) showed also the formation of multimolecular micelles of similar shape and size. On the contrary, by TEM imaging, unimolecular micelles ranging 15-20 nm were occasionally observed in some samples probably due to different conditions during sample preparations. As an example, in mPEG$_3$OOC(CH$_2$)COO-*g*-PDHU, isolated monomolecular micelles could be observed (Figure 5.6 a). Moreover, monomolecular micelles were detected surrounding some multimolecular micelles, at short distance in a uniform-like arrangement indicating the easiness of secondary unimolecular micelle aggregation processes.

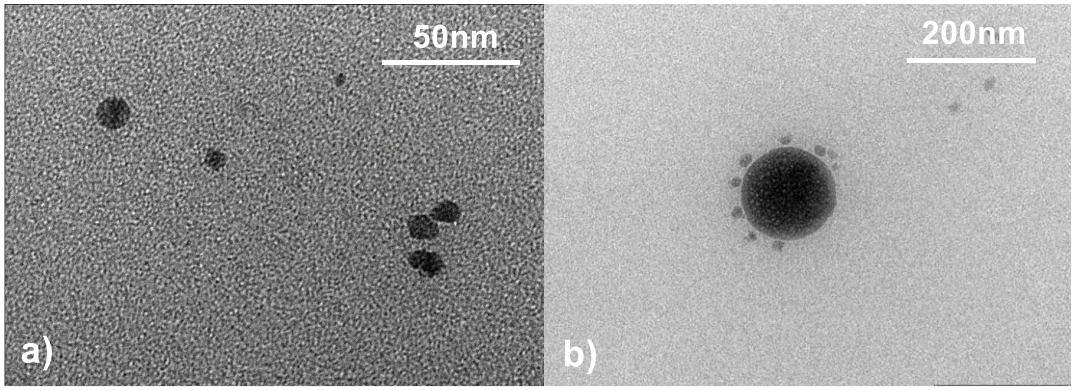

Figure 5.6 TEM images of mPEG$_3$OOC(CH$_2$)COO-*g*-PDHU micelles obtained in drying mode a) region showing isolated monomolecular micelles of 15-20 nm, b) region showing monomolecular micelles (15-20 nm) arranged around a multimolecular spherical micelle of 145 nm.

DLS intensity size distribution curves for mPEG$_{12}$-*b*-PDHU$_9$ and mPEG$_{12}$-*b*-PDHU$_{15}$ show quite narrow distributions with Z average size of about 240 and 300 nm respectively. Copolymers with longer mPEG moiety mPEG$_{45}$-*b*-PDHU$_9$ and mPEG$_{45}$-*b*-PDHU$_{15}$ present also secondary aggregation micelles of smaller size (100-140 nm) but with broader distribution. In fact, for mPEG$_{45}$-*b*-PDHU$_9$ a bimodal distribution with about 22 % of micelles of 40 nm were detected.

According to these results, the length of the flexible PEG moiety is not as determinant as the number of units that need to be assembled in a secondary aggregation to form a stable hydrophobic core.[28] Thus in the case of shorter mPEG$_{12}$ chains, higher number of copolymer units seem to be necessary leading to multimolecular micelles with larger hydrophobic cores and larger size. Usually, in the case of multimolecular micelles by self-assembly of linear block copolymers, the opposite behaviour is observed.[58] TEM images under negative stain (PTA) show nice micellar distributions in the case of mPEG$_{12}$-*b*-PDHU$_9$ and mPEG$_{12}$-*b*-PDHU$_{15}$ (Figure 5.7 a and Figure SI.19 a and SI.19 b) but in the case of mPEG$_{45}$-*b*-PDHU$_n$ micelles stick together into great glomerular aggregates in which the multicellular micelles retain somewhat the shape and size. (Figure SI.19 c and SI.19 d). This seem to indicate that under the imaging conditions the large mPEG$_{45}$ shells interact and come near as water evaporates. For all samples, size distribution histograms show broader distributions than

those observed by DLS. This can be attributed to changes during the TEM sample preparation, which clearly is the case of the cluster aggregates observed in the two $mPEG_{45}$-*b*-$PDHU_n$ samples. In any case, TEM images indicates that the micelles retain their roughly spherical shape.

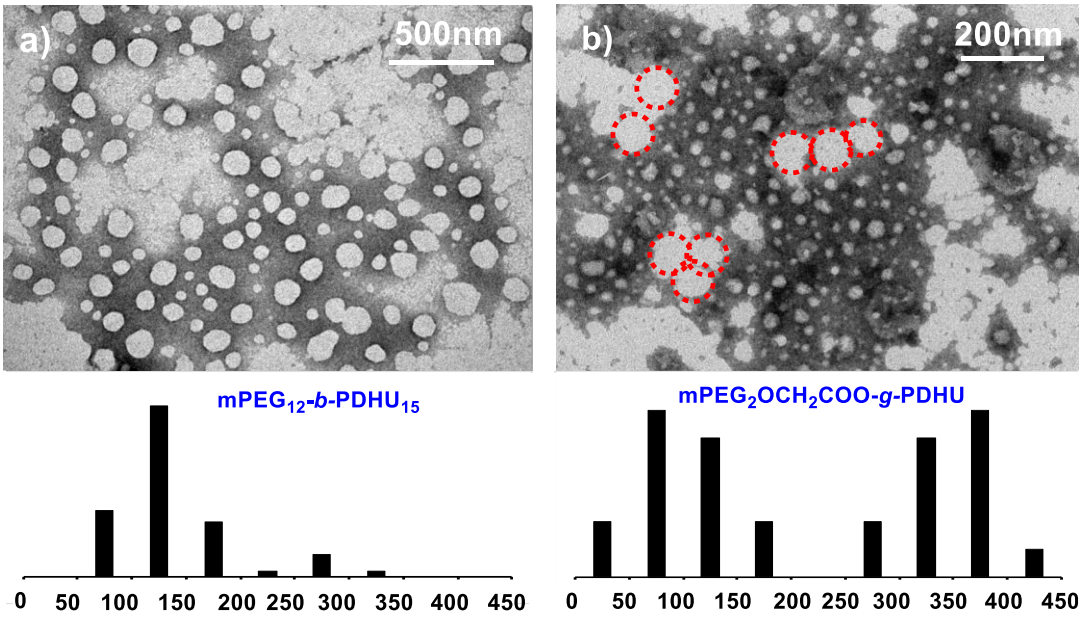

Figure 5.7 TEM images in negative stain mode (top) and size distribution histograms (analysed by ImageJ software (bottom) of a) $mPEG_{12}$-*b*-$PDHU_{15}$ and b) $mPEG_2OCH_2COO$-*g*-PDHU micelles obtained with a 0.5 mg/mL solution in water.

Microstructural analysis of grafted copolymers obtained from linear PEUA and branched PDHU proved to have similar hyperbranched structure with few differences in branching degree (20-30 %) and grafting percentage (45-60 %). Accordingly, a similar self-assembly behaviour could be expected for all these copolymers and this was confirmed by DLS measurement. All grafted copolymers show (Table 5.6 and Figure SI.20) two narrow micelle distributions of different size. The average size by intensity show a bimodal distribution with multimolecular micelles with Z average ranging 240-270 nm accompanied lower percentages (7-33 %) of smaller micelles of 100 nm or less. No significant differences were observed when comparing polymers grafted with $mPEG_2OCH_2COOH$ and $mPEG_3OOC(CH_2)_2COOH$. However, grafting onto linear PEUA seems to produce

multimolecular micelles of higher size and PdI which could be related to a more heterogeneous structure due to transesterification occurred during the grafting process. Thus, for $mPEG_3OOC(CH_2)_2COO$-*g*-PEUA two size distributions micelles were clearly detected (Figure 5.7 b). TEM imaging under drying and negative stain modes also show the presence of round shaped multimolecular micelles of different size (Figure SI.20 a, SI.20 c and SI.20 d) and in some cases great glomerular aggregates (Figure 5.7 b). The two modal distribution observed by DLS, is only observed in size distribution histogram of $mPEG_2OCH_2COO$-*g*-PDHU. For the other grafted copolymers very broad distributions were also observed (Figure SI.20 c and SI.20 d).

The self-assembling of mPEG/PDHU block copolymers and grafted polymers was confirmed by critical micelle concentration measurements (Table 5.7, Figure 5.8 and Figure SI.21) from the I_1/I_3 fluorescence intensity ratio using pyrene.[59] Block copolymers, $mPEG_{12}$-*b*-$PDHU_9$ and $mPEG_{45}$-*b*-$PDHU_9$ were analysed giving CMC of $2{\cdot}10^{-4}$ and $1{\cdot}10^{-4}$ $mg{\cdot}ml^{-1}$ respectively, indicating that above very low concentrations in water, unimolecular micelles spontaneously aggregate together forming supramolecular multimolecular micelles that increase the solubility of the fluorescent probe. Increasing the percentage of PDHU block seems not to affect the CMC as $mPEG_{12}$-*b*-$PDHU_{15}$ and $mPEG_{45}$-*b*-$PDHU_{15}$ gave similar values, $1{\cdot}10^{-4}$ and $3{\cdot}10^{-4}$ $mg{\cdot}ml^{-1}$.

CMC for grafted polymers, $mPEG_2OCH_2COO$-*g*-PDHU and $mPEG_3OOC(CH_2)_2COO$-g-PDHU was also determined. It was found an increase of the CMC necessary to produce the self-assembly to $2{\cdot}10^{-3}$ $mg{\cdot}l^{-1}$ for $mPEG_2OCH_2COO$-*g*-PDHU and to $32.4{\cdot}10^{-3}$ $mg{\cdot}ml^{-1}$ for $mPEG_3OOC(CH_2)_2COO$-g-PDHU, indicating that grafted polymers have less hydrophobic core, due to the statistical grafting and heterogeneous distribution of mPEG moieties. However, according to rapid increase of the I_1/I_3 intensity ratio in the fluorescence spectra of pyrene above CMC, higher loadings for grafted polymers than for block copolymers seems to occur. Anyway, CMC are much lower than the used for DLS measurements and TEM imaging (0.5 $mg{\cdot}l^{-1}$ solutions) confirming the predominant presence of multimolecular micelles at these concentrations.

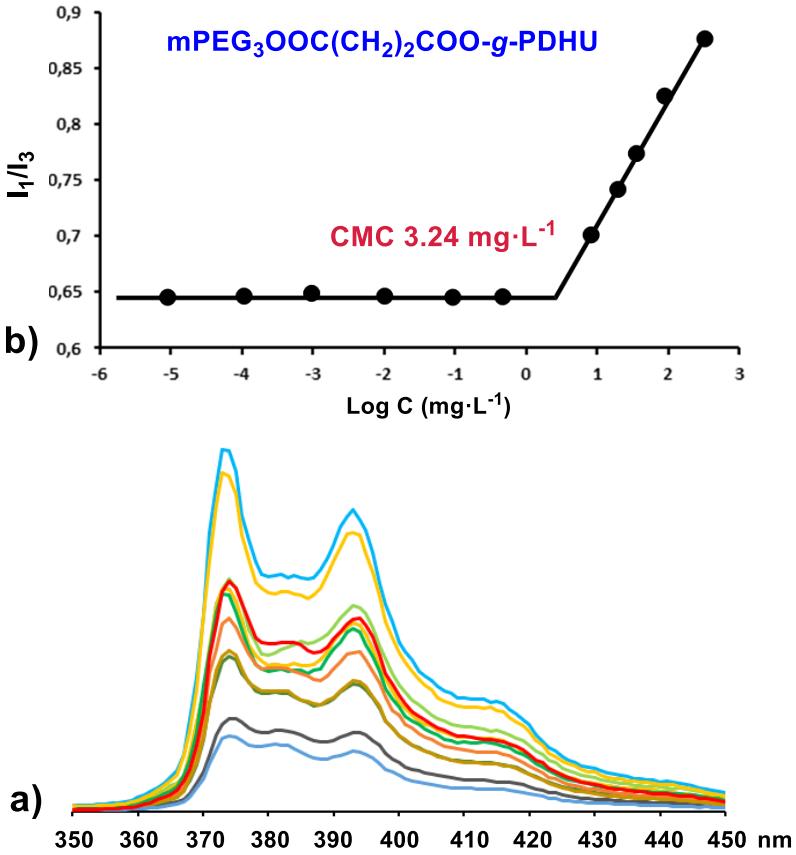

Figure 5.8 Fluorescence spectra of pyrene in mPEG$_2$OOC(CH$_2$)$_2$COO-*g*-PDHU micelles a) and calculation of the CMC of the multimolecular micelles using the I_1/I_3 diagram.

5.8 CONCLUSIONS

A renewable hydroxyl hyperbranched polyester: poly(10,11-dihydroxyundecanoic acid) (PDHU), by self-polycondensation of 10,11-dihydroxyundecanoic acid was successfully synthesized using CALB as catalyst and thus avoiding metallic catalysts. Branching and post polymerization transesterification processes seem to proceed indistinctly from both types of hydroxyl groups even though it is described that esterification occurs selectively at primary hydroxyl groups during polymerization.

The synthesis of model compounds and derivatization of polyesters allowed a detailed structural characterization of hyperbranched polyesters by ^{1}H, ^{13}C and ^{19}F NMR.

Chapter 5

Branched amphiphilic copolyesters by copolymerization with methoxypolyethylenglycols of different lengths (550 and 2000 $g \cdot mol^{-1}$) were successfully synthesized using CALB as catalyst. Incorporation of DHU units is lower than the feed in all cases.

Amphiphilic polyesters were also prepared by grafting carboxyl functionalized di and triethyleneglycols onto PEUA and PDHU hydroxypolyesters. 50-60 % extend of hydroxyl groups esterification was achieved. In linear PEUA grafting proceeds together with transesterification reactions leading to a branched structure.

The microstructure of these block copolymers and grafted polymers was determined by NMR by using models and ^{1}H-^{13}C heteronuclear bidimensional correlations. The self-assembly of these amphiphilic polyesters form well-defined micelles of 100-300 nm in aqueous solutions. Critical micellar concentration indicates that even at low concentration these copolymers self-assemble to lead multimolecular micelles, and that unimolecular micelles are scarcely observed.

5.9 REFERENCES

[1] Schneiderman D. K.; Hillmyer M. A.; 50th Anniversary Perspective: There is a great future in sustainable polymers, **2017**, *Macromolecules*, 50, 3733-3749.

[2] Gandini A.; Lacerda T. M.; Carvalho A. J. F.; Trovatti T.; The progress of polymers from renewable resources: furans, vegetable oils and polysaccharides, **2016**, *Chem. Rev*., 116, 1637–1669.

[3] Gandini A.; Lacerda T. M.; From monomers to polymers from renewable resources: Recent advances, **2015**, *Prog. Polym. Sci*., 48, 1-39.

[4] S Bigot.; Daghrir M.; Mhanna A.; Boni G.; Pourchet S.; Lecamp L.; Plasseraud L.; Undecylenic acid: A Tunable Bio-based Synthon for Materials Applications, **2016**, *Eur. Polym. J*., 74, 26-37.

[5] Seyednejad H.; Ghassemi A. H.; van Nostrum C. F.; T Vermonden.; Hennink W. E.; Functional aliphatic polyesters for biomedical and pharmaceutical applications, **2011**, *J. Controlled Released*, 152, 168-176.

[6] Oh J. K.; Polylactide (PLA)-based amphiphilic block copolymers: synthesis, self-assembly, and biomedical Applications, **2011**, *Soft Matter*., 7, 5096-5108.

[7] Vilela C.; Sousa A. F.; Fonseca A. C.; Serra A. C.; Coelho J. F. J.; Freire C. S. R.; Silvestre A. J. D.; The quest for sustainable polyesters – insights into the future, **2014**, *Polym. Chem*., 5, 3119-3141.

[8] Kolb N.; Winkler M.; Syldatk C.; Meier M. A. R.; Long-chain polyesters and polyamides from biochemically derived fatty acids, **2014**, *Eur. Polym. J*., 51, 159–166.

[9] Kunduru K. R.; Basu A.; Zada M. H.; Domb A. J.; Castor oil based biodegradable polyesters, **2015**, *Biomacromolecules*, 16, 2572-2587.

[10] Maisonneuve L.; Lebarbé T.; Grauab E.; Cramail H.; Structure–properties relationship of fatty acid-based thermoplastics as synthetic polymer mimics, **2013**, *Polym. Chem*., 4, 5472-5517.

[11] Beyazkilic Z.; Lligadas G.; Ronda J. C.; Galià M.; Cádiz V.; Vinylsulfide-containing polyesters and copolyesters from fatty acids: Thiol-yne monomer synthesis and thiol-ene functionalization, **2014**, *Macromol. Chem. Phys*., 215, 2248-2259.

[12] Beyazkilic Z.; Lligadas G.; Ronda J. C.; Galià M.; Cádiz V.; Synthesis and functionalization of vinylsulfide and ketone-containing aliphatic copolyesters from fatty acids, **2015**, *Polymer*, 79, 290-298.

[13] Lluch C.; Calle M.; Lligadas G.; Ronda J. C.; Galià M.; Cádiz V.; Versatile post-polymerization modifications of a functional polyester from castor oil, **2015**, *Eur. Polym. J*., 72, 64-71.

[14] Valverde C.; Lligadas G.; Ronda J. C.; Galià M.; Cádiz V.; Hydroxyl functionalized renewable polyesters derived from 10-undecenoic acid: polymer structure and postpolymerization modification, **2018**, *Eur. Polym. J.*, 105, 68-78.

[15] Türünç O.; Meier M. A. R.; Fatty Acid Derived Monomers and Related Polymers *Via* Thiol-ene (Click) Additions, **2010**, *Macromol. Rapid Commun*., 31, 1822-1826.

[16] Bao Y.; He J.; Li Y.; Facile and eficient synthesis of hyperbranched polyesters based on renewable castor oil, **2013**, *Polym. Int*., 62, 1457,1464.

[17] Testud D.; Pintori E.; Grau E.; Taton D.; Cramail H.; Hyperbranched polyesters by polycondensation of fatty acid-based AB_n-Type monomers, **2017**, *Green Chem*., 19, 259-269.

[18] You Z.; Cao H.; Gao J.; Shin P. H.; Day B. W.; Wang Y.; A functionable polyester with free hydroxyl groups and tunable physiochemical and biological properties, **2010**, *Biomaterials*, 31, 3129-3138.

[19] White J. E.; Earls J. D.; Sherman J. W.; López L. C.; Dettloff M. L.; Step-growth polymerization of 10,11-epoxyundecanoic acid. Synthesis and properties of a new hydroxy-functionalized thermoplastic polyester, **2007**, *Polymer*, 48, 3990-3998.

[20] Miao S.; Zhang S.; Su Z.; Wang P.; Chemoenzymatic synthesis of oleic acid-based polyesters for use as highly stable biomaterials, **2008**, *J. Polym. Sci. Part A: Polym. Chem*., 46, 4243-4248.

[21] De Smet S.; Lingier S.; Du Prez F. E.; MacroRAFT agents from renewable resources and their use as polymeric scaffolds in a grafting from approach, **2014**, *Polym. Chem*, 5, 3163-3169.

[22] Blasco E.; Sims M. B.; Goldmann A. S.; Sumerlin B. S.; Barner-kowollik C.; 50th Anniversary Perspective: Polymer functionalization, **2017**, *Macromolecules*, 50, 5215-5225.

[23] Kataoka K.; Harada A.; Nagasaki Y.; Block copolymer for drug delivery: design, characterization and biological significance, **2001**, *Adv. Drug Delivery Rev*., 47, 113-131.

[24] Gaucher G.; Dufresne M-H.; Sant V. P.; Kang N.; Maysinger D.; Leroux J-C.; Block copolymers micelles: preparation, characterization and application in drug delivery, **2010**, *J. Contol. Rel*., 109, 169-188.

[25] Kurniasih I. N.; Liang H.; Kumar S.; Mohr A.; Sharma S.K.; Rabe J. P.; Haag R.; A bifunctional nanocarrier based on amphiphilic hyperbranched polyglycerol derivatives, **2013**, *J. Mat. Chem. B*, 1, 3569-3577.

[26] Kamenova K.; Haladjova E.; Grancharov G.; Kyulavska M.; Tzankova V.; Aluani D.; Yoncheva K.; Pispas S.; Petrov P.; Co-assembly of block copolymers as a tool for developing novel micellar carriers of insulin for controlled drug delivery, **2018**, *Eur. Polym. J., 104*, 1-9.

[27] Mai Y.; Eisenberg A.; Self-assembly of block copolymers, **2012**, *Chem. Soc. Rev*., 41, 5969-5985.

[28] Hong H.; Mai Y.; Zhou Y.; Yan D.; Cui J.; Self-assembly of large multimolecular micelles from hyperbranched star copolymers, **2007**, *Macromol. Rapid Comm*., 28, 591-596.

[29] Fan X.; Li Z.; Loh X. J.; Recent developments of unimolecular micelles as functional materials and applications, **2016**, *Polym. Chem*., 7, 5898-5918.

[30] Zhou Y.; Yan D.; Supramolecular self-assembly of amphiphilic hyperbranched polymers at all scales and dimensions: progress, characteristics and perspectives, **2009**, *Chem. Commun*., 1172-1188.

[31] Saha A.; S Ramakrishnan.; Unimolecular micelles and reverse micelles based in hyperbranched polyethers. Comparative study of AB_2 + A-R and A_2 + B_3 + A-R type strategies, **2009**, J. *Polym. Sci. Part A: Polym. Chem*., 49, 80-91.

[32] Feng C.; Li Y.; Yang D.; Hu J.; Zhang X., Huang X., Well-defined graft copolímers: from controlled synthesis to multipurpose applications, **2001**, *Chem. Soc. Rev*., 40, 1282-1295

[33] Kutikov A. B.; Song J.; Biodegradable PEG-based amphiphilic block copolímers for tissue engineering applications, **2015**, *ACS Biomater. Sci, Eng*., 13, 463-480.

[34] Abbina S.; Parambath A.; PEGilation and its alternatives: A summary in engineering of biomaterials for graft delivery systems, **2018**, Chapter 14, 363-376. Woodhead publishing Series in Biomaterials.

[35] Xiong X-B.; Uludag H.; Lavasanifar A.; Biodegradable amphiphilic poly(ethylene oxide)-*block*-polyesters with grafted polyamines as supramolecular nanocarriers for efficient siRNA delivery, **2009**, *Biomaterials*, 30, 242-253.

[36] Hazer B.; Amphiphilic poly(3-hydroxy alcanoate)s: Potential candidates for Medical Applications, **2010**, *Int. J. Polym. Sci*., 1-8.

[37] S Stefani.; Kurniasih I. N.; S Sharma. K.; C Böttcher.; P Servin.; Haag R.; Triglycerol-based hyperbranched polyesters with an amphiphilic branched shell as novel biodegradable drug delivery systems, **2016**, *Polym. Chem*., 7, 887-898.

[38] Wu W-X.; Yang X-L.; Liu B-Y.; Deng Q-F.; Xun M-M.; Wang N.; Yu X-Q.; Lipase-catalyzed synthesis of oxidation-responsive poly(ethylene glycol)-*b*-poly(β)-thioether ester) amphiphilic block copolímers, **2016**, *RSC Adv*., 6, 11870-11879.

[39] Aouf C.; Durand E.; Lecomte J.; Figueroa-Espinoza M-C: Dubreucq E.; Fulcrand H.; Villeneuve P.; The use of lipases as biocatalysts for the epoxidation of fatty acids and phenolic compounds, **2014**, *Green Chem*., 16, 1740-1754.

[40] Kim K-R.; Oh D-K.; Production of hydroxyl fatty acids by microbial fatty acid-hydroxylation enzymes, **2013**, *Biotech. Adv*., 31, 1473-1485.

[41] Warwel S., gen Klaas M.R.; Chemo-enzymatic epoxidation of unsaturated carboxylic acids, **1995**, *J. Mol. Cat. B: Enzym*., 1, 29-35.

[42] Campanella A.; Fontanini C.; Baltanás M.A.; High Yield Epoxidation of Fatty Acid Methyl Esters with Performic Acid Generated *in situ*, **2008**, *Chem. Eng. J*., 144, 466-475.

[43] Logan R.L.; Park E.; US Patent 2.666.572, **1954**.

[44] Formic acid of renewable origin is commercially available from Aldrich and other suppliers.

[45] Liu X.; Li S.; Liu Y.; Cao Y.; Formic Acid: A Versatile Renewable Reagent for Green and Sustainable Chemical Synthesis, **2015**, *Chin. J. Cat*, 36, 1461-1475.

[46] Garaleh M.; Lahcini M.; Kricheldorf H.R.; Weidner S.M.; Syntheses of aliphatic polyesters catalyzed by lanthanide triflates, **2009**, *J. Polym. Sci. Part A: Polym. Chem*., 47, 170-177.

[47] Y Shibata.; Takasu A.; Shynthesis of polyester having pendent hydroxyl groups via regioselective dehydration polycondensations of dicarboxylic acids an diols by low temperature polycondensation, **2009**, *J. Polym. Sci. Part A: Polym. Chem*., 47, 5747-5759.

[48] Kobayashi S.; Lipase-catalyzed polyester synthesis. A green Polymer chemistry, **2010**, *Proc. Jpn. Acad., Ser*. *B*, 86, 338-365.

[49] Douka A.; S Vouyiouka.; L-M. Papaspyridi.; Papaspyres C.D.; A review on enzymatic polymerization to produce polycondensation polymers: The case of aliphatic polyesters, polyamides and polyesteramides, **2018**, *Prog. Polym. Sci*., 78, 1-25.

[50] Mahapatro A.; Kumar A.; Gross R.A.; Mild, solvent-free ω-hydroxy acid polycondensations by *Candida anatartica* Lipase B, **2004**, *Biomacromolecules*, 5, 62-68.

[51] Ebata H.; Toshima K.; Matsumura S.; Lipase-catalyzed synthesis and curing of high-molecular-weight polyricinoleate, **2007**, *Macromol. Biosci.*, 7, 798-803.

[52] Vossenberg P.; R Beeftink.; Stuart M. C.; Tramper H.; Effect of enzyme dehydration on alcalase-catalyzed synthesis in near-anhydrous organic media, **2013**, *Biotechnol. Prog*., 29, 870-875.

[53] Wang S.; Meng X.; H Zhou.; Liu Y.; Secundo F.; Liu Y.; Enzyme stability and activity in non-aqueous reaction systems: a mini review, **2016**, *Catalysts*, 6, 32, 1-16.

[54] Duan Z-Q.; Du W.; Liu De-H.; The solvent influence on thbe positional selectivity of Novozyl 435 during 1,3-diolein synthesis by esterification, **2010**, *Biores. Tech*., 101, 2568-2571.

[55] Khan A.; Sharma S.K.; Kumar A.; Watterson A.C.; Kumar J.; Parmar V.S.; Novozym 435-catalyzed syntheses of polyesters and polyamides of medicinal and industrial relevance, **2014**, *ChemSusChem*, 7, 379-390.

[56] Kumari M.; Singh A. K.; Kumar S.; Achazi K.; Gupta S.; Haag R.; Sharma S. K.; Synthesis of amphiphilic dendronized polymers to study their self-assembly and transport behaviour, **2014**, *Polym. Avd. Technol*., 25, 1208-1215.

[57] Sen S.; Puskas J.E.; Green polymer chemistry: Enzyme catalysts for polymer functionalization, **2015**, *Molecules*, 20, 9358-9379.

[58] Hsu H.J.; Sen S.; Pearson R.M.; Uddin S.; Král P.; Hong S.; Poly(ethylenglycol) corona chain length controls end group-dependent cell interactions of dendron micelles, **2014**, *Macromolecules*, 47, 6911-6918.

[59] Ray G.B.; Charkraborty I.; Moulik S.P.; Pyrene absorption can be a convenient method for probing critical micellar concentration (cmc) and indexing micellar polarity, **2006**, *J. Colloid. Interface. Sci*,. 294, 248-254.

UNIVERSITAT ROVIRA I VIRGILI
10-UNDECENOIC ACID-BASED BIODEGRADABLE HYDROXY POLYESTERS: A PLATFORM FOR AMINOACID BIOCONJUGATES AND PEG-DERIVED AMPHIPHILIC COPOLYMERS
Carmen Valverde Sarmiento

Chapter 6

Experimental part

UNIVERSITAT ROVIRA I VIRGILI
10-UNDECENOIC ACID-BASED BIODEGRADABLE HYDROXY POLYESTERS: A PLATFORM FOR AMINOACID BIOCONJUGATES AND PEG-DERIVED AMPHIPHILIC COPOLYMERS
Carmen Valverde Sarmiento

6.1 MATERIALS

1,2-epoxyhexane (97 %) (EH), n-hexanoic acid (99.5 %) (EA), 1,2-hexanediol (98 %), 1,6-hexanediol (99 %), 10-undecenoic acid (98 %) (UA), methyl 10-undecenoate (96 %), N-Boc-phenylalanine (99 %) (Boc-Phe-OH), N-Boc-serine metylester (95 %) (Boc-Ser-OMe), L-cysteine (97 %), 2-[2-(2-methoxyethoxy)ethoxy] acetic acid (technical grade), poly(ethylene glycol)methyl ether (Mn ~ 550) ($mPEG_{12}$), poly(ethylene glycol)methyl ether (Mn ~ 2000) ($mPEG_{45}$), (trimethylsilyl) diazomethane solution 2.0 M in diethyl ether ($TMS\text{-}CHN_2$), succinic anhydride (99 %), tri(ethylene glycol) monomethyl ether (95 %), pyrene (99.9 %), trichloroacetyl isocyanate (97 %) (TAI), trifluoroacetic anhydride (99 %) (TFAA), hydrogen peroxide (30 %), 2,2-dimethylthiazolidine-4-carboxylic acid (97 %), phosphotungstic acid (99.9 %) (PTA), 3,5-bis(trifluoromethyl)benzoic acid (98 %), sodium formate (99.98 %), poly(ε-caprolactone)diol (PCL) Mn 2.000 Da, titanium (IV) isopropoxide (97 %), methanesulfonic acid (99.5 %), tetrabutylphosphonium bromide (98 %) (TBPB), glacial acetic (99.8 %), acetic anhydride (99 %), hydrogen peroxide (30 %), formic acid (95 %), tetraethylammonium bromide (98 %) (TEAB), 1,5,7-triazobicyclo[4.4.0]dec-5-ene (98 %) (TBD), N-(3-dimethylamino-propyl)-N'-ethylcarbodiimide hydrochloride (98 %) (DECH), 4-dimethyl-aminopyridine (99 %) (DMAP), boron trifluoride diethyl etherate (46 %) (BF_3Et_2O), boron trifluoride diethyl etherate (99 %) (BF_3Et_2O), *Candida Antarctica* immobilized on acrylic resin (5.000 U/g) (CALB), *candida rugose* lipase immobilized on immobead 150 (100 U/g) (CR), lipase from porcine pancreas (100-500 U/g, pH 8.0, 37 °C), soda lime, cumene (99 %), propylene glycol monomethyl ether acetate (99 %) (Dowanol), trichlorofluoromethane (99.5 %) ($CFCl_3$) and phosphate buffered saline pH 7.4 (at 25 °C) from Sigma Aldrich. Anhydrous magnesium sulfate, maleic anhydride (99 %), potassium hydroxide (KOH) and tetramethylsilane (TMS) from Scharlau; ethylbenzene (99 %) from Baker; citric acid buffer solution pH 2.0 (20 °C) from Fluka, sodium azide and sodium borohydride from Probus; 1,1,2,2-tetrachloroethane-D_2 (TCE-D_2), chloroform-D ($CDCl_3$), deuterated dimethylsulfoxide (DMSO-d_6) and dimethylformamide-D_7 (DMF-D_7) from

euriso-top; toluene, tetrahydrofuran (THF), acetone, dimethylformamide (DMF), diethyl ether, dichloromethane (DCM), diphenyl ether (DPE) and 1,2-dichloroethane (DCE), ethanol (EtOH) and methanol (MeOH) from Scharlau. Analytical grade solvents were purified and dried by standard methods. 4 Å powdered molecular sieves were activated 24 h at 220˚C and cooled under vacuum prior use. Flash column chromatography was carried out using neutral silica-gel 60 F254 (from Panreac) and hexane-ethyl acetate as eluent.

6.2 INSTRUMENTATION AND ANALISYS

6.2.1 Nuclear Magnetic Resonance (NMR) analysis

^{1}H (400 MHz), ^{13}C (100.5 MHz) and ^{19}F (376.8 MHz) NMR spectra were recorded using a Varian Gemini 400 spectrometer. Spectra were recorded at room temperature using 10-15 mg (^{1}H and ^{19}F NMR) or 30-40 mg (^{13}C NMR) of sample in $CDCl_3$, DMF-D_7 or TCE-D_2 as solvent and TMS (^{1}H NMR) or $CFCl_3$ (^{19}F NMR) as internal standard. In ^{13}C NMR the central peak of the deuterated solvent was taken as reference and the chemical shifts given in ppm from TMS using the appropriate shifts conversions. Spectra for semi-quantitative measurements were degassed with helium and recorded using a D1=15 s and 32 transients in ^{1}H and ^{19}F NMR and a flip angle of 45 ˚, a D1=0.5 s and 10000 to 20000 transients in ^{13}C NMR. 2D ^{1}H-^{1}H homonuclear (gCOSY) and ^{13}C-^{1}H gradient heteronuclear Single Quantum Coherence (gHSQC) spectra were recorded as a means of obtaining the hh and hx correlation respectively.

6.2.2 Fourier Transform Infrared Spectroscopy (ATR-FTIR)

The FTIR spectra were recorded on a FTIR-680PLUS spectrophotometer with a resolution of 4 cm^{-1} in absorbance and transmittance modes. An attenuated total reflection (ATR) accessory with thermal control and a diamond crystal (Golden Gate heated single-reflection diamond ATR, Specac, Teknokroma) was used.

6.2.3 Liquid Chromatography-Mass Spectrometry (ESI MS)

The chromatographic system was an Agilent 1200 liquid chromatograph coupled to 6210 Time of Flight (TOF) mass spectrometer from Agilent Technologies (Waldbronn, Germany) with an ESI interface, using a Zorbax Eclipse XDB C18 column (4.6 mm × 150 mm × 5 µm) provided by Agilent Technologies.

6.2.4 Size exclusion chromatography (SEC)

The number-average molecular weight (Mn), weight average molecular weight (Mw) and molecular weight distribution (polydispersity, Đ, Mw/Mn) were measured by SEC. Polymer molecular weight analysis was carried out with an Agilent 1200 series system equipped with an Agilent 1100 series refractive-index detector. The analysis was performed on the three following column system: 3 µm PLgel MIXED-E, 5 µm PLgel MIXED-D, 20 µm PLgel MIXED-A at a nominal flow rate of 1.0 ml·min^{-1} and a sample concentration of 0.1 % w/w in THF as solvent. The instrument was calibrated with linear monodisperse polystyrene standards from Polymer Laboratories with molecular weights ranging from 500 to 400.000 Kg·mol^{-1}.

6.2.5 Thermogravimetric analysis (TGA)

Thermal stability studies were carried out on a Mettler TGA/SDTA851e/LF/1100 with N_2 as purge gas in the 30-800 °C temperature range at scan rates of 10 °C· min^{-1}.

6.2.6 Fluorescence Spectroscopy

The spectrofluorimetric data were acquired on an Aminco-Bowman series 2 Luminescence spectrometer (SLM Amino, Rochester, NY, USA) equipped with a 150 W continuous xenon lamp and a PMT detector.

6.2.7 Differential Scanning Calorimetry (DSC)

Calorimetric studies were carried out on a Mettler DSC3+ thermal analyser using N_2 as a purge gas (100 ml·min^{-1}). Calibration was made using an indium standard (heat flow calibration) and an indium-lead-zinc standard (temperature calibration). Samples of 5-7 mg were sealed in aluminium pans. A three-step procedure was applied at scanning rate of 10 °C·min^{-1}: first, heating up to 30-40 °C above the melting temperature of the polymer and holding for 5 min, to erase the thermal history; second, cooling down to -80 °C and holding for 5 min; finally, a second heating from -80 °C to the same temperature at the first heating. The second heating scans were used to characterize the crystallinity and melting behaviour. The crystallinity was calculated according to the equation (6.1).

$$\chi_\chi\ (\%) = \Delta H_m / \Delta H_m^0 \times 100 \qquad \text{equation 6.1}$$

where the melting enthalpy (ΔH_m) is the value of the second heating run and ΔH_m^0 is the melting enthalpy reported for a 100 % pure crystalline polyester. The average value of three measurements were given.

6.2.8 Contact angle

Contact angle measurements were determined at 25 °C using deionized water on polymer surfaces prepared by casting and curing monomers over glass slides. The water drop method (3 mL) was used on an OCA 15EC contact angle setup (Neutek Instruments) equipped with a motorized pipet.

6.2.9 Atomic Force Microscope (AFM)

Atomic Force Microscope (AFM) AFM analysis was performed in Agilent 5500/SPM microscope in acoustic AC (AAC) mode at room temperature in air, using silicon cantilevers.

6.2.10 Environmental scanning electron microscope (ESEM)

Environmental scanning electron microscopy (ESEM) images were obtained with a FEI QUANTA 600 instrument using low vacuum and an accelerating potential of 20 KV.

6.2.11 Transmission electron microscopy (TEM)

Transmission electron microscopy (TEM) observations were carried out on a JEOL 1011 high-resolution transmission electron microscope at an accelerating voltage of 80 kV. Samples were imaged in bright field at tension of 80 Kv using an ITEM imaging software.

6.2.12 Dynamic Light Scattering measurements (DLS)

Dynamic Light Scattering measurements were performed on a Malvern NanoZS instrument, equipped with an avalanche photodiode detector and a solid-state laser He-Ne laser with output power was 4 mW at λ = 632.8 nm) at a scattering angle of 90°.

6.2.13 X-ray diffraction (XRD)

XRD measurements were made using a Siemens D5000 diffractometer (Bragg-Brentano parafocusing geometry and vertical θ-θ goniometer) fitted with a curved graphite diffracted-beam monochromator, incident and diffracted-beam Soller slits, a 0.06 º receiving slit and scintillation counter as a detector. The angular 2θ diffraction range was between 15 and 30 º. The data were collected with an angular step of 0.03 º at 6 s per step and sample rotation. A low background Si (510) wafer was used as sample holder. $Cu_{k\alpha}$ radiation (λ= 1.5418 Å) was obtained from a copper X-ray tube operated at 40 kV and 30 mA. Each diffractogram was fitted as a sum of several pseudo-Voigt functions representing the crystalline and the amorphous part with the software TOPAS 6.0 (Bruker, TOPAS V6. Bruker AXS, Karlsruhe, Germany). The percentage of crystallinity was then calculated as the area ratio between the peaks associated to the crystalline part and the amorphous part.

6.2.14 Polymer solubility

In a 25 mL vial, 0.25 g of finely grounded polymer and 2 mL of each solvent was mixed and stirred, for 2 h at room temperature.

6.2.15 Water uptake

In a closed chamber, accurately weighted disk samples were kept in a constant humidity environment (saturated solution of $Na_2CO_3 \cdot 10H_2O$) at 37 or 45 ˚C for 48 h. Next, samples were weighted and the water uptake was determined by difference and was expressed as weight increase percentage. An average of three measurements was taken.

6.3 SYNTHESIS MODEL COMPOUNDS

6.3.1 Reaction between 1,2-epoxyhexane and n-hexanoic acid

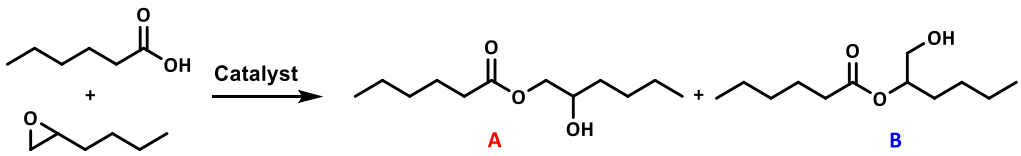

Scheme 6.1 Model reaction between 1,2-epoxyhexane and n-hexanoic acid.

Reactions were carried out in a 2 mL cylindrical flask with a screwed cap and teflon®/silicon septa with stirring and under argon. 0.25 g (2.5 mmol) of 1,2-Epoxyhexane, 0.29 g (2.5 mmol) of n-hexanoic acid and the catalysts of choice (1 % molar for organic and organometallic catalysts) were heated in bulk or in toluene solution (2.5 M) at 100 ˚C. For enzymatic catalysts (10 % w/w) the mixture was heated in bulk or in solution (2.5 M in toluene or DMF) at 90 ˚C during 24 h.

6.3.2 Synthesis of 2-Hydroxyhexyl hexanoate (A) and 1-hydroxyhexan-2-yl hexanoate (B)

An equimolar mixture of 1,2-epoxyhexane (0.5 g, 4.3 mmol), n-hexanoic acid (0.5 g, 4.3 mmol) and TBPB (0.01 g, 0.04 mmol) was heated at 100 °C for 24 h. The resulting oil was purified by column chromatography using hexane/ethyl acetate (8:2) as eluent yielding 0.54 g (64 %) of the mixture of A and B as a colourless oil.

2-Hydroxyhexyl hexanoate (A): ESI-TOF MS: m/z calc.: 216.17725; found: 216.1727. ^{1}H NMR ($CDCl_3$/TMS, δ ppm): 4.15(dd, 1H, $COOCH_2$-COH), 3.95(dd, 1H, $COOCH_2$-COH), 3.83(m, 1H, COO-$(CH_2)_2$-CH-OH), 2.33(t, 2H, CH_2-CH_2-COO), 1.63-1.32(m, 12H, $(CH_2)_n$), 1.31 (t, 1H, -OH), 0.90 (t, 6H, CH_2-CH_3).

^{13}C NMR ($CDCl_3$, δ ppm): 174.4 (s, 1C, COO), 70.3 (d, 1C, COO-CH_2), 68.8 (t, 1C, HOCH), 34.5 (t, 1C, CH_2-COO), 33.3-22.9 (t, 6C, $(CH_2)_n$), 14.3 (q, 2C, CH_2-CH_3).

1-Hydroxyhexan-2-yl hexanoate (B): ESI-TOF MS: m/z calc.: 216.17725; found: 216.1727. ^{1}H NMR ($CDCl_3$/TMS, δ ppm): 4.92(m, 1H, $(CH_2)_2$-CH-OOC), 3.71(dd, 1H, HO-CH_2-CH), 3.62(dd, 1H, HO- CH_2-CH), 2.33(t, 2H, CH_2-CH_2-COO), 1.63-1.32(m, 12H, $(CH_2)_n$), 0.90(m, 6H, CH_2-CH_3).

^{13}C NMR ($CDCl_3$, δ ppm): 174.7 (s, 1C, COO), 75.6 (d, 1C, CH_2-CH-OCO), 66.0 (t, 1C, OH- CH_2-CH), 34.8 (t, 1C, CH_2-CH_2-COO), 31.6-22.6 (t, 6C, $(CH_2)_n$), 14.2 (q, ,2C, CH_2-CH_3).

6.3.3 Synthesis of hexane-1,2-diyl dihexanoate (C)

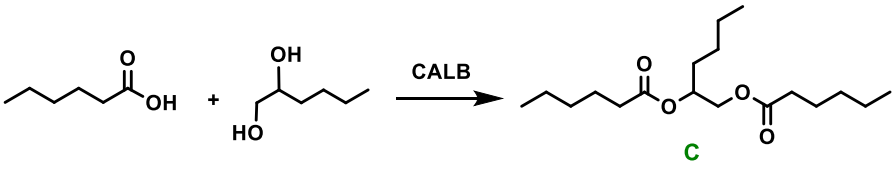

Scheme 6.2 Synthesis of hexane-1,2-diyl dihexanoate (C).

An equimolar mixture of 1,2-hexanediol (0.25 g, 2.1 mmol), n-hexanoic acid (0.48 g, 4.2 mmol) and CALB (0.050 g, 10 % wt) was heated at 90 °C for 24 hours in toluene (2.5 M). After solvent evaporation under reduced pressure, the resulting oil was purified by column chromatography using hexane/ethyl acetate (8:2) as eluent yielding 0.48 g (73 %) of C as a colourless oil.

Hexane-1,2-diyl dihexanoate (C): ESI-TOF MS: m/z calc.: 314.2457; found: 314.2464. ^{1}H NMR ($CDCl_3$/TMS, δ ppm): 5.12(m, 1H, $(CH_2)_2$-C<u>H</u>-OOC), 4.22(dd, 1H, COOC<u>H_2</u>-CH), 4.04(dd, 1H, COOC<u>H_2</u>-CH), 2.33(t, 4H, CH_2-C<u>H_2</u>-COO), 1.63-1.32(m, 18H, $(CH_2)_n$), 0.90(m, 9H, CH_2-C<u>H_3</u>).

^{13}C NMR ($CDCl_3$, δ ppm): 173.8 (s, 1C, COO), 173.6 (s, 1C, COO), 71.4 (d, 1C, $(CH_2)_2$-<u>C</u>H-O), 65.1 (t, 1C, O- <u>C</u>H_2-CH), 34.9 (t, 1C, CH_2-<u>C</u>H_2-COO), 34.8 (t, 1C, CH_2-<u>C</u>H_2-COO), 31.5-21.3 (t, 9C, $(CH_2)_n$), 13.9 (q, 3C, CH_2-<u>C</u>H_3).

6.3.4 ^{1}H and ^{19}F NMR "*in situ*" model derivatization

Derivatization with trichloroacetylisocyanate (TAI) and trifluoroacetic anhydride (TFAA) of A and B was carried out to determine the chemical shifts of methylene and methine signals arising from the hydroxyester moieties. [1,2,3]

6.3.4.a Reaction of A and B with TAI

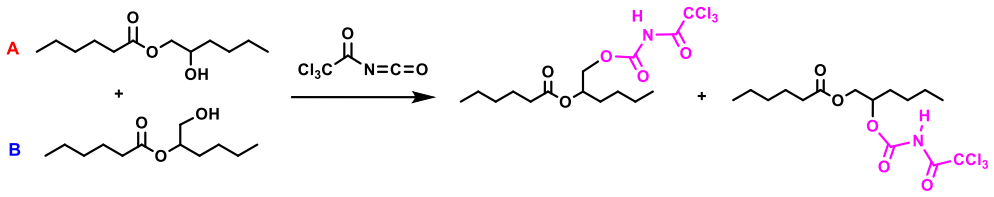

Scheme 6.3 Reaction of derivatization of A and B with TAI.

In a NMR tube, 25 mg (0.025 mmol) of a mixture of A and B was dissolved in $CHCl_3$ (0.7 mL). TAI (0.05 mL) was added drop to drop and the mixture was stirred for 2 minutes to lead to the corresponding trichloroacetylcarbamates.

2-(((2,2,2-trichloroacetyl)carbamoyl)oxy)hexyl hexanoate: ^{1}H NMR ($CDCl_3$/TMS, δ ppm): 5.15 (m, 1H, COO-CH_2-C<u>H</u>-OCONH), 4.32 (dd, 1H, COO-C<u>H</u>$_2$-CH-OCONH), 4.12 (dd, 1H, COO-C<u>H</u>$_2$-CH-OCONH), 2.33 (t, 2H, CH_2-C<u>H</u>$_2$-COO), 1.66-1.33(m, 9H, -CH_2), 0.90 (m, 6H, CH_2-C<u>H</u>$_3$).

1-(((2,2,2-trichloroacetyl)carbamoyl)oxy)hexan-2-yl hexanoate: ^{1}H NMR ($CDCl_3$/TMS, δ ppm): 5.15 (m, 1H, CH_2-C<u>H</u>-CH_2-OCONH), 4.42 (dd, 1H, COO-CH-C<u>H</u>$_2$-OCONH), 4.25 (dd, 1H, COO-CH-C<u>H</u>$_2$-OCONH), 2.33 (t, 2H, CH_2-C<u>H</u>$_2$-COO), 1.66-1.33(m, 9H, CH_2), 0.90 (m, 6H, CH_2-C<u>H</u>$_3$).

6.3.4.b Reaction of A and B with TFAA

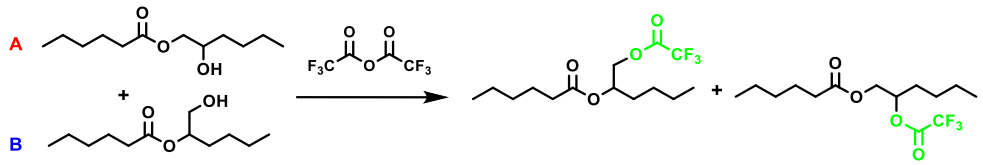

Scheme 6.4 Derivatization of A and B with TFAA.

In a 5 mL flask under inert atmosphere, 100 mg (0.0045 mmol) of a mixture of A and B was dissolved in CH_2Cl_2 (2 mL), and TFAA (0.6 mL) was added. The mixture was heated under reflux for 20 minutes and the solvent evaporated under vacuum to dryness, and the resulting oils analysed by ^{1}H NMR.

2-(Trifluoroacetoxy)hexyl-1-hexanoate: ESI-TOF MS: m/z calc.: 259.2548. ^{1}H NMR ($CDCl_3$/TMS, δ ppm): 5.28 (m, 1H, $(CH_2)_2$-C<u>H</u>-OOC-CF_3), 4.38 (dd, 1H, COO-C<u>H</u>$_2$-CH-OOC-CF_3), 4.09 (dd, 1H, COO-C<u>H</u>$_2$-CH-OOC-CF_3), 2.33(t, 2H, CH_2-C<u>H</u>$_2$-COO), 1.63-1.32(m, 12H, CH_2), 0.90(m, 6H, CH_2-C<u>H</u>$_3$).

^{19}F NMR ($CDCl_3$/$CFCl_3$, δ ppm): -75.21 (s, CF_3-COO-CH-).

1-(Trifluoroacetoxy)-hexan-2-yl hexanoate: ESI-TOF MS: m/z calc.: 259.2548. ^{1}H NMR ($CDCl_3$/TMS, δ ppm): 5.18 (m, 1H, CF_3-COO-CH_2-C<u>H</u>-OOC), 4.52 (dd, 1H, CF_3-COO-C<u>H_2</u>-CH-COO), 4.31 (dd, 1H, CF_3-COO-C<u>H_2</u>-CH-COO), 2.33(t, 2H, CH_2-C<u>H_2</u>-COO), 1.63-1.32(m, 12H, CH_2), 0.90(m, 6H, CH_2-C<u>H_3</u>).

^{19}F NMR ($CDCl_3$/$CFCl_3$, δ ppm): -75.02 (s, CF_3-COO-CH_2).

6.3.4.c Synthesis of hexane-1,2-diyl bis(2,2,2)-trifluroacetate

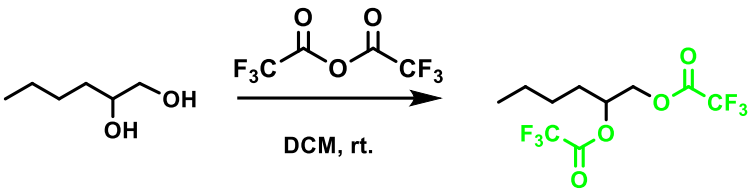

Scheme 6.5 Synthesis of hexane-1,2-diyl bis(2,2,2,)-trifluoroacetate.

In a 5 mL flask under inert atmosphere, 875 mg (7.4 mmol) of 1,2-hexanediol was dissolved in CH_2Cl_2 (3 mL), and TFAA (2 mL) was added. The mixture was heated under reflux for 20 minutes and the solvent evaporated under vacuum to dryness, and the resulting oils analysed by ^{1}H NMR.

^{1}H NMR ($CDCl_3$/TMS, δ ppm): 5.37 (m, 1H, CF_3-COO-CH_2-C<u>H</u>-OOC), 4.60 (dd, 1H, CF_3-COO-C<u>H_2</u>-CH-COO), 4.42 (dd, 1H, CF_3-COO-C<u>H_2</u>-CH-COO), 1.77 (m, 2H, C<u>H_2</u>-CHO), 1.39 (m, 4H, $(CH_2)_2$), 0.94 (m, 3H, CH_3).

^{19}F NMR ($CDCl_3$/$CFCl_3$, δ ppm): -75.45 (s, CF_3-COO-CH_2), -75.50 (s, CF_3-COO-CH).

6.3.5 Purification of 2-[2-(2-Methoxyethoxy)ethoxy]acetic acid (mPEG$_2$CH$_2$COOH)

The commercial grade product from Aldrich was dried by azeotropic distillation with toluene and further evaporation under vacuum.

6.3.6 Synthesis of decane-1,2- diyl bis(2-(2-(2-methoxyethoxy)ethoxy)acetate

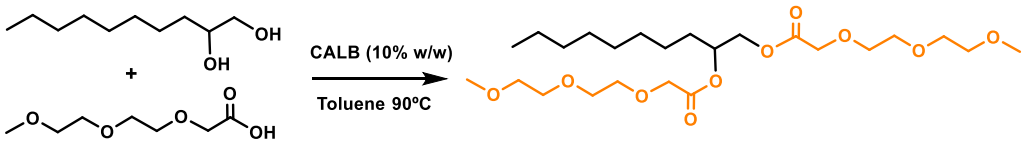

Scheme 6.6 Synthesis of decane-1,2diyl bis(2-(2-(2-methoxyethoxy)ethoxy) acetate.

In a 5 mL flask 500 mg (2.87 mmol) of 1,2-decanediol and (2-(2-(2-methoxyethoxy)ethoxy) acetic acid 777 mg (4.30 mmol) were dissolved in toluene (3 mL) and 127 mg CALB (10 % w/w) was added. The mixture was heated at 80 °C for 24h. The resulting solution was diluted in dichloromethane (3 mL) and extracted with water several times. Finally, the solvent was evaporated under vacuum to dryness, and the resulting oil analysed by ^{1}H NMR.

6.4 MONOMERS SYNTHESIS

6.4.1 10,11-Epoxyundecanoic acid

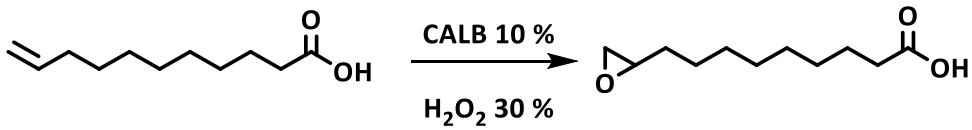

Scheme 6.7 Synthesis of 10,11-epoxyundecanoic acid (EUA).

In a 250 mL two necked round bottomed flask, 15.0 g (80.5 mmol) of 10-undecenoic acid in 90 mL of toluene, 6.6 mL (130 mmol) of 30 % hydrogen peroxide and 3.0 g (10 % w/w) of CALB were vigorously stirred at 40˚C for 24 h. Enzyme was filtered off and the resulting solution diluted in toluene, washed several times with water, dried over anhydrous magnesium sulfate, concentrated and dried under vacuum. The product was obtained as a white solid (yield 98 %) with melting point of 49-52 ˚C (lit. 50 ˚C).[4]

ESI-TOF, exact mass m/z 200.1414 [M+H] (Theoretical mass: 200.1412).

^{1}H NMR ($CDCl_3$/TMS, δ ppm): 2.91 (m, 1H, $(CH_2)_2$-C<u>H</u>-O, in oxirane ring), 2.75 (dd, 1H, J_{cis} = 5.2 Hz, CH-C<u>H</u>$_2$-O), 2.47 (dd, 1H, J_{trans} = 2.4 Hz, CH-C<u>H</u>$_2$-O), 2.33 (t, 2H, C<u>H</u>$_2$COOH), 1.64-1.32 (m, 12H, CH_2).

^{13}C NMR ($CDCl_3$, δ ppm): 180.72 (s, 1C, COOH), 139.26 (d, 1C, CH_2-<u>C</u>H-O), 114.29 (t, 1C, CH-<u>C</u>H$_2$O-), 34.25-25.78 (t, 8C, CH_2).

6.4.2 Methyl-11-hydroxyundecanoate

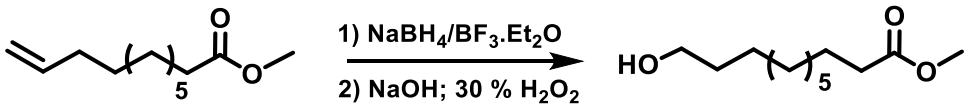

Scheme 6.8 Methyl 11-hydroxyundecanoate synthesis.

In a 250 mL round bottomed flask under argon, 2.46 g (65 mmol) of sodium borohydride were suspended in anhydrous THF (120 mL) and 47.2 mL (210 mmol) of methyl 10-undecenoate were added with stirring. The mixture was cooled on an ice-bath and 9.9 mL (80 mmol) of freshly distilled boron trifluoride diethyletherate were added drop wise during 1 h. The ice-bath was removed and mixture stirred for two additional hours and cooled again with a new ice-bath. Next, 21 mL of 3 M NaOH and 21 mL of 30 % H_2O_2 were added in this order in small portions during 1 h and the mixture kept at room temperature overnight. After neutralization with a concentrated NaH_2PO_4 solution, the organic layer was extracted several times with diethyl ether. After solvent evaporation, the resulting yellow oil was distilled under vacuum (120-125 °C, 0.8 mmHg) to afford 31.7 g of colourless oil (yield 72 %).[5]

^{1}H NMR ($CDCl_3$/TMS, δ ppm): 3.68 (s, 3H, $COOCH_3$); 3.63 (t, 2H, C<u>H</u>$_2$OH); 2.32 (t, 2H, CH_2COO); 1.71-1.50 (m, 4H, C<u>H</u>$_2$CH$_2$COO and C<u>H</u>$_2$CH$_2$OH); 1.40-1.20 (m, 12H, $(CH_2)_6$).

^{13}C NMR ($CDCl_3$, δ ppm): 174.2 (s, 1C, COO); 63.2 (t, 1C, CH_2OH); 51.4 (q, 1C, CH_3); 33.8 (t, 1C, <u>C</u>H$_2$COO); 32.1 (t, 1C, <u>C</u>H$_2$CH$_2$OH); 29.7-29.0 (t, 5C, $(CH_2)_5$); 25.6 and 25.0 (t, 2C, <u>C</u>H$_2$CH$_2$COO and <u>C</u>H$_2$CH$_2$OH).

6.4.3 10,11-Dihydroxyundecanoic acid

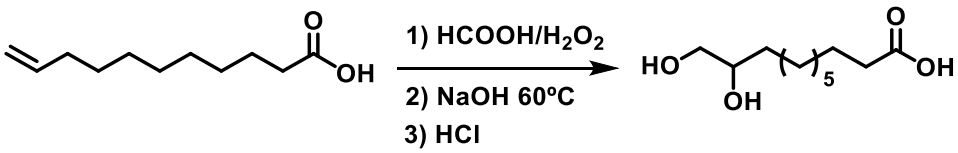

Scheme 6.9 10,11-Dihydoxyundecanoic acid synthesis (DHU).

Based on a reported procedure, 15.0 g (80.0 mmol) of 10-undecenoic acid and 73 mL (130 mmol) of formic acid were introduced in a 500 mL two necked round bottomed flask.[6] Next, 5.5 mL (98 mmol) of 50 % (w/w) hydrogen peroxide was added drop by drop with vigorous stirring during 20 min and the reaction mixture maintained at 40 ˚C for 1.5 h. Excess of formic acid was removed under reduced pressure and the resulting oil refluxed with 1.5 M NaOH solution (200 mL, 300 mmol) for 2 h. The clear solution was cooled in a water-ice bath, adjusted to pH 2 using 1 M HCl and stirred for 1 h. The resulting supernatant white solid was filtered, washed several times with water and dried under reduced pressure for 48 h. The product was obtained as a white solid (yield 96 %) with melting point of 92-94 ˚C (lit. 87-88˚C).[7]

ESI-TOF, exact mass m/z 218.1518 (Theoretical mass: 218.1518).

^{1}H NMR ($CDCl_3$/TMS, δ ppm): 3.72 (m, 1H, $HOCH_2$-C<u>H</u>OH-), 2.75 (dd, 1H, HOC<u>H</u>$_2$-CHOH), 2.47 (dd, 1H, HOC<u>H</u>$_2$-CHOH), 2.33 (t, 2H, C<u>H</u>$_2$COOH), 1.64-1.32 (m, 12H, $(CH_2)_6$).

^{13}C NMR ($DMSOd_6$, δ, ppm): 174.6 (s, 1C, COO), 71.2 (d, 1C, CHOH), 66.01 (t, 1C, CH_2OH), 33.7, 33.5 (t, 2C, <u>C</u>H_2COOH and CHOH-<u>C</u>H_2), 29.4 to 28.7 (t, 6C, $(CH_2)_n$), 24.6 (t, 2C , <u>C</u>H_2CH_2COOH).

6.4.4 Synthesis of (tri(ethylene glycol) monomethyl ether)succinic acid mono ester

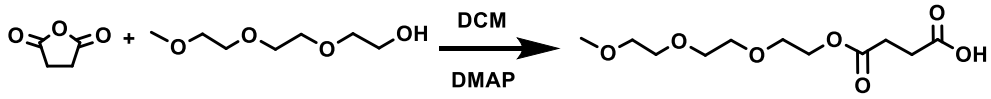

Scheme 6.10 (Tri(ethylene glycol)monomethyl ether)succinic acid mono ester synthesis ($mPEG_3$-$OOC(CH_2)_2COOH$).

In a 250 mL flask with a Dean-Stark apparatus tri(ethylene glycol) monomethyl ether (16.4 g, 100 mmol) and 1,2-dichloroethane (150 mL) were heated under reflux for 1 h to remove water. Next the solution was concentrated to 100 mL and succinic anhydride (25.0 g, 250 mmol) and N,N-dimethylaminopyridine (1.2 g ,10 mmol) were added. A condenser was adapted and the mixture heated under reflux for 24 h. Next, the solvent was distilled off and the crude reaction mixture dissolved in water, extracted with a mixture of hexane-ethyl acetate 1:1 and extracted again with dichloromethane. The dichloromethane solution was dried over $MgSO_4$ and concentrated under vacuum. The resulting product was dried overnight under vacuum to give 22.4 g (83 %) of a colourless viscous oil.

^{1}H NMR ($CDCl_3$/TMS, δ ppm): 9.49 (s, 1H, COOH), 4.26 (m, 2H, COO-CH_2), 3.72-3.67 (m, 8H, CH_2-O), 3.60 (m, 2H, CH_3-O-CH_2), 3.40 (s, 3H, CH_3), 2.67 (m, 4H, $OOC(CH_2)_2$-COOH).

^{13}C NMR ($CDCl_3$, δ ppm): 176.6 (s, 1C, COO), 172.2 (s, 1C, $COOCH_2$), 71.7 (t, 1C, CH_3-O-CH_2), 70.3 (t, 2C, -O-CH_2CH_2-O-CH_2-), 68.9 (t, 1C, -CH_2CH_2-OOC-), 63.8 (t, 1C, -CH_2CH_2-OOC-), 58.9 (q, 1C, CH_3), 28.9 (t, 1C, CH_2-COOH).

6.5 POLIMERS SYNTHESIS

6.5.1 10,11-Epoxyundecanoic acid polymerization tests with organic and enzymatic catalysts

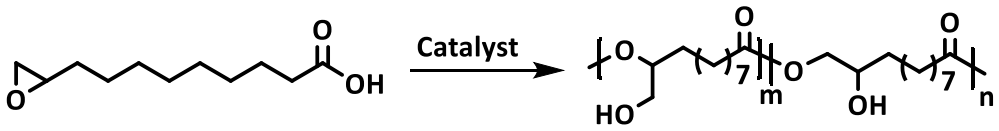

Scheme 6.11 Polymerization of 10,11-epoxyundecanoic acid (PEUA).

Polymerization tests were carried out in 5 mL cylindrical flasks with a Teflon coated screwed cap with a small stirring bar. 0.50 g (2.5 mmol) of EUA and the necessary amount of TBPB (1 % mol) or CALB (10 % w/w) catalysts were carefully weighted followed by the addition of 1.0 mL of solvent (toluene or DMF) if necessary. Flasks were closed, the content homogenized by stirring 30 min at 60 ˚C and fitted in oil bath at 100 ˚C (TBPB) or 90 ˚C (CALB). At present times (2, 4, 8, 24 or 48 h), a small sample was taken, dried under vacuum and analysed by ^{1}H NMR. Polymers were isolated by adding THF (3 mL), shaking the flask for 5 min and precipitating the clear solution in cold diethyl ether (100 mL). The resulting white polymer was collected by filtration and dried under vacuum. CALB beads and insoluble materials (when formed) were separated by decantation and rinsing with fresh THF.

6.5.2 10,11-Epoxyundecanoic acid polymerization kinetics with TBPB

1.0 g (5.0 mmol) of EUA was dissolved in 2.0 mL of toluene, ethylbenzene or cumene (2.5 M). Next, the necessary amount of TBPB (0.5, 1.0 or 2.0 mol %) was added. Using a syringe, 0.20 mL aliquots of each mixture were introduced in 2.0 mL screwed cap cylindrical flasks with a small stirring bar. The flasks were closed and heated and stirred in an oil bath at 100 ˚C (toluene), 130 ˚C (ethylbenzene) or 150 ˚C (cumene). At prefixed times, flasks were

cooled down, the solvent evaporated under vacuum, and the resulting solid mixture analysed by ^{1}H NMR and SEC.

6.5.3 Synthesis of linear PEAU-1, branched PEAU-2 and crosslinked PEUA-3

6.5.3.a Synthesis of linear PEUA-1

EUA polymerization (10.0 g, 50.0 mmol) was carried out with 1 % of TBPB in a 2.5 M solution in toluene at 100 ˚C for 8 h. The reaction mixture was dissolved in THF and then it was precipitated twice into cold diethylether. In this way, a white polymer with Mn 9800 g·mol^{-1} and Đ 3.4 was obtained in 87 % yield. The NMR data ascertaining the constitution and purity of this polyester are described below.

^{1}H NMR ($CDCl_3$/TMS, δ ppm): 4.90 (m, HO-H_2C-C<u>H</u>-OCO, abnormal unit), 4.13 and 3.96 (dd, OCO-C<u>H</u>$_2$-CHOH, normal unit), 3.82 (m, (-OCOCH_2-C<u>H</u>-OH, normal unit), 3.69 and 3.62 (dd, OCOCH-C<u>H</u>$_2$-OH, abnormal unit), 2.35 (m, 2H, OOC-CH_2), 1.62-1.29 (m, 14H, $(CH_2)_7$).

^{13}C NMR ($CDCl_3$, δ ppm): 174.5 (s, 1C, COO, abnormal unit), 174.2 (s, 1C, COO, normal unit), 75.4 (d, 1C, HOH$_2$C-<u>C</u>H-OCO, abnormal unit), 70.1 (s, 1C, -OCOCH_2-<u>C</u>H-OH, normal unit), 68.7 (t, 1C, OCO-<u>C</u>H$_2$-CHOH, normal unit), 64.9 (t, 1C, OCOCH-<u>C</u>H$_2$-OH, abnormal unit), 34.6 (t, 1C, <u>C</u>H$_2$-COO, abnormal unit, 34.3 (t, 1C, <u>C</u>H$_2$-COO, normal unit), 25.6-25.1 (t, 7C, $(CH_2)_7$).

6.5.3.b Synthesis of branched PEUA-2 and crosslinked PEUA-3

EUA polymerization (2.0 g, 10.0 mmol) was carried out with 1 % of TBPB in bulk at 100 ˚C for 8 h. The insoluble fraction was filtered off and rinsed several times with THF (28 % yield). The soluble polymer fraction was isolated by precipitation in diethylether resulting a white polymer with Mn 12400 g·mol^{-1} and Đ 4.1 in 62 % yield.

6.5.4 Preparation of poly(11-hydroxyundecenoate) by polymerization of methyl 11-hydroxyundecanoate initiated by 1,6-hexanediol

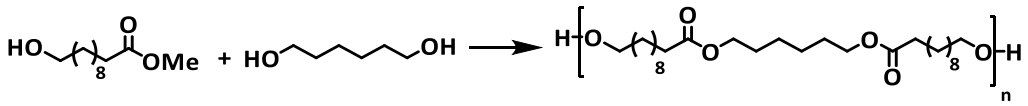

Scheme 6.12 Polymerization of methyl 11-hydroxyundecanoate initiated by 1,6-hexanediol.

In a 50 mL Schlenk flask 5.4 g (25 mmol) of methyl 11-hydroxyundecanoate and 0.25 g (2.1 mmol, molar ratio 12:1) of 1,6-hexanediol were melted with stirring under argon atmosphere at 130 °C. Over the resulting homogeneous clear mixture, 0.07 mL (0.00025 mol, 1 % molar) of titanium tetraisopropoxide was added and the temperature raised to 190 °C with the application of vacuum (2 mmHg). After 4 h the mixture was cooled and the resulting solid white mass was dissolved in 25 mL of THF and precipitated twice over 1000 mL of cold diethylether. The resulting white solid was collected by filtration, rinsed with diethyl ether, and dried under vacuum. (Yield: 92 %, Mn: 3520 g·mol^{-1}, by ^{1}H NMR, and 3900 g·mol^{-1}, Đ 2.0 by SEC).

^{1}H NMR ($CDCl_3$/TMS, δ ppm): 4.86 (m, 2H, C$\underline{H}_2$-OH (end group), 4.05 (t, 8H, COO-C$\underline{H}_2$-CH_2), 3.64 (t, 4H, HO-C$\underline{H}_2$) (end group), 2.29 (t, 4H, C$\underline{H}_2$-COO), 1.61 (m, 20H, -COO-CH_2-C$\underline{H}_2$; HO-CH_2-C$\underline{H}_2$; C$\underline{H}_2$-CH_2-COO), 1.28 (m, 56H, $(CH_2)_n$).

^{13}C NMR ($CDCl_3$, δ ppm): 175.1 (s, 2C, COO), 64.4 (t, 2C, C$\underline{H}_2$-OOC), 63.0 (t, 2C, CH_2-OH), 34.4 (t, 2C, C$\underline{H}_2$-COO), 29.4-25.0 (t, 20 C, $(CH_2)_n$.

6.5.5 Purification of PCL

Commercial PCL-diol was solved in THF and precipitated twice in cold methanol yielding a white solid that was filtered and dried under vacuum. (Yield: 88 %, Mn: 2580 g·mol^{-1}, by ^{1}H NMR, and 3600 g·mol^{-1}, Đ 1.9 by SEC).

6.5.6 Polymerization of 10,11-dihydoxyundecanoic acid

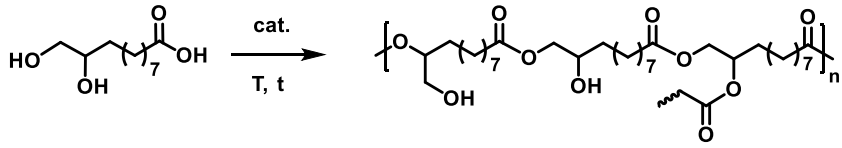

Scheme 6.13 Polymerization of 10,11-dihydroxyundecanoic acid (PDHU).

Polymerization tests were carried out in cylindrical Schlenk flasks with 0.28 g (1.3 mmol) of DHU. In the case of bulk polymerizations, vacuum (2 mmHg) was applied after 1 h of reaction. Polymerizations in solution were carried out using a 2.5 M monomer concentration in the appropriate solvent. 0.25 g of 4 Å activated molecular sieves were added in anhydrous tests. Samples of the reaction mixture were taken at present times an analysed by ^{1}H NMR. Finally, the polymer was isolated by adding chloroform (2 mL) and filtered to remove insoluble material (CALB beads or molecular sieves). The resulting clear solution was precipitated in cold diethyl ether (200 mL) and the resulting solid collected by filtration, dried under vacuum and analysed by SEC and ^{1}H NMR.

^{1}H NMR ($CDCl_3$/TMS, δ ppm): 5.11 (m, 1H, OCO-C<u>H</u>-CH_2-OCO, 1H, branched unit), 4.94 (m, 1H, HO-H_2C-C<u>H</u>-OCO, abnormal unit), 4.24 and 4.03 (dd, 2H, OCO-C<u>H_2</u>-CHOCO, branched unit), 4.12 and 3.96 (dd, 2H, OCO-C<u>H_2</u>-CHOH, normal unit), 3.85 (m, 1H, OCOC<u>H_2</u>-C<u>H</u>-OH, normal unit), 3.70- 3.58 (m, 2H, OCOCH-C<u>H_2</u>-OH, abnormal unit; 1H, OH-C<u>H_2</u>-CHOH, and 1H OH-CH_2-C<u>H</u>OH, end groups), 3.45 (m, 1H, OH-C<u>H_2</u>-CHOH, end group), 2.34 (m, 2H, C<u>H_2</u>-COO), 1.62-1.29 (m, 14H, $(CH_2)_7$).

^{13}C NMR ($CDCl_3$, δ ppm): 174.4 (s, 1C, COO, abnormal unit), 174.2 (s, 1C, COO, normal unit), 173.8 and 173.6 (s, 1C, COO, branched units), 75.4 (d, 1C, HOH_2C-<u>C</u>H-OCO, abnormal unit), 72.4 (d, 1C, OH-CH_2-<u>C</u>HOH, end group), 71.4 (d, 1C, OCOC<u>H_2</u>-<u>C</u>H-OCO, branched unit), 70.0 (d, 1C, OCOC<u>H_2</u>-<u>C</u>H-OH, normal unit), 68.7 (t, 1C, OCO-<u>C</u><u>H_2</u>-CHOH, normal unit), 66.9 (t, 1C, OH-<u>C</u><u>H_2</u>-CHOH, end group), 65.1 (t, 1C, OCOCH-<u>C</u><u>H_2</u>-OCO, branched unit), 64.9 (t, 1C, OCOCH-<u>C</u><u>H_2</u>-OH, abnormal unit), 34.6-33.4 (t, 1C, <u>C</u><u>H_2</u>-COO), 29.6-25.0 (t, 7C, $(CH_2)_7$).

6.5.6.a Scaled polymerization of 10,11-dihydoxyundecanoic acid

Scaled polymerization of 10,11-dihydroxyundecanoic with CALB in toluene following the conditions: in a 25 mL Schleck flask under inert atmosphere 3.0 g DHU (13.8 mmol) were dissolved in 5.5 mL of toluene (2.5 M) and with vigorous stirring 0.3 g (10 % (w/w)) of CALB and 0.5 g of 4 Å MS were added. The mixture was heated at 80 °C with stirring during 24 h. The resulting polymerization mixture was diluted in 25 mL of chloroform and solids (CALB beards and MS) removed by filtration and rinsed with some free solvent. Chloroform was removed under reduce pressure and the resulting solid dissolved in THF and precipitated twice into cold diethylether (400 mL). The resulting fine solid collected by filtration and dried under vacuum for 24h. Yield 98 %; molecular weight 15800 g·mol^{-1}; Đ 2.7; percentage of branching units 22.1 %, percentage of secondary hydroxyl units 57.5 % and percentage of primary hydroxyl units 20.3 %. ^{1}H and ^{13}C NMR and the heteronuclear single quantum correlation (HSQC) spectra of PDHU was recorded.

6.6 DERIVATIZATION POLYMERS

6.6.1 PEUA trifluoroacetylation

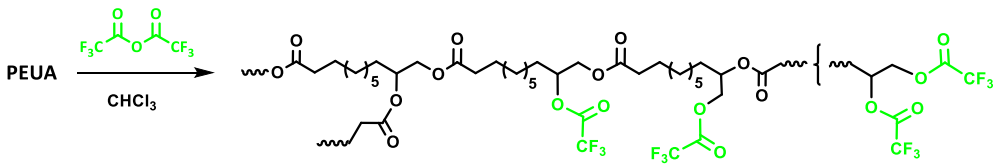

Scheme 6.14 Derivatization of PEUA with TFAA.

In 10 mL round bottomed flask under inert atmosphere 50 mg (0.02 mmol) of PEUA-1 or PEUA-2 were dissolved in $CHCl_3$ (2 mL) and TFAA (0.2 mL) was added. The mixture was heated at 40 °C for 30 minutes and further concentrated to dryness under vacuum for 2 h (soda-lime trap protection) to remove solvent and excess of reagent. The resulting PEUA trifluoroacetates were characterized by ^{1}H and ^{19}F NMR and the assignments made according to the corresponding trifluoroacetates of model compounds A and B.

^{1}H NMR ($CDCl_3$/TMS, δ ppm): 5.26 (m, 1H, $(CH_2)_2$-C<u>H</u>-OOC-CF_3), 5.15 (m, 1H, $(CH_2)_2$-C<u>H</u>-OOC), 4.51 (dd, 1H, CF_3-COO-C<u>H_2</u>-CH), 4.36 (dd, 1H, COO-C<u>H_2</u>-CH), 4.29 (dd, 1H, CF_3-COO-C<u>H_2</u>-CH), 4.06 (dd, 1H, COO-C<u>H_2</u>-CH), 2.30 (t, 2H, CH_2-C<u>H_2</u>-COO), 1.63-1.32 (m, CH_2), 0.90 (m, CH_2-C<u>H_3</u>).

^{19}F NMR ($CDCl_3$/ $CFCl_3$, δ ppm): -75.46 (s, CF_3-COO-CH_2-), -75.67 (s, CF_3-COO-CH-).

6.6.1.a PEUA-1 hydroxyl content and molecular weight determination

The absolute primary and secondary hydroxyl content was determined by ^{19}F NMR spectroscopy using an internal reference.[3] In a NMR tube, accurate amounts of dried PEUA-1-TFA (14.57 mg) and 3,5-bis(trifluoromethyl)benzoic acid (14.22 mg) were dissolved in 0.65 mL of $CDCl_3$. By comparing the intensity of the signals of trifluoroacetate groups in the PEUA-TFA and trifluoromethyl groups of the internal standard, the amount of primary (0.169 Eq_{OH} per 100 g of polymer) and secondary (0.353 Eq_{OH} per 100 g of polymer) alcohols was estimated using equation 6.2.

$$\frac{Eq_{OH}}{100\ g_{pol}} = \frac{I_{OH}}{I_{st}} x \frac{W_{st}}{W_{pol}} x \frac{200}{FW_{st}} \qquad \text{equation 6.2}$$

I_{OH}: Intensity of PEUA-1-TFA signal.
I_{st}: Intensity of 3,5-bis(trifluoromethyl) benzoic acid.
W_{st}: Weigh of 3,5-bis(trifluoromethyl) benzoic acid.
W_{pol}: Weigh of PEUA-1-TFA.
FW_{st}: 3,5-Bis(trifluoromethyl) benzoic acid FW (258.12 g·mol^{-1}).

From the total hydroxyl content (0.522 Eq_{OH}/100 g polymer) and considering a linear structure with one carboxylic acid and one hydroxy end groups, the polymerization degree was estimated using equation 6.3:

$$\frac{Eq\ OH}{100g\ Polym.} = \frac{n+1}{M\ unit + M\ water};\ n = 19 \qquad \text{equation 6.3}$$

M_{unit}: Mass of the repeating unit (200.28 g·mol^{-1}).
M_{water}: FW of water (18 g·mol^{-1}).
n: Polymerization degree.

6.6.2 PEUA derivatization with trimethylsilyldiazomethane

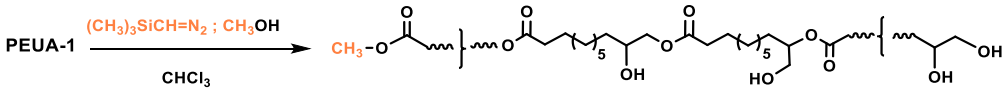

Scheme 6.15 PEUA-1 TMS-CHN_2 derivative.

In a 10 mL flask under argon atmosphere, 0.02 g (0.12 mmol) of PEUA-1 was dissolved in 1 mL of a mixture of $CHCl_3$ and CH_3OH (2:1). A 2 M solution of TMS-CHN_2 in hexane (0.1 mL, 0.2 mmol) was added using a syringe until a yellow colour persists.[8,9] The mixture was stirred at r.t. for 1 h, evaporated under vacuum to dryness and analysed by ^{1}H NMR.

^{1}H NMR ($CDCl_3$/TMS, δ ppm): 4.90 (m, 1H, OC<u>H</u>-CH_2), 4.13 (dd, 1H, OC<u>H</u>$_2$-CH), 3.96 (dd, 1H, OC<u>H</u>$_2$-CH), 3.82 (m, 1H, $(CH_2)_2$-C<u>H</u>-OH), 3.67 (dd, 1H, CH-C<u>H</u>$_2$-OH), 3.65 (s, 3H, CH_3-OCO), 3.61 (dd, 1H, CH-C<u>H</u>$_2$-OH), 2.32 (m, 2H, CO-C<u>H</u>$_2$-CH_2), 1.61-1.28 (m, 28H, CH_2-C<u>H</u>$_2$).

Molecular weight was calculated by comparing the intensity of the $COOCH_3$ end group and the CH_2COO methylene of the repeating unit according to equation 6.4:

$$n = \frac{3}{2}\frac{I_{\propto CH2}}{I_{COOCH3}} = \frac{3}{2}\frac{I_{2.35-2.25}}{I_{3.70-3.64} - I_{3.62-3.55}} \; ; \; n \sim 19 \quad \text{equation 6.4}$$

$I_{\alpha CH2}$= Intensity of the signal at 2.30 ppm.
I_{COOCH3}= Intensity of signals from 3.55 to 3.62 ppm – intensity of signals from 3.64 to 3.70 ppm.

6.6.3 PDHU trifluoroacetylation

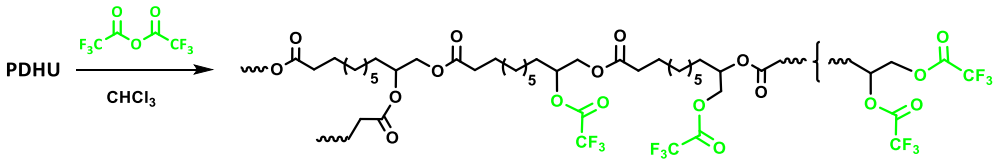

Scheme 6.16 Derivatization of PDHU with TFAA.

In 10 mL round bottomed flask under inert atmosphere 75 mg (0.03 mmol) of PDHU were dissolved in $CHCl_3$ (3 mL) and TFAA (0.4 mL) was added. The mixture was heated at 40 °C

for 30 minutes and further concentrated to dryness under vacuum for 2 h (soda-lime trap protection) to remove solvent and excess of reagent. The resulting PDHU trifluoroacetates were characterized by ^{1}H and ^{19}F NMR and the assignments made according to the corresponding trifluoroacetates of model compounds A and B and the bis-trifluoroacetate of 1,2-hexanediol.

^{1}H NMR ($CDCl_3$/TMS, δ ppm): 5.35 (m, 1H, CH-OOCCF$_3$ end group), 5.28 (m, 1H, CH-OOCCF$_3$ normal unit), 5.14 (m, 1H, CH-OOCCF$_3$ abnormal unit), 5.07 (m, 1H, CH-OOC branched unit), 4.58 (dd, 1H, CH$_2$-OOCCF$_3$ end group), 4.50 (dd, 1H, CH$_2$-OOCCF$_3$ abnormal unit), 4.42 (dd, 1H, CH$_2$-OOCCF$_3$ end group), 4.39 (dd, 1H, CH$_2$-OOCCF$_3$ normal unit), 4.29 (dd, 1H, CH$_2$-OOCCF$_3$ abnormal unit), 4.20 (m, 1H, CH$_2$-OOC branched unit), 4.06 (dd, 1H, CH$_2$-OOCCF$_3$ normal unit), 4.02 (dd, 1H, CH$_2$-OOC branched unit), 2.30 (m, 2H, CH$_2$COO), 1.73-1.28 (m, 14H, (CH$_2$)$_7$).

^{19}F NMR ($CDCl_3$/ $CFCl_3$, δ ppm): -75.48 (s, CF$_3$COO-CH abnormal units), -75.52 (s, CF$_3$COO-CH$_2$ end group), -75.68 (m, CF$_3$COO-CH normal units and CF$_3$COO-CH end group).

6.6.3.a PDHU hydroxyl content and molecular weight determination

The absolute content of primary and secondary hydroxyl groups in PDHU was determined by integration of the ^{19}F NMR signals using accurately weighted amounts of PDHU-TFA and bis(trifluoromethyl)benzoic acid as internal).

In a NMR tube, accurate amounts of dried PDHU-TFA (22.20 mg) and 3,5-bis(trifluoromethyl)benzoic acid (12.45 mg) were dissolved in 0.65 mL of $CDCl_3$. By comparing the intensity of the signals of trifluoroacetate groups in the PEUA-TFA and trifluoromethyl groups of the internal standard, the amount of primary (0.215 Eq_{OH} per 100 g of polymer) and secondary (0.297 Eq_{OH} per 100 g of polymer) alcohols was estimated using equation 6.5.

$$\frac{Eq_{OH}}{100g_{pol}} = \frac{I_{OH}}{I_{st}} x \frac{W_{st}}{W_{pol}} x \frac{200}{FW_{st}} \quad \text{equation 6.5}$$

$I_{OH:}$ Intensity of PEUA-1-TFA signal.
I_{st}: Intensity of 3,5-bis(trifluoromethyl) benzoic acid.
W_{st}: Weigh of 3,5-bis(trifluoromethyl) benzoic acid.
W_{pol}: Weigh of PEUA-1-TFA.
FW_{st}: 3,5-Bis(trifluoromethyl) benzoic acid FW (258.12 g·mol^{-1}).

From the total hydroxyl content (0.512 Eq_{OH}/100 g polymer) and considering the branched structure, the polymerization degree can be estimated using equation 6.6:

$$\frac{Eq\ OH}{100g\ Polym.} = \frac{n+1}{M\ unit + M\ water}; \quad n \sim 36 \quad \text{equation 6.6}$$

M_{unit}: Mass of the repeating unit (200.28 g·mol^{-1}).
M_{water}: FW of water (18 g·mol^{-1}).
n: Polymerization degree.

In this way, 0.215 and 0.295 equivalents of primary and secondary hydroxyl per 100 g of polymer were determined. According to a branched structure and one hydroxyl group per repeating unit and one hydroxyl end group it is possible to roughly estimate a Mn of 7200 g·mol^{-1} for this sample, which is about one half of that determined by SEC (15800 g·mol^{-1}). Molecular weights determined by SEC are over or under estimated as consequence of differences in the hydrodynamic volume with the polystyrene standards used in the calibration.

6.7 POST-POLYMERIZATION MODIFICATION

6.7.1 PEUA modification with N-Boc-phenylalanine

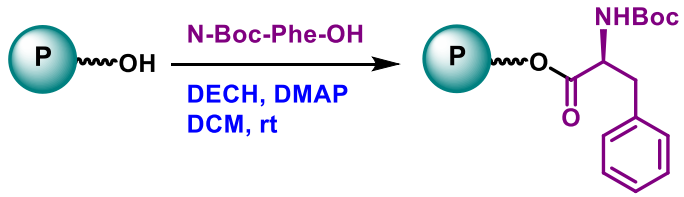

Scheme 6.17 Post-polymerization modification of PEUA-1 with N-Boc-Phe-OH.

In a 100 mL flask, 0.5 g (2.5 mmol) of PEUA 0.73 g (2.75 mmol) of Boc-Phe-OH, 0.96 g (5.01 mmol) of DECH and 0.02 g (0.13 mmol) of DMAP were dissolved in DCM (40 mL). The mixture was stirred at 20 ˚C under inert atmosphere for 24 h. After solvent evaporation, the resulting solid was dissolved in THF (3 mL) and precipitated twice in deionized water. The modified polymer was dried under vacuum for 24 h. Yield: 81 %. Mn = 15700 g·mol^{-1}; Đ = 2.4.

^{1}H NMR ($CDCl_3$/TMS, δ ppm): 7.30-7.19 (m, 5H, H_{ar}), 5.10 (m, 1H, NH), 4.98 (m, N-Boc-Phe-Ala-O-C<u>H</u>-CH_2OCO, normal unit), 4.77 (m, N-Boc-Phe-Ala-O-CH_2-C<u>H</u>-COO, abnormal unit), 4.57 (s, 1H, HN-C<u>H</u>-COO), 4.19 and 4.01 (m, 2H, N-Boc-Phe-Ala-O-CH-C<u>H_2</u>-COO, normal unit), 4.12 and 3.81 (N-Boc-Phe-Ala-O-C<u>H_2</u>-CH-COO, abnormal unit), 3.11 and 2.92 (m, 2H, Ph-CH_2), 2.29-2.35 (m, 2H, CH_2-COO), 1.64-1.26 (m, 23H, $(CH_2)_7$ and $C(CH_3)_3$).

^{13}C NMR ($CDCl_3$, δ ppm): 174.1 (s, 1C, COO, abnormal unit), 173.6 (s, 1C, COO, normal unit), 171.8 (s, 1C, HN-CH-<u>C</u>OO-CH), 155.1 (s, 1C, HNCOO), 136.1, 129.4, 128.6 and 127.1 (Ph), 80.0 (s, 1C, <u>C</u>$(CH_3)_3$), 73.7 and 73.1 (d, 1C, N-Boc-Phe-Ala-O- <u>C</u>H-CH_2-COO, normal unit), 70.0 (d, 1C, N-Boc-Phe-Ala-O-CH_2-<u>C</u>H-COO, abnormal unit), 65.9 (s, 1C, t-Boc-Phe-Ala-O-<u>C</u>H_2-CH-COO, abnormal unit), 64.9 and 64.7 (s, 1C, N-Boc-Phe-Ala-O-CH-<u>C</u>H_2-COO, normal unit), 54.4 (d, 1C, OOC-<u>C</u>H-NH), 38.3 (s, 1C, Ph-<u>C</u>H_2-CH), 34.4 (s, 1C, <u>C</u>H_2-COO), 30.7-24.8 (s, 7C, $CH_2)_7$ and (q, 3C, C(<u>C</u>$H_3)_3$).

6.7.2 PEUA modification with 2,2-dimethylthiazolidin-3-(N-formyl)-4-carboxylic acid

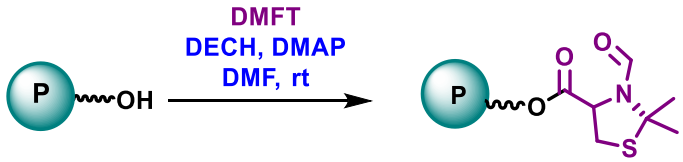

Scheme 6.18 Post-polymerization modification of PEUA-1 with 2,2-dimethylthiazolidin-3-(N-formyl)-4-carboxylic acid (DMFT).

6.7.2.a Synthesis of 2,2-dimethylthiazolidin-3-(N-formyl)-4-carboxylic acid

Synthesis of DMFT was accomplished following a two-step synthetic approach.

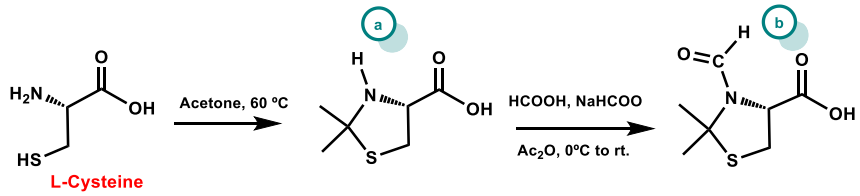

Scheme 6.19 Synthesis of a) 2,2-dimethylthiazolidin-4-carboxylic acid and b) 2,2-dimethylthiazolidin-3-(N-formyl)-4-carboxylic acid from L-cysteine.

Synthesis of 2,2-dimethylthiazolidin-4-carboxylic acid

Synthesis was carried out using a reported procedure. 36.3 g (0.30 mol) of L-cysteine, 880 mL of dry acetone (12 mol) and 1 mL of glacial acetic acid were refluxed with stirring until all solid dissolves (6 h). The warm solution was filtered and the clear solution stand in the refrigerator (-20 ˚C) for crystallization. The white solid was collected by filtration, washed with cool acetone and dried to yield 42.8 g of crystalline product. Yield (88.0 %). Melting point 152-154 ˚C (lit. 163-165 ˚C).

ESI-TOF, exact mass m/z 161.0513 (Theoretical mass: 161.0510).

^{1}H NMR (DMSOd_6/TMS, δ ppm): 13.05 (s, 1H, -COOH), 4.00 (dd, 1H, C<u>H</u>-NH-), 3.33 (dd, 1H, -CH_2-S-), 2.96 (dd, 1H, -CH_2-S-), 2.09 (s, 1H, -NH), 1.59 (s, 3H, CH_3-), 1.43 (s, 3H, CH_3-).

^{13}C NMR ($DMSOd_6$, δ, ppm): 172.6 (s, 1C, C=O), 75.8(s, 1C, -CH-NH), 64.4 (s, 1C, $\underline{C}(CH_3)_2$), 32.2 (t, 1C, $-CH_2S-$), 29.9 (q, 1C, CH_3).

Synthesis of 2,2-dimethylthiazolidin-3-(N-formyl)-4-carboxylic acid

Based on a reported procedure, a solution of 13.6 g (0.2 mol) of sodium format in 260 mL formic acid was cooled to 0˚C and 32.2 g of 2,2-dimethylthiazolidin-4-carboxylic acid were added and stirred until solution. Next, 100 mL of acetic anhydride were added dropwise during an hour. When the addition was complete the mixture was stirred at room temperature for two hours and a white precipitate separate. 200 mL of cool water were added, the mixture cooled to 0-5 ˚C and the solid filtered, washed with cool water and dried under vacuum over KOH to produce 33.0 g (86 %) of crude product that was purified by recrystallization in 750 mL EtOH/H_2O (1:1) to give 29.8 g (78 %) of white crystalline solid. Yield (75 %). Melting point 211˚C (lit. 221-222 ˚C).

ESI-TOF, exact mass m/z 189.0466 (Theoretical mass: 189.0460).

^{1}H NMR ($DMSOd_6$/TMS, δ ppm): 13.00 (s, 1H, -COOH), 8.39, 8.21 (s, 1H, -CHO), 5.05, 4.82 (dd, 1H, -C<u>H</u>-NCHO-), 3.43, 3.36 (dd, 1H, $-CH_2-S-$), 3.17, 3.14 (dd, 1H, $-CH_2-S-$), 2.09 (s, 1H, -NH), 1.74, 171 (s, 6H, CH_3).

^{13}C NMR ($DMSOd_6$, δ, ppm): 172.6 (s, 1C, COOH), 160 (s, 1C, N-CHO), 75.8 (d, 1C, -<u>C</u>H-N-CHO), 64.4 (s, 1C, $\underline{C}(CH_3)_2$), 32.2 (t, 1C, $-CH_2S-$), 29.9 (q, 1C, CH_3).

6.7.2.b PEUA modification with 2,2-dimethylthiazolidin-3-(N-formyl)-4-carboxylic acid

In a 50 mL flask, 0.5 g (2.5 mmol) of PEUA 0.73 g (2.75 mmol) of DMFT, 0.96 g (5.01 mmol) of DECH and 0.02 g (0.13 mmol) of DMAP were dissolved in DMF (10 mL). The mixture was stirred at 20 ˚C under inert atmosphere for 24 h. The solution was precipitated twice in deionized cool water. The modified polymer was dried under vacuum for 24 h. Yield: 86 %. Mn = 11630 g·mol^{-1}; Đ = 2.9.

^{1}H NMR ($CDCl_3$/TMS, δ ppm): 8.33, 8.25 (s, 1H, CHO), 5.12-5.02 (m, 1H, O-CH_2-CH-COO, normal and abnormal units), 4.33-3.99 (m, 2H, O-CH-CH_2-COO, normal and abnormal units), 3.32-3.22 (m, 3H, CO-CH-, CH-CH_2-S), 2.29-2.35 (m, 2H, CH_2-COO), 1.64-1.26 (m, 23H, $(CH_2)_7$ and $C(CH_3)_3$).

^{13}C NMR ($CDCl_3$, δ ppm): 173.6 (COO, normal and abnormal units), 169.1(s, 1C, COO), 159.1 (d, 1C, N-CHO), 73.3 (d, 1C, -O-CH_2-CH-COO, normal and abnormal units),64.7 (d, 1C, O-CH_2-CH-COO, normal and abnormal units), 70.3 (d, 1C, -CH-N-CHO), 62.6 (t, 1C, -CH_2S-), 29.3(s, 1C, $C(CH_3)_2$), 29.7 (q, 1C, CH_3), 30.7-24.8 (t, 7C, $CH_2)_7$ and (s, 1C, $C(CH_3)_3$).

6.7.3 Modification with succinic anhydride (PEUA-Succinate)

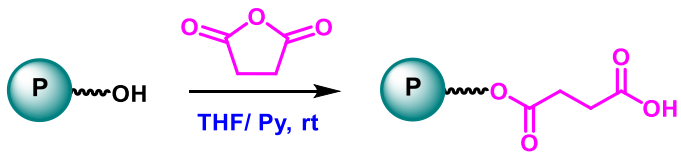

Scheme 6.20 Post-polymerization modification of PEUA-1 with succinic anhydride.

Following a described procedure, in a 50 mL flask under inner atmosphere 0.50 g (2.5 mmol) of PEUA-1 were dissolved in anhydrous THF (5 mL). Next, 0.8 mL (0.79 g, 10 mmol) of anhydrous pyridine and 0.76 g (7.5 mmol) of succinic anhydride were added in this order. The mixture was stirred at room temperature for 24 h and precipitated twice in deionized water. The resulting PEUA-monoester dried was under vacuum for 24 h. Yield: PEUA-succinate (84 %). Mn = 10500 g·mol^{-1}; Đ = 2.8.[10]

^{1}H NMR ($CDCl_3$/TMS, δ ppm): 5.01 (m, 1H, CH-OCO), 4.16 and 3.97 (m, 2H CH_2-OCO), 2.55 (m, 4H, OC-CH_2CH_2COOH), 2. 23 (m, 2H, CH_2-COO), 1.6-1.22 (m, 14H $(CH_2)_7$).

^{13}C NMR ($CDCl_3$ + DMF-d_7, δ ppm): 174.3 (s, 1C, COOH), 173.5 (s, 1C, COO, normal unit), 173.4 (s, 1C, COO, abnormal unit), 172.3 (s, 1C, COO succinate in abnormal unit), 172,13 (s, 1C, COO succinate in normal unit), 71.8 (d, 1C, CH-OCO, normal unit), 71.2 (d, 1C, CH-OCO,

abnormal unit), 65.3 (t, 1C, $\underline{C}H_2$-OCO, abnormal unit), 64.8 (t, 1C, $\underline{C}H_2$-OCO, normal unit), 34.4 (t, 1C, $\underline{C}H_2$-COO), 34.1-24.8 (q, 7C, $(CH_2)_7$.

6.7.4 Modification of PEUA-succinate with N-Boc-serine methylester

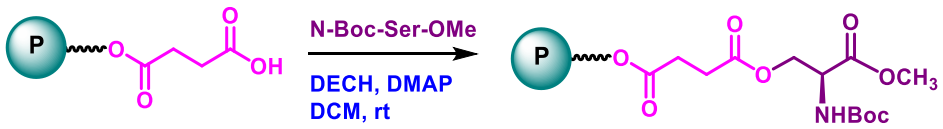

Scheme 6.21 Post-polymerization modification of PEUA-1 with N-Boc-Ser-OMe.

In a 25 mL flask, 0.34 g (1.12 mmol) of PEUA-Succinate and 0.24 g (1.12 mmol) of Boc-Ser-OMe were dissolved in anhydrous DCM (10 mL). The mixture was stirred and 0.38 g of DECH (2.06 mmol) and 0.006 g (0.06 mmol) of DMAP were added. The reaction was kept at room temperature under inert atmosphere for 24 h. The resulting suspension was washed several times with water and concentrated. The resulting polymer was dissolved in the minimum quantity of THF and precipitated over deionized water. The final product was dried under vacuum for 24 h. Yield: 64 %. Mn = 16250 g·mol^{-1}; Đ = 2.8.

^{1}H NMR ($CDCl_3$/TMS, δ ppm): 5.38 (s, 1H, -NH), 5.07 (m, 2H, CH_2-OCO), 4.57 (m, 1H, -C$\underline{H}$-NH), 4,45-4.36 (m, 2H, NH-CH-C$\underline{H}_2$-OCO), 4,30-4.21 (m, 2H, -CH_2-OCO), 3.77 (s, 3H, OCH_3), 2.61 (s, 4H, COO-C$\underline{H}_2$-C$\underline{H}_2$-OCO), 2.30 (m, 2H, -CH_2-COO), 1.62-1.29 (m, 23H, $(CH_2)_7$, $C(CH_3)_3$).

^{13}C NMR ($CDCl_3$, δ ppm): 172.5 (s, 1C, COO Succinate), 170.7 (s, 1C, COO abnormal unit), 170.6 (s, 1C, COO normal unit); 169.6 (s, 1C, $\underline{C}OOCH_3$); 154.9 (s, 1C, O-CO-NH); 79.9 (s, 1C, $\underline{C}(CH_3)_3$); 71.3 (d, 1C, $\underline{C}HCH_2OOC$ normal unit); 70.2 (d, 1C, $\underline{C}H$-OOC abnormal unit); 64.5 (t, 1C, $\underline{C}H_2CHOOC$ abnormal unit); 63.8 (t, 1C, $\underline{C}H_2OOC$ normal unit); 63.5 (t, 1C, NHCH$\underline{C}H_2$OOC); 56.1 (d, 1C, NH$\underline{C}$HCH$_2$OOC); 51.7 (q, 1C, OCH_3); 28.7-21.7 (t, 7C, $(CH_2)_7$, $OOCCH_2CH_2COO$, (s, 3C, $C(\underline{C}H_3)_3$).

6.8 DEGRADATION PROCEDURES

Sample disks (12.0 mm x ~0.40 mm; surface area to volume ratio equal to 0.1 cm^{-1}) weighting about 50 mg, were prepared by compression moulding (4 ton) using a manual hydraulic press 15 ton sample pressing (SPECAC) equipped with a water cooled heater. Finely grounded samples were introduced into the preheated (40 °C) mould and after 3 h pressed under vacuum and kept at room temperature for 1 h. Disks were demoulded under cool N_2 and dried under vacuum to constant weight (m_0). After incubation in the selected media for the scheduled period of time, three samples of each polymer were rinsed thoroughly with distilled water and weighted immediately after wiping the surface with a filter paper to absorb the surface water to obtain the wet weight (m_w). Next, the samples were vacuum-dried for 48 h and weighted again to obtain the dry weight (m_d).

6.8.1 Hydrolytic degradation

For hydrolytic degradation, samples were immersed in Falcom tubes containing about 24 ml of citric acid buffer (pH 2.0) and kept sterile by adding 0.03 % (w/v) of NaN_3. Incubation took place at 45 °C. Samples were removed at specific intervals, cleaned and dried under vacuum to constant weight.

Weight loss was determined by equation (6.7).

$$WL\ \% = [(m_0 - m_d)/m_0] \times 100 \qquad \text{equation 6.7}$$

where m_0 is the initial mass, m_t is the final mass after drying at a predetermined time. An average of three measurements was taken.

6.8.2 *In vitro* enzymatic degradation

In vitro enzymatic degradation tests were carried out in a similar way using a phosphate buffer (pH 7.2) containing lipase from porcine pancreas (20 mg). Buffered enzyme solution

was replaced every 72 h to maintain enzyme activity. Incubation took place at 37 °C. Samples were removed at specific intervals, cleaned and dried under vacuum to constant weight. Weight loss was determined by equation (6.7).

6.8.3 Accelerated degradation

500 mg of powdered polymer were mixed with methanesulfonic acid water solution (1 M, 20 mL) and the mixture was heated under reflux. After 24 hours the solution was neutralized with Na_2CO_3 saturated solution and the organic products were extracted with DCM, concentrated under vacuum and analysed by SEC and ^{1}H NMR.

6.8.4 PEUA accelerated degradation: kinetic study

180 mg of PEUA were mixed with methanesulfonic acid water solution (0.5 M, 8 mL), and heated under reflux. At prefixed times, aliquots of solutions were taken, cooled down, neutralized with Na_2CO_3 saturated solution and the organic products extracted with DCM. The solvent was removed under vacuum and products analysed by SEC and ^{1}H NMR.

6.9 COPOLYMERIZATION

6.9.1 Block polymerization of mPEG-OH and DHU

In a typical procedure, in a 15 mL Schlenck flask, the necessary amount of monomethoxy poly(ethylene glycol) 550 ($mPEG_{12}$) or 2000 ($mPEG_{45}$) and dihydroxyundecanoic acid (DHU) (0.5 g, 2.3 mmol), were dissolved in 3mL of toluene. The used feed molar ratios of mPEG/DHU were 1:20 and 1:30. CALB (10 % (w/w) vs. total substrates) was transferred into the flask and the mixture heated with stirring at 80 °C for 48 h. The reaction was quenched with chloroform (5mL mL) and the enzyme was removed by filtration and rinsed with free solvent. The clear solution was concentrated under vacuum, dissolved in 1,2-dichloroethane and stirred with 20 mL of distilled water at 80 °C during 2 h. The aqueous phase was removed off and the extraction was repeated four times with new portions of

water (total amount 100 ml) every two hours and the last kept overnight. The organic phase was dried with anhydrous $MgSO_4$, concentrated and the resulting polymer dried under vacuum at room temperature for 48 h.

^{1}H NMR ($CDCl_3$/TMS, δ ppm): 5.07 (m, CH-OOC, branched unit), 4.90 (m, HO-H_2C-C<u>H</u>-OOC, abnormal unit), 4.22 (m, 2H, O-CH_2C<u>H_2</u>-OOC and 1H, COO-CH_2, branched unit), 4.13 (dd, 1H, COO-CH_2, normal unit), 4.11 (dd, 1H, COO-CH_2, branched unit), 3.96 (dd, 1H, COO-CH_2, normal unit), 3.82 (m, 1H, C<u>H</u>-OH, normal unit), 3.69-3.62 (m, 4H, C<u>H_2</u>-OH, abnormal unit and C<u>H</u>OHC<u>H_2</u>OH end group), 3.60 (m, 24H or 88H, O(CH_2)$_2$O), 3. 54 (m, 2H, CH_3-O-C<u>H_2</u>), 3.43 (m, 1H, C<u>H_2</u>OH end group), 3.38 (s, 3H, CH_3O), 2.35 (m, 2H, COOCH_2), 1.62-1.29 (m, 14H, (CH_2)$_7$).

^{13}C NMR ($CDCl_3$, δ ppm): 174.5 (s, 1C, COO, abnormal unit), 174.2 (s, 1C, COO, normal unit), 173.6 (s, 1C, <u>C</u>OO-CH_2<u>C</u>H_2-O), 172.5 and 172.3 (s, 1C, COO, branched unit), 75.1 (d, 1C, <u>C</u>H-OOC, abnormal unit), 72.2 (d, 1C, <u>C</u>HOHCH_2OH end group), 71.8 (t, 1C, CH_3OCH_2<u>C</u>H_2), 71.2 (d, 1C, <u>C</u>H-OOC, branched unit), 70.5 (t, 1C, O-<u>C</u>H_2-<u>C</u>H_2), 69.7 (d, 1C, CH_2-<u>C</u>H-OH, normal unit), 69.1 (t, 1C, O-<u>C</u>H_2CH_2-OOC), 68.5 (t, 1C, COO-<u>C</u>H_2-CHOH, normal unit), 66.7 (t, 1C, CHOH<u>C</u>H_2OH, end group), 64.9 (t, 1C, COOCH-<u>C</u>H_2, branched unit), 64.4 (t, 1C, COOCH-<u>C</u>H_2-OH, abnormal unit), 63.3 (t, 1C, OCH_2<u>C</u>H_2-OOC), 59.0 (q, 1C, CH_3O), 34.6 (t, 1C, <u>C</u>H_2-COO, abnormal unit, 34.3 (t, 1C, <u>C</u>H_2-COO, normal unit), 25.6-25.1 (t, 7C, (CH_2)$_7$).

6.9.2 Grafting of mPEG$_2$OCH$_2$COOH onto PEUA and PDHU

In a 50 mL flask with a condenser, 0.5 g (2.3 mmol) of PEUA or PDHU were dissolved under reflux with 25 mL of toluene. After 2 h, temperature was dropped to 80 °C and 0.82 g (4.6 mmol) of 2-[2-(2-methoxyethoxy)ethoxy]acetic acid and CALB (10 wt % vs. total substrates) were added. After stirring at 80 °C for 24 h the mixture was quenched with chloroform (10 mL), the enzyme was removed by filtration and after concentration dissolved in 1,2-dichloroethane and extracted with hot water following the procedure described in the block copolymerization.

mPEG$_2$OCH$_2$COO-graft-PEUA and mPEG$_2$OCH$_2$COO-graft-PDHU:

^{1}H NMR ($CDCl_3$/TMS, δ ppm): 5.15 (m, 1H, CH-OOC-mPEG normal unit), 5.05 (m, 1H, CH-OOC branched unit), 4.95 (m, 1H, CH-OOC-mPEG abnormal unit), 4.88 (m, 1H, CH-OOC abnormal unit), 4.31-4.23 (m, 1H, C$\underline{H}_2$-CH-COOmPEG), 4.14 (m, 1H, CH_2-OOC normal unit and 1H, CH_2OOC branched unit), 4.10 and 4.04 (s, 2H, mPEG-OC$\underline{H}_2$COO), 3.98 (m, 1H, C$\underline{H}_2$-CH-COOmPEG), 3.67 (m, 1H, CH_2-OOC normal unit and 1H, CH_2OOC branched unit), 3.82 (m, 1H, C$\underline{H}$OH normal unit), 3.73, 3.69 and 3.65 (m, 6H, CH_3O-C$\underline{H}_2$C$\underline{H}_2$-O-C$\underline{H}_2$-), 3.55 (m, 2H, C$\underline{H}_2$O-CH_2COO), 3.35 (s, 3H, CH_3O), 2.30 (m, 2H, CH_2COO), 1.59-1.28 (m, 14H, $(CH_2)_7$).

^{13}C NMR ($CDCl_3$, δ ppm): 174.5 (s, 1C, COO, abnormal unit), 174.2 (s, 1C, COO, normal unit), 172.6 and 172.4 (s, 1C, COO, branched unit), 170.6, 170.4 and 170.2 (s, 1C, O-$CH_2\underline{C}$OO grafted end groups and normal and abnormal units), 76.3 (d, 1C, $\underline{C}$HOOC grafted abnormal unit), 75.3 (d, 1C, $\underline{C}$HOOC, abnormal unit), 72.3 (d, 1C, $\underline{C}$HOOC grafted normal unit), 71.9 (t, 1C, $CH_3O\underline{C}H_2$), 71.3 (d, 1C, $\underline{C}$H-OOC, branched unit), 70.9 (t, 1C, $\underline{C}H_2OOCCH_2O$), 70.6 and 70.5 (t, 1C, O-$\underline{C}H_2$-$\underline{C}H_2$), 69.9 (d, 1C, CH_2-$\underline{C}$H-OH, normal unit), 68.6 and 68.4 (t, 1C, $\underline{C}H_2$OOC grafted units), 66.8 (t, 1C, $\underline{C}H_2$OH end group) , 65.4 (t, 1C, $\underline{C}H_2OOCCH_2O$ grafted unit), 64.8 (t, 1C, COO$\underline{C}H_2$, branched unit), 64.7 (t, 1C, CH_2-OH, abnormal unit), 59.1 (q, 1C, CH_3O), 34.5-33.9 (t, 1C, $\underline{C}H_2$COO), 25.6-24.6 (t, 7C, $(CH_2)_7$).

6.9.3 Grafting of mPEG$_3$OOC(CH$_2$)$_2$COOH onto PEUA and PDHU

In a 50 mL flask with a condenser 0.5 g (2.3 mmol) of PEUA or PDHU were heated under reflux with 25 mL of toluene. After 2 h, temperature was dropped to 80 °C and 1.2 g (4.6 mmol) (tri(ethylene glycol)monomethyl ether)succinic acid monoester and CALB (10 wt % vs. total substrates) were added. After stirring at 80 °C for 24 h the mixture was quenched with chloroform (10 mL), the enzyme was removed by filtration and after concentration dissolved in 1,2-dichloroethane and extracted with hot water following the procedure described in the block copolymerization.

$mPEG_3OOC(CH_2)_2COO$-g-PEUA and $mPEG_3OOC(CH_2)_2COO$-g-PDHU

^{1}H NMR ($CDCl_3$/TMS, δ ppm): 5.08 (m, 1H, CH-OOC-mPEG normal unit and 1H, CH-OOC branched unit), 4.98 (m, 1H, CH-OOCmPEG abnormal unit), 4.91 (m, 1H, CHOOC abnormal unit), 4.28-4.23 (m, 2H, $C\underline{H}_2$-$OOC(CH_2)_2COO$), 4.18 (m, 1H, CH_2OOC normal unit), 4.15-4.12 and 4.08-4.04 (m, 2H, CH_2-$OOC(CH_2)_2COO$mPEG, 1H CH-$OOC(CH_2)_2COO$mPEG, 1H CH_2OOC normal unit and 2H, CH_2OOC branched unit), 3.84 (m, 1H, CHOH normal unit), 3.77 (m, 2H, $C\underline{H}_2CH_2OOC(CH_2)_2COO$, 3.62 (m, 6H, $CH_2O\underline{CH}_2\underline{CH}_2O$), 3.57 (m, 2H, $CH_3O\underline{CH}_2$), 3.40 (s, 3H, CH_3), 2.66 (m, 4H, $OOC(CH_2)_2COO$), 2.33 (m, 2H, CH_2COO) 1.61-1.29 (m, 14H, $(CH_2)_7$).

^{13}C NMR ($CDCl_3$, δ ppm): 174.3 (s, 1C, COO, abnormal unit), 174.2 (s, 1C, COO, normal unit), 172.6 and 172.4 (s, 1C, COO, branched unit), 172.4 (s, 1C, O-$CH_2\underline{C}OO$ grafted), 75.2 (d, 1C, $\underline{C}HOOC$ grafted abnormal unit), 75.1 (d, 1C, $\underline{C}HOOC$, abnormal unit), 72.3 (d, 1C, $\underline{C}HOOC$ grafted normal unit), 71.9 (t, 1C, $CH_3O\underline{C}H_2$ and CHOH end group), 71.2 (d, 1C, $\underline{C}H$-OOC, branched unit), 70.9 (t, 1C, $CH_2O\underline{C}H_2\underline{C}H_2O$), 69.9 (d, 1C, CHOH normal unit), 69.2 (t, 1C, $\underline{C}H_2OOC$ grafted normal unit), 69.1 (t, 1C, $\underline{C}H_2OOC(CH_2)_2COO$), 68.50 (t, 1C, $\underline{C}H_2$-CH-OH, normal unit), 66.8 (t, 1C, $\underline{C}H_2OH$ end group), 65.0 (t, 1C, $\underline{C}H_2OOC$ branched unit), 64.6 (t, 1C, $\underline{C}H_2OH$ abnormal unit), 64.0 (t, 1C, $\underline{C}H_2OOC(CH_2)_2COO$), 63.4 (t, 1C, $\underline{C}H_2OOC$ grafted abnormal unit), 59.1 (q, 1C, CH_3O), 34.5-33.9 (t, 1C, $\underline{C}H_2COO$), 25.6-24.6 (t, 7C, $(CH_2)_7$)

6.10 COPOLYMERS SELF-ASSEMBLY BEHAVIOR

6.10.1 Preparation and characterization of micelles by self-assembly

Block and graft copolymer micelles were prepared by the co-solvent evaporation nano-precipitation method. Samples of $mPEG_n$-*b*-$PDHU_m$, $mPEG_2OCH_2COO$-*g*-PDHU or $mPEG_3OOC(CH_2)_2COO$-*g*-PDHU were directly dissolved in HPLC grade THF (1 mL·5 mg^{-1}) and added dropwise to deionized water at room temperature with stirring (800 rpm). THF was gradually evaporated by bubbling argon during 60 min and the resulting micellar solution filtered through a membrane syringe filter (0.20 μm) and diluted with HPLC water to obtain

a 0.5 mg·mL^{-1} concentration. Average size, size distribution and Z-average of micelles were determined by Dynamic Light Scattering (DLS) at 20 ^{o}C.

The Stokes-Einstein equation was used by the instrument to calculate Z-average size. Size and morphology of the polymeric micelles were analysed by transmission electron microscopy (TEM) in drying and negative stain mode. Typically, a drop of 25-50 μg·ml^{-1} was dropped onto a cooper grid coated with carbon film and drying in air at room temperature and atmospheric pressure at least for 12 h was allowed. In the stain mode, a solution of 2 % phosphotungstic acid (PTA) was added to the droplet. Samples were imaged in bright field at tension of 80 Kv using an ITEM imaging software.

6.10.2 Critical micelle concentration (CMC) measurements

The critical micelle concentration of copolymers was determined by the pyrene 1:3 ratio.[11] Typically, stock mater solution of fluorescent probe (6.0·10^{-7} M) in THF were prepared and pre-calculated volumes were transferred to vials followed by argon flow evaporation. Different concentrations (from 0.4 mg·mL^{-1} to 1·10^{-8} mg·mL^{-1}) of block or graft copolymer solutions in water were added and the mixture stirred overnight protected from light. Samples were excited at 335 nm, and the emission spectra were recorded from 350 to 500 nm at room temperature. The intensity values of fluorescence emission, I_{372} and I_{382} at 372 nm and 382 nm, respectively, were used from the subsequent calculations. The CMC was determined from the plots of the I_{382}/I_{372} ratio versus the logarithm of the polymer concentration using the intersection of the linear regression lines as the CMC values. All solutions were filtered through filters of 0.20 μm pore size before DSL measurements that were made by triplicate.

6.11 REFERENCES

[1] Woodlett V. W., Use on *In situ* Reactions for Characterization of Alcohols and Glycols by Nuclear Magnetic Resonance, **1965**, *Anal. Chem.,* 37, 431-432.

[2] Ranganathan M., Balaram P., Trifluoroacetic anhydride. A convenient NMR solvent for carbohydrates, 270 MHz ^{1}H NMR studies of 2-acetamido-2-deoxyhexoses, **1980**, *Org. Magn. Reson.,* 13, 220-223.

[3] Rajan M., Cotiuga I., Ma Y., Picchioni F., Agarwal U. S., Determination of acid and hydroxyl end-groups in end-functionalized polystyrenes using ^{19}F NMR, **2003**, *e-Polymers*, 46, 1-7.

[4] Harris P. L.; Smith J. C., Addition of hydrogen bromide to triple and to double bonds. Undecynoic, undecenoic, and 10,11-epoxyundecoic acids, **1935**, *J. Chem. Soc.,* 1572-1576.

[5] K. Kakihuchi, T. Tsugaru, Y. Tobe, Y. Odaira, Acid-catalyzed rearrangement of [5.*n*.2]propella-ε-lactones, **1981**, *J. Org. Chem*., 46, 4204-4208.

[6] Vinczer P., Baán G., Novák L.; A novel stereocontrolled synthesis of (z,z)-3,13-octadecadien-1-yl acetate, the sex pheromone of synanthedon species, **1984**, *Tetrah. Lett.*, 25, 2701-2704.

[7] Vinczer P., Juvancz Z., Novak L., Szantay C.; *Acta Chim. Hung*., **1988**, 125 125,797-820.

[8] Presser A., Hüfner A.; Trimethylsilyldiazomethane – a mild and efficient reagent for the methylation of carboxylic acids and alcohols in natural products, **2004**, *Monatsh. Chem.*, 135, 1015-1022.

[9] Kühnel E., Laffan D. D. P, Lloyd-Jones G. C., del Campo T. M., Shepperson I. R., Slaughter J. L.; Mechanism of methyl esterification of carboxylic acid by trimethylsilyldiazomethane, **2007**, *Angew. Chem. Int. Ed.*, 46, 7075-7078.

[10] Bories-Azeau X., Mérian T., Weaver J. V. M., Armes S. P., van der Haak H. J. W., Synthesis of near-monodisperse acidic homopolymers and block copolímers from hydroxylated methacrylic copolímers using succínic anhydride under mild conditions, **2004**, *Macromolecules*, 37, 8903-8910.

[11] Aguiar J., Carpena P., Molina-Bolívar J.A., Ruiz C.C.; On the determination of the critical micelle concentration by the pyrene 1:3 ratio method*,* **2003**, *J. Colloid Interface Sci.,* 258, 116-122.

UNIVERSITAT ROVIRA I VIRGILI
10-UNDECENOIC ACID-BASED BIODEGRADABLE HYDROXY POLYESTERS: A PLATFORM FOR AMINOACID BIOCONJUGATES AND PEG-DERIVED AMPHIPHILIC COPOLYMERS
Carmen Valverde Sarmiento

Chapter 7

General conclusions

UNIVERSITAT ROVIRA I VIRGILI
10-UNDECENOIC ACID-BASED BIODEGRADABLE HYDROXY POLYESTERS: A PLATFORM FOR AMINOACID BIOCONJUGATES AND PEG-DERIVED AMPHIPHILIC COPOLYMERS
Carmen Valverde Sarmiento

7. GENERAL CONCLUSIONS

It has been demonstrated in this Thesis that it is possible preparing renewable functional polyesters from platform chemicals derived from vegetable oils, and developing environmentally friendly monomers and polymer synthesis strategies to keep moving toward more sustainable polymer chemistry.

The general conclusions of these research are summarized as follows:

- Biobased linear and branched hydroxyl functionalized aliphatic polyesters using AB (10,11-epoxyundecanoic acid, EUA) and AB_2 (10,11-dihydroxyundecanoic acid, DHU) monomers, were successfully synthesized *via* ROP or polycondensation with organic or enzymatic catalysts and thus avoiding metallic catalysts.

- The synthesized hydroxypolyesters (poly(10,11-epoxyundecanoic acid), PEUA) and poly(10,11-dihydroxyundecanoic acid), PDHU) and their block and grafted copolymers, were structurally characterized in detail, on the basis of model compounds, by ^{1}H, ^{13}C and ^{19}F NMR spectroscopy and ^{1}H-^{13}C heteronuclear bidimensional correlations.

- The enzymatic and hydrolytic degradation behaviour of hydroxy polyester PEUA, was studied and compared to that of poly(11-hydroxyundecanoate) and commercial poly(ε-caprolactone). The presence of hydrophilic pending groups together with the superior amorphous character in PEUA are determinant in its enhanced enzymatic and hydrolytic degradation rates.

- PEUA degradation proceeds through bulk erosion mechanism whereas commercial poly(ε-caprolactone) degraded through a surface erosion mechanism.

- The post-polymerization modification of the linear hydroxypolyester has been carried out with N-Boc protected, L-phenylalanine, L-serine and a cysteine derivative, as model for polymer bioconjugates

- Branched amphiphilic copolyesters by copolymerization with methoxypolyethylenglycols of different lengths (550 and 2000 $g \cdot mol^{-1}$) were successfully synthesized using CALB as catalyst. Incorporation of DHU units into a hyperbranched arrangement is lower than the feed in all cases.

- Grafting onto PEUA and PDHU hydroxypolyesters using carboxyl functionalized di and triethyleneglycols proceed with 50-60 % hydroxyl esterification. In linear PEUA grafting proceeds together with transesterification reactions leading to a branched structure.

- The self-assembly of these amphiphilic polyesters form well-defined micelles of 100-300 nm in aqueous solutions. Critical micellar concentration indicates that even at low concentration these copolymers self-assemble to lead multimolecular micelles and unimolecular micelles are scarcely observed.

Annex A

UNIVERSITAT ROVIRA I VIRGILI
10-UNDECENOIC ACID-BASED BIODEGRADABLE HYDROXY POLYESTERS: A PLATFORM FOR AMINOACID BIOCONJUGATES AND PEG-DERIVED AMPHIPHILIC COPOLYMERS
Carmen Valverde Sarmiento

SI.1 Synthesis of 10,11-epoxyundecanoic acid monomer (EUA)

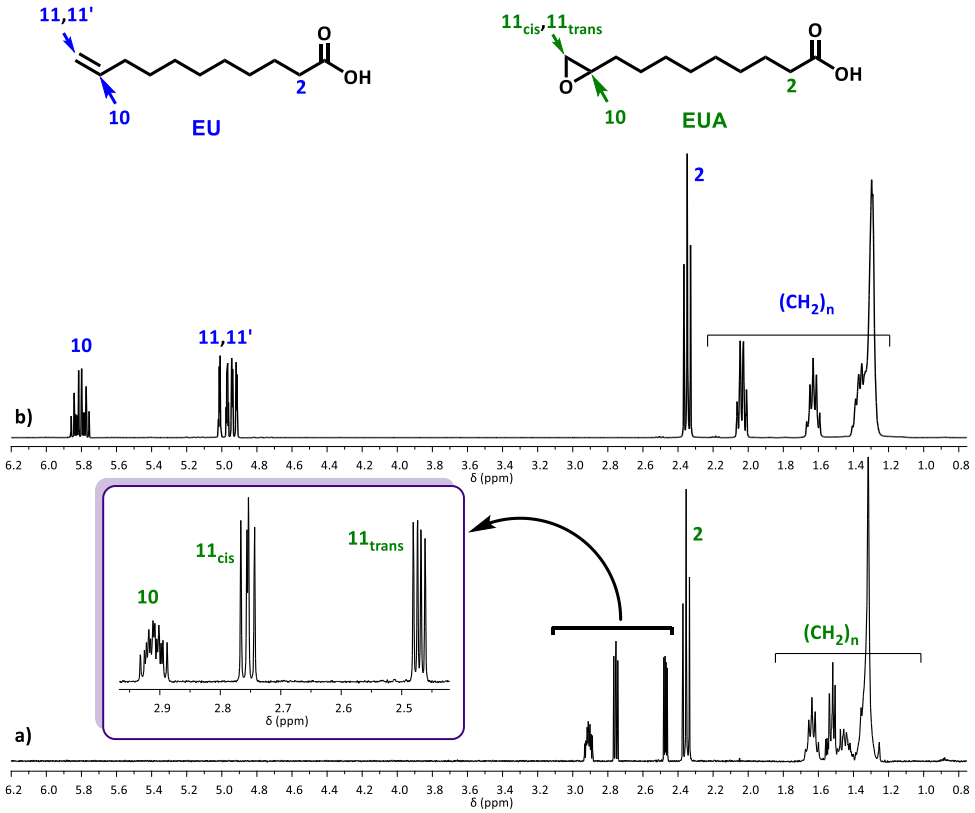

Figure SI.1 ^{1}H NMR spectra of a) EUA monomer and b) UA.

Annex A

SI.2 Synthesis of 2-hydroxyhexyl hexanoate (A) and 1-hydroxyhexan-2-yl hexanoate (B).

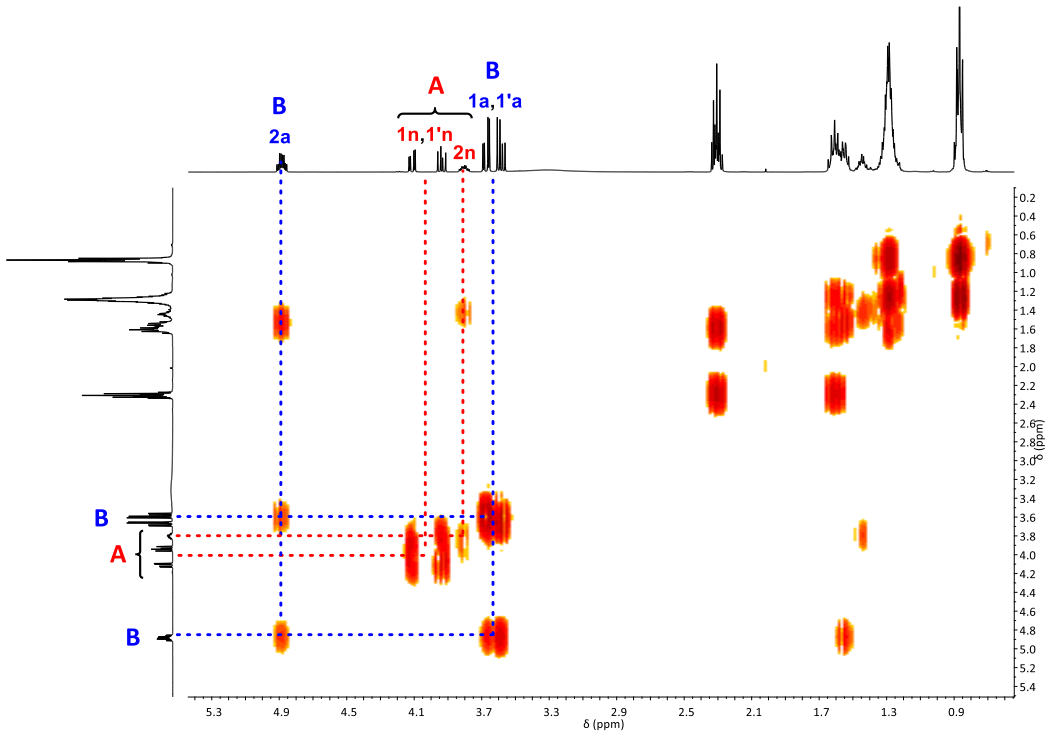

Figure SI.2 2D-^{1}H NMR gCOSY of A and B mixture.

SI.3 Synthesis of 2-(((2,2,2-trichloroacetyl)carbamoyl)oxy)hexyl hexanoate and 1-(((2,2,2-trichloroacetyl)carbamoyl)oxy)hexan-2-yl hexanoate

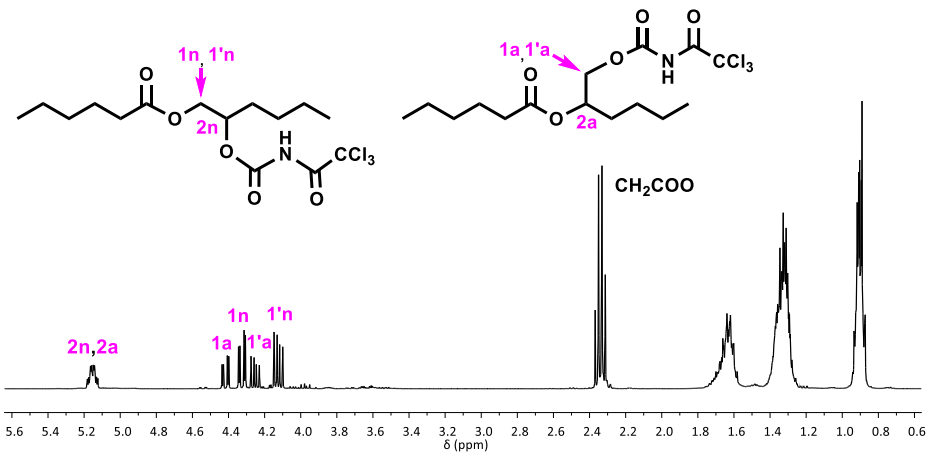

Figure SI.3 ^{1}H NMR spectrum of the mixture of A and B with TAI.

SI.4 Synthesis of 2-(trifluoroacetoxy)hexyl-1-hexanoate and 1-(trifluoroacetoxy)-hexan-2-yl hexanoate

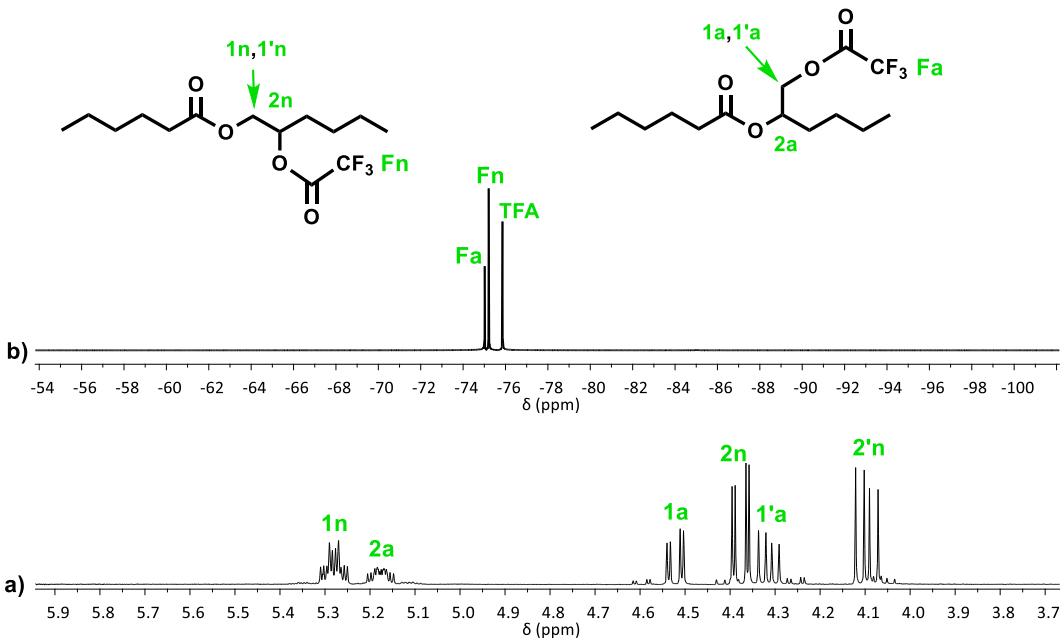

Figure SI.4 a) ^{1}H and b) ^{19}F NMR spectra of the mixture of A and B with TFAA.

In Table SI.1 are collected the chemical shifts of the hydroxyester moieties in A and B and their TAI and TFAA derivatives. For TAI derivatives upfield shielding of 0.6-0.7 for the methylene protons of primary alcohol and 1.20 ppm for the methine protons of secondary alcohols were observed. For TFAA derivatives upfield shielding of 0.7-0.8 for the methylene protons of primary alcohol and 1.33 ppm for the methine protons of secondary alcohols were observed. All these values are in good agreement to those reported in the literature.

Annex A

Table SI.1. ^{1}H and ^{19}F NMR chemical shifts of the hydroxyester moieties in A and B and their TAI and TFAA derivatives.

Position	δ ROH	δ ROCONHOCCl$_3$	Δ δ	δ ROOCCF$_3$	Δ δ	δ ^{19}F NMR
Compound A						
2_n	3.95	5.15	+ 1.20	5.28	+1.33	-75.21
1_n	4.15			4.38	+0.23	
$1'_n$	3.83			4.09	0.26	
Compound B						
2_a	4.92			5.18	+0.26	-75.02
1_a	3.71	4.42	+ 0.71	4.52	+0.81	
$1'_a$	3.62	4.25	+ 0.63	4.31	+0.69	

SI.5 Synthesis of PEUA

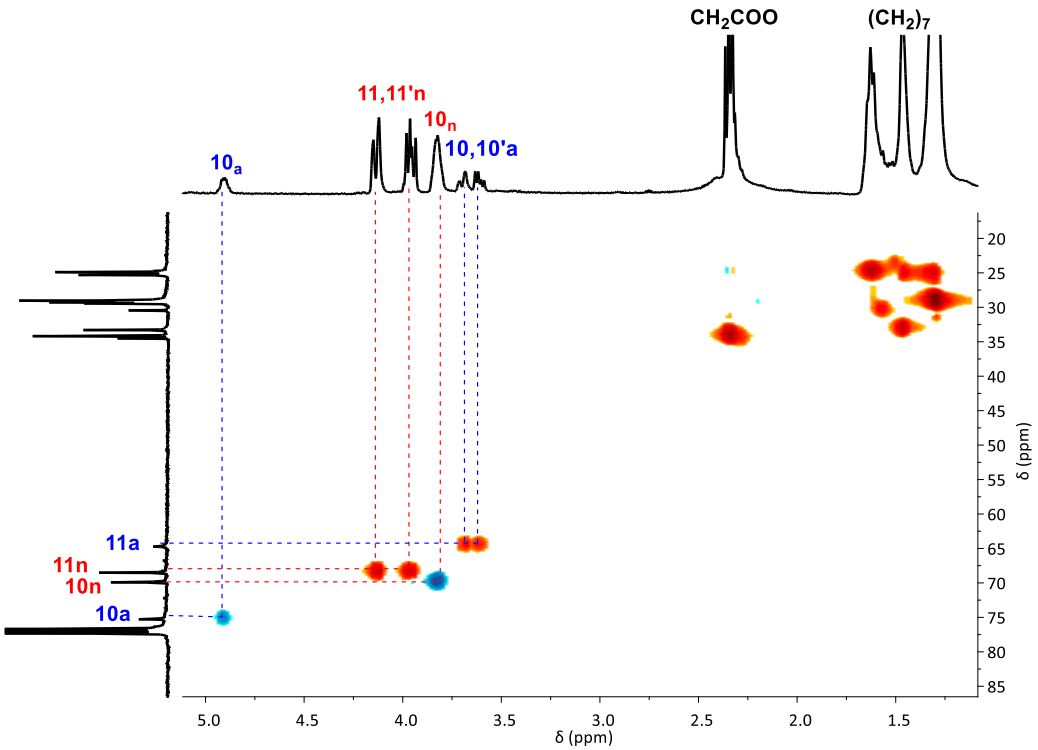

Figure SI.5 Heteronuclear single quantum correlation (HSQC) spectra of PEUA-1.

SI.6 PEUA hydroxyl content and molecular weight determination

Table SI.2 ^{1}H NMR chemical shifts of CH_2 and CH hydroxyester units in PEUA-2 and their trifluoroacetyl derivative.

Position	δ R-OH	δ R-OOC-CF_3	Δ δ
Normal units			
10_n	3.81	5.26	+ 1.45
11_n	4.13	4.36	+ 0.23
$11'_n$	3.96	4.06	+ 0.10
Abnormal units			
10_a	4.90	5.15	+ 0.25
11_a	3.70	4.51	+ 0.81
$11'_a$	3.60	4.29	+ 0.69
Branched units			
10_b	5.08	5.08	0.00
11_b	4.22	4.22	0.00
$11'_b$	4.03	4.03	0.00
1,2-Diol end groups			
10_e	3.62	5.34	+ 1.72
11_e	3.67	4.59	+ 0.92
$11'_e$	3.42	4.40	+ 0.98

Annex A

SI.7 Synthesis of cysteine derivatives

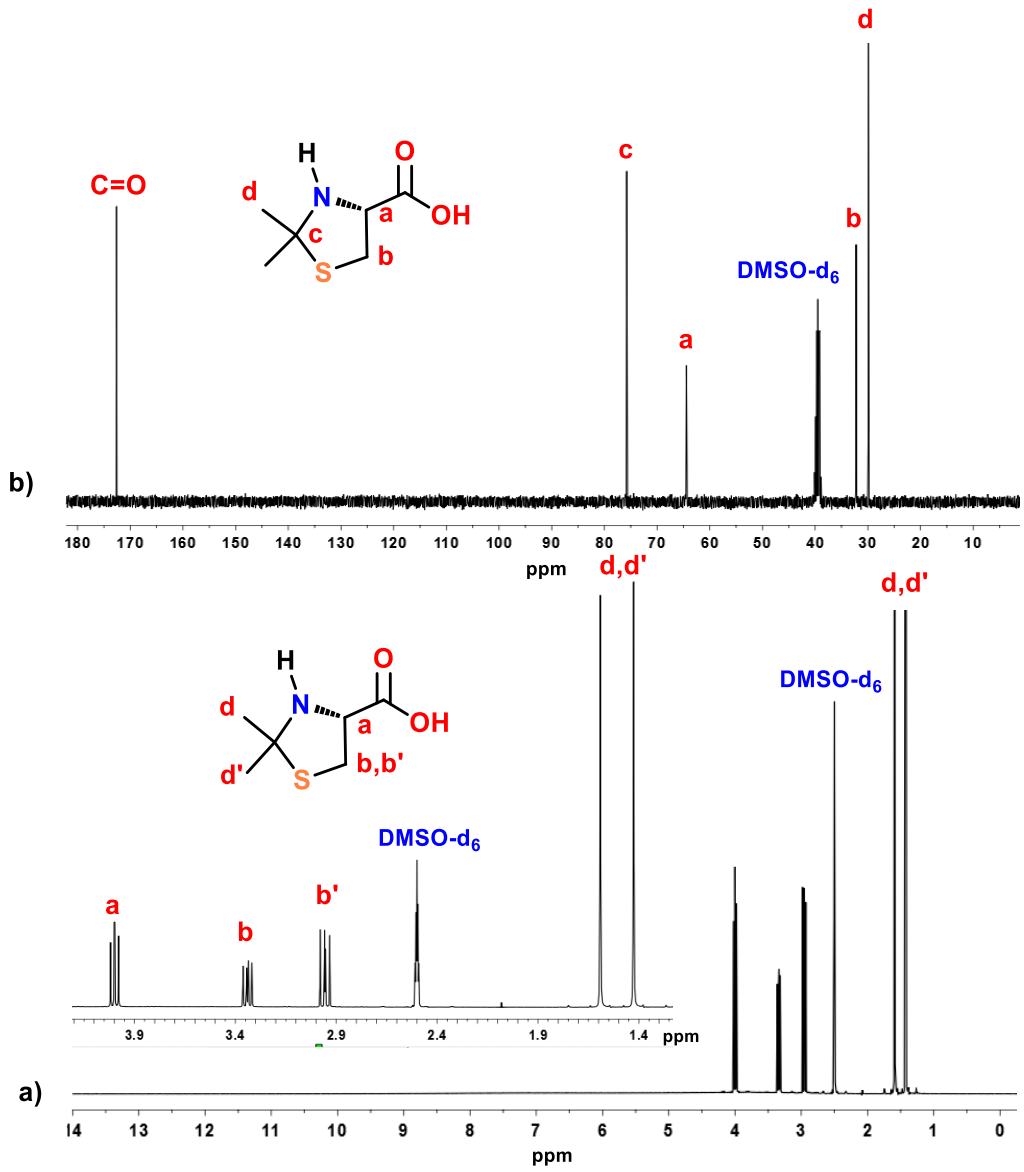

Figure SI.6 a) ^{1}H and b) ^{13}C NMR spectra of 2,2-dimethylthiazolidin-4-carboxylic acid (DMT) in DMSO-d_6.

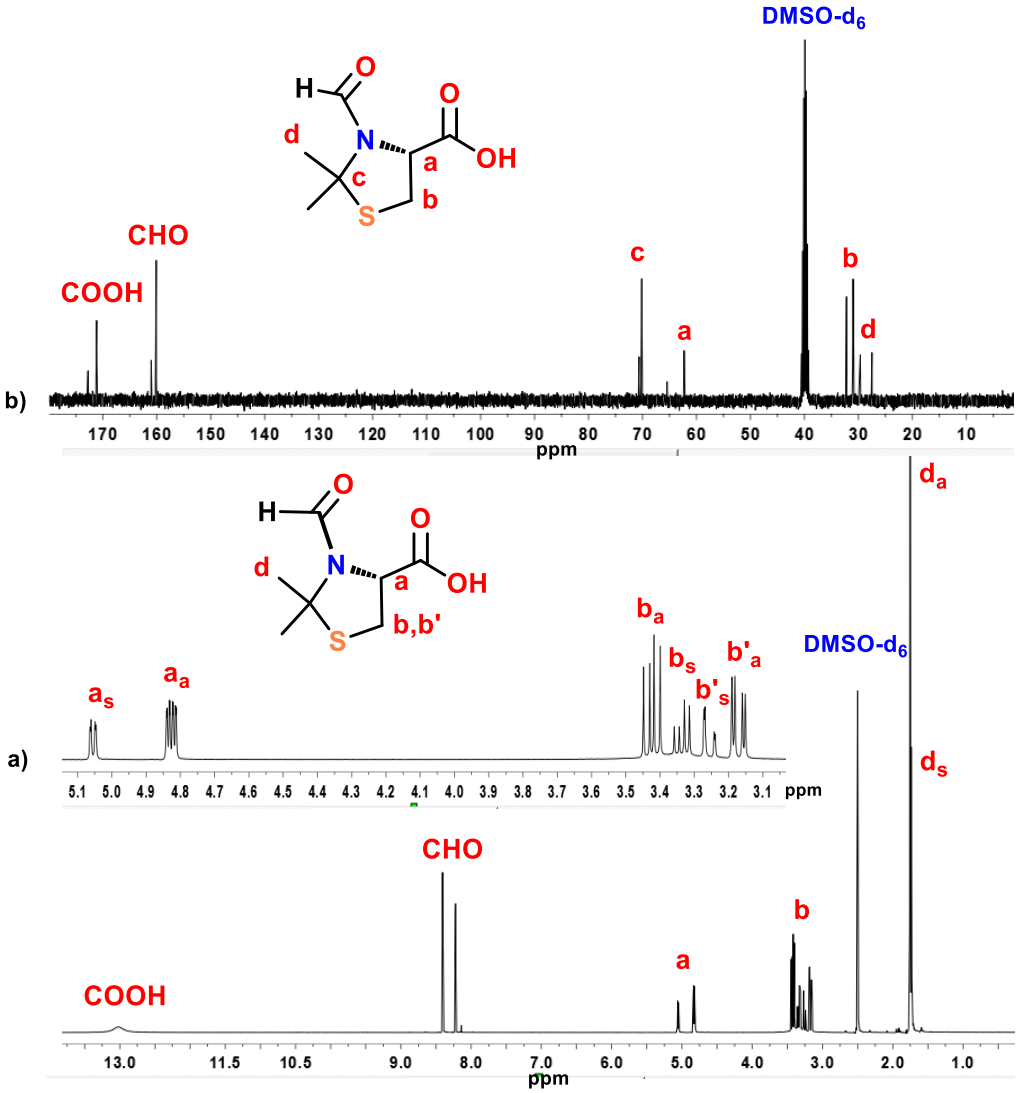

Figure SI.7 a) ^{1}H and b) ^{13}C NMR spectra of 2,2-dimethylthiazolidin3-(N-formyl)-4-carboxylic acid (DMFT) in DMSO-d_6.

UNIVERSITAT ROVIRA I VIRGILI
10-UNDECENOIC ACID-BASED BIODEGRADABLE HYDROXY POLYESTERS: A PLATFORM FOR AMINOACID BIOCONJUGATES AND PEG-DERIVED AMPHIPHILIC COPOLYMERS
Carmen Valverde Sarmiento

Annex B

UNIVERSITAT ROVIRA I VIRGILI
10-UNDECENOIC ACID-BASED BIODEGRADABLE HYDROXY POLYESTERS: A PLATFORM FOR AMINOACID BIOCONJUGATES AND PEG-DERIVED AMPHIPHILIC COPOLYMERS
Carmen Valverde Sarmiento

SI.1 Synthesis of PEUA

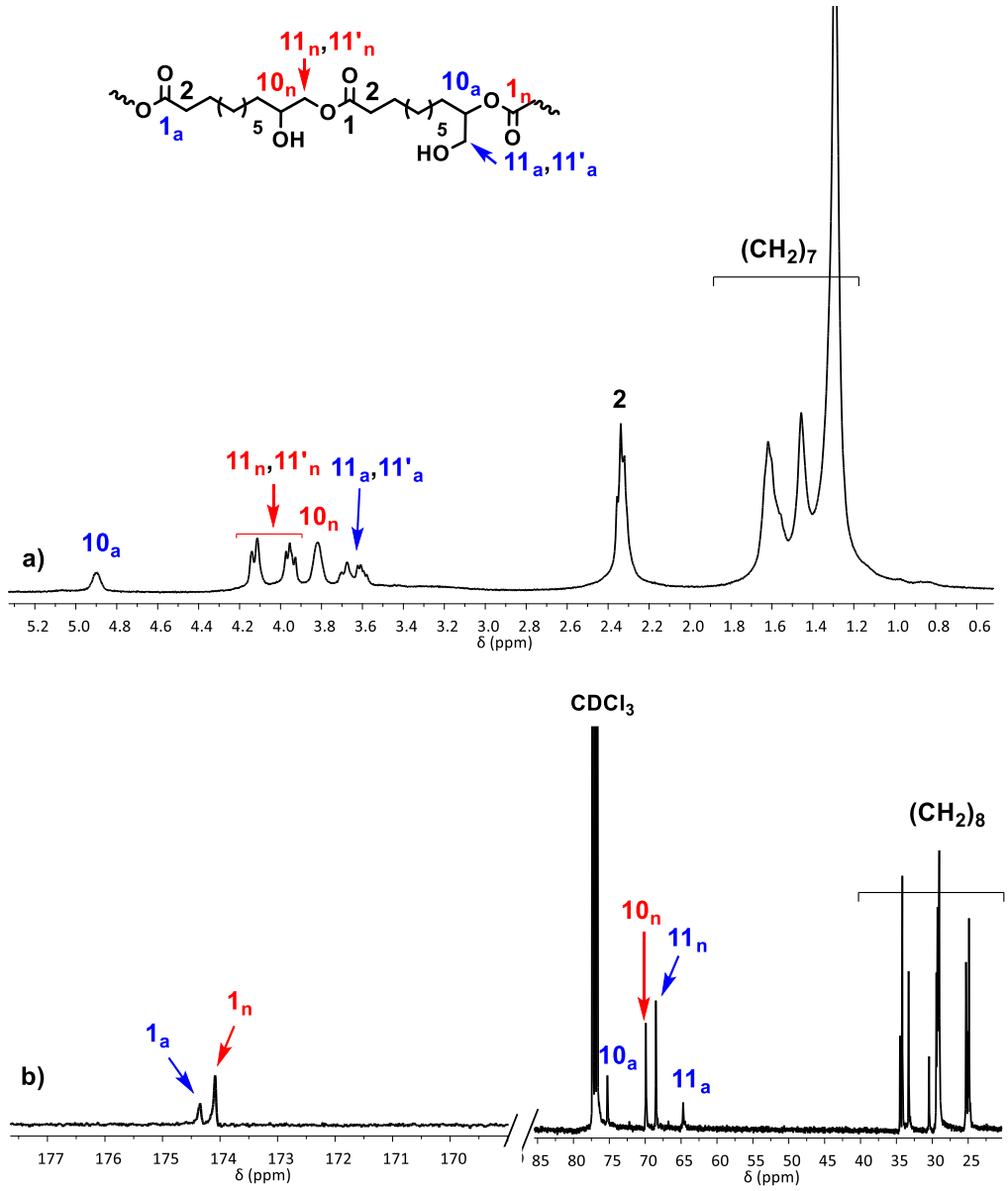

Figure SI.1 a) ^{1}H NMR and b) ^{13}C NMR spectra of PEUA.

Annex B

SI.2 Synthesis of PHU

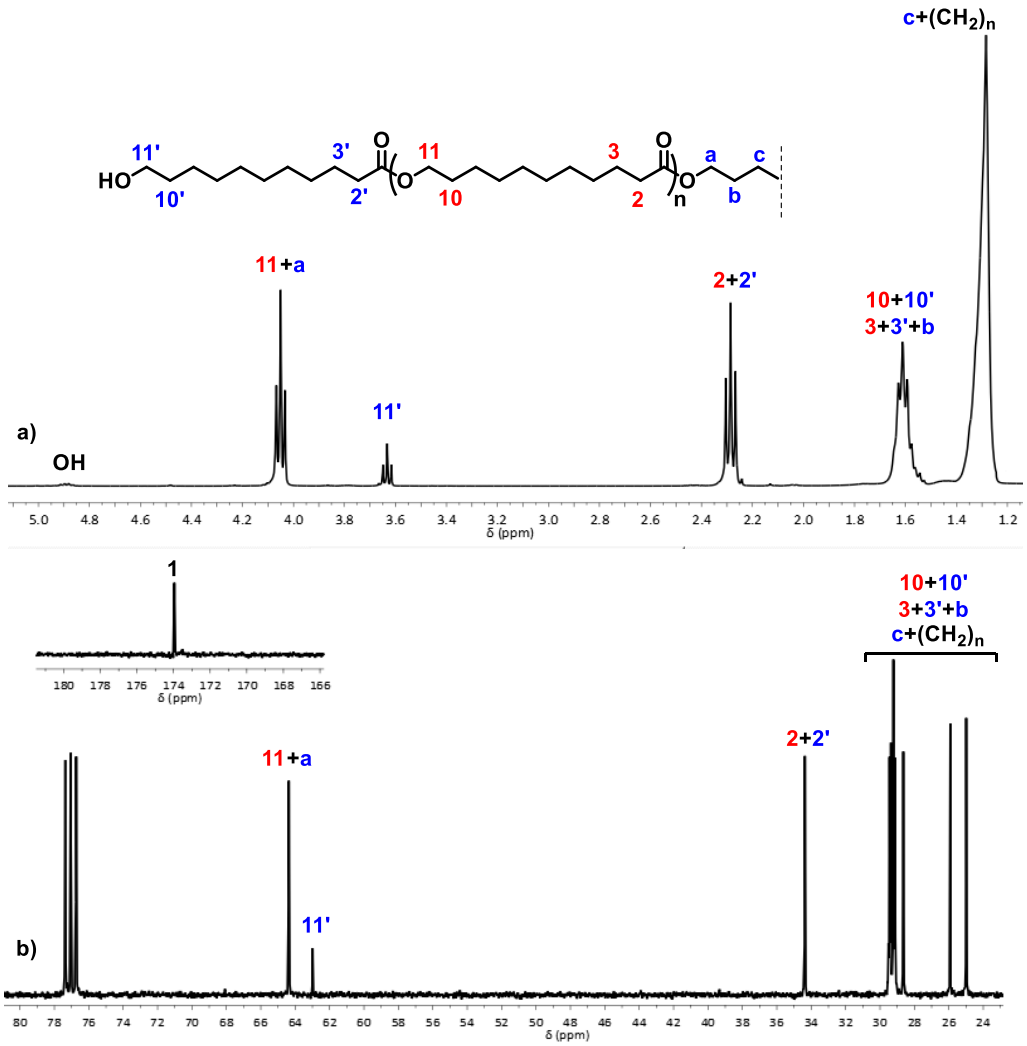

Figure SI.2 a) ^{1}H NMR and b) ^{13}CNMR spectra of PHU.

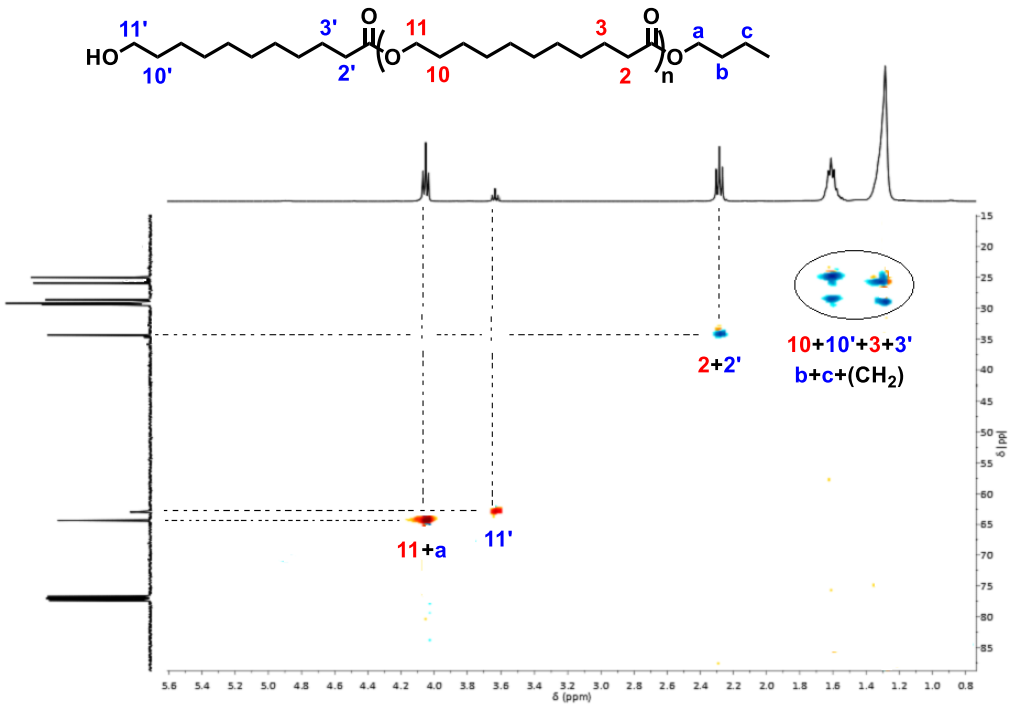

Figure SI.3 Heteronuclear single quantum correlation (HSQC) spectra of PHU.

UNIVERSITAT ROVIRA I VIRGILI
10-UNDECENOIC ACID-BASED BIODEGRADABLE HYDROXY POLYESTERS: A PLATFORM FOR AMINOACID BIOCONJUGATES AND PEG-DERIVED AMPHIPHILIC COPOLYMERS
Carmen Valverde Sarmiento

Annex C

UNIVERSITAT ROVIRA I VIRGILI
10-UNDECENOIC ACID-BASED BIODEGRADABLE HYDROXY POLYESTERS: A PLATFORM FOR AMINOACID BIOCONJUGATES AND PEG-DERIVED AMPHIPHILIC COPOLYMERS
Carmen Valverde Sarmiento

SI.1 Synthesis of 2-hydroxyhexyl hexanoate (A), 1-hydroxyhexan-2-yl hexanoate (B) and hexane-1,2-diyl dihexanoate (C)

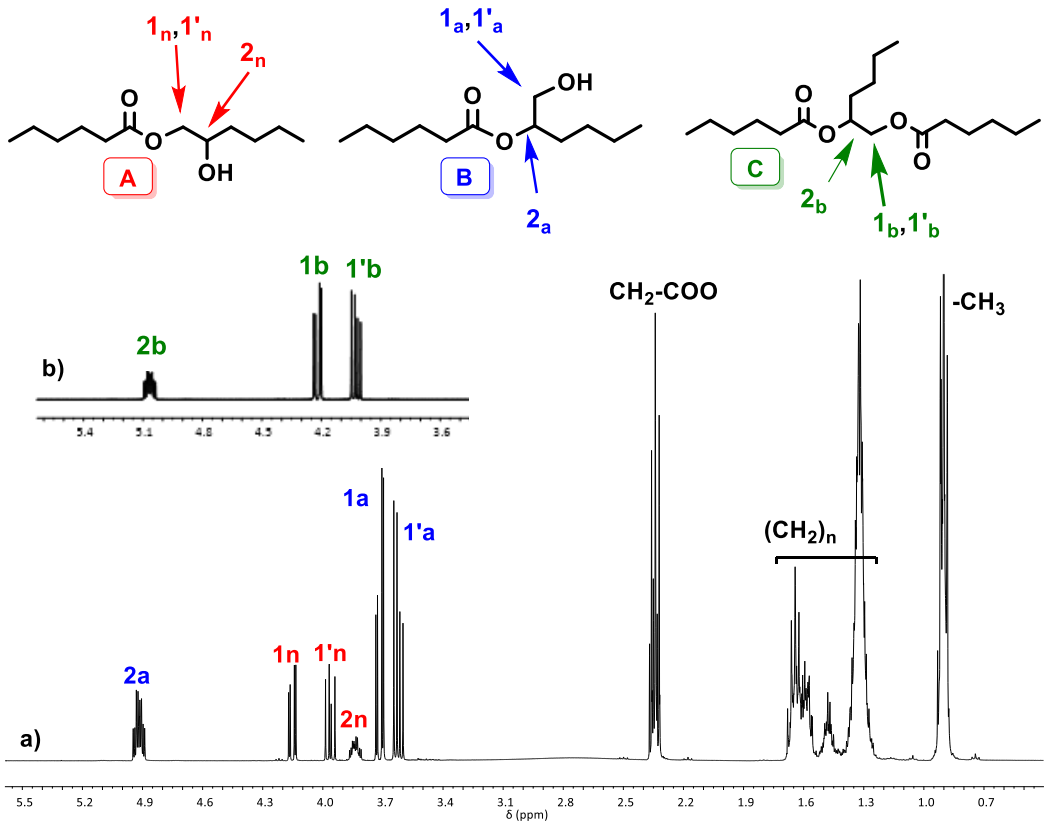

Figure SI.1 ^{1}H NMR spectra of a) A, B mixture and b) C**.**

Annex C

SI.2 Synthesis of 2-(trifluoroacetoxy)hexyl-1-hexanoate, 1-(trifluoroacetoxy)-hexan-2-yl hexanoate and hexane-1,2-diyl bis(2,2,2,)-trifluoroacetate

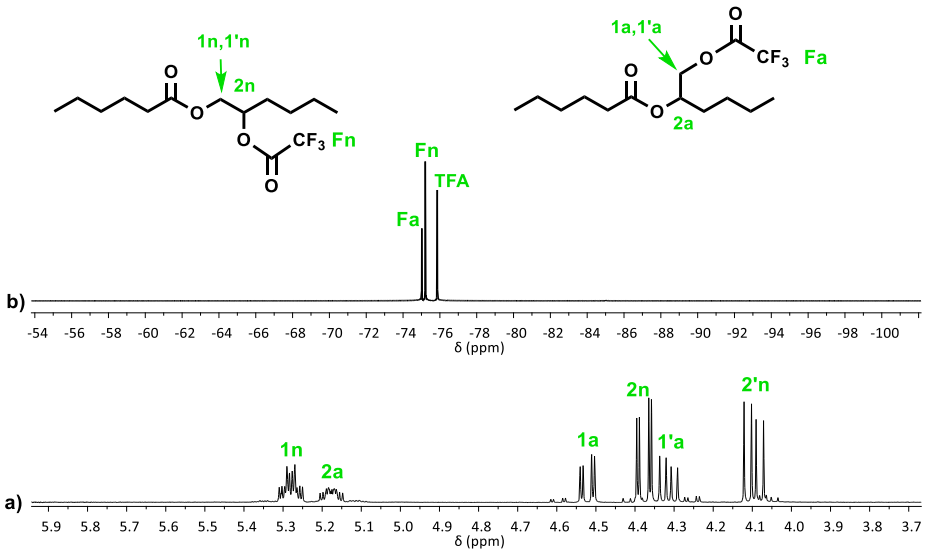

Figure SI.2 a) ^{1}H and b) ^{19}F NMR spectra of A and B trifluoroacetates with the corresponding assignments.

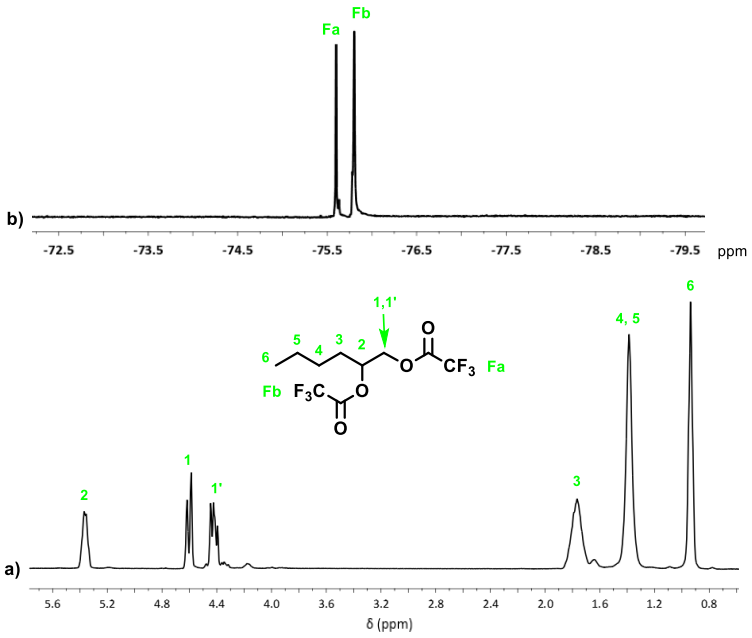

Figure SI.3 a) ^{1}H and b) ^{19}F NMR spectra of hexane-1,2-diyl bis(2,2,2,)-trifluoroacetate with the corresponding assignments.

SI.3 Synthesis of PDHU

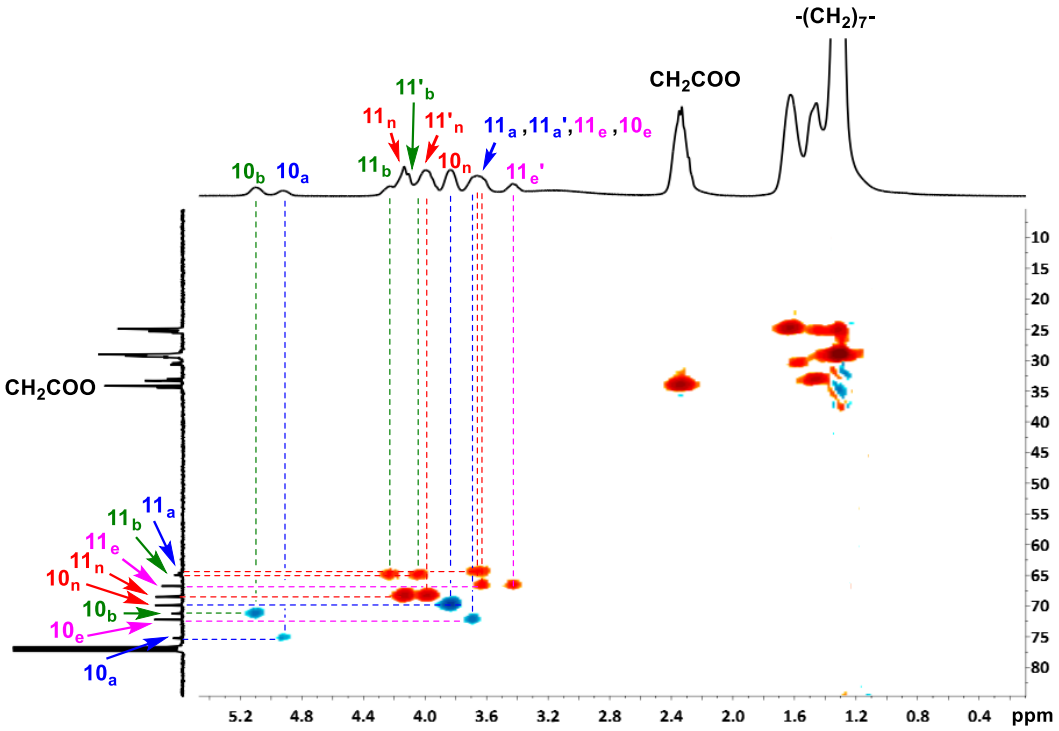

Figure SI.4 Heteronuclear single quantum correlation (HSQC) spectra of PDHU recorded in $CDCl_3$.

Annex C

SI.4 PDHU hydroxyl content and molecular weight determination

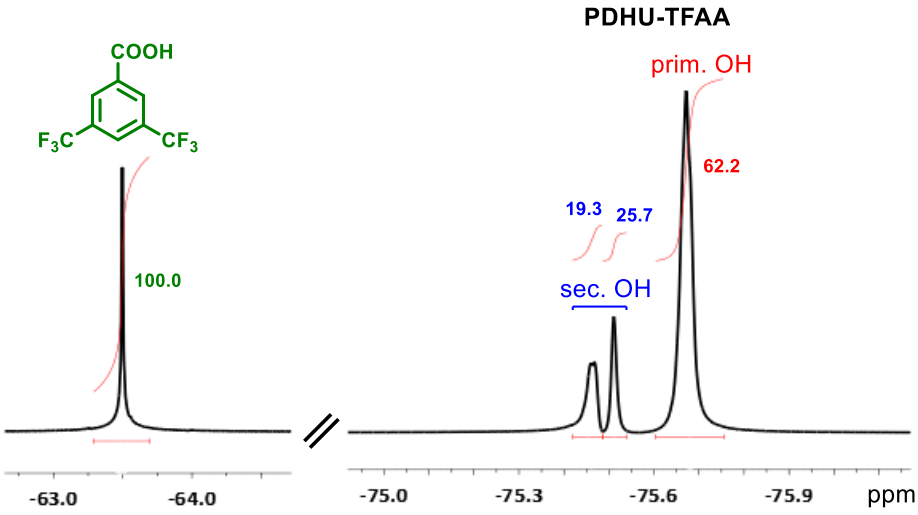

Figure SI.5 ^{19}F NMR spectrum of the PDHU-1-TFA and 3,5-bis(trifluoromethyl)benzoic acid mixture.

Table SI.1 ^{1}H NMR chemical shifts in ppm, of CH_2 and CH hydroxyester units in PDHU and PDHU-TFA.

Position	δ R-OH	δ R-OOC-CF_3	Δ δ
Normal units			
10_n	3.81	5.26	+ 1.45
11_n	4.13	4.36	+ 0.23
$11'_n$	3.96	4.06	+ 0.10
Abnormal units			
10_a	4.90	5.15	+ 0.25
11_a	3.70	4.51	+ 0.81
$11'_a$	3.60	4.29	+ 0.69
Branched units			
10_b	5.08	5.08	0.00
11_b	4.22	4.22	0.00
$11'_b$	4.03	4.03	0.00
1,2-Diol end groups			
10_e	3.62	5.34	+ 1.72
11_e	3.67	4.59	+ 0.92
$11'_e$	3.42	4.40	+ 0.98

SI.5 Structural characterization of mPEG-b-PDHU copolymers

^{1}H and ^{13}C NMR spectra of copolymers and the corresponding peak assignments made on the basis of the starting reagents and reported data are shown in Figures SI.6, SI.7, SI.8 and SI.9.[1]

^{1}H NMR spectra of $mPEG_{12}$-*b*-$PDHU_9$, $mPEG_{12}$-*b*-$PDHU_{15}$, $mPEG_{45}$-*b*-$PDHU_9$ and $mPEG_{45}$-*b*-$PDHU_{15}$ (Figures SI.6 and SI.8) show the same patterns where signals of branched PDHU block and starting $mPEG_n$ moieties are clearly identified. The actual comonomer composition (Table 5.3 in Chapter 5) was estimated from the relative signals intensities of α-methylene to the ester at 2.35 ppm in PDHU moiety and methyl at 3.38 ppm in $mPEG_n$ moiety. The branched structure of grown PDHU was confirmed by the methine signals at 5.07, 4.90 and 3.82 ppm. It must be pointed out that non-reacted mPEG-OH cannot be distinguished by ^{1}H NMR because signals appear overlapping and only ^{13}C NMR allow confirm that it has been completely removed during the work-up. Thus, in ^{13}C NMR spectra (Figures SI.7 and SI.9) the absence of signal of CH_2OH in mPEG-OH at 61.3 ppm, and the presence of the signal of CH_2-OOC in mPEG-*b*-PDHU at 63.3 ppm is the main feature that confirm the copolymer structure. The carbonyl of this block-linking ester bond can be also observed at 173.6 ppm. Moreover, characteristics C signals of both moieties appear well resolved at defined chemical shift. The methine and methylene region of the ^{13}C NMR spectra of m-PEG_{12}-b-$PDHU_9$ and m-PEG_{12}-b-$PDHU_{15}$ also show some extra small intensity signals (marked with an asterisk in figure SI.7) which can be attributed to the unit directly linked to the m-PEG moiety, as they are almost not detected in the block copolymers with major mPEG content (m-PEG_{45}-*b*-$PDHU_9$ and m-PEG_{45}-*b*-$PDHU_{15}$).

Annex C

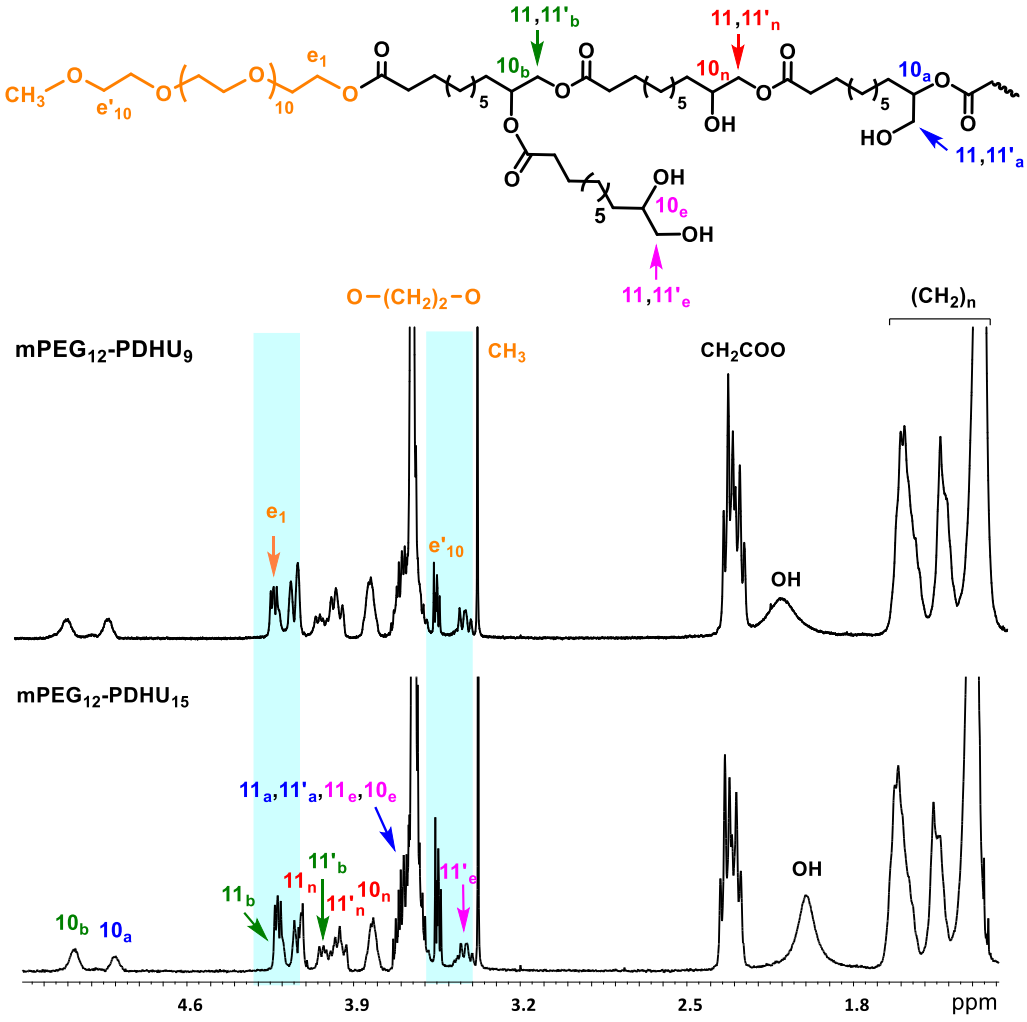

Figure SI.6 ^{1}H NMR spectra recorded in $CDCl_3$ of mPEG$_{12}$-*b*-PDHU$_9$ and mPEG$_{12}$-*b*-PDHU$_{15}$ block copolymers with the corresponding assignments.

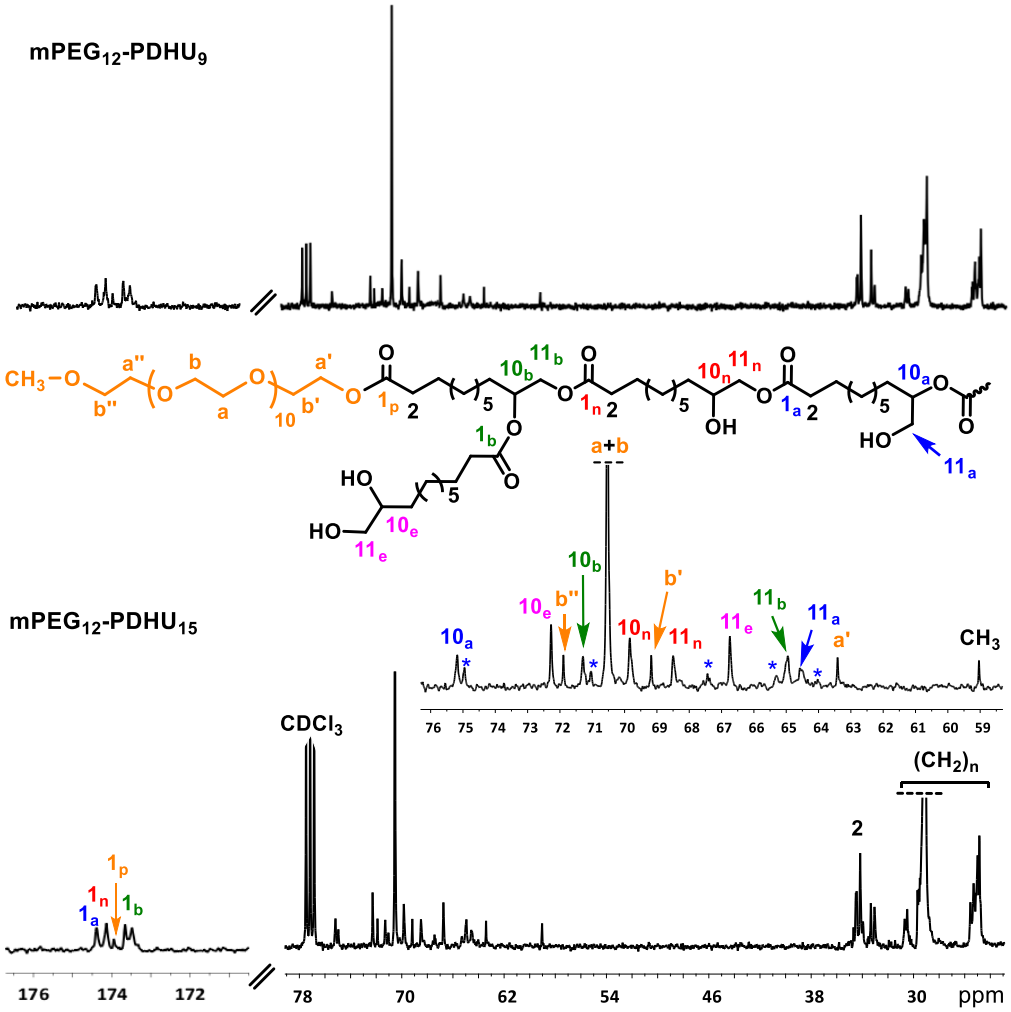

Figure SI.7 ^{13}C NMR spectra recorded in $CDCl_3$ of $mPEG_{12}$-*b*-$PDHU_9$ and $mPEG_{12}$-*b*-$PDHU_{15}$ block copolymers with the corresponding assignments.

Annex C

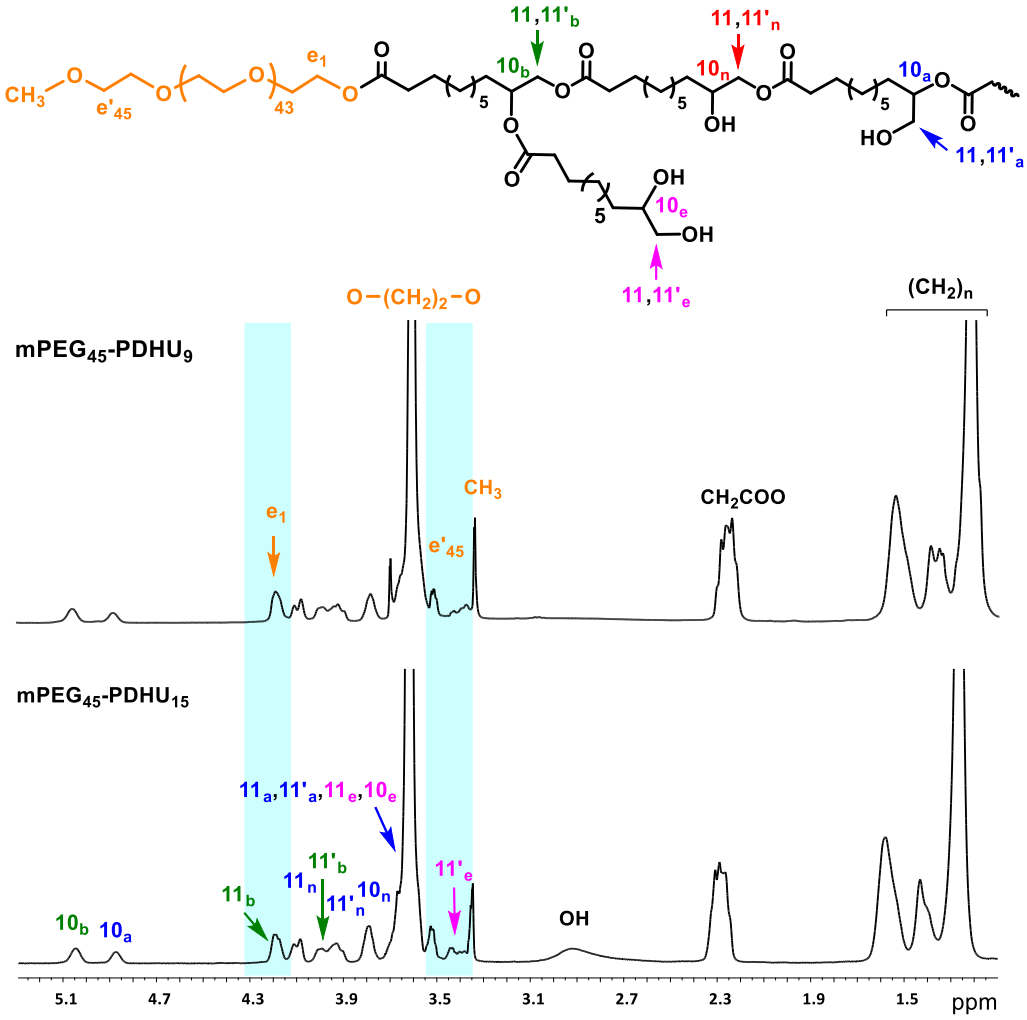

Figure SI.8 ^{1}H NMR spectra recorded in $CDCl_3$ of mPEG$_{45}$-*b*-PDHU$_9$ and mPEG$_{45}$-*b*-PDHU$_{15}$ block copolymers with the corresponding assignments.

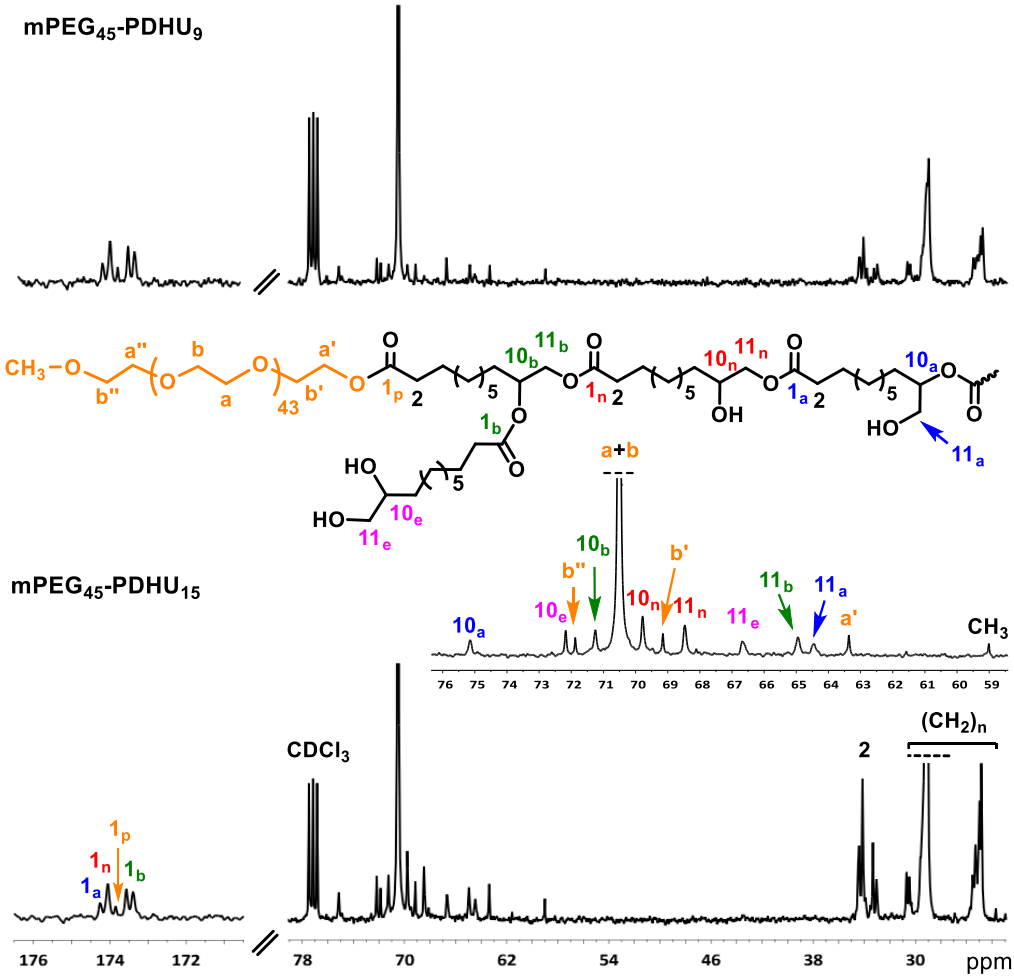

Figure SI.9 ^{13}C NMR spectra recorded in $CDCl_3$ of mPEG$_{45}$-*b*-PDHU$_9$ and mPEG$_{45}$-*b*-PDHU$_{15}$ block copolymers with the corresponding assignments.

Annex C

SI.6 Structural characterization of PDHU and PEUA grafted with $mPEG_2OCH_2COOH$ and $mPEG_3OOC(CH_2)_2COOH$

^1H and ^{13}C NMR spectra and the corresponding peak assignments made on the basis of the chemical shifts of parent polymers the starting reagents and model compounds, heteronuclear single quantum correlation (HSQC) spectra and data reported in the literature are shown in Figures SI.10, SI.11, SI.12, SI.13, SI.14 and SI.15.[1]

^1H NMR of polymers grafted with $mPEG_2OCH_2COOH$ (Figures SI.10b and SI.12b) were undertaken taking into account that alkoxyacetyl ester units produce a higher up-shielding than regular aliphatic ester units in the repeating PEUA and PDHU units (Figures SI.10a and SI.12a). This was inferred by comparing the spectra of model compounds A, B and C (Figure SI.1) compounds with the mixture of 1,2-decanediol 2-(2-(2-methoxyethoxy)ethoxy) acetate esters (Figure SI.17). In this way the unequivocal assignment of methine signals in repeating units at 5.15 ppm (normal unit grafted with mPEG), 5.05 (branched unit), 4.95 (abnormal unit) and 3.82 (normal unit) was made. From these signals the percentage of the different units were estimated (Table 5.4 in Chapter 5). The main features of the grafted moiety are the methylene of the O-CH_2COO linking unit at 4.04 ppm, the polyoxyethylene chain at 3.69-3.55 ppm and the methyl end group at 3.35 ppm. This last signal was used to estimate the grafting degree by comparing to that of the α-CH_2COO in the repeating unit (Table 5.4 in the Chapter 5). ^{13}C NMR spectra signals (Figures SI.11b and SI.13b) were undertaken using the same methodology with the aid of heteronuclear single quantum correlation (HSQC) spectra (Figures SI.14 and SI.15). The main feature is the carbonyl of the grafted moiety that appears at 170.6, 170.4 and 170.2 ppm due to the different chemical shifts of signals arising from grafting onto normal, abnormal and diol end group units. This difference can be also observed on the methine and methylene signals of the different repeating units.

^1H NMR of polymers grafted with $mPEG_3OOC(CH_2)_2COOH$ (Figures SI.10c and SI.12c) were undertaken in a similar way as above, in this case methine in the grafted normal unit

appears at lower chemical shift and overlapped with the methine corresponding to the branched units at 5.08 ppm. The grafted abnormal unit appears at 4.98 ppm and the non-grafted abnormal and normal units appear respectively at 4.91 and 3.84 ppm and from their relative intensity the percentage of the different units could be estimated (Table 5.4 in Chapter 5). Signals of the grafted moiety appear at 4.28 and 3.77-3.57 for the polyoxyethylene protons, 3.40 for the methoxy end group and 2.66 for succinic methylene units. From the intensity of these last two signals, the percentage of grafting was estimated by comparing to that of the α-CH_2COO in the repeating unit at 2.33 ppm (Table 5.4 in Chapter 5). In ^{13}C NMR (Figures SI.11c and SI.13c) the most significant signals are those of the grafted units, the carbonyls that appear at 172.4 ppm and the methine and methylene of the normal, abnormal and end diol units appear at different chemical shifts and that could be distinguished from the signals corresponding to the unmodified polymer.

The most relevant structural feature is that for both grafting reagents, $mPEG_2OCH_2COOH$ and $mPEG_3OOC(CH_2)_2COOH$, the spectra obtained from grafting PEUA and PDHU contain identical signals with differences in their relative intensity which reveal a branched structure for all polymers.

Annex C

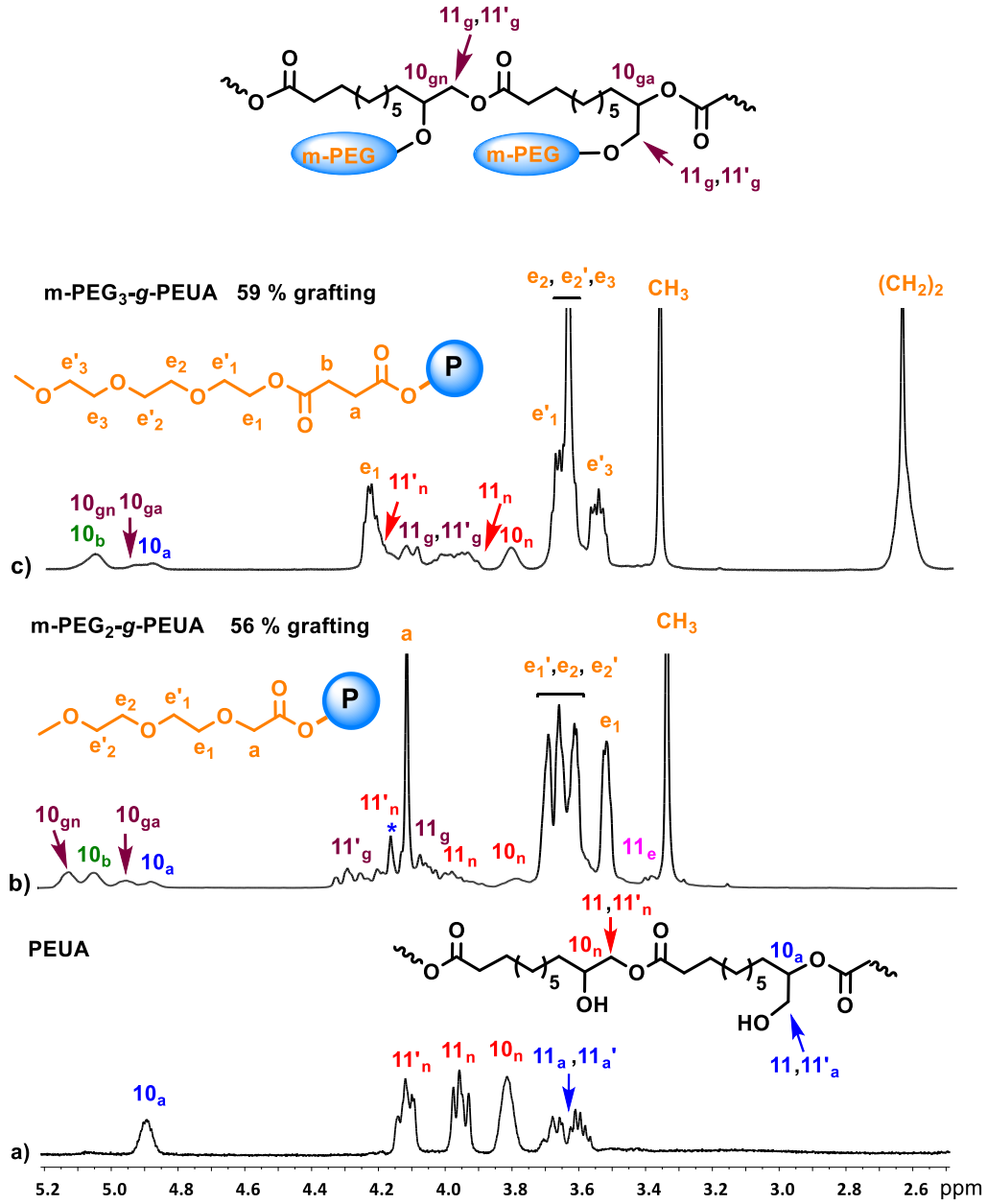

Figure SI.10 ^{1}H NMR spectra recorded in $CDCl_3$ of PEUA grafted with $mPEG_2OCH_2COOH$ and $mPEG_3OOC(CH_2)_2COOH$ with the corresponding assignments.

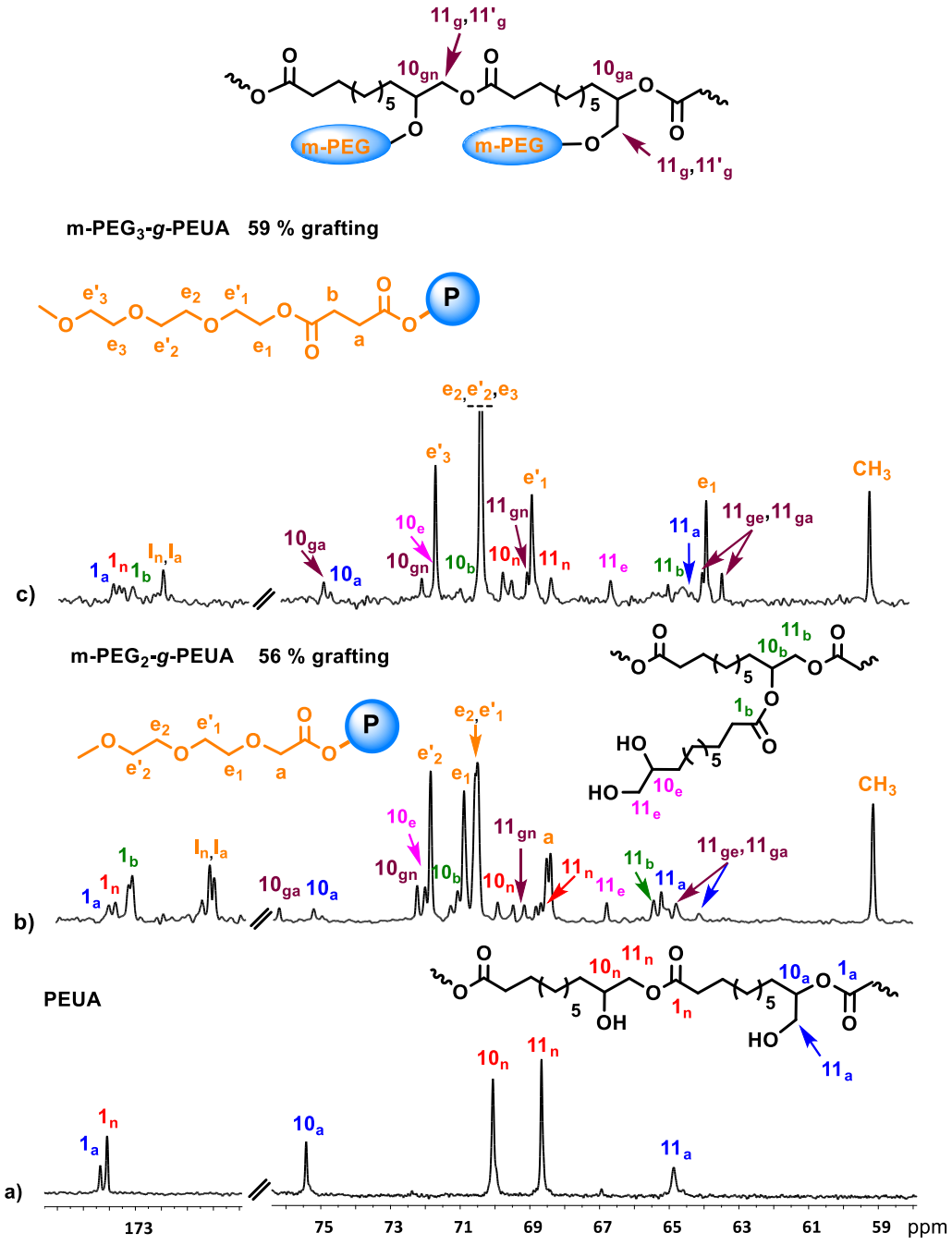

Figure SI.11 ^{13}C NMR spectra recorded in $CDCl_3$ of PEUA grafted with $mPEG_2OCH_2COOH$ and $mPEG_3OOC(CH_2)_2COOH$ with the corresponding assignments.

Annex C

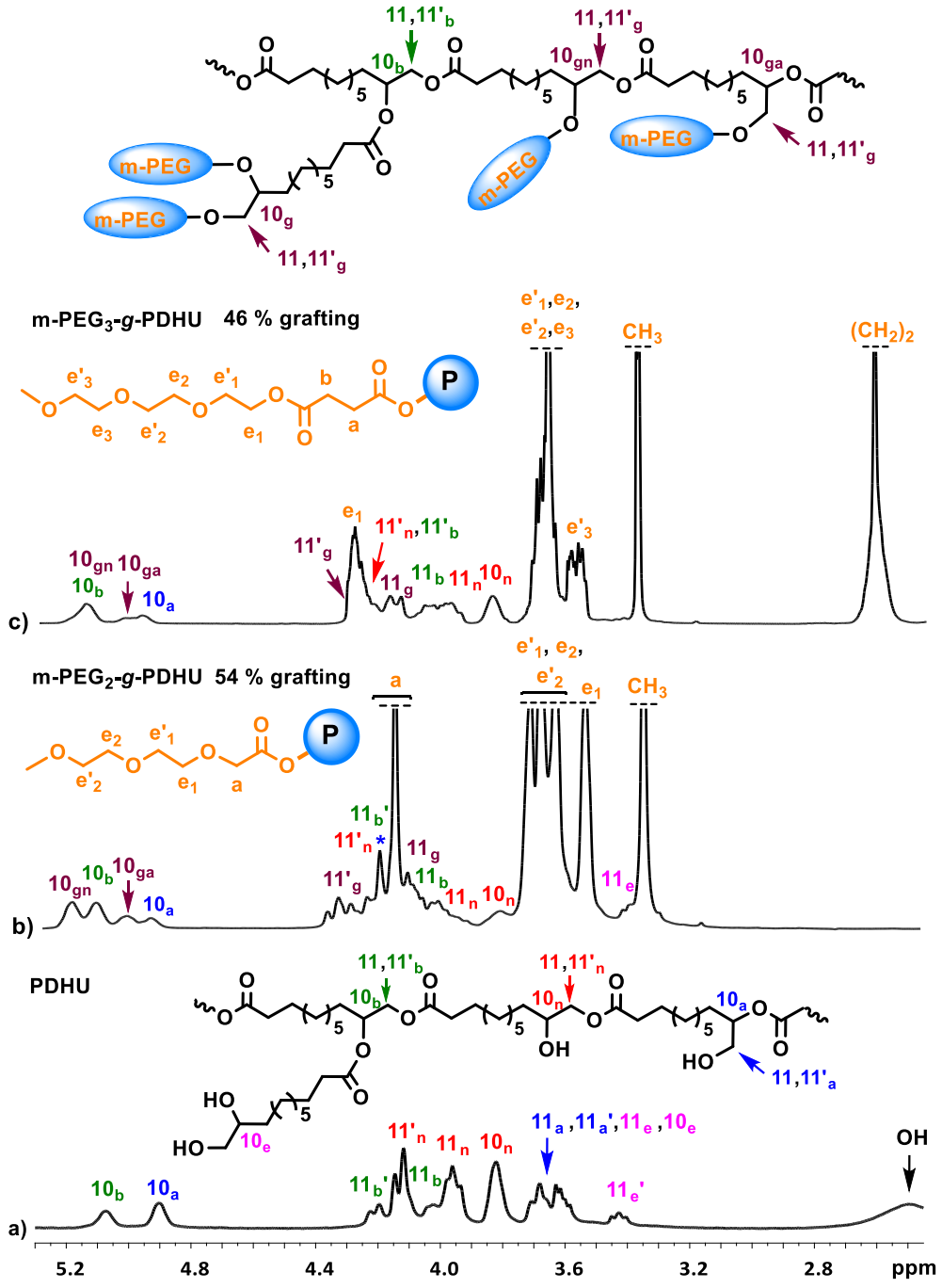

Figure SI.12 ^{1}H NMR spectra recorded in $CDCl_3$ of PDHU grafted with $mPEG_2OCH_2COOH$ and $mPEG_3OOC(CH_2)_2COOH$ with the corresponding assignments.

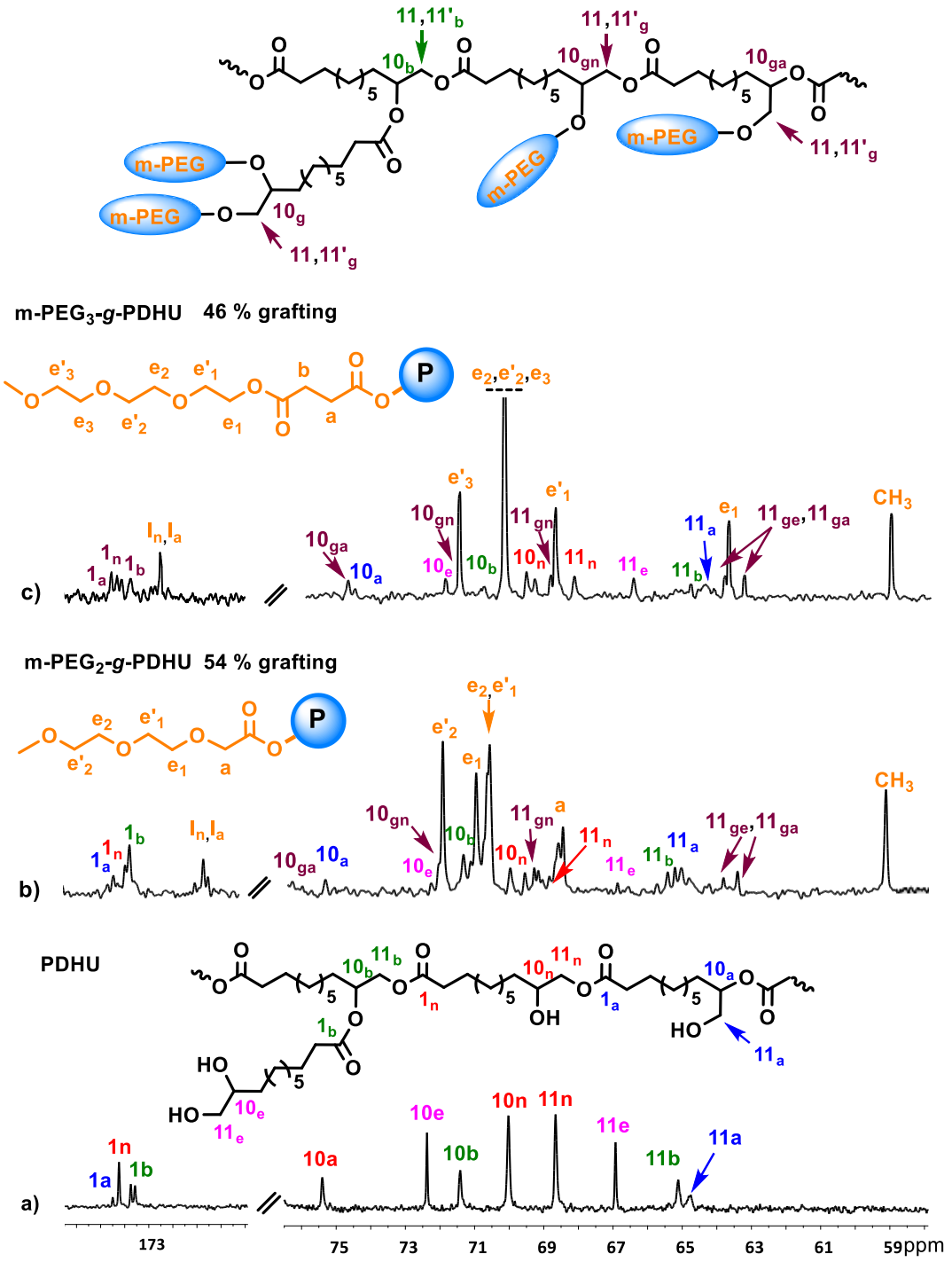

Figure SI.13 ^{13}C NMR spectra recorded in $CDCl_3$ of PDHU grafted with $mPEG_2OCH_2COOH$ and $mPEG_3OOC(CH_2)_2COOH$ with the corresponding assignments.

Annex C

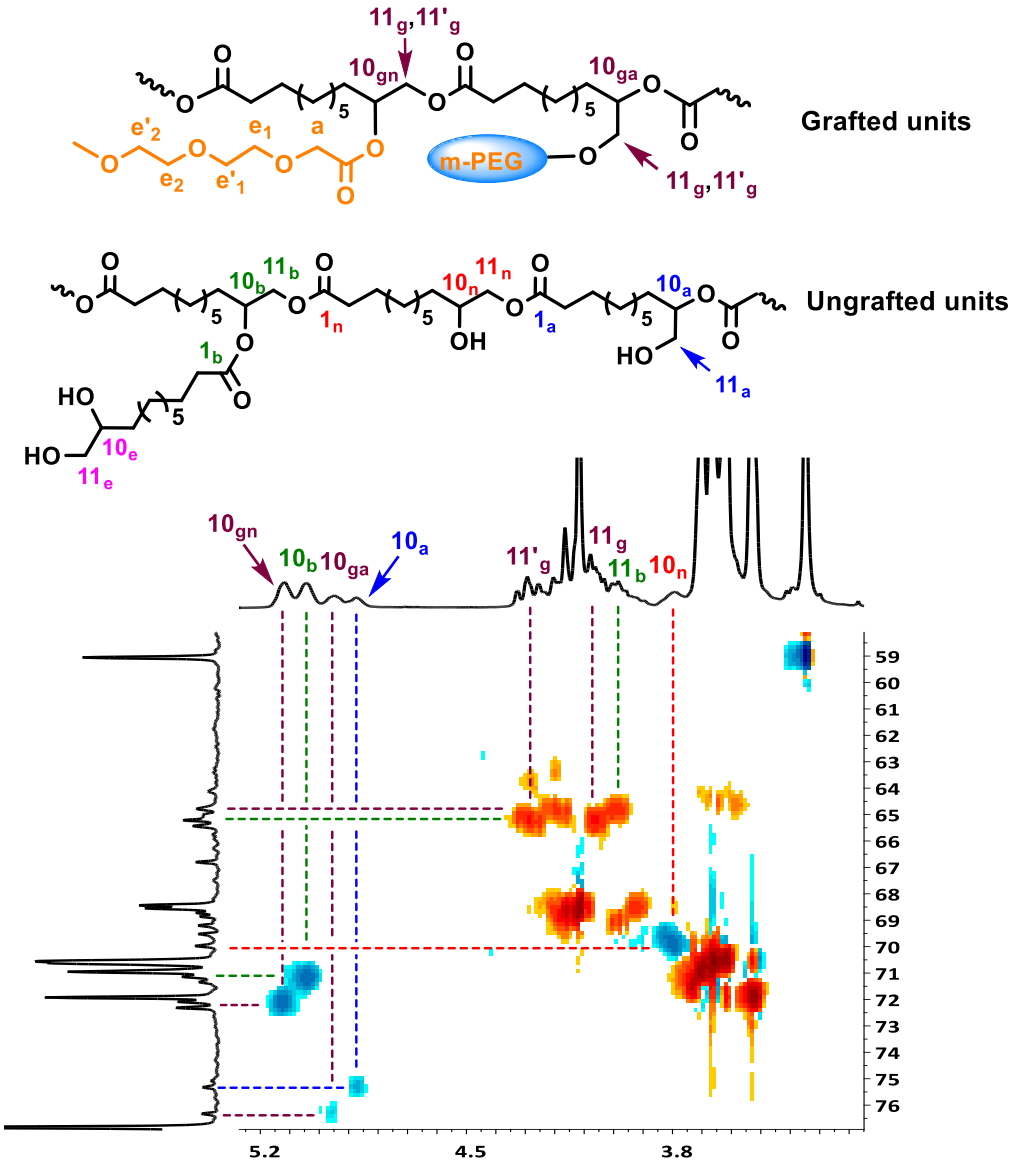

Figure SI.14 Heteronuclear single quantum correlation (HSQC) spectra recorded in $CDCl_3$ of PDHU grafted with $mPEG_2OCH_2COOH$.

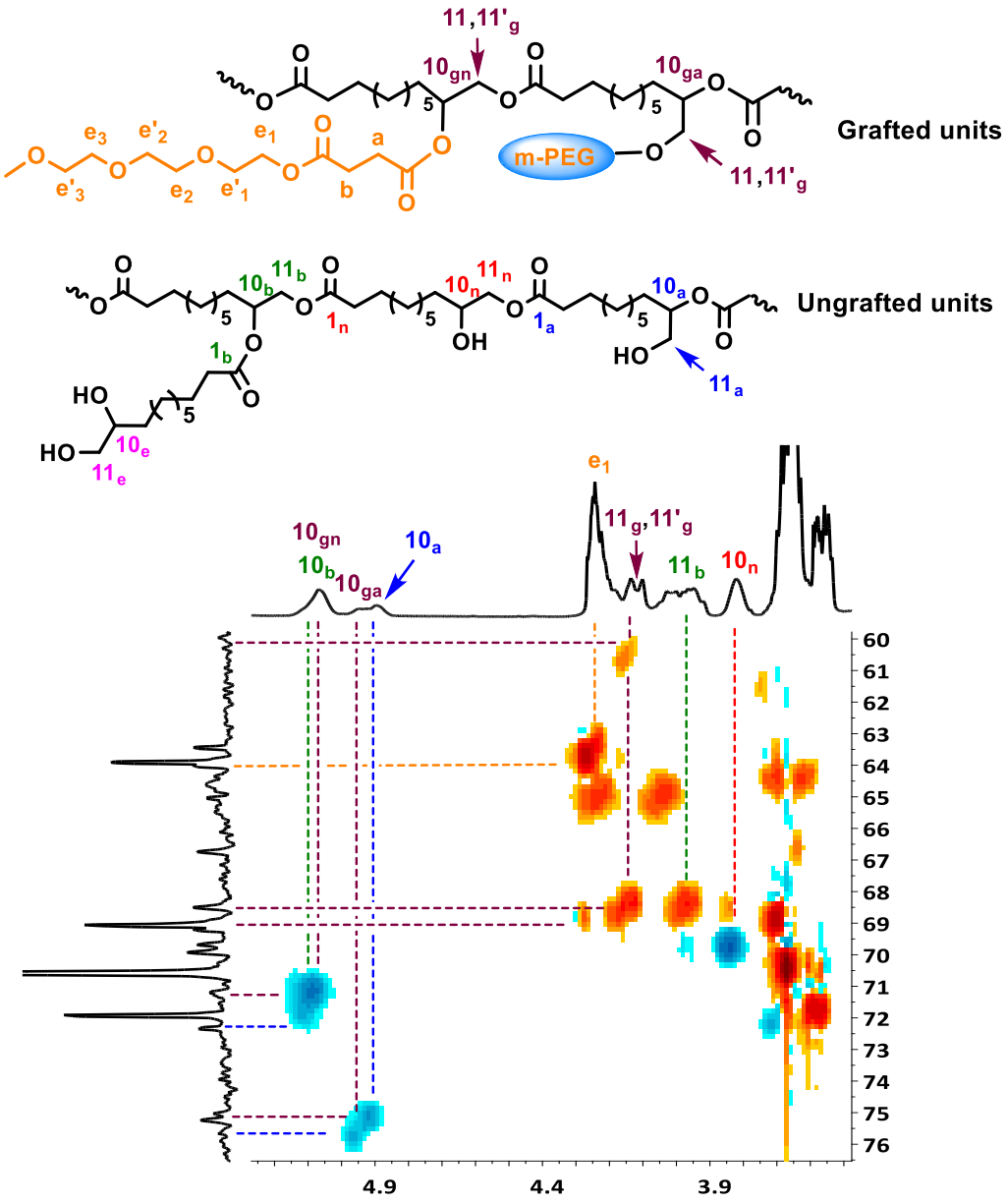

Figure SI.15 Heteronuclear single quantum correlation (HSQC) spectra recorded in $CDCl_3$ of PDHU grafted with $mPEG_3OOC(CH_2)_2COOH$.

Annex C

SI.7 Synthesis of (tri(ethylene glycol) monomethyl ether)succinic acid mono ester (mPEG$_3$-OOC(CH$_2$)$_2$COOH)

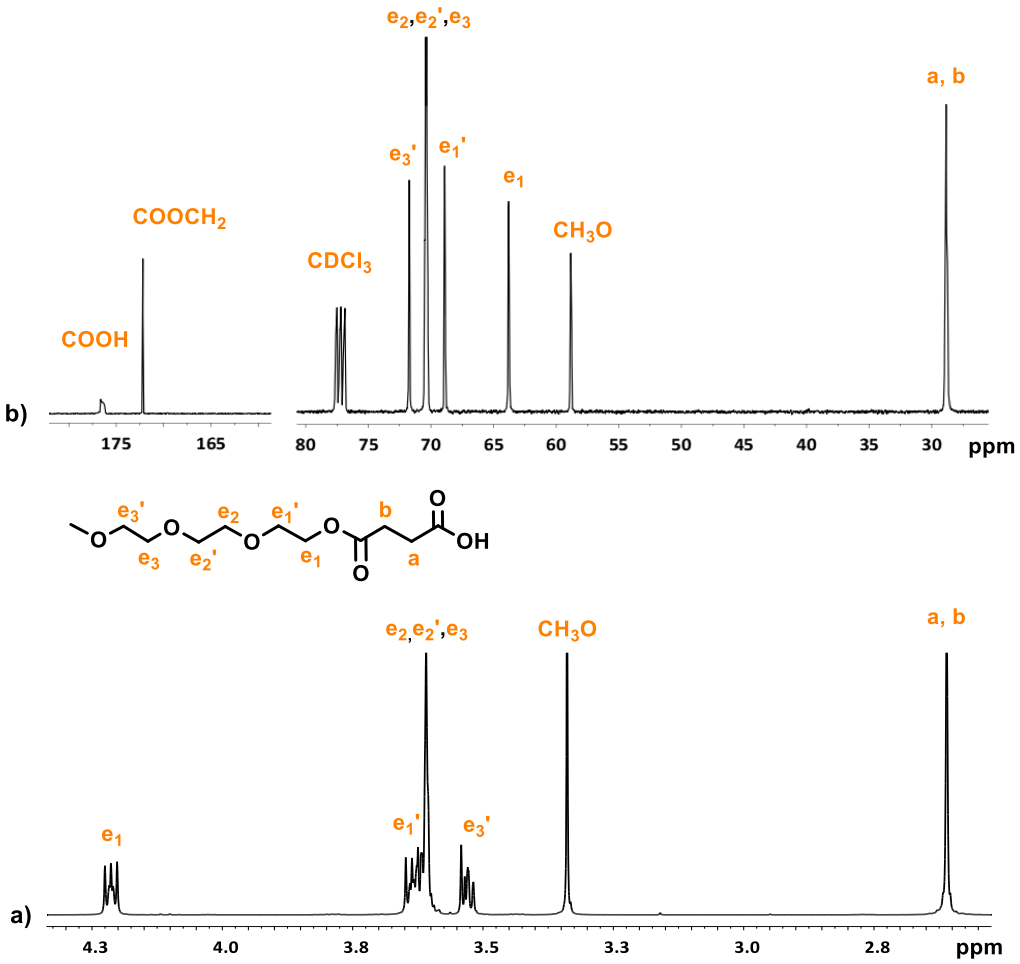

Figure SI.16 a) ^{1}H and b) ^{13}C NMR spectra of *mPEG$_3$-OOC(CH$_2$)$_2$COOH* recorded in $CDCl_3$ with the corresponding assignments.

SI.8 Synthesis of decane-1,2diyl bis(2-(2-(2-methoxyethoxy)ethoxy) acetate

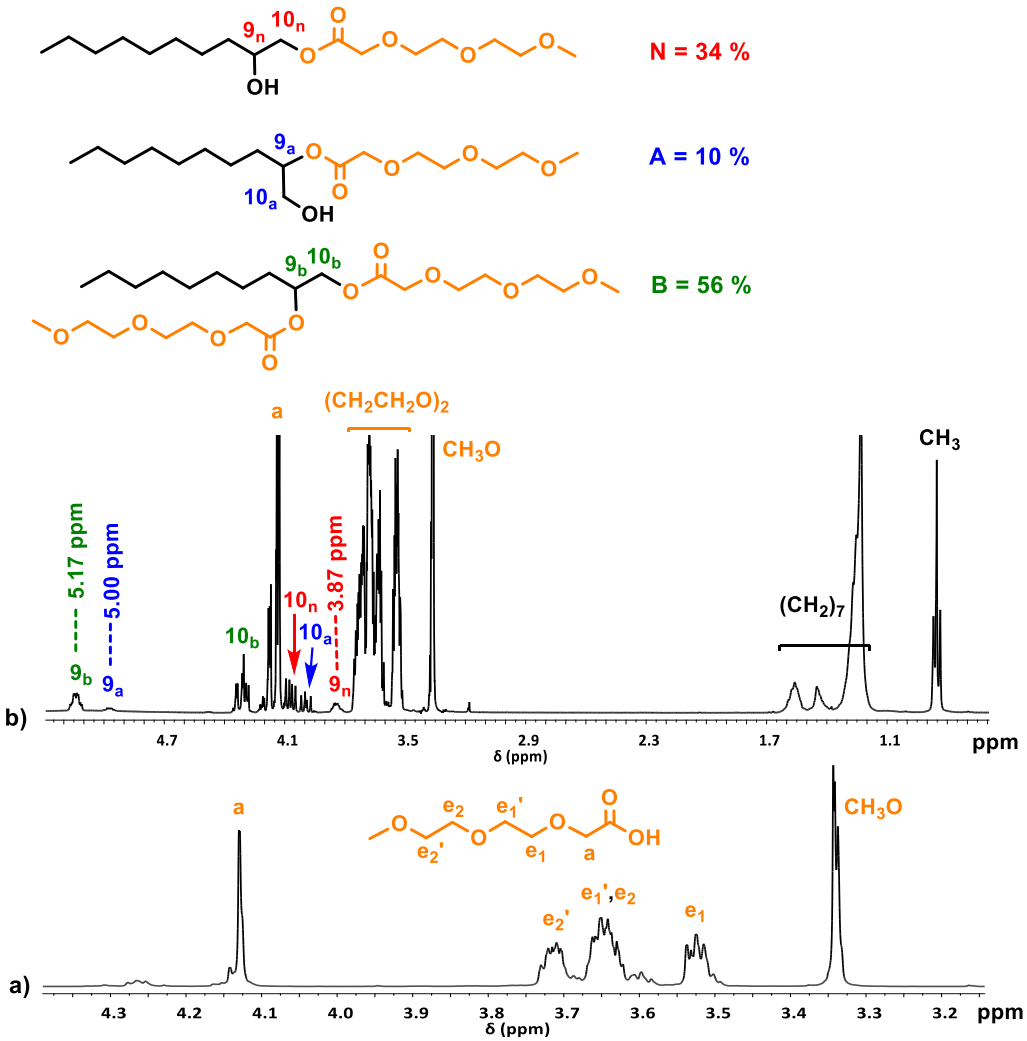

Figure SI.17 ^{1}H NMR spectra of a) 2-(2-(2-methoxyethoxy)ethoxy) acetic acid and b) crude reaction mixture with 1,2-decandiol with the corresponding assignments.

Annex C

SI.9 Dynamic light scattering of mPEG-b-PDHU and mPEG-g-PDHU copolymers

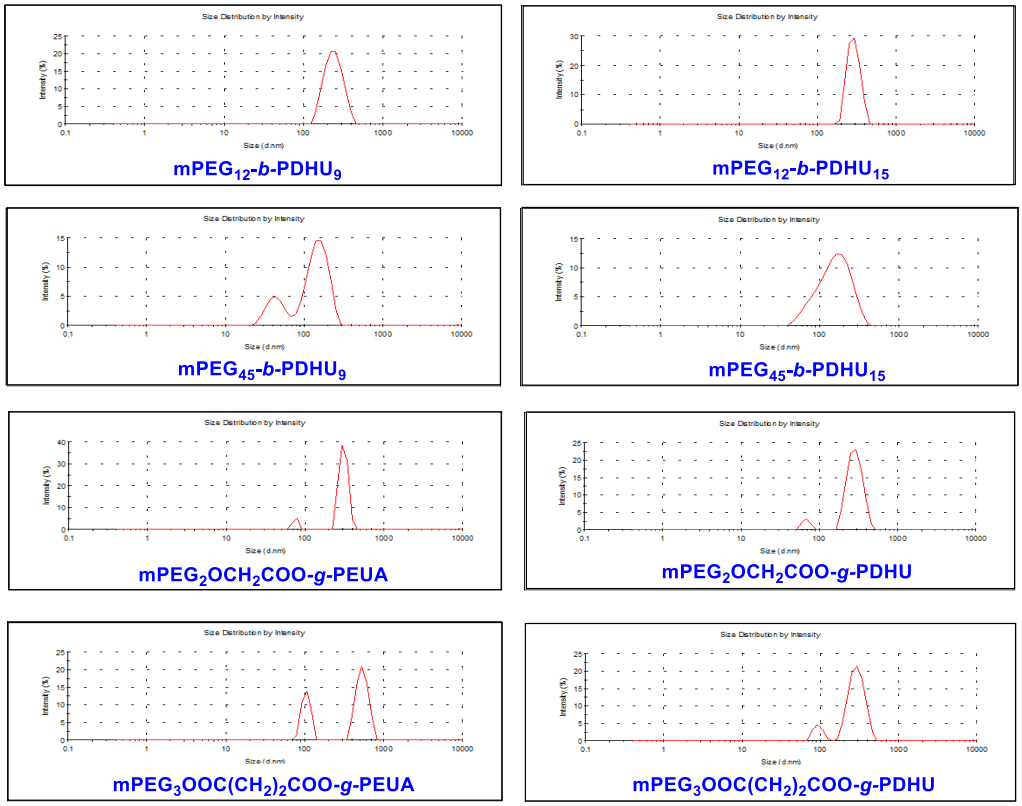

Figure SI.18 Hydrodynamic diameter distributions by intensity of the block and graft copolymers determined by DLS in water (0.5 mg·ml^{-1}).

SI.10 TEM imaging of mPEG-b-PDHU and mPEG-g-PDHU copolymers

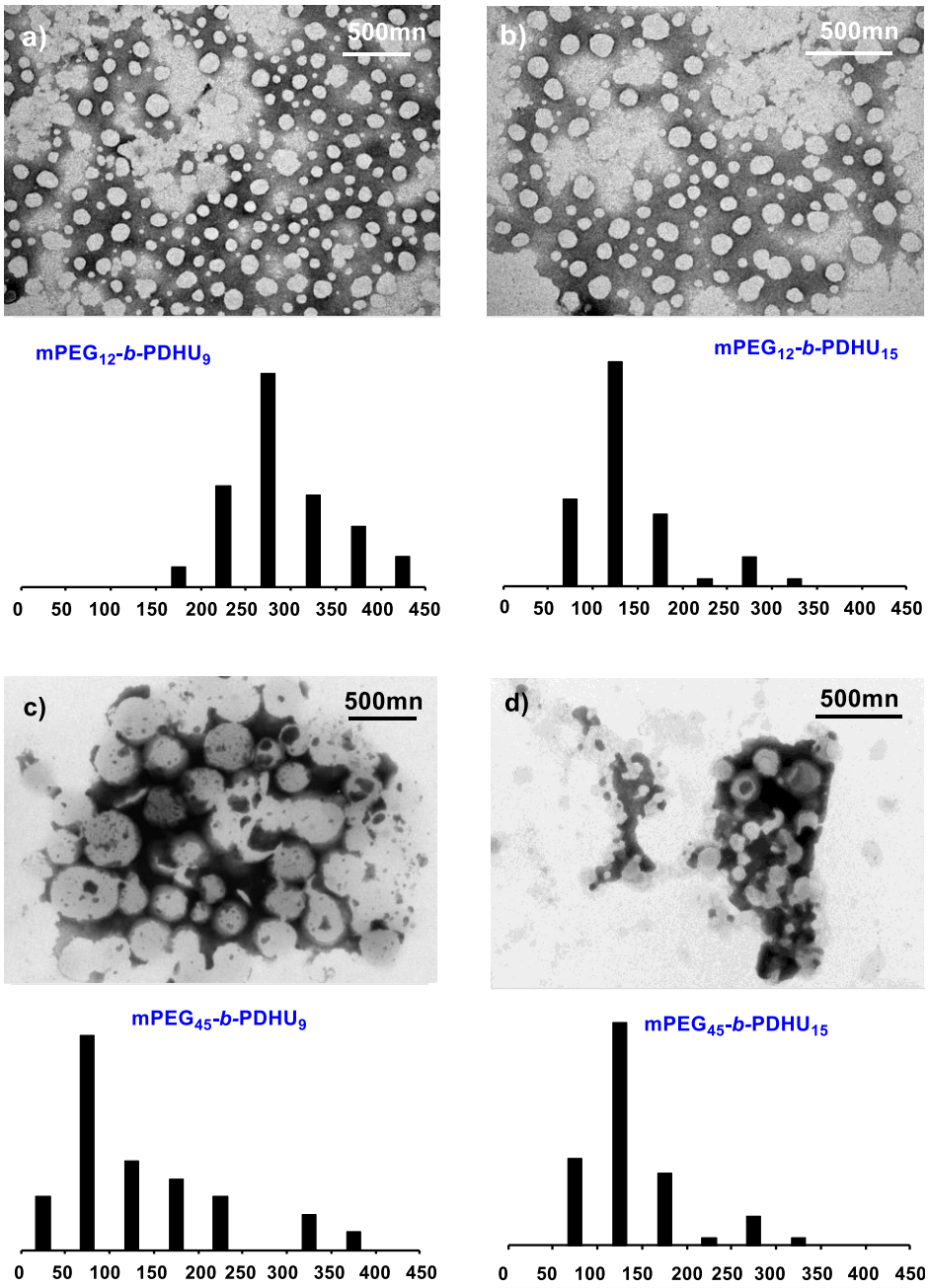

Figure SI.19 TEM images at images under negative stain mode (top) and size distribution histograms (bottom) (analysed by ImageJ software using various TEM images and a minimum of 40 micelles). a) mPEG$_{12}$-*b*-PDHU$_9$, b) mPEG$_{12}$-*b*-PDHU$_{15}$, c) mPEG$_{45}$-*b*-PDHU$_9$, d) mPEG$_{45}$-*b*-PDHU$_{15}$.

Annex C

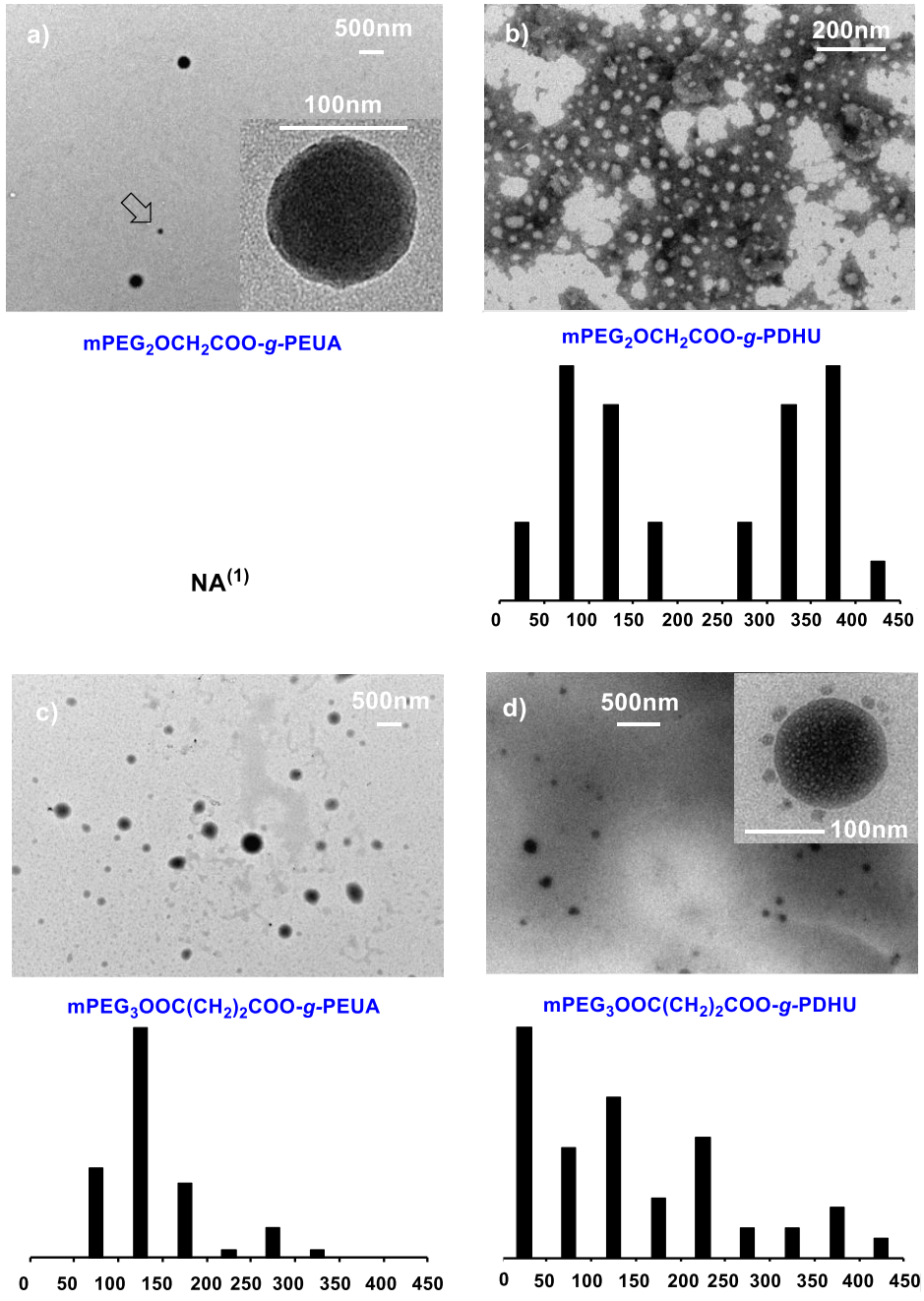

Figure SI.20 TEM images at different magnifications (top) and size distribution histograms (bottom) (analysed by ImageJ software using various TEM images and a minimum of 40 micelles). a) $mPEG_2OCH_2COO$-*g*-PEUA in drying mode, b) $mPEG_2OCH_2COO$-*g*-PDHU in negative stain mode, c) $mPEG_3OOC(CH_2)_2COO$-*g*-PEUA in drying mode, and d) $mPEG_3OOC(CH_2)_2COO$-*g*-PDHU in drying mode. (1) No analysed.

SI.11 Critical micelle concentration determination of mPEG-b-PDHU and mPEG-g-PDHU copolymers

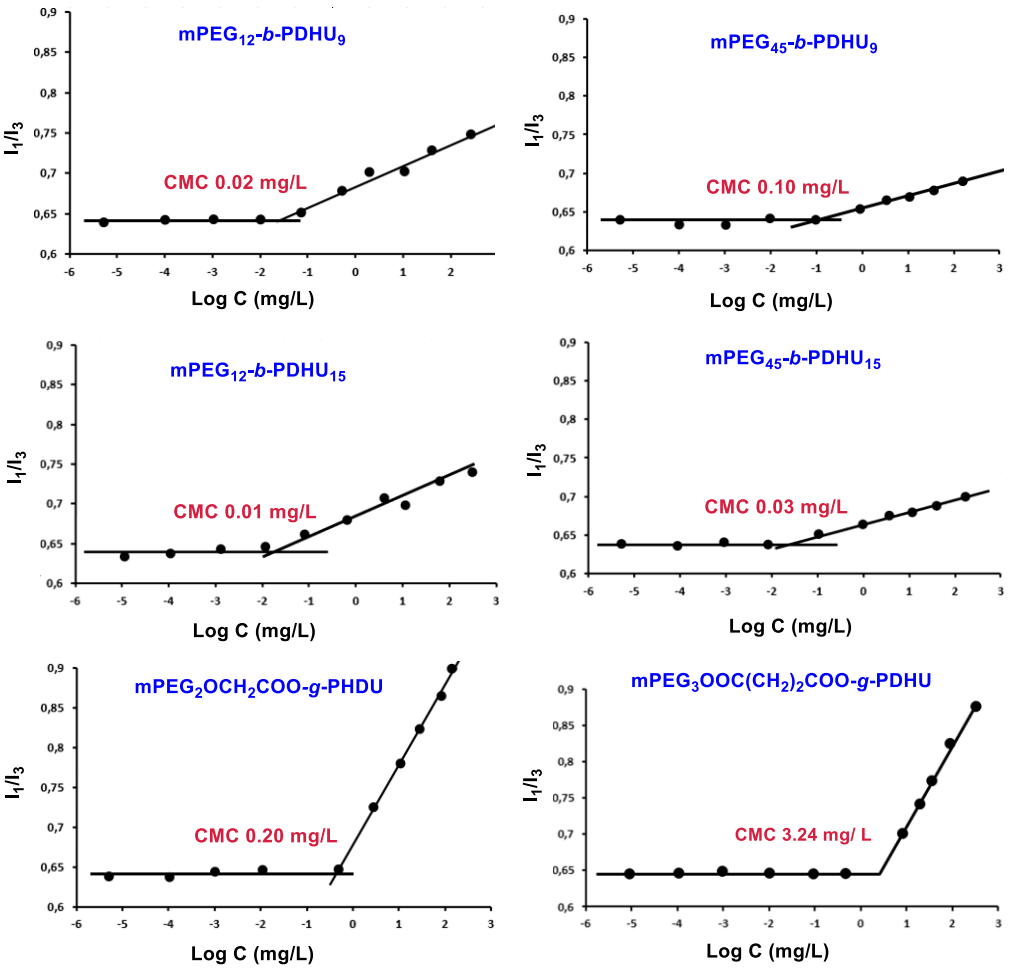

Figure SI.21 Calculation of CMC of selected multimolecular micelles using the I_1/I_3 intensity ratio method based on the fluorescence spectra of pyrene.

Annex C

REFERENCES

[1] Barrelle M., Béguin C., Tessier S., Carbon-13 NMR of oxygenated derivatives of polyoxyethylenes, **1982**, *Org. Mag. Res*., 19, 102-104.

List of abbreviations

$Sc(OTf)_3$	Scandium(III) triflate
[bmim]Br	1-Butyl-3-methylmidazolium bromide
[bmim]Cl	1-Butyl-3-methylmidazolium chloride
[hmim]Br	1-Hexyl-3-methylmidazolium bromide
µm	micrometres
^{13}C NMR	Carbon nuclear magnetic resonance
^{19}F NMR	Fluorine nuclear magnetic resonance
^{1}H NMR	Proton nuclear magnetic resonance
Å	Amstrong
AcOH	Acetic acid
AFM	Atomic force microscopy
Be	Beryllium
$BF_3.Et_2O$	Boron trifluoride diethyl etherate
B_u	Branching units
C. tropicalis	Candida tropicalis
ca.	Calculated
CALA	Candida antarctica lipase A
CALB	Candida antarctica Lipase B
Cat.	Catalyst
$CDCl_3$	Deuterated chloroform
$CFCl_3$	trichlorofluoromethane
CL	ε-Caprolactone
CLEAs	Cross-linked enzyme aggregates
CMC	Critical micelle concentration
Conv.	Conversion
d	Doublet
DCC	Diclyclohexylcarbodiimide
DCM	Dichloromethane
dd	Doublet of doublets
DDL	12-Dodecanolide
DECH	N-(3-Dimethylaminopropyl)-N-ethylcarbodiimide hydrochloride
DHU	10,11-Dihydroxyundecanoic acid
DLS	Dynamic Light Scattering
DMAP	4-(Dimethylamino)pyridine
DMF	N,N-Dimethylformamide

DMF-D_7	Deuterated dimethylformamide
DMFT	2,2-dimethylthiazolidin-3-(N-formyl)-4-carboxylic acid
DMSO	Dimethyl sulfoxide
DMSO-d_6	Deuterated dimethyl sulfoxide
DMT	2,2-Dimethylthiazolidin-4-carboxylic acid
Dowanol PMA™	Propylene glycol monomethyl ether acetate
DPE	Diphenyl ether
DSC	Differential scanning calorimetry
Đ	Polydispersity by SEC
EAM	Enzyme-activated monomer
EC 3.1.1.3	Triacylglycerol acylhydrolase
EH	1,2-epoxyhexane
Ent.	Entry
eROP	Enzymatic ring-opening polymerization
ESEM	Enviromental scanning electron microscopy
ESI MS	Liquid chromatography-mass spectrometry
EtOH	Ethanol
E_u	Etherificated units
EUA	10, 11-Epoxyundecanoic acid
FDA	United States governamental agency for Food and Drug Administration
FDCA	Furandicarboxylic acid
FT-IR	Fourier-transform infrared spectroscopy
γ-BL	γ-Butyrolactone
gCOSY	Gradient 2D 1H-1H Homonuclear NMR spectra
GHG	Green house gases
gHSQC	Gradient 2D 1H-13C Heteronuclear Single Quantum Coherence
h	Hours
HA	Hexanoic acid
HDL	16-Hexadecanolide
HSO_3Cl	Chlorosulfuric acid
IF	Insoluble fraction
IM-PC	Pseudomonas cepacia immobilized on ceramics
J	Coupling constant
Kv	Kilovolt
LA	Latic acid
lipase A	Aspergillus niger
lipase CA	Candida Antarctica
lipase CC	Candida cylindracea

Lipase CR or CR	Candida rugosa
lipase MM	Mucor meihei
lipase PC	Pseudomonas cepacia
lipase PF	Pseudomonas fluorescens
lipase PR	Penicillium roqueforti
lipase RJ	Rhizopus japonicus
lipase RM	Rhizomucor meihei
lipase YL	Yarrowia lipolytica
m	Multiplet
M	Molar ($g \cdot mol^{-1}$)
m.p.	Melting point
MARPOL	Marine pollution
m_d	Dry weight
μg	Micrograms
MHz	Megahertz
min.	Minutes
Mn	Number average molecular weight
$mPEG_2OCH_2COOH$	2-(2-(2-Methoxyethoxy)ethoxy)acetic acid
$mPEG_3OOC(CH_2)_2COOH$	2-(2-(2-Methoxyethoxy)ethoxy)ethyl monosuccinate
$mPEG_n$	Methoxypolyetileneglycol moieties
$mPEG_n$-OH	Methoxypolyetileneglycol
MR	Methyl ricinolate
MS	Molecular sieve
Mt	Megatonne
Mw	Weight average molecular weight
m_w	Wet weight
N_a	Abnormal units
N-Boc-Phe-OH	N-*tert*-butoxylcarbonyl phenylalanine
N-Boc-SerOMe	N-*tert*-butoxylcarbonyl serine methyl ester
nm	Nanometres
NMR	Nuclear magnetic resonance
N_u	Normal units
Θ	Contact angle in degrees (º)
OL	8-Octanoline
PBS	Poly(butylene succinate)
PBT	poly(butylene terephthalate) or Poly(butylene tartrate)
PBT-b-PTMG	poly(butylene adipate-co-terephthalate)
PBT-b-PTMG	poly(buthylene terephthalate)
PCL	poly(ε-caprolactone)
PDHU	Poly(10,11-dihydroxyundecanoic acid)

PDI	Polydispersity by DLS
PDL	15-Pentadecanolide
PE	Polyethylene
PEF	Poly(ethylene furanoate)
PEG	Polyethylene glycol
PET	Poly(ethylene terephthalate)
PEUA	Poly (10,11-epoxyundecanoic acid)
PGA	poly(glycolic acid)
PHA	Poly(hydroxyalkanoate)
PHFA	Poly(dihydroferulic acid)
PHP	Poly(hydroxypropionic acid)
PHU	Poly(11-hydroxyundecanoate)
PL	ß-Propiolactone
PLA	Polylactic acid
PLGA	Poly(lactic-co-glycolic acid)
PMMA	Poly(methylmethacrylate)
POC	1,8-Octanediol-co-citrate
Poly(12-HD-co-12HS)	Poly(12-hydroxydodecanoic acid)-co-(methyl-12-hydroxysterate)
PP	Polypropylene
PPC	Polypropylene carbonate
PPL	Porcine pancreas lipase
ppm	Part per million
PPT	Polypropylene terephthalate
PRA	Poly(ricinoleic acid)
PS	Polyestirene
PSeD	Poly(sebacoyl diglyceride)
PTA	Phosphotungstic acid
PTMC	Poly(trimethylene carbonate)
PTSA	p-Toluensulfonic acid
PTT	Poly(trimethylene terephthalate)
PVC	Polyvinylchloride
Py	Pyridine
q	Quartet
r.t.	Room temperature
RA	Ricinioleic acid
ROP	Ring-opening polymerization
rt	Room temperature
s	Singlet
$Sc(OTf)_3$	Scandium (III) triflate

$scCO_2$	Supercritical carbon dioxide
SEC	Size exclusion chromatography
SF	Soluble fraction
SI	Supporting information
$Sn(Oct)_2$	Tin(II) 2-ethylhexanoate
S_N2	Bimolecular nucleophilic substitution
Solv.	Solvent
Succ.	Succinic acid
t	Triplet or time
T	Temperature
t_0	Initial time
t_{10}	After 10 weeks time
$T_{5\%}$	Temperature of 5% weight loss
TAI	Trichloroacetylisocyanate
TBAS	Bis(tetrabutylammonium) sebacate
TBD	7-Methyl-1,5,7-triazabicyclo[4.4.0]dec-5-ene
TBPB	Tetrabutylphosphonium bromide
Tc	Crystallization temperature
TCE-d_2	Deuterated tetrachloroethane
TEAB	Tetrabutylammonium bromide
TEM	Transmission electron microscopy
TFA	Trifluoroacetic acid
TFAA	Trifluoroacetic anhydride
Tg	Glass-transition temperature
TGA	Thermogravimetric analysis
THF	Tetrahydrofuran
Tm	Melting temperature
Tmax	Temperature of maximum degradation rate
TMS	Tetramethylsilane
TMS-CHN_2	Trimethylsilyldiazomethane
TOF	Time of Flight
Tol.	Toluene
U	Unit.
UA	10-Undecenoic acid
UDL	11-Undecanolide
VL	δ-Valerolactone
Vos	Vegetable oils
w/w	Weight/weight
XRD	X-Ray diffraction
δ	Chemical shift (ppm)

ΔHc	Crystallization enthalpy
ΔHm	Melting enthalpy
ΔT	ΔT=Tm-Tc
χ_c	Fractional crystallinity

List of Publications

Title: Hydroxyl functionalized renewable polyesters derived from 10-undecenoic acid: Polymer structure and post-polymerization modification.

Authors: C. Valverde, G. Lligadas, J. C. Ronda, M. Galià, V. Cádiz.

Reference: European Polymer Journal, Vol. 105, pp. 68-78, 2018, DOI 10.1016/j.eurpolymj.2018.05.026. Polymer Science, I.F. 3,741.

Title: Hydrolytic and enzymatic degradation studies of aliphatic 10-undecenoic acid-based polyesters

Authors: C. Valverde, G. Lligadas, J. C. Ronda, M. Galià, V. Cádiz.

Reference: Polymer Degradation and Stability, Vol. 155, pp. 84-94, 2018, DOI 10.1016/j.polymdegradstab.2018.07.012. Polymer Science, I.F. 3,193.

Title: PEG-modified poly(10,11-dihydroxyundecanoic acid) amphiphilic copolymers. Grafting *versus* macromonomer copolymerization approaches using CALB

Authors: C. Valverde, G. Lligadas, J. C. Ronda, M. Galià, V. Cádiz.

Reference: DOI 10.1016/j.eurpolymj.2018.09.032, European Polymer Journal, Polymer Science, I.F. 3,741.

Meeting Contributions

Autors: C. Valverde, G. Lligadas, J. C. Ronda, M. Galià, V. Cádiz.

Oral Presentation: Polyesters from castor oil-derived 10-undecenoic acid.

JIP-JEPO (Jornadas de Jovenes Investigadores en Polímeros and Journées d'Etudes des Polymères), September 2015, San Sebastian, Spain.

Autors: C. Valverde, G. Lligadas, J. C. Ronda, M. Galià, V. Cádiz.

Poster Presentation: Synthesis and modification of functionalized polyesters derived from 10-undecenoic acid.

XIV Meeting of the Group of Polymers (GEP) of the Spanish Royal Chemistry and Royal Physics Societies, September 2016, Burgos, Spain.

UNIVERSITAT ROVIRA I VIRGILI
10-UNDECENOIC ACID-BASED BIODEGRADABLE HYDROXY POLYESTERS: A PLATFORM FOR AMINOACID BIOCONJUGATES AND PEG-DERIVED AMPHIPHILIC COPOLYMERS
Carmen Valverde Sarmiento

UNIVERSITAT ROVIRA I VIRGILI
10-UNDECENOIC ACID-BASED BIODEGRADABLE HYDROXY POLYESTERS: A PLATFORM FOR AMINOACID BIOCONJUGATES AND PEG-DERIVED AMPHIPHILIC COPOLYMERS
Carmen Valverde Sarmiento

UNIVERSITAT ROVIRA I VIRGILI
10-UNDECENOIC ACID-BASED BIODEGRADABLE HYDROXY POLYESTERS: A PLATFORM FOR AMINOACID BIOCONJUGATES AND PEG-DERIVED AMPHIPHILIC COPOLYMERS
Carmen Valverde Sarmiento

UNIVERSITAT
ROVIRA i VIRGILI